OXIDATION OF ORGANIC COMPOUNDS IN MOLTEN SALTS

A thesis submitted by

EMAD FADHIL AL-MUSLIH

to the

FACULTY OF ENGINEERING,
UNIVERSITY OF ASTON IN BIRMINGHAM

for the degree of

DOCTOR OF PHILOSOPHY

Department of Chemical Engineering,
University of Aston in Birmingham.
June 1984.

ACKNOWLEDGEMENTS

The Author is indebted to the following:
Dr.J.K.Maund, who supervised the major part of the work, for his help and guidance;

Dr.B.W.Hatt, who supervised the initial stages of the research, for his helpful discussions on the project;

the technical staff of the chemical engineering department Mrs.Overton for typing the thesis and Mr.R.Hill for his support and optimism.

TO

MUM AND DAD

THE UNIVERSITY OF ASTON IN BIRMINGHAM

OXIDATION OF ORGANIC COMPOUNDS IN MOLTEN SALTS

EMAD FADHIL AL-MUSLIH Ph.D 1984

SUMMARY

The objective of this research was to investigate the oxidation of organic compounds in molten alkali metal hydroxides containing manganates. It has been shown that controlled oxidation can be readily achieved with high specificity to give products in high yield with very short reaction times. The concurrent changes in the melt were monitored using a vibrating platinum indicator electrode with a quazi-reference electrode which was successfully developed for use in molten (Na-K)OH eutectic at 523K.

Henry's Law constants for water in the molten eutectic system (Na-K)OH have been measured and used to calculate the water concentration in the melt. The electrochemistry of manganates in molten (Na-K)OH eutectic at 523K has been studied using the vibrating platinum electrode, and the existence of the species Mn(II), Mn(III), Mn(IV), Mn(V) and Mn(VI) in such melts has been investigated at various water concentrations. The half-wave potentials of the voltammetric waves were measured versus the cathodic limit of the melt. The stability of Mn(V) or Mn(VI) in the melt was achieved by varying the water concentration.

A range of organic chemicals has been passed through molten (Na-K)OH at 523K and the reactions of these chemicals with the melt have been studied. The same organics were then passed through molten (Na-K)OH containing stabilized Mn(V) or Mn(VI) without violent reaction. Methanol, allyl alcohol, propane 1, 2 diol, 1-heptene and acetone were oxidized by Mn(V) and Mn(VI). Ethanol was only oxidized by Mn(VI), iso-propanol and benzyl alcohol were only oxidized by Mn(V). N-propanol, butanol, 2 methyl propan-2-ol, n-hexane, n-heptane toluene and cyclohexane were unchanged by both Mn(V) and Mn(VI). Detailed experiments have been performed on the reactions of ethanol, iso-propanol and methanol in molten (Na-K)OH containing stabilized Mn(V) or Mn(VI), and reaction mechanisms have been postulated.

Ethanol and iso-propanol were oxidized to acetaldehyde and acetone respectively with a potential for useful chemical process The oxidation of methanol could be developed as a basis for an industrial methanol disposal process.

KEYWORDS

Molten hydroxides, Manganates, Oxidation, Voltammetry, Alcohols.

LIST OF CONTENTS

Chapter Page

5. Electroanalysis of Manganates in Molten (Na-K)OH Eutectic

5.7 Effect of Adding Carbonate and Peroxide to (Na-K)OH Eutectic Containing $KMnO_4$

LIST OF TABLES

LIST OF FIGURES

CHAPTER 1

INTRODUCTION

Molten salts offer many potential advantages as reaction media for the industrial synthesis of chemicals at high temperature. They have high thermal stability, an extremely wide liquidus range, high electrical and thermal conductivity, and are excellent solvents for salts, metals, metal oxides and many gases. They are also generally inexpensive. The excellent heat transfer properties of molten salts enable easy control of exothermic or endothermic reactions. Molten salts also have the ability to stabilize unusually high or low oxidation states of various chemical species. The major disadvantages in the use of molten salts are the problems associated with handling any liquid at high temperature such as the possibility of vapour explosions caused by the accidental addition of liquids such as water. To handle high temperature molten salts, special equipment has to be designed to deal with these and other potential problems; for example valves, pumps and pipes must be heated so that the molten salt does not solidify and cause blockage. If water is present in the system hydrolysis of the salt may occur. The equipment must also be constructed of a material which resists the corrosive nature of the molten salt system and which is able to withstand the required high working temperatures. The possibility of accidents due to the formation of a solid cap of molten salt followed by a pressure increase and finally an explosion must also be eliminated. These problems and others have been overcome by some of the industrial processes using molten salts, e.g. pyrolysis, isomerization, dehydration, nitration, fuel cells, nuclear power, electrowinning and the syntheses of many organic and organometallic compounds. Molten salts provide a suitable environment for a wide range of chemical reactions. Sundermeyer (114) divided chemical processes in molten salts into three categories: (i) reactions in which the melt acts as a catalyst. (ii) reactions involving the participation of the melt and the consumption of one or more of its components with no simple means for regenerating the latter. (iii) reactions in which the melt acts as a solvent for the reactants. Reviews of chemical reactions in molten salts have been made by Sundermeyer (115), Kerridge (116) and Parodi, Bonomi and Gentaz (117). Gentaz and Bonomi (118) have reviewed molten salt processes, molten salt technology, and commented on possible future trends in the use of molten salt media.

This project set out to investigate an area of organic reactions in molten salts with a view to developing a basis for an industrial process. Certain practical aspects of the project were considered, these included: (i) the reaction must take place at relatively low temperature (not more than 573K) and at atmospheric pressure. (ii) the reaction must provide a suitably varied area for research. (iii) the reaction must give products which are volatile at the molten salt operating temperature and (iv) electrolysis of the molten salt could provide an active reactant species.

A survey of the possible reaction areas which employed molten salt media was carried out with a view to the study of one of these areas in the research project. Oxidation-reduction reactions were chosen as the most suitable. It was thought that an organic oxidation reaction might be performed with an inorganic oxidizing agent dissolved in the melt and that reactions might be more specific than if pure oxygen or air were used. The regeneration of the oxidizing agent using oxygen or electrolysis was also considered a practical possibility. It was known that unusual oxidation states of chromium and manganese had been found in some molten salts. The oxidation states of manganates that are soluble in some molten salts were chosen as the inorganic oxidizing agents. Eluard and Tremillon (7) had found that several manganese oxidation states could be stabilized in molten hydroxides; also Read (49) had performed some organic oxidation reactions in molten salts using manganates as the oxidizing agents.

Molten alkali metal hydroxides have been the subject of chemical and electrochemical investigations by several workers. The aim then of the research project was to study the oxidation of organic compounds in molten hydroxides by stabilized oxidation states of manganese.

CHAPTER 2

The Physical and Chemical Properties of Molten (Na-K)OH Eutectic Mixture

2.1 The Melt Composition

In the course of investigating the physical, chemical and electrochemical properties of the melt, more than one melt composition has been used. Von Hevesy (1) gave the composition of the NäOH-KOH eutectic as 63.1 mol% NaOH, melting point 185°C, describing it as a solid solution. More recent work (2, 3) has shown that the system is eutectic. The composition of the eutectic is taken to be 51 mol% NaOH and its melting point 170°C, in agreement with both the more recent references. Eluard and Tremillon (4 - 8) have also adopted this composition, although their earlier work was done on the melt composition given by Von Hevesy. The addition of LiOH to the binary melt does not lower the melting point significantly (3), and it is therefore reasonable to standardize all fused hydroxide work on the binary melt. The changes in experimental values resulting from the differences between the eutectic composition of 51 mol% NaOH and the equimolar one are well within the experimental error of the measurements.

Fused hydroxides can be used up to at least 775°K, although the problem of corrosion of container materials becomes more serious with increasing temperature.

2.2 Physical Properties

Arndt and Ploetz (9), have measured the density of pure NaOH and found it to be $1.746\{1-2.74 \times 10^{-4}(t-400)\}$

kg/l; that of pure KOH was 1.717{1-2.56 x 10^{-4}(t-400)} Kg/l. A weighted average extrapolated to 500K is 1.81 kg/l, which is taken to be the density of an equimolar melt (10). Extrapolation and interpolation from the data of Klochko and Godneva (11), give 1.84 kg/l for an equimolar melt containing 0.8 mol% water; this agreement is reasonable.

In later (12), the density of the molten NaOH-KOH eutectic mixture was measured at temperatures ranging from 451K to 688K. The molar volume of the melt was found to increase linearly with temperature. Also the water concentration dependency of the density of the melt has been measured (13) in a concentration range extending from the dry mixture to a mole fraction of water of 0.09. The viscosity of the anhydrous eutectic melt does not appear to have been measured; the values of Arndt and Ploetz (9) are for NaOH and KOH at much higher temperatures. The best estimate available is 2.4 NS/m^2 (2.4 cp) for an equimolar melt containing 0.8 mol% water at 200°C from Klochko and Godneva (11); extrapolation of the data of Arndt and Ploetz gives rough agreement.

The potential range of the melt is about 1.4V in both acidic and basic media, but the anodic and cathodic limiting reactions are dependent on the pH_2O of the melt. The anodic (oxidation) melt limit in acidic melts is the oxidation of OH^- to O_2^- or, beyond, to oxygen gas, whereas in basic melts oxidation to O_2^{-2} is possible before O_2^- formation. The cathodic (reduction) melt limit in acidic melts is the reduction of water to hydrogen, whereas in basic melts Na or K metal or both are produced instead. The potential range of NaOH or KOH is similar (14). Claes and Glibert (15), discussed the transport properties in ionic melts, of particular interest are those of molten hydroxides.

When the equivalent conductance (in $\Omega^{-1}cm^2eq^{-1}$) of the dry pure eutectic mixture is compared with that of fused sodium and potassium salts, the values are surprisingly similar (12), although molten hydroxides differ from simple ionic liquids in many ways. The interactions between the ions in a hydroxide melt are not strictly comparable with electrostatic interactions between ionic "hard spheres", [the formation of aggregates by hydrogen bonding between hydroxide ions has been deduced from Infra-red spectroscopic investigations (16)]. In the case of molten salts, cations seem to play the major role in transport processes; in most cases the transport number of the cation is about 0.6, (17). Shvedov and Yvanov (18) measured the transport numbers of Na^+ and K^+ ions in molten NaOH and KOH. They found $t_{Na^+} = 0.10 \pm 0.03$ and $t_{K^+} = 0.03 \pm 0.03$; thus current conduction is almost entirely associated with the anions. In order to interpret these results, a rather special transport mechanism has to be invoked. A proton transfer conduction mechanism similar to that proposed for water and aqueous solutions may be suitable. In molten hydroxides, proton transfer might occur through the direct involvement of water molecules and/or of oxide ions; these would then take on the role of hydronium and hydroxide ions, respectively, corresponding to aqueous solutions. The concentration of oxide ions and water molecules in the dry eutectic mixture is about 10^{-9} mol/cm^3 at 500K (19). This seems to be too low a concentration to explain the electrical conductance of molten hydroxides by a simple proton transfer mechanism via H_2O or O^{2-}. At 523K, the conductivity of the neutral melt is 0.87 Ω^{-1} cm^{-1} and it rises to only 1.08 Ω^{-1} cm^{-1} for a mole fraction of water of 0.1 (i.e., for a concentration of water 10^5 higher than in the neutral melt). The high conductivity of the neutral melt could be explained if it is assumed that proton transfer is particularly rapid in this case; a reason for this might lie in a favourable mutual reorientation of hydroxide ions. The experimental results give no information about such an effect, but, if this interpretation is correct, the structure of the molten hydroxide should exert a large influence on the migration processes.

The conductivity of the dry melt and of solutions of water from $X_w = 0$ to $X_w = 0.1$ were investigated between 451 and 723K (12). It was measured using a compact alumina capillary cell. The conductivity of the molten eutectic mixture increased from 0.436 Ω^{-1} cm^{-1} at 451°K to 1.783 Ω^{-1} cm^{-1} at 723°K. The specific conductances were extrapolated to infinite frequency.

The conductivity of the melt was also measured as a function of the oxoacidobasicity of the melt at concentrations ranging from a mole fraction of sodium oxide of 0.16 to a mole fraction of water of 0.09, (13). The conductivity of the melt was enhanced when the water concentration increased while it decreased when oxide ions were dissolved into the liquid except at low water concentrations the conductivity of the melt was directly proportional to the water concentration. The conductivity of the acidic melt is described by the following equation:

$$\text{Conductivity}_{\text{acidic melt}} = K + \mu\, F\, C_{H_2O} - A(C_{H_2O})^{\frac{1}{2}} \quad (2\text{-}1)$$

where K is the conductivity of the dry melt.

μ is the conventional mobility of the proton by transfer from H_2O to OH^-.

F is the Faraday constant.

C_{H_2O} is the water concentration.

and A is a mathematically suitable constant.

The specific conductance of pure NaOH and pure KOH were both measured earlier by Arndt and Ploetz (9), a weighted extrapolation gives 1.40 Ω^{-1} cm^{-1}.

2.3 Preparation of the Melt

The major problem in preparation of fused hydroxide melts is the removal, or perhaps more accurately the analysis and control of water concentration. Water is the only significant impurity in reagent-grade hydroxides other than carbonates, which may be removed as CO_2 by the purification process or is electrochemically inactive.

Water, which is present as over 10% by weight in some reagent-grade hydroxides, can be essentially quantitatively removed by heating the fused hydroxides at 450-500°C for several hours, which is reported to reduce the water content to below 20 ppm (20). Williams et al. (21), who also used this dehydration procedure, warned that water is held tenaciously by fused sodium hydroxide at temperatures below 400°C, even under high vacuum. Addition of metallic sodium, which reacts to evolve hydrogen, has been used to remove water (19); addition of water can be carried out effectively by the addition of hydroxide of known water content or it can be introduced indirectly by the addition of silica, which reacts with molten hydroxides to produce water (22).

The solubility data for water in molten hydroxides and the experimental techniques used, has been reviewed by the author in a recently published paper, (23). The Henry's law constants for water in the molten eutectic system NaOH-KOH have been measured; other workers measured the constant in molten sodium hydroxide only.

These solubility data are shown in table 2-1:

Melt	Ref.	Temperature K	Solubility data (as given by authors)	Henry's Law Constant (atm $mol^{-1}Kg$)	Experimental Technique
NaOH	24	623-773	Linear relation between solubility, pressure and the H_2O vapour	$10^{(4.88-3210/T)}$	Gravimetry
NaOH	25	640	84 μ mol mol^{-1} $torr^{-1}$	0.63	Volumetric
NaOH	25	690	44 μ mol mol^{-1} $torr^{-1}$	1.02	Volumetric
NaOH-KOH (63.1:36.9mol%)	23	523-723	Linear relation between Henry's Law constant and temperature	$e^{-(8081)/T+10.8}$	Gravimetry

Table 2-1 Solubility Data of Water in Molten Hydroxides

Hydrogen gas is only slightly soluble in the melt at 1 atm.pressure. The solubility of hydrogen in acidic (Na-K)OH,(51-49) mol% melts, at 500K, was measured by Eluard (26) using the coulometric method developed by Vogēl and Smith (27). It was found to be 2.24 x 10^{-8} mol cm^{-3} atm^{-1}, this value is in good agreement with the one determined in aqueous KOH at 473K (28).

Rahmel and Krueger have measured and reported the solubility of oxygen in sodium hydroxide melt (24).

2.4 Conditions of Use

Molten hydroxides must be studied under a dry inert atmosphere to prevent pickup of atmospheric moisture by the melt. The melt must also be kept away from oxygen, which is extremely oxidizing in the fused hyroxide system in which it can oxidize oxide and water to the superoxide ion. Corrosion of container materials can be a serious problem in fused hydroxides. Goret and Tremillon (19,20) successfully used Teflon crucibles. These are reported to be satisfactory up to 300°C but are attacked in higher temperature environments. In extremely reducing melts in which sodium metal is dissolved, the Teflon crucibles are attacked chemically even below 300°C. Ceramic materials are attacked in basic melts, although alumina withstands some acidic melts. Vitreous carbon is not attacked in fused hydroxides (19) at any pH_2O but in extremely reducing melts sodium metal will attack it, and in the presence of oxygen at these temperatures it is unlikely that it would remain unattacked. Most metals can withstand high temperatures but are attacked by fused hydroxides. Agar and Bowden (29) used a nickel crucible in their study of fused NaOH; the crucible rapidly became covered with a black oxide film that prevented, or more probably drastically reduced, corrosion of the crucible. Goret and Tremillon (19,20) report that nickel is attacked by oxygen in this melt and that the protective oxide coating, which is useful in acidic melts, dissolves in basic melts. The reactivity of nickel has also been demonstrated by Stern and Carlton (30), who employed a gold crucible. They reported that the gold was not attacked by fused NaOH up to 500°C, but Goret and Tremillon (31) showed that this was only true in neutral melts.

2.5 The Chemistry of Hydroxide Melts

The interrelationship in fused hydroxides between oxidation-reduction and acid-base behaviour makes their chemistry complex. The general chemical properties and the acid-base characteristics of these melts have been described by Goret and Tremillon (19,20,32).

Molten alkali hydroxides are completely dissociated into Na^+, K^+, or Li^+ and OH^-. As the OH^- ions are partially dissociated into H_2O and O^{2-} (19,33-35) water will play a fundamental role in these media as was earlier emphasized by Agar and Bowden (35) and then by Lux et al. (36,37). The acid-base behaviour of molten hydroxides can be described formally by the dissociation equilibrium which can be represented by:

$$2OH^- \rightleftarrows H_2O + O^{2-} \qquad (2\text{-}2)$$

In writing an equilibrium constant for this solvent system, the standard state of hydroxide ion is taken to be the actual state in the fused hydroxide eutectic, while the standard states of both water and oxide ion are Henrian. That is, the standard state of these species is a solution of unit concentration on some concentration scale having the properties of the species at infinite dilution in the melt.

The equilibrium constant is then simplified to:

$$K_{OH} = [H_2O]\ [O^{2-}] \qquad (2\text{-}3)$$

and its value in an equimolar melt at 500K has been estimated to be (given most easily here as pK_{OH}), (20):

$$pK_{OH} = 11.5 \pm 0.7 \text{ (in unit moles per litre)}$$

The Bronsted acid-base concept has been retained in molten hydroxides, so that a substance acting as proton-donor (with respect to OH^-) and forming H_2O according to:

$$HA + OH^- \rightleftarrows H_2O + A^- \qquad (2\text{-}4)$$

is defined as an "acid", while a proton-acceptor species

$$B + OH^- \rightleftarrows BH^+ + O^{2-} \qquad (2\text{-}5)$$

is defined as a "base", and in other words water being the conjugate acid of hydroxide ion and oxide ion being its conjugate base. It should be pointed out that water in these media may also behave as an acid according to the Bronsted theory, for water may be considered as the "solvated" proton in hydroxide melts; then it plays the same role as the H_3O^+ cation in aqueous solutions, thus water is also the strongest acid that can exist in the melt.

Analagous to the pH (pH_3O^+) scale employed in aqueous solutions, (the autoprotolysis constant for water)

$$K_{H_2O} = [H_3O^+][OH^-] \quad pK_{H_2O} = 14.0 \qquad (2-6)$$

a pH_2O scale has been formulated for molten hydroxides and its use exactly parallels the use of pH in aqueous solutions. Moreover the use of Pourbaix, or E-pH_2O, diagrams is as useful in these melt as in water, where they have the more usual E-pH form.

Considering the equilibrium constant, it is understandable that the accessible pH_2O range in this melt at 500K is about 12.0 units, located between the most concentrated water solutions and the most concentrated oxide solutions (corresponding to the sodium oxide solubility in this melt i.e. 0.05 mol/kg). The melt is said to be "acidic" or "basic" when the pH_2O is, respectively, lower or higher then 5.8. The role of water in molten hydroxides is directly related to the oxoacidobasic properties of the melts themselves, as the autodissociation equilibrium (2-2) is nothing but the reverse reaction involving the oxoacid properties of water:

$$H_2O + O^{2-} \rightleftarrows 2OH^- \qquad (2-7)$$

By considering the dissociation constant value (31, 38, 4, 6-8) determined experimentally at 500K, an equilibrium constant may be ascribed to reaction (2-7) of a value equal to $10^{-12.5}$ in the molality scale. From the work of Tremillon and Doisneau (39) a correlation can be found between this value and the corresponding ones at different temperatures and compositions in molten alkali hydroxides. For example, in pure NaOH at 593K a constant close to 10^{-10} could be found. The acid-base equilibria of water and corresponding equilibrium constant values is given in table 2-2.

Composition	T(K)	Acid-base Equilibrium	pK=-logK*	Ref.	Note
NaOH-KOH (51-49mol%)	500	$2OH^- \rightleftarrows O^{2-} + H_2O$	12.5	19,38 31,4,6-8	
NaOH	700	$2OH^- \rightleftarrows O^{2-} + H_2O$	7.5	39	a
NaOH	800	$2OH^- \rightleftarrows O^{2-} + H_2O$	6.0	39	a
NaOH	873	$2OH^- \rightleftarrows O^{2-} + H_2O$	5.0	39	a
NaOH	1000	$2OH^- \rightleftarrows O^{2-} + H_2O$	3.75	39	a
NaOH	623	$2OH^- \rightleftarrows O^{2-} + H_2O$	9.7	39	b
NaOH	750	$2OH^- \rightleftarrows O^{2-} + H_2O$	7.4	39	b
NaOH	850	$2OH^- \rightleftarrows O^{2-} + H_2O$	6.2	39	b
NaOH	1000	$2OH^- \rightleftarrows O^{2-} + H_2O$	5.0	39	b
LiOH	750	$2OH^- \rightleftarrows O^{2-} + H_2O$	2.5	39	b
LiOH	850	$2OH^- \rightleftarrows O^{2-} + H_2O$	1.8	39	b
LiOH	1000	$2OH^- \rightleftarrows O^{2-} + H_2O$	1.1	39	b
KOH	750	$2OH^- \rightleftarrows O^{2-} + H_2O$	10.3	39	b
KOH	850	$2OH^- \rightleftarrows O^{2-} + H_2O$	8.8	39	b
KOH	1000	$2OH^- \rightleftarrows O^{2-} + H_2O$	7.1	39	b

a - combination of experimental and thermochemical data

b - values obtained through thermochemical data only

* K calculated in molality and atmosphere units

Table 2-2 Acid-Base Equilibria of Water and Corresponding Equilibrium Constant Values for Hydroxide Melts.

2.6 Applications Related to the Acidobasicity and Redox Properties of Water in Molten Hydroxides

Fused hydroxides have long been known to be corrosive to metals, and many studies of this corrosion have been made. No quantitative data could be deduced from any of these studies, however, because either the atmosphere was not controlled or the water content of the melt was significant so such studies have not been cited. The part played by water in molten hydroxides is fundamental as this compound is the strongest oxoacid in these melts. Thus the solubilities of metal oxides will depend greatly on the concentration of water in the melts as demonstrated by Tremillon et al. (38,31,4,6-8,39) through reactions such as:

$$M^{n+} + nOH^- \rightleftarrows MO_{n/2} \downarrow + \frac{n}{2} H_2O \qquad (2-8)$$

whose equilibrium constant K_A can be related to the solubility product value K_s and to the solvent autodissociation constant K_i:

$$K_s = K_i \ (K_A)^{-n/2} \qquad (2-9)$$

According to these authors, the water concentration ranges corresponding to the precipitation or to the dissolution (for $[M^{n+}]=10^{-2}$) of various metal oxides are represented in Fig. 2-1. In pure molten NaOH, the determinations made by Doisneau and Tremillon (40) at 623K enabled these authors to predict that titanium could be separated from iron by varying the water content of melts in which ilmenite ($FeTiO_3$) is dissolved.

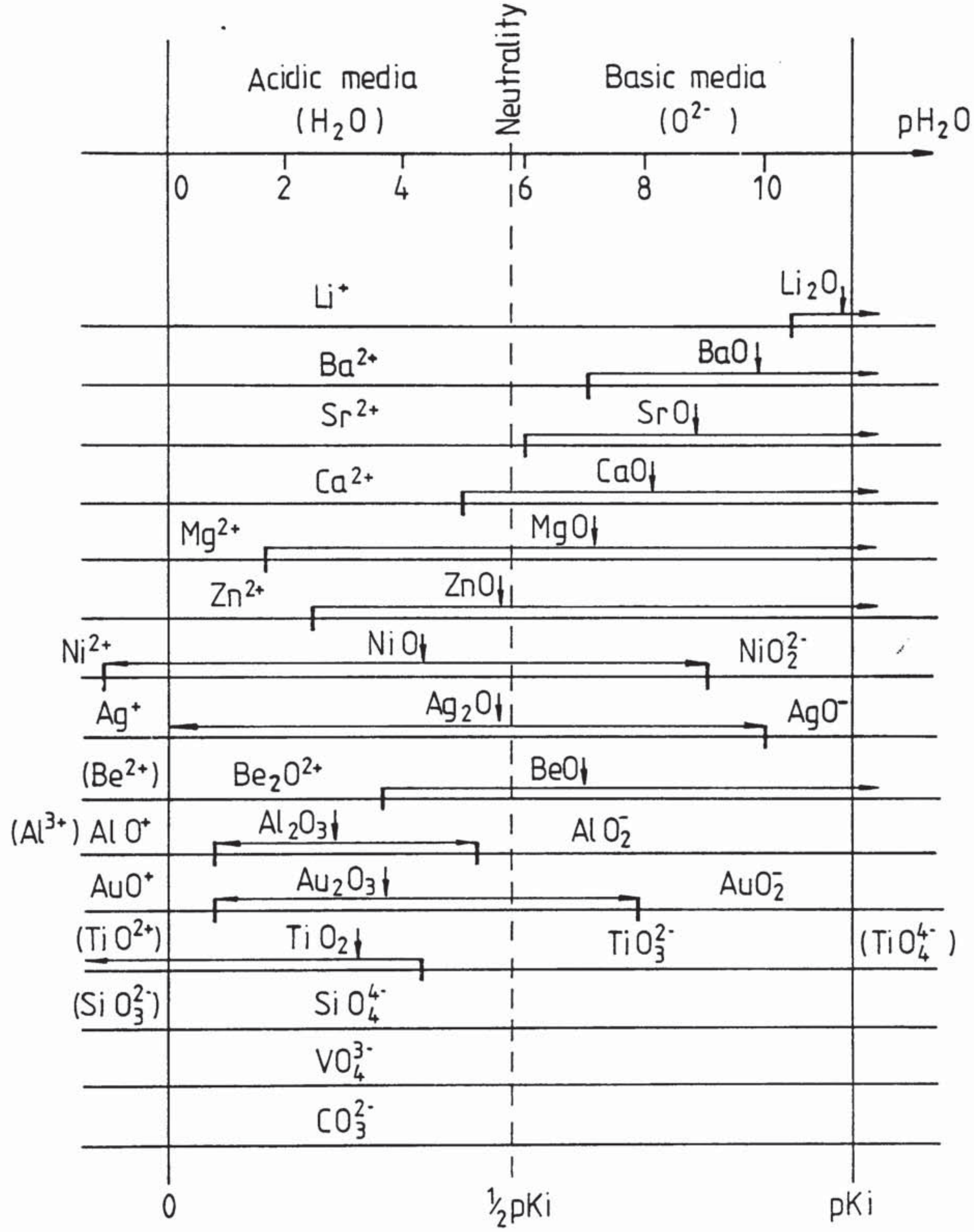

Figure 2-1 Solubility diagram of various metal oxides in molten NaOH-KOH at 500K. (According to Tremillon et al. 31,38)

Predictions about the effects of water on some species can be made by looking at the corresponding acidic part of the E-pO^{2-} or E-pH_2O diagrams. The lower limit of these diagrams corresponds to the reduction of water except in very basic media where this limit is due to the formation of hydride. Tremillon and co-workers (19,38,31,4,6-8,39) concluded that for example copper and manganese oxides which precipitate in neutral media, can be separated by the progressive addition of water, only copper oxide is dissolved. Then manganese oxide can be dissolved by the formation of MnO_4^{3-} when adding an oxidizing compound to the melt. More generally it has been shown that in concentrated water melts (acidic media), silver, gold, mercury, nickel, and platinum oxides were insoluble both in oxidizing and reducing conditions.

Moreover the use of nickel as a crucible material for hydroxide melts, was shown to be justified as the oxide of this element is also insoluble and adherent in oxidizing basic melts. Some predictions have also been made for the corrosion of some metals in NaOH-KOH at 500K through the Pourbiax-type diagrams represented in Fig. 2-2. As can be seen, the effect of increasing water concentration is to reduce corrosion. Most of the considered elements are passivated except for silver, which on the contrary is immune over a large range of acidity and potential. A comparable study has been made by Doisneau and Tremillon (40) for iron in pure molten NaOH at 623K.

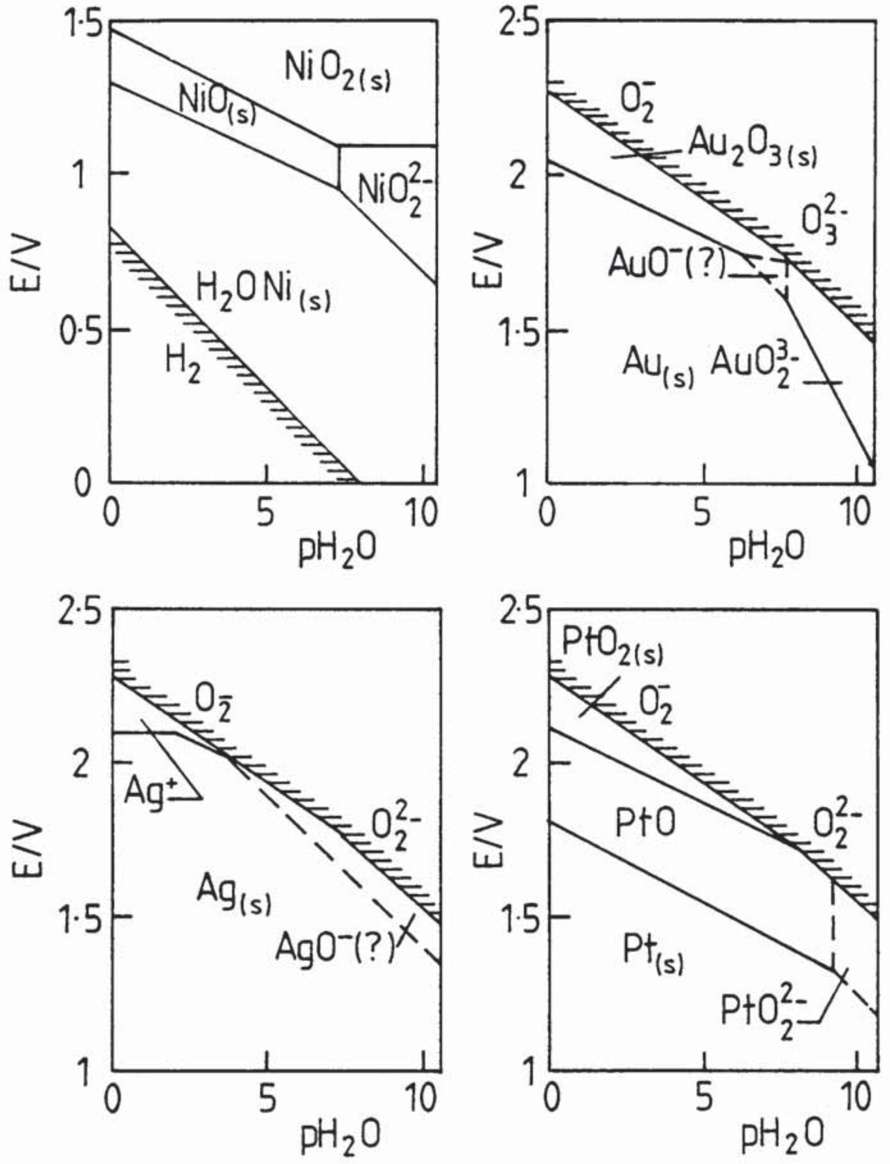

Figure 2-2 Pourbaix-type diagrams for various noble metals in molten (Na-K)OH at 500 K (according to Tremillon et al 4, 6-8)

Water would have a deleterious effect on the solubilization of Fe(III) oxides, except if introduced in large quantities (very acidic media), by the formation of FeO^+. Moreover, these authors have shown that water in this melt (acidic media) would significantly corrode iron by the formation of Fe^{2+} and hydrogen. These latter results, obtained by electrochemical methods (potentiometry and voltammetry), are in good agreement with those of Newman et al. (41) who followed the hydrogen evolution on Cr-Mo steels in molten hydrated NaOH in a temperature range 1030-1270K. Such kinds of predictions can be made for other temperatures and for other molten hydroxides from the thermochemical data calculations as shown by Doisneau and Tremillon (39,42) for LiOH, NaOH, KOH at various temperatures. These latter authors established the validity of such predictions through comparisons with some experimental determinations (43) and the main results were not found to be significantly different from those obtained in molten NaOH-KOH eutectic.

CHAPTER 3

The Electrochemistry of Pure Molten Hydroxides and Molten Hydroxides Containing Manganates

3.1 The electrochemistry of molten (Na-K)OH eutectic

The theoretical background to electrochemical techniques of analysis has been thoroughly reviewed by W.D. Read in his thesis (49) or it can be found in many other textbooks.

3.1.1 The electrochemistry of water and hydrogen in the molten hydroxides

In neutral or acidic melts water can be reduced either by the alkali metals or electrochemically, where the cathodic limiting reaction is hydrogen evolution. Palladium tube electrodes (50) were used in studying the water reduction, where the limiting current was controlled by the diffusion of hydrogen through the metal walls. Rotating platinum wire electrodes (19, 38, 31) were also widely used in these studies.

For the electrode reaction:

$$2H_2O + 2e^- \rightleftarrows H_2 + 2OH^- \qquad (3\text{-}1)$$

the $H_2O/H_2(g)$ electrode reaction appears to be voltammetrically reversible on platinum in NaOH-KOH at 500°K, and linear plots of potential against $\log[(i_L - i)^2/i]$ are obtained. The potential of the waves measured shifts to more anodic values as the water concentration decreases, as expected from the Nernst relation. Platinization of the platinum does increase the height of the hydrogen oxidation wave, but the water reduction wave does not appear to be affected. When relatively large amounts of Na_2O

added to dehydrate the melt, the reduction of water was preceded by another process, (22). This process, which occurs at a potential of about 1V lower or more anodic than the reduction of water, is probably the reduction of superoxide ions (coming from the dismutation of peroxide present as an impurity in the added Na_2O) according to the reaction, (20):

$$O_2^- + 2H_2O + 3e^- \rightleftarrows 4OH^- \qquad (3\text{-}2)$$

This coreduction wave for H_2O and O_2^- appears to limit the cathodic potential excursions. The peak current for the direct reduction of water in NaOH-KOH eutectic at 170°C at stationary platinum micro-electrodes is directly proportional to the concentration of water, (51) The partial pressures of oxygen and water vapour also influence the voltammetric responses at platinum, gold, silver, nickel and iron electrodes in the hydroxide melts (52). Thus, the anodic dissolution of platinum is enhanced in the presence of water, whilst water is directly reduced. The standard states for the water/hydrogen couple are a 1 mole/l solution for water and the gas at 1 atm pressure for hydrogen.

In his thesis, Goret (32) reports a standard potential value of 0.78 ± 0.05V (versus a "standard sodium" electrode) at $pH_2O = 0$, for the reduction of water, deduced from the $E_{\frac{1}{2}}$ value of reaction (3-1) and most probably refers to the couple $H_2O/H_{2(soln)}$. Subsequently, Tremillon (53) determined a value of 0.82V, versus the same reference, on the basis of a potential vs. pH_2O diagram, and this value is explicitly attributed to the couple $H_2O/H_2(g)$.

The interdiffusion coefficient of water in molten, equimolar NaOH-KOH has been evaluated (22) by chronopotentiometry between 193 and 263°C. Water was introduced indirectly by the addition of silica. Silica reacts with molten hydroxides according to (38):

$$SiO_2 + 4OH^- \rightleftarrows SiO_4^{4-} + 2H_2O \qquad (3\text{-}3)$$

The stoichiometry of this reaction can be verified by titrating the liberated water with sodium oxide. The water reduction potential on a platinum electrode was found to be equal to -0.815 ± 0.02V vs. a cu/cu(I) reference electrode, on the evidence of chronopotentiometric data. After conversion to the "sodium" reference scale, the value reported was practically coincident with the value given by Goret. The standard potential value; based on $[H_2O] = 1$ mol kg^{-1} and $P_{H_2} = 1$ atm. was found to be equal to 1.04V with respect to a standard sodium reference electrode. This value explains why the reduction of hydroxide ions can never occur since, taking into account the autodissociation constant value ($10^{-12.5}$), the standard potential of the corresponding reaction:

$$2OH^- + 2e^- \rightleftarrows H_2 + 2O^{2-} \qquad (3\text{-}4)$$

would be equal to:

$$E_1^o = E_o^o + \frac{RT}{F} \log K_A \qquad T = 227°C \qquad (3\text{-}5)$$

where all the notations have its usual meaning.

$$E_1^o = E_o^o - 0.1\ pK_A \qquad (3\text{-}6)$$

therefore

$$E_1^o = 1.04 - 0.1 \times 12.5 = -0.21V \qquad (3\text{-}7)$$

and this value is more negative than that of sodium ions, so no hydrogen evolution can be observed because solvent cations are more easily reduced than OH^- itself. Another consequence is that dissolving Na or K in this melt does not produce the strongest basic medium, since the pO^{2-} value corresponding to a zero potential value for the hydrogen electrode is $pO^{2-} = 2.1$.

When metallic Na is added to acidic melts, water is consumed (19) according to the reaction:

$$2H_2O + 2Na \rightleftarrows H_2 + 2Na^+ + 2OH^- \qquad (3\text{-}8)$$

and the hydrogen produced can react with the excess metallic sodium to form sodium hydride. NaH may then undergo an oxidation process (following the oxidation of the residual sodium) according to the reaction:

$$2NaH \rightleftarrows 2Na^+ + H_2 + 2e^- \qquad (3\text{-}9)$$

This reaction was also observed when metallic Na was added to a hydrogen-containing anhydrous melt. In basic melts, hydrogen is not formed electrochemically, and the limiting cathodic reaction is alkali metal deposition. Additionally, cathodic evolution of hydrogen was obtained by electroreduction of ammonia dissolved in the melt according to:

$$NH_3 + e^- \rightleftarrows \tfrac{1}{2} H_2 + NH_2^- \qquad (3\text{-}10)$$

Water cannot be oxidized in molten NaOH-KOH since oxide or hydroxide ions (according to the pO^{2-} value) are easier to oxidize to peroxide and superoxide species, (19, 31, 83). Results obtained either with thermochemical data or with experimental determinations by Doisneau and Tremillon (42) on other alkali hydroxides (particularly for pure NaOH), are in good agreement with those given above.

Potential data in both strongly acidic solutions of $pH_2O = 0$ and in strongly basic solutions of $pH_2O = 10.5$ (corresponding to an oxide concentration of 0.1 molar, the greatest oxide concentration achievable experimentally) are given in table 3-1.

Couple	E^o_M (Na), V (pH_2O, 0)	E^o_M (Na), V (pH_2O, 10.5)	Comments
$H_2O/H_2(g)$	+0.78	nonexistent	Reversible
O_2^{2-}/O^{2-}	nonexistent	+1.50	Reversible
O_2^-/O^{2-}	nonexistent	+1.62	Calculated
O_2^-/O_2^{2-}	nonexistent	+1.75	Reversible
$O_2(g)/O^{2-}$	nonexistent	+1.78	Thermo-dynamic Calculation
O_2^-/OH^-	+2.27	nonexistent	Voltametric estimate
$O_2(g)/O_2^-$	+2.33	+2.33	Calculated

Table 3-1 Hydrogen and Oxygen Potentials in Molten Hydroxides

3.1.2 The nature of oxygen species in the hydroxide melts

The equilibria and redox chemistry of oxygen in molten alkali hydroxides are complex because they depend on the acidity of the melt. Most of the information available is from a voltammetric study at a rotating platinum electrode, (20). In anhydrous molten NaOH-KOH between 450 and 500°C, chemical as well as electrochemical data indicate that free O^{2-}, O_2^{2-}, O_2^- and dissolved oxygen are in equilibrium and they have limited ranges of stability in solution. The pourbaix diagram of the melt-Oxygen system is shown in Figure 3-1. This diagram is based on the work of Tremillon and co-workers. Antropov and Tkalenko (54) produced similar diagrams for the NaOH-O_2 and KOH-O_2 systemsat 427°C using published thermochemical data. The various oxygen species are discussed below in the order of their oxidizing power.

i) Oxide

The oxide ion O^{2-} is the strongest base and reductant in hydroxide melts. It reacts with the acid water to give hydroxide ion according to the equilibrium:

$$2OH^- \rightleftarrows H_2O + O^{2-} \qquad (3\text{-}11)$$

whose equilibrium constant $[H_2O][O^{2-}]$, called here K_{OH}, has been calculated by Goret and Tremillon (20) from voltammetric data. They gave the value 11.5±0.7 for pK_{OH}. From this value it is clear that oxide ion is virtually nonexistent in acidic melts. Oxide can be added to the melt as Na_2O to give an oxide concentration of up to about 0.1 mol/l, such that the maximum practical

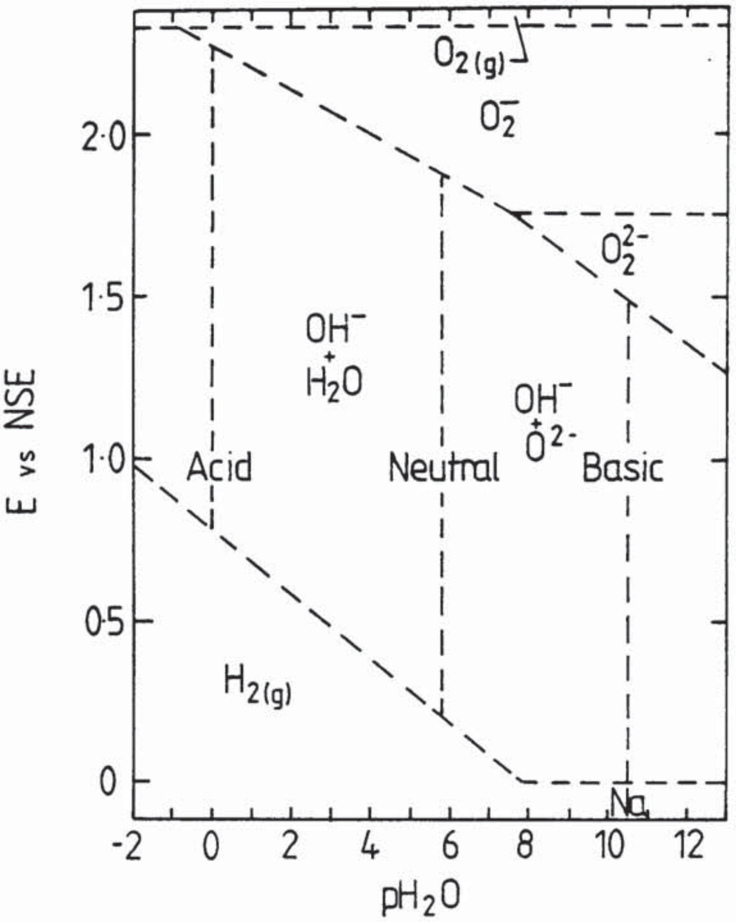

Figure 3-1 Pourbaix diagram for molten (Na, K) OH

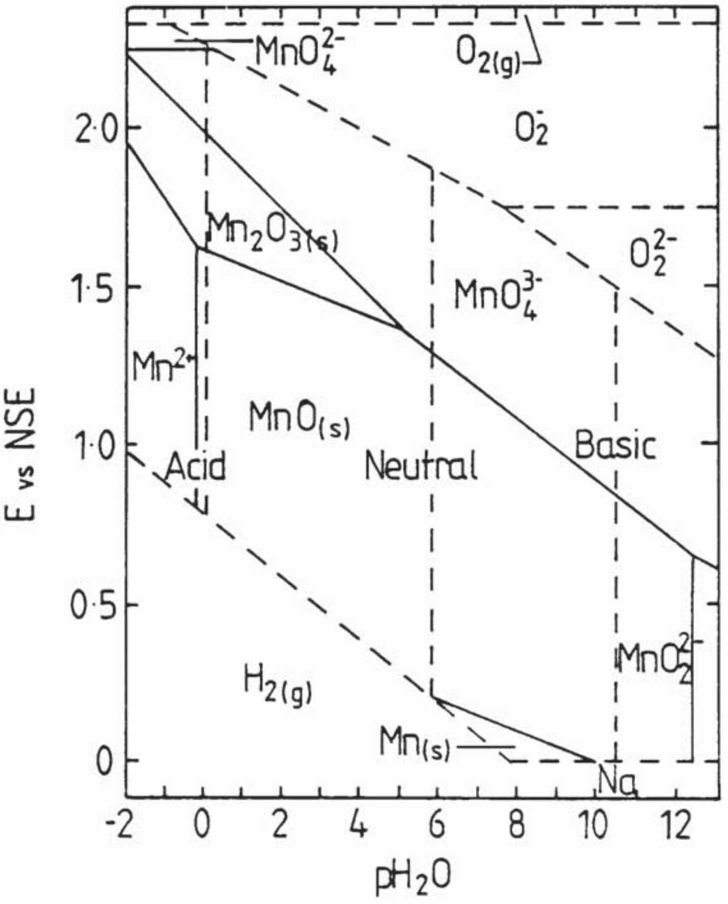

Figure 3-3 Pourbaix diagram for manganese in molten (Na, K) OH

value of pH_2O in the melt is about 10.5. In basic melts, oxide ion is not reducible but can be oxidized. The oxidation is generally to peroxide ion, and can be carried out anodically at a rotating platinum electrode (20) or chemically with oxygen gas (in which case oxidation continues to superoxide ion if the oxygen is present in excess):

$$2O^{2-} - 2e^- \rightleftarrows O_2^{2-} \qquad (3\text{-}12)$$

$$O_2^{2-} - e^- \rightleftarrows O_2^- \qquad (3\text{-}13)$$

ii) Peroxide

The peroxide ion, like oxide, is stable only in basic melts, in which it is generated by dissolution of sodium peroxide or by anodic oxidation of oxide. It reacts quantitatively with water and decrease in the limiting current of the peroxide oxidation wave is observed on the addition of small amounts of water to a melt containing peroxide leading to the generation of superoxide:

$$3\,O_2^{2-} + 2H_2O \rightleftarrows 4OH^- + 2O_2^- \qquad (3\text{-}14)$$

which may further react with water to liberate oxygen. Peroxide ion added as the slightly soluble Na_2O_2 is reduced to oxide rapidly on a nickel oxide electrode but more slowly on platinum. The O_2^{2-}/O^{2-} couple is therefore reversible, and Goret and Tremillon gave its standard potential as +1.40 ± 0.05V against the NSE at pH_2O of 11.5.

Since the electrochemical reduction is:

$$O_2^{2-} + 2e^- \rightleftarrows 2O^{2-} \qquad (3\text{-}12)$$

the potential changes by 100 mV/pH_2O unit and is +1.50±0.05V at a pH_2O of 10.5 (see table 3-1).

Peroxide can also be quantitatively oxidized to the superoxide ion by oxygen gas or anodically at the rotating platinum electrode. The resulting superoxide ion is easily reducible to peroxide at the same electrode and appears voltammetrically reversible. From these oxidation and reduction curves Goret and Tremillon (20) calculated the standard potential of the O_2^-/O_2^{2-} couple to be +1.75V against the NSE at a pH_2O of 11.5. The precision, although not given, is probably ±0.05V. The reduction is independent of pH_2O, being:

$$O_2^- + e^- \rightleftarrows O_2^{2-} \qquad (3\text{-}13)$$

and the potential is therefore unchanged at +1.75V at a pH_2O of 10.5. The thermodynamics of the Pt/O_2 electrode in fused NaOH has been discussed by Krueger et al. (52) in terms of the controlling reaction:

$$O_2 + 2e^- \rightleftarrows O_2^{2-} \qquad (3\text{-}15)$$

While their data cannot be compared quantitatively with the values given above, the general trend is similar.

In the same context, Lux et al. (36) reported that peroxide is formed by oxygen in fused NaOH and in fused KOH while superoxide is also formed in KOH (and to an even greater extent in RbOH and CsOH); the reactions depend on the partial pressures of both oxygen and water vapour.

iii) Superoxide

The superoxide ion is stable in basic melts (see the phase diagram of the KO_2-KOH system in Tsentsiper et al. (55) where it can be reduced reversibly to peroxide, as discussed above and further to the oxide ion:-

$$O_2^- + e^- \rightleftarrows O_2^{2-} \qquad (3\text{-}13)$$

$$O_2^{2-} + 2e^- \rightleftarrows 2O^{2-} \qquad (3\text{-}12)$$

In acidic melts the reduction is to hydroxide:

$$O_2^- + 2H_2O + 3e^- \rightleftarrows 4OH^- \qquad (3\text{-}2)$$

The superoxide ion is not oxidized to oxygen, it reacts with water according to:

$$4O_2^- + 2H_2O \rightleftarrows 3O_2(g) + 4OH^- \qquad (3\text{-}16)$$

but the equilibrium constant is unfavourable except at high local concentrations of superoxide or water.

In acidic melts the observed evolution of oxygen on oxidation at platinum electrodes can be explained on this basis. The standard potential of the O_2^-/OH^- couple was estimated to be +2.27 at a pH_2O of 0.0.

Although the potential of the O_2^-/O^{2-} couple cannot be directly measured, its standard potential in basic solution, +1.52 ± 0.07V at a pH_2O of 11.5, can be calculated from the standard potentials already cited. The potential is pH_2O dependent and its value at a pH_2O of 10.5 would be +1.62V.

iv) Oxygen gas

Couples involving oxygen gas cannot be measured directly owing to the peroxide and superoxide intermediates. Indirect thermodynamic calculations by Eluard and

Tremillon (4) employing the measured potentials of nickel and nickel oxide couples and the free energy of formation of NiO at 500K, which is -193.01 KJ/mole (-46.13 Kcal/mol) permit the calculation of the standard potential of the $O_2(g)/O^{2-}$ couple at a pH_2O of 11.5; the value is +1.72V. The potential changes by 50mV/ pH_2O unit and is therefore +1.78V at a pH_2O of 10.5. The standard state of oxygen is the gas under 1 atm. pressure.

Using this value of the standard potential of the $O_2(g)/O^{2-}$ couple, the standard potential of the $O_2(g)/O_2^-$ couple was calculated, and it is a highly oxidizing +2.33V ,which is more positive than the value +2.27V for the O_2^-/OH^- couple at a pH_2O of 0; this indicates that oxygen evolution should not be possible on oxidation in the melt, although the unfavourable potential is so small that it is in fact easily overcome.

The older studies by Agar and Bowden (29), which indicate that the mechanism of oxygen evolution in fused NaOH is different in melts described here as acidic and basic, are of interest in this regard,although quantitative thermodynamic data are not given in them. Afanasev and Gamazov (56), studying the platinum reference electrode in fused NaOH, found its potential to vary with oxygen partial pressure.

3.2 Reference electrodes used in molten hydroxides

The construction of a suitable reference electrode in fused hydroxide melts is not a simple problem. Although it would be desirable to have an electrode whose potential was fixed by the fixed activities of components of the melt itself, such as the aluminium reference in fused chloroaluminates, this is not possible in hydroxide melts.

All reference electrodes require an isolation compartment that prevents mixing of the electrolytes in the two half-cells but permits electrolytic contact. Teflon compartments with holes drilled in the bottom or with the bottom closed by a porous graphite disk can serve this purpose. Metal compartments are not useful for isolation purposes since insulators must be used.

The Na(I)/Na(O) couple can serve as a useful electrode only in basic melts, since sodium metal reacts with water in acidic melts. Moreover, the activity of metallic sodium is difficult to fix because the metal is soluble in the melt. Nor can it safely be assumed, even in basic melts, that only sodium and not a sodium-potassium alloy is being deposited on cathodization, or that the potential does not involve a sodium-electrode metal alloy.

An equilibrium Na(I)/Na(O) reference has not been attempted in this melt, nevertheless, Goret and Tremillon (20, 31, 38) have been able to use this couple as a voltammetric reference. Voltammetric curves can be compared (±50 mV) by superimposing the limiting anodic or cathodic potentials.

In basic melts the limiting cathodic process is alkali metal deposition. If the soluble alkali metal has the concentration 1.0 mol/l and is entirely sodium, a Na(I)/Na(O) couple is thereby defined and this can therefore be used as a reference electrode. The standard states are as follows: sodium ion, the actual state of Na(I) in the melt, which is fixed by the melt composition; and sodium metal, a 1.0 mol/l solution in the melt. The potential of this electrode is taken to be exactly 0.0V and it is called the normal sodium electrode (NSE), following Tremillon. This electode is more suitable for voltammetric work than for potentiometric studies.

Kern and Bloch (44) studied the half-cell Au(O)/ $Au_2O_{3(saturated)}$ in NaOH-KOH and suggested its use as a reference electrode. They employed a gold electrode, the potential of which is probably determined by the gold (III) - gold couple and is given as +1.550 V with respect to a hydrogen electrode, in excellent agreement with the work of Goret and Tremillon. The reference half-cell, Fig.3-2 (A) consisted of an impervious alumina tube with its bottom closed with a porous graphite disc, and the top with a cork bung. The electrode was a gold wire immersed in an NaOH-KOH eutectic that contained gold oxide inside the alumina compartment. The Au_2O_3 was obtained by extensive anodization of the gold electrode in weakly basic melts. The electrode was apparently indifferent to the presence of nitrogen, hydrogen, oxygen or water vapour in the atmosphere above the melt. Although water vapour probably does

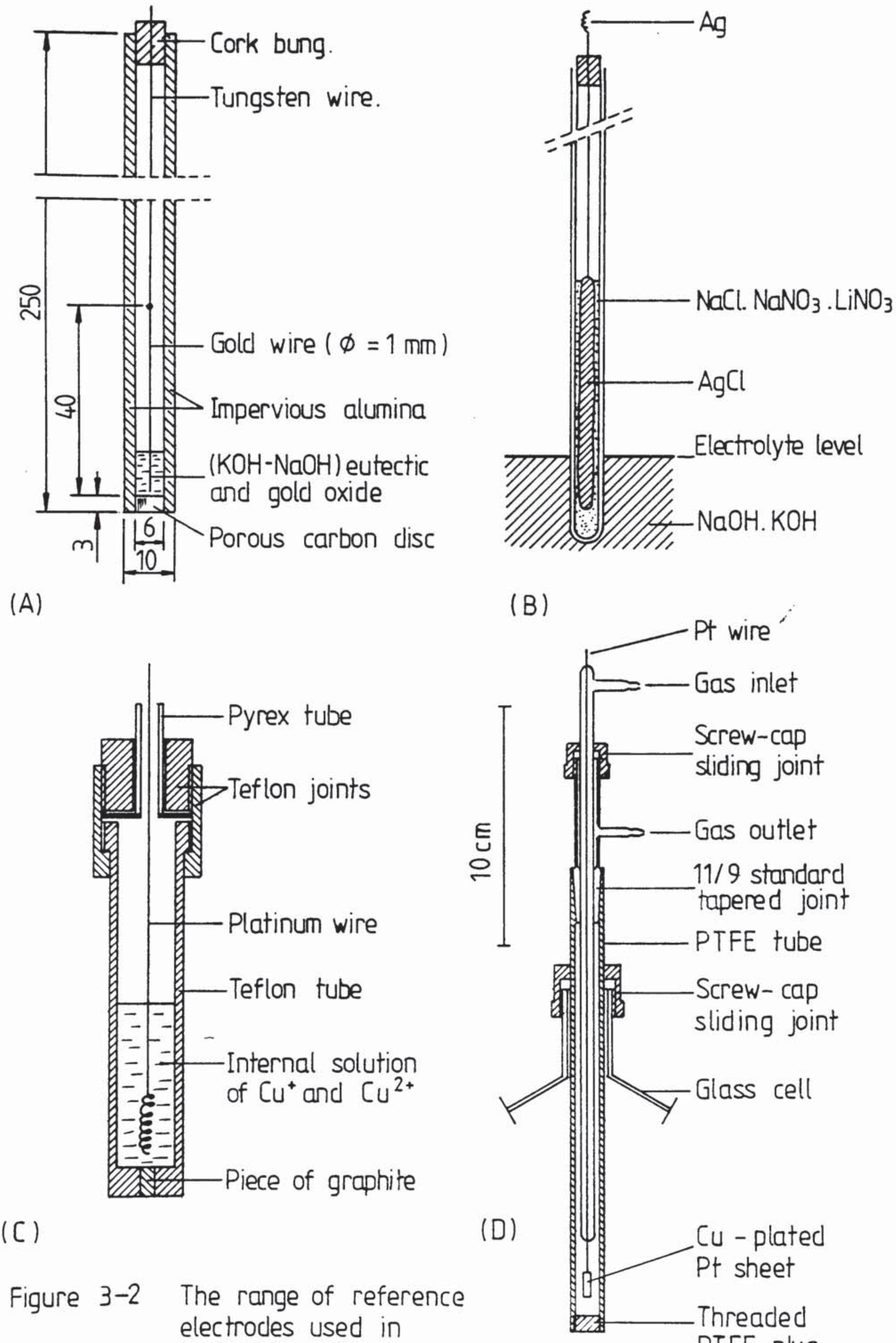

Figure 3-2 The range of reference electrodes used in hydroxide melts.

have a significant effect, the conditions were not specified in detail. The electrode was tested by measuring the half wave potential of the water reduction wave in (Na-K)OH eutectic at 300°C, using a gold wire working electrode. The melt was flushed continuously with Argon gas to reduce the water concentration in the melt.

It was found that the half-wave potential of the water reduction was not changing with time and its value was very close to the theoretical value calculated using the Nernst equation.

The reversibility of the half-cell was tested by micropolarization. Two identical half-cells were dipped in the same melt at 400°C, and a potential difference of 200 mV was imposed upon the two electrodes. The electrode returned to its equilibrium potential in a short time when the circuit was disconnected. At current values lower than the gold oxide diffusion limiting current, the current-potential curve was appreciably linear, so Kern and Bloch claimed that their reference half-cell was reversible, reproducible, stable and nonpolarizable within the temperature range (200°C - 500°C). Bonnemay et al. (45) proposed the use of the reference electrode Ag/AgCl(S) in $NaCl-LiNO_3-KNO_3$.

The Ag-AgCl electrode was immersed in a chloride-nitrate solution contained in an alumina tube, Fig. 3-2 (B). Apparently the idea of this half-cell was based on the well known, silver-silver halide half-cell used mainly in aqueous solutions (46), where the electrode has a solid phase in the form of sparingly soluble salt (here AgCl with a melting point of 455°C) in equilibrium with a saturated solution of this salt participating in the electrode reaction. This type of electrode is normally prepared by an anodically formed AgCl layer on the silver wire. The characteristics of the half-cell were studied by setting up the following cell:

$$\mathrm{Ag_I\,AgCl}\left|\begin{array}{l}\mathrm{NaCl}\\ \text{conc.}X_I\\ \text{dissolved in}\\ \text{molten nitrate}\end{array}\right|\begin{array}{c}\text{the alumina}\\ \text{junction}\end{array}\left|\begin{array}{l}\mathrm{NaCl}\\ \text{conc.}X_{II}\\ \text{dissolved in}\\ \text{molten nitrate}\end{array}\right|\mathrm{AgCl\ Ag_{II}}$$

where X is the mole fraction of NaCl:

$$X_{NaCl} = \frac{nNaCl}{n(NaCl)+n(NaNO_3)+n(LiNO_3)} \qquad (3\text{-}17)$$

The NaCl concentration in compartment II was kept constant while it was varied in compartment I by varying the amount of NaCl dissolved in the molten nitrate, thus the electrode potential of the second half-cell (compartment II) was fixed and the electrode potential of the first half-cell (compartment I) was measured for each NaCl concentration change in that compartment. The measured value of the potential difference was then compared with the theoretical value calculated at 330°C, and it was found that the measured value agreed with the theoretical value for the concentration range of $X_{NaCl} = 5\times10^{-3}$ to $X_{NaCl} = 5\times10^{-2}$. The reproducibility, stability, reversibility and nonpolarizabili of the half-cell were tested and proved to be satisfactory.

Goret and Tremillon (20) suggested a half-cell based on copper, Pt/Cu(II), Cu(I) in NaOH-KOH, Fig. 3-2(C), and employed this as a potentiometric reference electrode in an acidic (hydrated) medium. This half-cell has however, a limited range of applicability, owing to the use of a porous graphite plug to establish electrolytic contact with the experimental solution. So the above authors found it more convenient to use the half-wave potential of the superoxide-peroxide couple to establish the origin of the potential scale in voltammetric measurements. The accuracy of the potential values determined in this way is reported as ±30mV.

More recently, Schiavon et al.(47) proposed a reference half-cell based on the copper(I) - copper couple. This couple was chosen in view of the independence of its potential on the concentration of water in a relatively wide range and was preferred to the Cu(II) - Cu(I) couple mainly because the concentration of one species only needs to be fixed in order to determine its potential. All the parts of the reference electrode in contact with the melt were made of PTFE, Fig. 3-2 (D) and the electrode was a copper-plated platinum sheet, supported by a Pyrex tube which acted also as a gas inlet. A solution of known Cu(I) concentration was prepared by dissolving Cu_2O in (Na,K)OH melt. This half-cell stability, reproducibility and reversibility were also tested and proved to be satisfactory.

A platimun quazi-reference electrode was used by Wiaux and Claes (48) in their studies of the electrochemical behaviour of nitrate and nitrite ions in the molten

(Na,K)OH eutectic, where all potential values were referred to the cathodic limit of the solvent.

The half-cells $Au/Au_2O_3(s)$ in NaOH-KOH and Ag/AgCl(s) in $NaCl-LiNO_3-KNO_3$ have the advantage of not being directly responsive to the pH_2O of the melt as do others, but it was reported that the half-cell $Au/Au_2O_3(s)$ in NaOH-KOH potential is dependant on the pO^{-2} of the unhydrated (basic) melt. Unfortunately, no extensive measurements using either the Ag/AgCl or Cu(I)/Cu(O) reference electrodes appear to have been made. Moreover, it should be pointed out that the reference electrodes Au/Au_2O_3 and Ag/AgCl apparently were not actually tested in molten hydroxides.

3.3 <u>Oxidation states of manganese in molten hydroxides and concentrated aqueous alkaline solutions</u>

In his thesis, W.D. Read (49) reviewed the reactions of compounds of manganese in molten alkali nitrates and nitrites as well as in molten hydroxides. The stabilization of compounds of manganese, and the influence of the cations Na^+ and K^+ on the oxidation states of manganese in molten nitrates were also reviewed. It is interesting that hydroxide added to nitrate melts containing manganates stabilizes Mn(V) and/or Mn(VI) depending on the added hydroxide concentration. The main reference for the reactions of compounds of manganese in molten hydroxides is the French paper by Eluard and Tremillon (7). A translation of part of that paper appeared in the thesis mentioned above. However, a short review of the Eluard and Tremillon paper is essential. Using the electroanalytical technique of voltammetry with a rotating disk electrode for analysis, they performed experiments on manganates in molten (Na-K)OH at 500K. They found that the equilibria of manganates in the melt was a function of the water concentration present in the melt, they therefore carried out experiments in acidic, slightly acidic/ neutral and basic solutions.

3.3.1 Acidic (hydrated) melts

In acidic melts Mn(II), Mn(III) Mn(V) and Mn(VI) were found to exist. Manganese metal reacts with water quantitatively to give Mn(II) with evolution of hydrogen:

$$Mn(O) + 2H_2O \rightleftarrows Mn^{2+} + 2OH^- + H_2 \qquad (3\text{-}18)$$

the solution obtained was colourless. Upon oxidation of such solutions at a nickel electrode, a brown precipitate of Mn_2O_3 is formed:

$$2Mn^{2+} + 6OH^- \rightleftarrows Mn_2O_3 + 3H_2O + 2e^- \qquad (3\text{-}19)$$

The same process can be carried out chemically, since oxygen takes Mn(II) solutions to Mn_2O_3; however, after prolonged treatment with oxygen the precipitate redissolves as blue manganate ion, MnO_4^{3-}, which contains Mn(V). The manganate solutions can also be prepared by addition of permanganate to the melt, which oxidizes it with reduction to Mn(V):

$$3MnO_4^- + 8OH^- \rightleftarrows 3MnO_4^{3-} + 2O_2^- + 4H_2O \qquad (3\text{-}20)$$

or by oxidation of the dioxide MnO_2. Under an atmosphere of oxygen the solutions of Mn(V) are partially oxidized to Mn(VI) as the ion MnO_4^{2-}; a wave appears at about +2.25V against the "sodium electrode", corresponding to the reduction of MnO_4^{2-}. The dioxide MnO_2 is unstable in these melts, disproportionating to MnO_4^{3-} and Mn_2O_3(s):

$$4MnO_2 + 6OH^- \rightleftarrows Mn_2O_3 + 2MnO_4^{3-} + 3H_2O \qquad (3\text{-}21)$$

and MnO_4^{3-} is reduced to Mn_2O_3 by addition of Mn(II) as $MnSO_4$:

$$2MnO_4^{3-} + 4Mn^{2+} + 2OH^- \rightleftarrows 3Mn_2O_3 + H_2O \qquad (3\text{-}22)$$

The addition of MnOOH to the melt precipitates Mn_2O_3, showing that the solubility of MnO^+ in the melt is negligible.

In slightly less acidic melts, MnO precipitates from solutions of Mn(II). When an acidic melt containing Mn(II) ions was dehydrated, a brown precipitate of MnO was found and the existence of the following equilibrium was suggested:

$$Mn^{2+} + 2OH^- \rightleftarrows MnO + H_2O \qquad (3\text{-}23)$$

and when K is defined as: $K = \dfrac{[H_2O]}{[Mn(II)]}$

pK is about 1.6. From this and the other experimental data (5), the solubility of Mn(II) at a pH_2O of 0.0 is about 6.3×10^{-1} mol/l, and at a pH_2O of -0.9 it is about 5 mol/l. These data are consistent with the reported corrosion of manganese (21) in NaOH.

3.3.2 Basic (oxide) Melts

Manganese metal reacts with basic melts to give the slightly soluble manganese (II) oxide, (MnO), which in very basic melts goes into solution as MnO_2^{2-}. Introduction of

Mn(III) or Mn(IV) as Mn_2O_3 or MnO_2 gives a blue solution characteristic of the MnO_4^{3-} ion:

$$3Mn_2O_3 + 7O^{2-} \rightleftarrows 4\ MnO_2^{2-} + 2MnO_4^{3-} \qquad (3\text{-}24)$$

The addition of permanganate ion MnO_4^-, gives the blue MnO_4^{3-} and peroxide ion, which has been identified voltammetrically. The standard potentials in basic solution, at a pO^{2-} of 0.0 or a pH_2O of 11.5, are +2.25V for the couple MnO_4^{2-}/MnO_4^{3-}; about +1.84V for the couple $MnO_4^{3-}/MnO(s)$; +1.03V for the couple $Mn_2O_3(s)/MnO(s)$; +0.64V for the couple MnO_4^{3-}/MnO_2^{2-}; and -0.08V for the couple MnO(s)/Mn(O). These values are given in Table 3-2, and the Pourbaix diagram for manganese is shown in Fig. 3-3. For more details about the voltammograms and its interpretation it is necessary to refer to the original paper (7) or its translated version in (49). The electrochemical redox reactions of manganates in the melt are shown in Table 3-3.

Qualitative manganese studies have been done in other hydroxide melts (57-59). Lux and Niedermaier (36) used a spectrophotometric technique in the analysis of manganate equilibria in molten NaOH at temperatures of 533K, 583K and 633K. They found that at these temperatures Mn(V) was the stable oxidation state of manganese regardless of the oxygen and water pressure above the melt in the gas phase. In molten KOH using the same technique and temperatures they found that Mn(VI) was also present. The amount of Mn(VI) in equilibrium with Mn(V) was found to decrease with increasing temperature, but increase with increasing O_2 or H_2O pressure above

Couples	E^{o}_{M}(Na),V (pH_2O,0)	E^{o}_{M}(Na),V (pH_2O,10.5)	Comments
MnO(s)/Mn(0)	Nonexistent	about 0.0.	Mn reacts
Mn(II)/Mn(0)	+0.505	Nonexistent	Mn reacts
MnO_4^{3-}/MnO_2^{2-}	Nonexistent	+0.64	Voltammetric
Mn_2O_3(s)/MnO(s)	+1.03	Nonexistent	Voltammetric
Mn_2O_3(s)/Mn(II)	+1.585	Nonexistent	Voltammetric
MnO_4^{3-}/MnO(s)	Nonexistent	1.74	Voltammetric
MnO_4^{2-}/MnO_4^{3-}	+2.25	Nonexistent	Voltammetric

Table 3-2 Manganese potentials in molten hydroxides

Acid melt

$$MnO_4^{2-} + e^- \rightleftarrows MnO_4^{3-}$$

$$2\,MnO_4^{3-} + 5H_2O + 4e^- \rightleftarrows Mn_2O_3(s) + 10OH^-$$

$$Mn_2O_3(s) + 3H_2O + 2e^- \rightleftarrows 2Mn^{2+} + 6OH^-$$

Slightly acidic/neutral melt

$$2MnO_4^{3-} + 5H_2O + 4e^- \rightleftarrows Mn_2O_3(s) + 10OH^-$$

$$Mn_2O_3(s) + H_2O + 2e^- \rightleftarrows 2MnO\ (s) + 2OH^-$$

Basic melt

$$MnO_4^{3-} + 3H_2O + 3e^- \rightleftarrows MnO(s) + 6OH^-$$

$$MnO(s) + H_2O + 2e^- \rightleftarrows Mn(s) + 2OH^-$$

Very Basic melt

$$MnO_4^{3-} + 2H_2O + 3e^- \rightleftarrows MnO_2^{2-} + 4OH^-$$

Table 3-3 Electrochemical Redox Reactions of Manganates in (Na-K)OH Eutectic the melt. Quantitative analysis of their results indicated that O_2 is reduced to superoxide.

Carrington and Symons (60) studied the structure and reactivity of the manganese oxyanions MnO_4^-, MnO_4^{2-} and MnO_4^{3-} in concentrated alkaline aqueous solutions.

The manganate systems were analysed using U.V. visible spectrophotometry, together with electrode potential measurement of the couples MnO_4^-/MnO_4^{2-} and MnO_4^{2-}/MnO_4^{3-}. From their results and observations they proposed several possible reactions of the manganese oxyanions. The differences between NaOH and KOH were accounted for in terms of the effect of the metal cation. They found that the potentials measured in NaOH were consistently higher than in KOH and that the reactivity of the manganese ions was also much higher in NaOH than in KOH. Galus et al.(61) studied the influence of the ionic strength, pH and nature of the background electrolyte and its concentration as well as the influence of the electrode material on the electrode kinetics of the two couples mentioned above, using cyclic voltammetry and the rotating disk electrode method of analysis.

CHAPTER 4

Experimental Equipment

4.1 Equipment layout

The basic experimental equipment layout is shown in Fig.4-1, in the form of a simplified block diagram. The diagram shows the system used for the oxidation of an organic vapour by a stabilized oxidation state of manganese in molten (Na-K)OH eutectic. In Fig.4-2 is a photograph of the front of the rig. In the following sections each major part of the experimental equipment will be described in detail.

4.2 Nitrogen purification system

The nitrogen purification system used in this work for the removal of oxygen and water, was designed and used by W.D.Read in his work (49), but it was necessary to regenerate the oxygen and water removal systems. The oxygen removal system consisted of two copper columns containing copper turnings at 573 K. Oxygen was removed by the passage of nitrogen through these two copper columns, in which the oxygen reacts with the copper turnings to form copper oxide. This system was regenerated by passing hydrogen at 723 K through the copper turnings, to make sure that the copper oxide was reduced back to copper. The water removal system consisted of a column containing a 4A molecular sieve, at the exit gas end of which was positioned a section of self-indicating silica gel. This system was regenerated by removing the molecular sieve

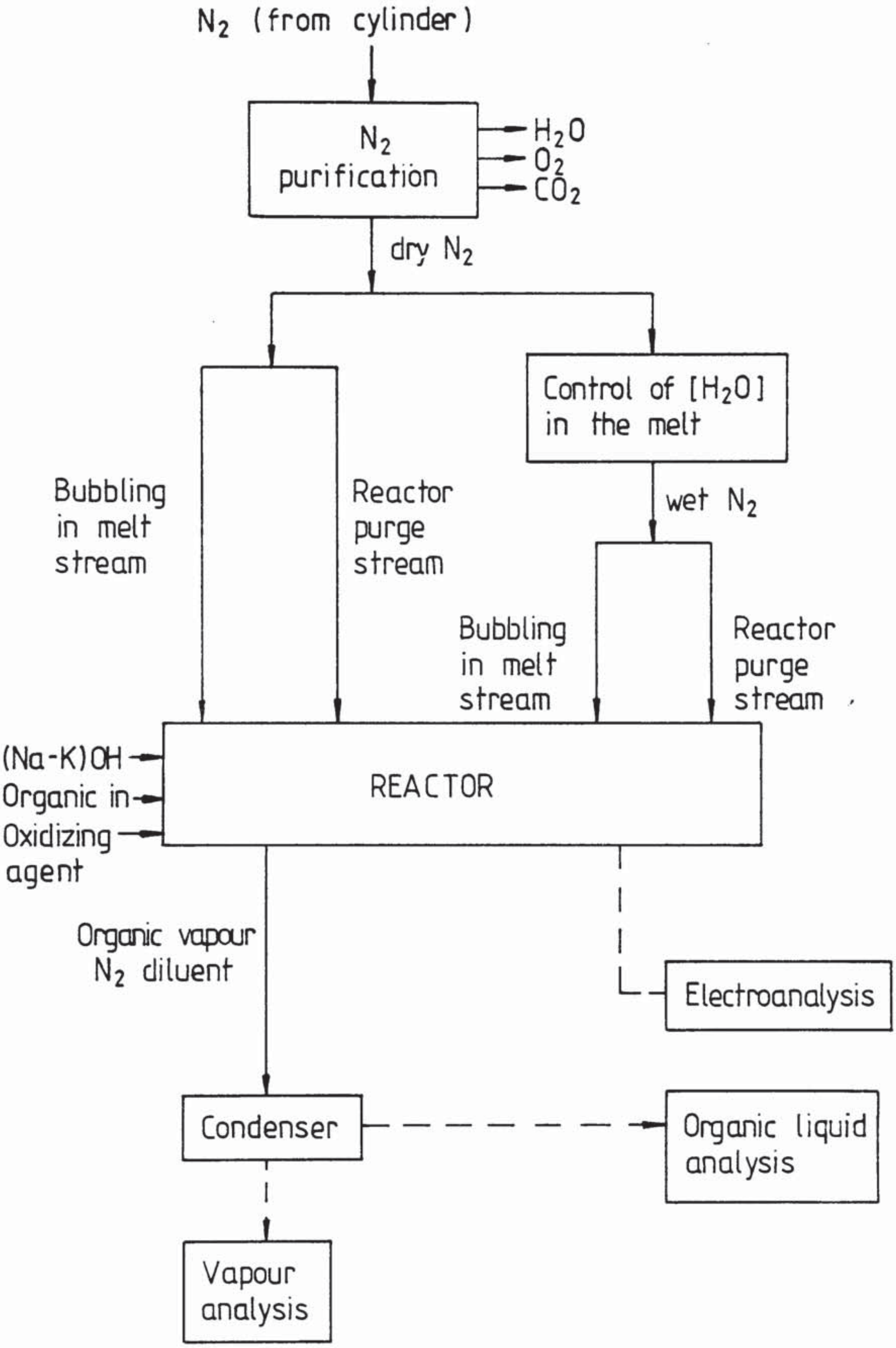

Figure 4-1 Block diagram of equipment for the oxidation of organic vapours in molten salts.

Figure 4-2

Experimental Rig

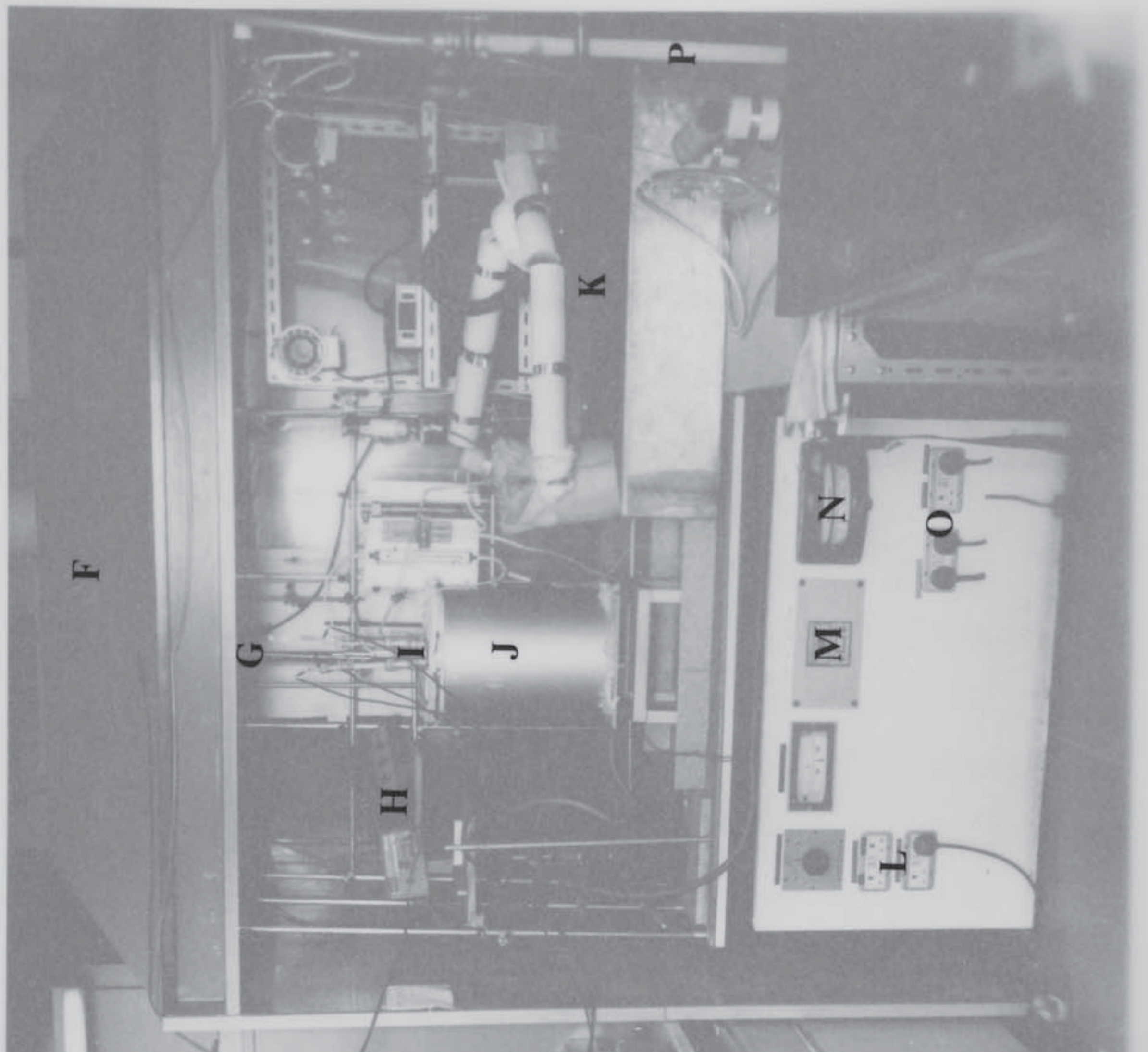
A
B
C
D
E
F
G
H
I
J
K
L
M
N
O
P

and the silica gel from the column and placing it in an oven for several hours at 373 K to drive off the water. They were then returned to the column ready for use. Another unwanted impurity in "white spot" nitrogen is carbon dioxide, since it reacts with molten hydroxides. The removal of carbon dioxide was carried out simply by the passage of nitrogen through a column packed with sodium hydroxide pellets.

4.3 Reactor furnace and electrical control panel

The reactor furnace was also designed and used by W.D.Read, (49). It was controlled by an Ether Digi controller, positioned together with the temperature controller for the tubular furnace used in the nitrogen purification system, and a number of power sockets, on an electrical control panel, fitted underneath the main reactor table.

4.4 Reactor vessel

A diagram of the Pyrex glass reactor vessel used in the detailed organic reaction experiments is shown in Fig.4-3. The diagram shows the reactor with the electrode system present in the melt. The reactor was made up of three main parts, the reactor head, the reactor base, and the PTFE beaker positioned inside the reactor base. The reactor head had four B.10 sockets and two SQ24 screw thread sockets. Using the four B.10 sockets, the organic input tube, product output tube, nitrogen purge tube and indicator electrode were sealed into the reactor. Using

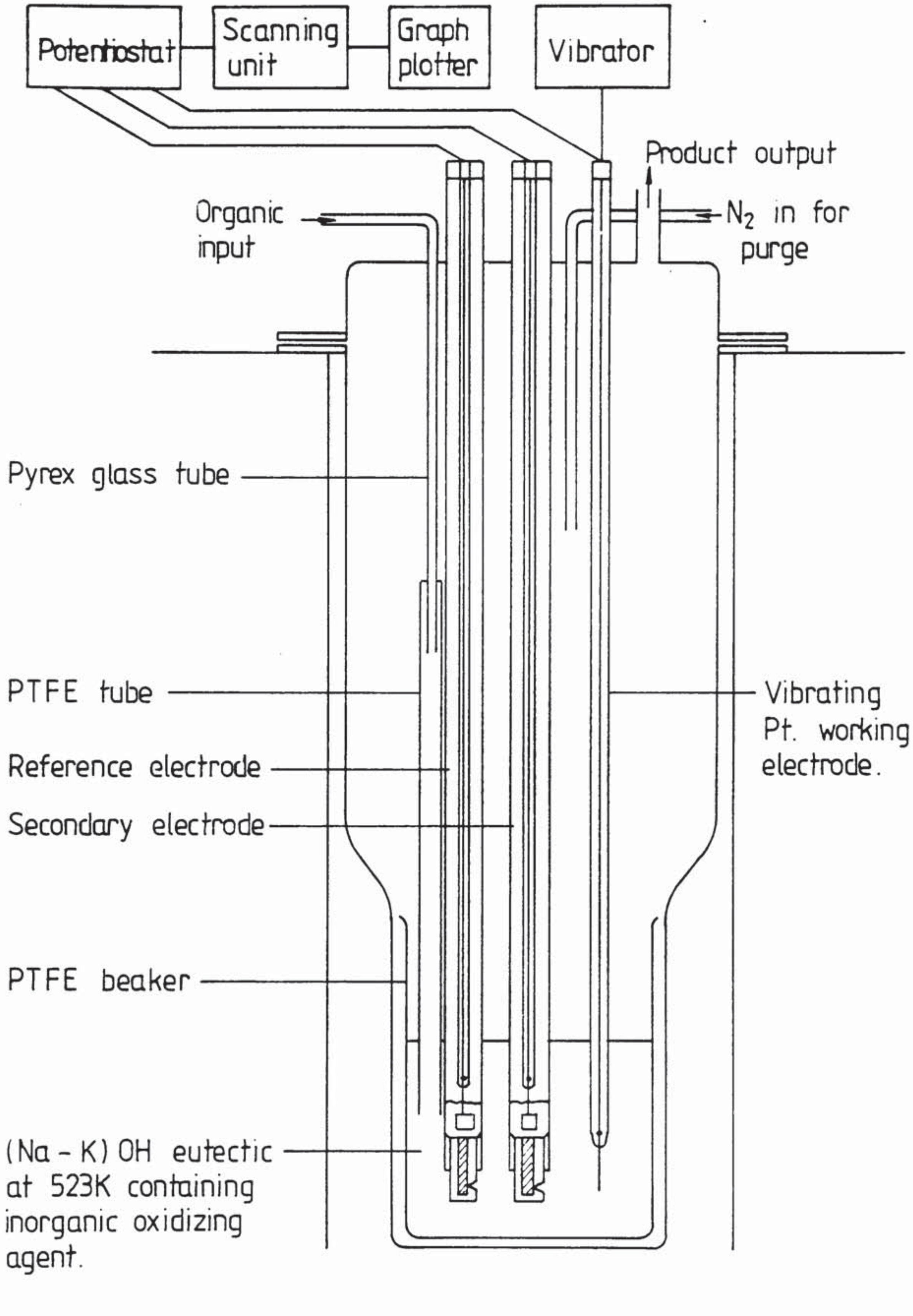

Figure 4-3 Reactor system.

the two SQ24 screwthread sockets, the reference and secondary electrodes were fitted into the reactor using QC 24/12 plastic caps and washers. The reactor base was 7.5cm i.d reduced to 5.5cm i.d, at its lower section for a length of 7.0cm so as to fit the o.d of a 100.0cc PTFE beaker. The thickness of the Pyrex glass used was 0.5cm, and the total length of the reactor was approximately 30.0cm. The reactor head and base were connected together by a ground glass flange of 12.0cm o.d. The reactor length was chosen so that the molten salt was positioned near the centre of the furnace where a steady temperature was maintained. The thermocouple was placed outside the reactor between the furnace and the reactor wall at a point where a constant difference between the set temperature and the temperature of the molten salt had been found. The reactor was supported on the top of the furnace by a stainless steel support ring, covered with Kao wool insulation. Fig.4-4 shows a photograph of the Pyrex reactor base and head, together with the vibrating indicator electrode, reference electrode, and secondary electrode.

Figure 4-4

Electrodes and Reactor Equipment

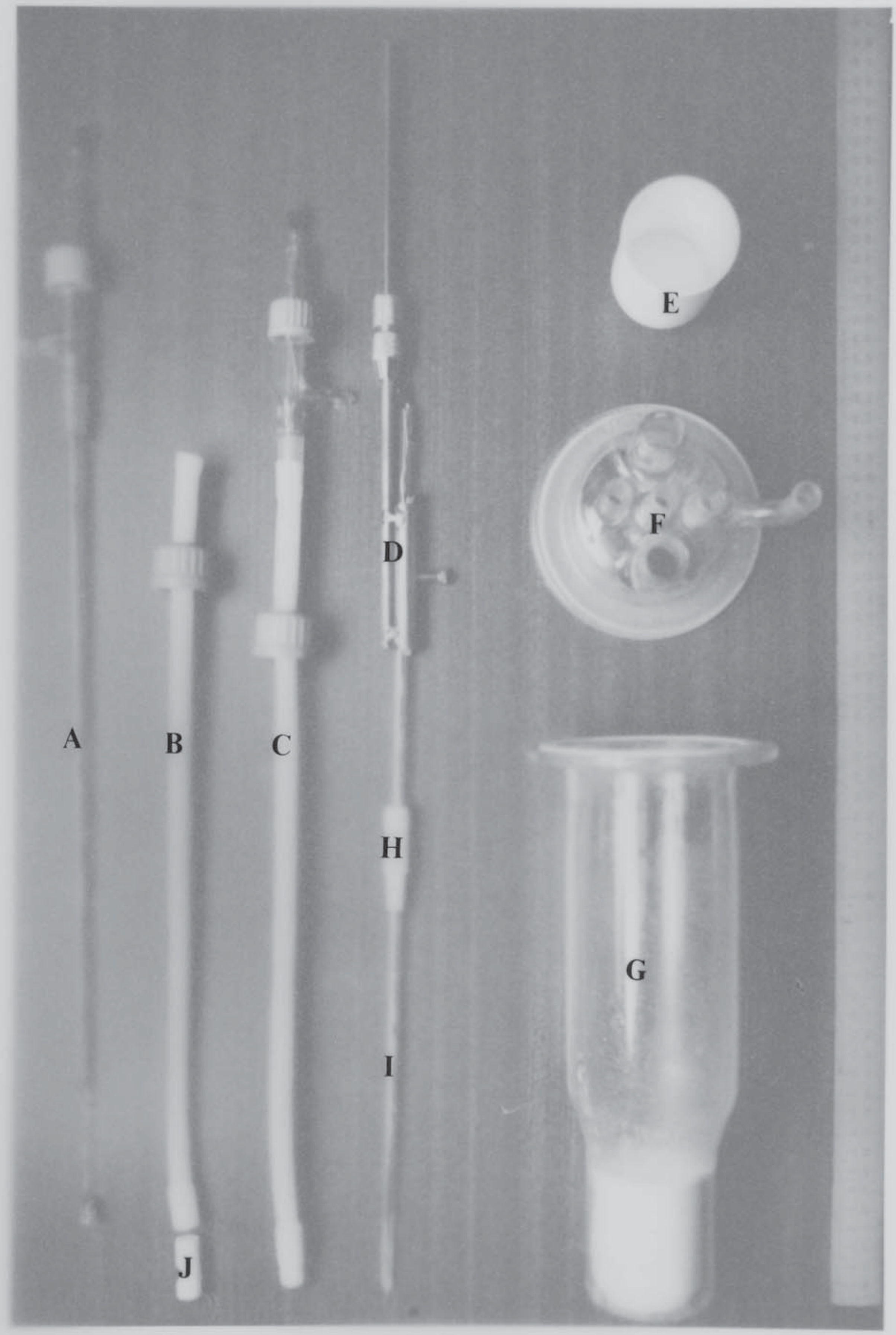
E
F
D
A
B
C
H
G
I
J

4.5 Organic feed preparation

A syringe pump made by Sage Instruments (Model 351) was used to inject the organic liquid feed from a 20cc glass syringe into the reactor via a 1mm i.d PTFE tube. The organic was admitted to the system as shown in fig. 4-5 in which dry O_2 - free N_2 was passed with the organic vapour into the reactor. The N_2 produced a steady stream of bubbles through the molten salt; the organic vapour was added dropwise to this stream as it entered the reactor head, becoming entrained, vaporized and then carried down the delivery tube into the molten salt. The syringe pump was capable of delivering the organic liquid at various flowrates ranging from 0.15 to 60ml min^{-1}. Various syringe sizes could be used in the range 5-100cc. Heating tapes used to prevent reflux in the reactor head and on the first section of the delivery lines to the condenser.

4.6 Condenser system

In preliminary experiments condensation of the organic vapour was simply performed using two Dreschel bottles immersed in ice and salt. However these proved to be inadequate so a more sophisticated condenser system was used, as shown in Fig.4-6. The Dreschel bottles were replaced by a single glass coiled condenser and the ice bath replaced by a chiller circulator system. This consisted of a Grants chiller-circulator employing

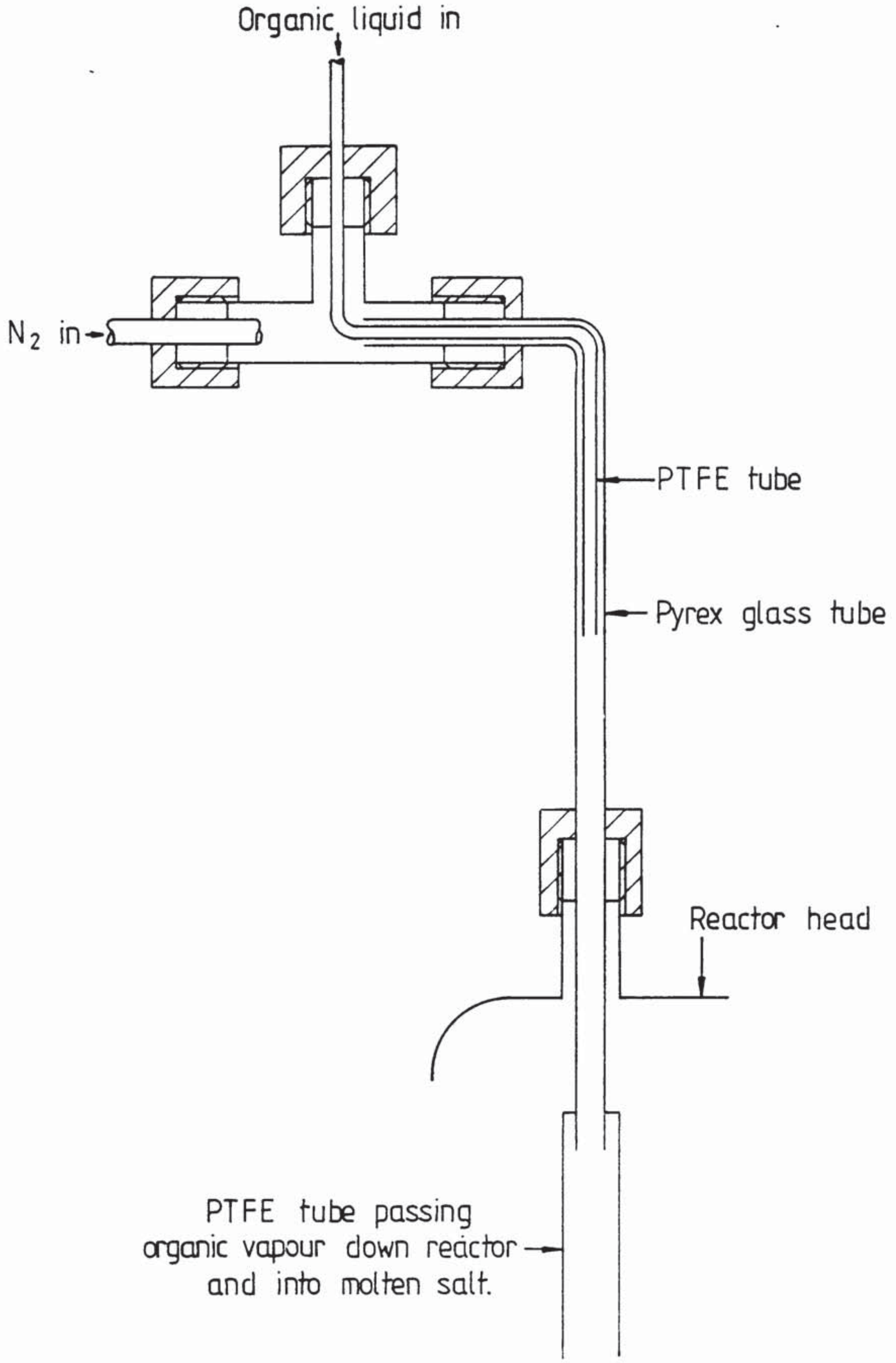

Figure 4-5 Equipment used for injection of organics.

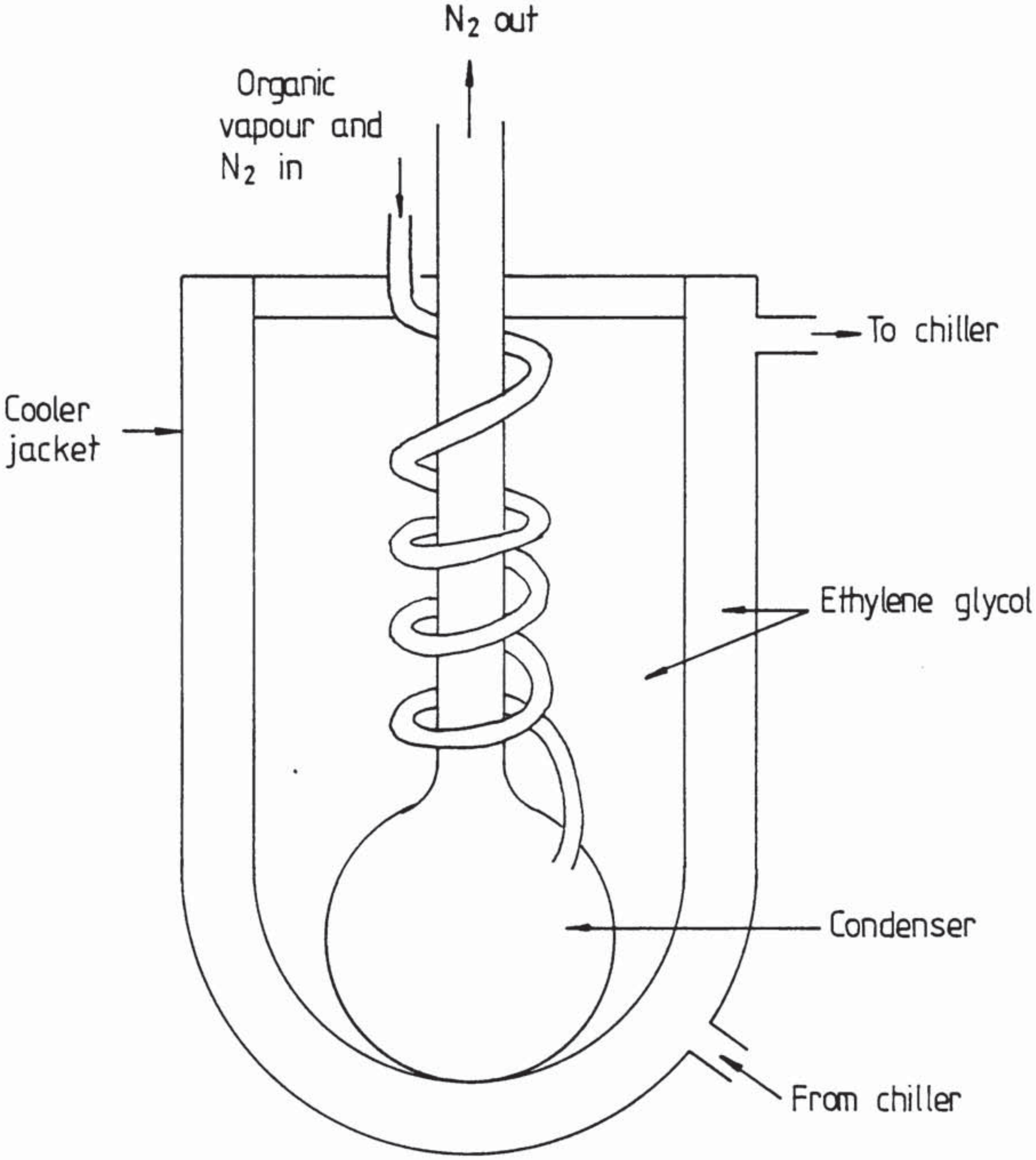

Figure 4-6 Condenser system

ethylene glycol in the form of Holts antifreeze as the coolant, which was connected to a constant temperature jacket, 10cm i.d, 12cm o.d and 25cm long through which the chilled ethylene glycol was circulated. The ethylene glycol was also placed in the inner section of the jacket, which was open to the atmosphere. Temperatures down to 258 K were easily obtained. Lagging with fibre glass insulation was employed to reduce heat gain. The condenser to reactor delivery line was made of glass tubing and connections were made by ball and socket fitments. Leak trays were used to collect any loss of the coolant from the condenser system.

4.7 Electronic equipment used for voltammetric studies

The electronic equipment consisted of a potentiostat, made by Hermes Controls Ltd. Model No.V40, series 200, a voltage sweep generator, also made by Hermes Controls Ltd. Model TWS-1 (triangular waveform synthesiser), an X-Y chart recorder made by Bryans, Model 2900, A3, a decade resistance box and a Philips digital volt meter.

A descriptive outline of the potentiostat controls, terminals and output specifications were all given in (49) as well as connections and setting up procedures.

The other equipment required no elaborate setting up and are simple in their operations, their specifications are also given in the same reference.

A simple wiring diagram of the voltammetric system is shown in Fig. 4-7.

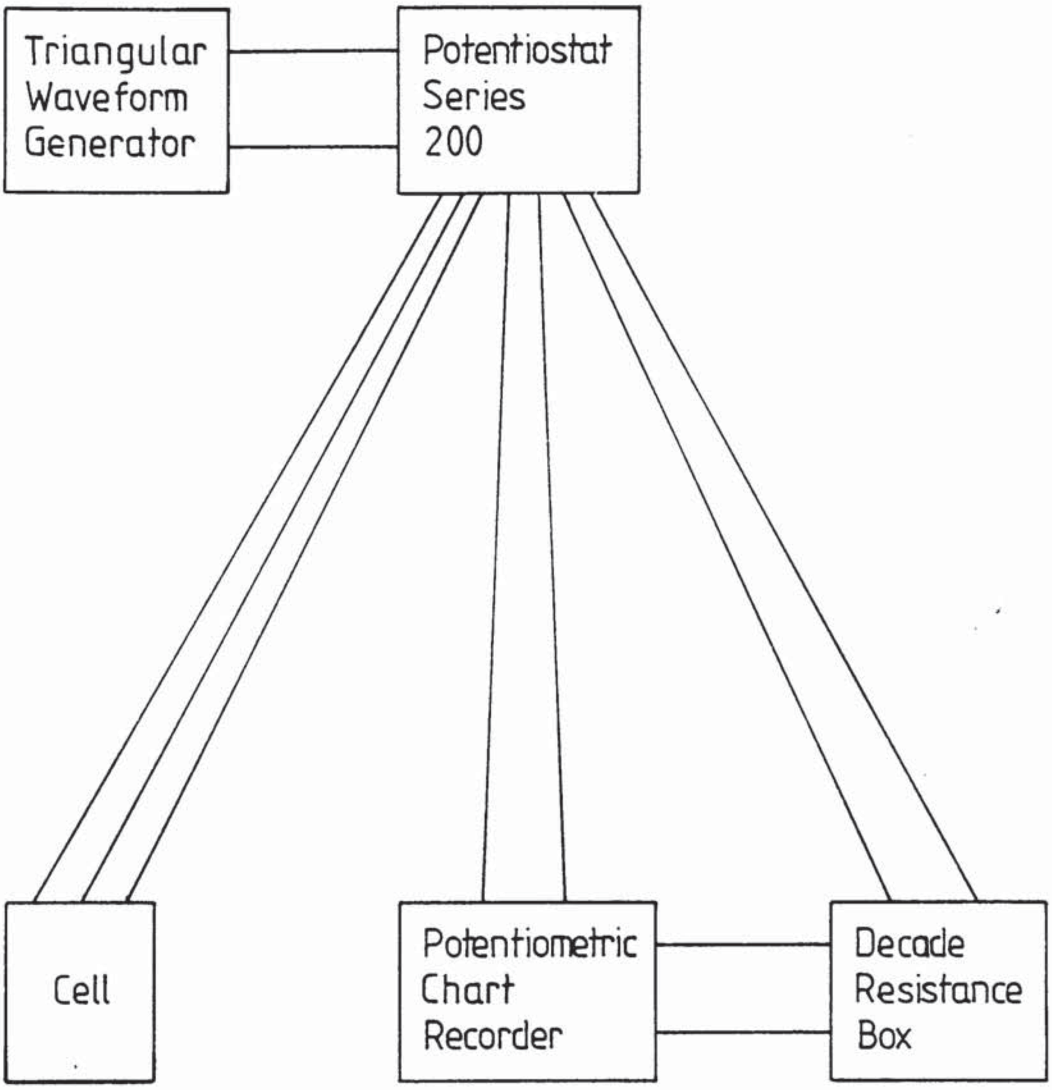

Figure 4-7 Simplified wiring diagram of voltammetric system.

4.8 Chemical analysis equipment

The main equipment used for chemical analysis of the reaction system was a series 204 Pye Unicam, gas-liquid chromatograph (G.L.C), a Centronic mass spectrometer and a thermobalance. Simple equipment such as PH - meters and laboratory glassware, were used for titrations and other standard analytical techniques.

The G.L.C was used for analysis of the condensed liquid product. It operated using either a flameionization detector system (F.I.D) or a thermal conductivity detector system (T.C.D). Both systems are capable of detecting 10^{-10}g/μl of sample and have a good quantitative response over a wide range. F.I.D responds to all compounds containing carbon and hydrogen and the response to different substances is closely related to their carbon content. Although it responds to most compounds, with chemicals such as formic acid and water the response is poor, so T.C.D was used instead for all samples containing water. T.C.D responds to any volatile material, simply on the basis of its difference in thermal conductivity from the carrier gas, but this detector is less sensitive than F.I.D.

The column selected was packed with Porapak N, which provided good separation for most organic chemicals and water. Liquid injection was performed using an S.G.E (Scientific glass engineers) syringe.

The amount usually injected was 0.5×10^{-6} ℓ (0.5μℓ).

The G.L.C output was recorded using a Philips PM 8251 single pen chart recorder, peak areas were measured using a Venture MKll digital integrator.

The setting up of the G.L.C was carried out using the carrier gas (Nitrogen for F.I.D and Helium for T.C.D) at a flow rate of approximately 50ml/min. This was measured at the gas exit end of the column using a bubble flowmeter. The flame of the F.I.D used a mixture of hydrogen and oxygen. The setting up of the instrument was relatively simple and is given stepwise in the manufacturer's handbook.

The organic product, usually $0.5\mu\ell$, was injected through a septum into the column. The main factors which affected the separation of the individual components of the liquid product were column temperature and the carrier gas flowrate. The injection region of the G.L.C was also capable of being heated so as to ensure that the liquid product entered the column as a vapour. The peak separation was optimized by the variation of column temperature using the oven and by variation of the carrier gas flowrate. The usual settings for temperature were 250°C for the injector, 250°C for the detector and 175°C for the column. A suitable attenuation was chosen to give the output peak heights within the recorder range. With the G.L.C satisfactorily set up the liquid product sample was injected several times until identical or reasonably similar peak areas and retention times for the liquid product components were obtained. Standard concentrations of various probable organic constituents of the liquid product were injected and if possible the major components of the liquid product were identified.

Standards of those major components were then made up and injected to confirm the G.L.C response was such that the peak area of the components was proportional to their concentration. Having confirmed this, in future experiments only two standards were made up, one at a higher concentration of the liquid product components and one lower. The constant of proportionality between peak area and concentration was calculated and hence the concentration of the component in the liquid product was found using its peak area and the constant of proportionality. The Centronic 200 M.G.A mass spectrometer was used for analysis of the gaseous product at the exit from the condenser. A full description of the mass spectrometer and its specifications are given in (49).

The use of the centronic mass spectrometer enables all the outout gases to be monitored simultaneously using an oscillographic display of the mass spectra. Concentration changes and new component appearances could be observed if in the mass range 0 to 200. It was also possible to record the results digitally, or on chart paper.

With the mass spectrometer the main standard used was simply laboratory air which was assumed to have its major components at concentrations in volume % of nitrogen 78, oxygen 21, carbon dioxide 0 and argon 1. Then having set up the machine, the usual method employed was to tune the mass spectrometer to the mass numbers of possible gaseous components such as nitrogen, oxygen, carbon dioxide and methane and by switching channels to record their concentrations. The mass spectrometer was then switched to full scan and the oscilloscope watched for anything new or unusual. If a new peak was obtained it was possible whilst still on the scan to find its mass number and hence its likely composition.

In measuring Henry's law constants for water in the molten eutectic system (Na-K)OH gravimetrically a Stanton-Redcroft recording thermobalance, sensitive to changes of 0.1mg or more, was used for the weight determinations. A detailed description of the experimental technique used in these measurements and the results can be found in (23)

4.9 The indicator electrode and its construction

Two types of micro-electrodes were used in the voltametric studies carried out, both were used as stationary and vibrating indicator electrodes. The first type was a platinum wire electrode which was used in the majority of the electrochemical experiments producing satisfactory results and reproducible voltammograms. It consisted of a 5.0mm o.d, 4.0mm i.d, 50cm long soda-glass tube, into which a 20 s.w.g tinned copper wire fused to a 0.5mm o.d platinum wire was inserted. The platinum was sealed into the soda glass at one end and a length of 1.0cm of the platinum wire was left protruding; a measured length of this wire (0.5cm) was then dipped into the melt. This provided a large effective electrode area and therefore the problems of electrode surface oxidation and the formation of an insulating film were minimised.

The vibrating solid micro-electrode used consisted basically of the solid stationary platinum micro-electrode mentioned above, modified to facilitate electrode vibration. The indicator electrode was clamped in a stainless steel connector which fitted into a vibro-mixer. The vibro-mixer was a standard vibrating stirrer model E1 made by Chemap. It consisted of a precision electro-magnetic vibrator incorporating variable amplitude adjustment. The vibro-mixer was restricted for use on mains frequency so was fixed at 50 cycles per second. The electrode to reactor connection seal was a simple PTFE B10 cone bored with a 7.0mm diameter hole. This allowed ± 1.0mm clearance for the irregularities in the glass tube diameter. The general arrangement of the electrode and vibrator can be seen in fig.4-3, showing the reactor system. The PTFE cone was a sufficiently good seal, since an inert atmosphere was to be maintained over the melt during experiments. The vibrating electrode system was clamped above the reactor, the B10 cone fitting into the reactor top.

Electrode height and positioning was possible by adjustment of the clamps.

The second type used was a Nickel electrode. This electrode was used to confirm some of the results obtained using the platinum wire electrode. The construction of the Ni electrode was the same as the Pt electrode except that the Pt wire was replaced by a thin nickel sheet, which was available in the laboratory, cut into a small 3.0 mm by 10mm rectangle, then sealed into the soda glass and the glass drawn out to a slight taper. The electrode was then ground flat. The two types of indicator electrodes are shown in Fig.4-8.

4.10 The reference and secondary electrodes and their construction

A quasi-reference electrode was found to be the only suitable reference electrode for use in molten hydroxides. The construction of both the reference and the secondary electrodestherefore, were the same. They consisted of a 12.0mm o.d, 10.0mm i.d thin wall PTFE tube with a length of 40.0cm. One end of the PTFE tube was closed by using a 12.0mm diameter, 3.0cm length PTFE rod. In order to ensure a seal, the PTFE tube had to be heated using a hot air gun, then the PTFE plug was inserted.

To establish the necessary electrical contact between the reference electrode and the bulk electrolyte without bulk mixing by diffusion, many methods were tried, (see Chapter 5).

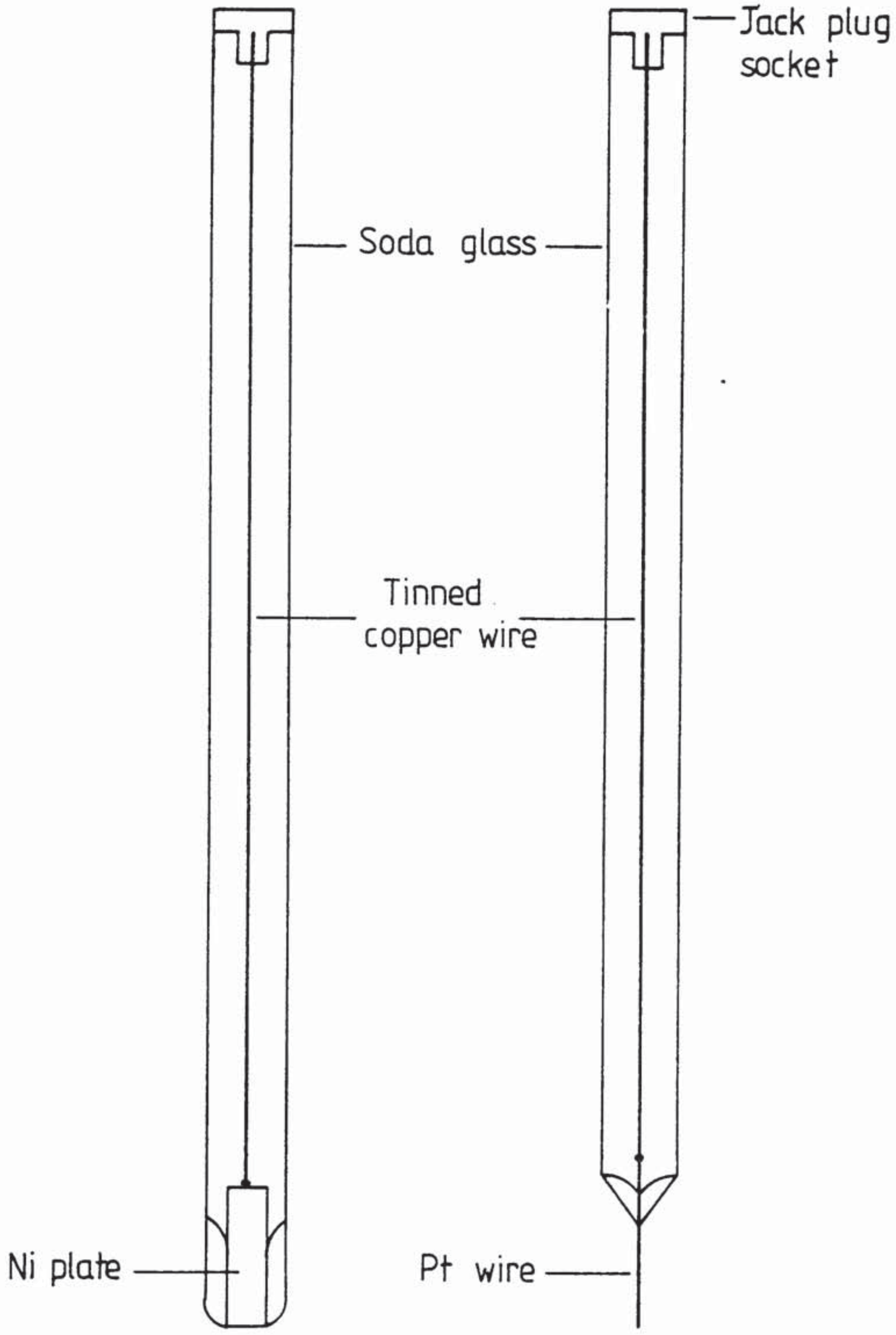

Figure 4-8 Indicator electrodes

Recrystallised alumina (Al_2O_3) was found to be the best material to provide electrical contact because of its stability in molten hydroxides and its properties of being porous and wettable by the melt. So a 3.0mm o.d, 2.5cm length of alumina tube was inserted into a 2.0mm diameter, 2.5cm long hole drilled into the PTFE rod, after heating it up, then a cut was made using a Stanley knife, to expose a small part of the alumina to the melt to enable the electrical contact to be established. The molten (Na-K)OH eutectic used in the bulk of the reactor was also used inside the PTFE outer compartment.

The inner electrode consisted of a Pyrex glass tube, 6mm o.d, 5mm i.d in which was sheathed a tinned copper wire of 20 s.w.g. To the copper wire was fused a 3.0cm long platinum wire 0.5mm o.d.

The platinum wire was then sealed into the glass at one end; the protruding platinum wire was fused to a $1cm^2$ platinum flag, cut from a very thin platinum sheet. This electrode then fitted into the PTFE outer compartment so that the platinum flag was immersed in the melt, using a tube with a standard tapered joint at one end and a screw-thread socket with a screw cap and washers at the other. These fittings were used to make a sliding joint, to fit the inner electrode into the PTFE outer compartment. The different parts of the electrode are shown in Fig.4-9. The three electrode system was initially tested in molten (Na-K)NO_3 eutectic, to ensure that the electro-analysis system was working properly and that the

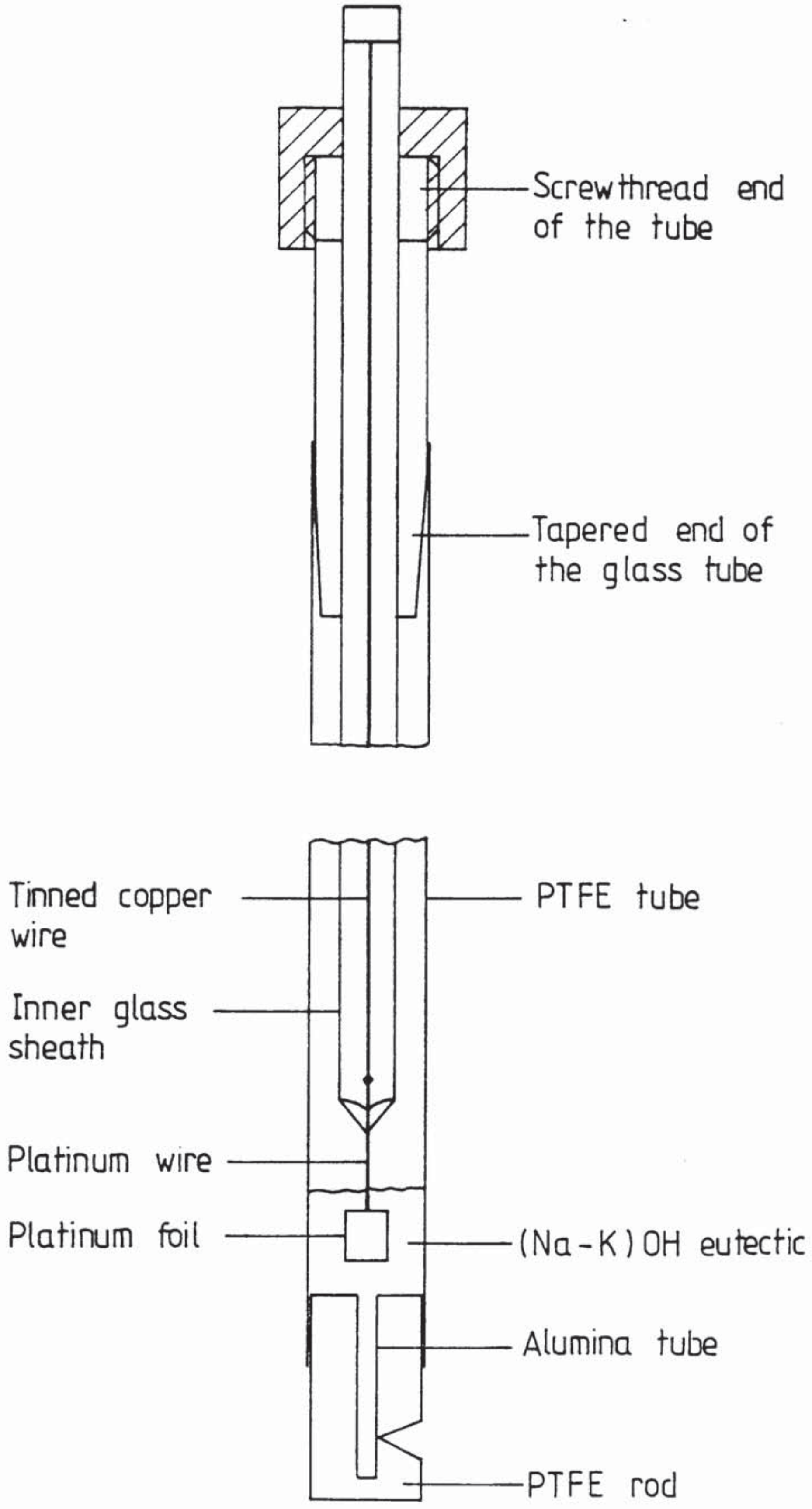

Figure 4-9 Reference and secondary electrodes. (Only one is shown because the electrodes are identical.)

voltammograms obtained were reliable. The usual voltammogram of the nitrate melt was obtained and it was similar to that obtained by several workers e.g. (87, 49).

4.11 Safety equipment

The main source of potential hazards in the experimental equipment and experimental chemical reactions are the following:

i. Explosive chemical oxidation reaction.
ii. Spillage of molten hydroxide.
iii. Unwanted additions to the molten hydroxide, e.g. water.
iv. Ignition of organic vapour.
v. Suck-back of condensate into the reactor.
vi. Electrical hazards : electrocution, sparks.
vii. Furnace overheating.
viii. Reactor inlet and outlet tube blocking during a chemical oxidation reaction.

Keeping these hazards in mind, the concentrations of the reactants were maintained at a level such that the safety equipment would be of sufficient volume to contain any explosion.

Using a tubular furnace, the explosion should be directed vertically rather than horizontally. A cone-shaped metal hood was available and this was positioned above the reactor close fitting to the furnace top. With the metal hood in place an explosion would be directed downwards through the furnace. At the bottom of the reactor a catch tray was placed to contain and minimise splashes of any molten salt, glass, etc. directed down through the furnace. The whole of the reactor assembly, furnace and condenser was positioned in a large fume hood constructed of plastic safety panels. The hood was open at the front for access, so a heavy duty movable safety screen was placed around the furnace and over the reactor. The fume hood extractor was operated during all experiments.

Personal safety equipment was also used. This consisted of a safety visor, safety spectacles, heat proof gloves and a laboratory coat. During the organic reactions a second person was present at a safer distance from the rig. In the event of an accident breathing apparatus, fire extinguishers, an eye bath, a body shower and first aid equipment were at hand. The rig design enabled easy shut-down. Since most of its components were electrical, a main junction box was incorporated which when switched off, switched off all the power to the rig, thus stopping the organic injection by the syringe pump, furnace heating, electrode vibration and nitrogen purification furnaces. The only remaining thing to be switched off was the nitrogen gas line, and nitrogen being inert, did not present a hazard.

CHAPTER 5

Electroanalysis of Manganates in Molten (Na-K)OH Eutectic

5.1 Preliminary Experiments

To obtain experience of working with molten salts in general, the initial experiments were carried out using molten (Na-K)NO_3 or mixtures of (Na-K)NO_3/(Na-K)OH rather than using (Na-K)OH alone, due to its corrosive nature and the difficulty of handling it. The preliminary experiments were performed whereby chemicals such as $KMnO_4$ were added to the melt at 523K, the melt was contained in a 50 cc PTFE beaker placed at the bottom of a Pyrex glass tubular reactor (6.0 cm o.d x 25.0 cm long). The Pyrex glass reactor head had six B.10 sockets, and the reactor head and base were connected by a ground glass flange of 8.5 cm o.d. The nitrate melt was 38.246 g of A.R. grade $NaNO_3$ and 55.61 g of A.R. grade KNO_3.

Voltammograms of nitrate melt containing high hydroxide concentrations >0.1M K/NaOH were obtained initially using the three electrodes system used by W.D. Read (49). New electrodes were constructed, the indicator electrode was a Pt wire sealed in soda glass tube and drawn into a taper ground flat end. The reference electrode was of the metal/metal ion type using Ag/Ag^+ couple. The secondary electrode was similar in construction to that of the reference electrode except that a Pt flag replaced the Ag electrode and no $AgNO_3$ was added.

Later on, the working electrode was modified to be more suitable for use in hydroxide melts Fig. 5-1 the Pt wire end of the glass electrode was drawn out into a

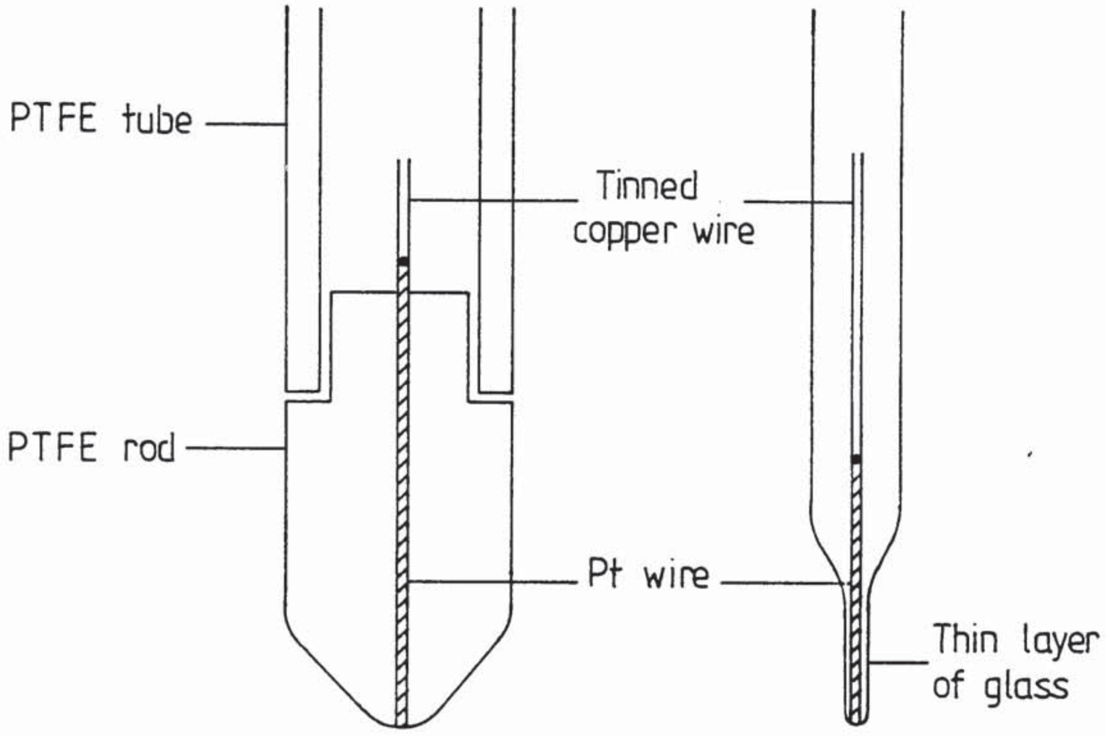

Figure 5-1 The working electrodes used in the preliminary experiments.

long taper with the minimum thickness that could just cover about 0.5 cm of the Pt wire, the electrode was then ground flat using 3F, 1F and 360-fine carborundum with glycerol on a perspex sheet, then 00 emery cloth moistened with glycerol. The resulting surface had a mirror-finish. The modified electrode provided a minimum contact between glass and melt. Soda glass was chosen because of its alkaline nature. Also the electrode was not to be left in the melt for more than the time required to obtain the voltammograms.

Arrangements were made so that only the tip of the electrode was immersed in the melt by using a milliammeter to observe the start of a current being passed between the indicator and the secondary electrodes. When the electrode was tested in hydroxide melt, the part immersed in the melt was corroded and chipped quickly, that made it impractical to use as more than one electrode was needed for each experiment. Another design also presented in Fig. 5-1 was constructed out of a PTFE tube and PTFE rod reduced in diameter to fit inside the tube; the rod was tapered at its free end and a fine hole (0.4 mm) was drilled at the centre of the rod, where a 0.5mm o.d Pt wire was pushed into it then the tip of the electrode was ground. When this electrode was tested in the melt, the PTFE softened by the heat and the melt climbed up the hole, giving an electrode without fixed area therefore this design had to be abandoned.

The only Pt working electrode design that gave satisfactory and reproducible results was the Pt wire electrode where a fixed length of the Pt wire (5.0 mm) was immersed in the melt (see section 4.9 for details). It was found that a working electrode with a smaller area was very easily coated with an insulating film of oxide or a precipitate especially in hydroxide melts containing $KMnO_4$ at potentials near the anodic end of the melt and when organic compounds were passed through the melt. As for the reference electrode development, PTFE tubes initially replaced the glass tubes of the Ag/Ag^+ reference electrode. The outer compartment was 7 mm i.d. PTFE tube,the inner electrode consisted of another PTFE tube 1 mm i.d, in which was sheathed a tinned copper wire, to this wire was fused a small length of Pt wire 0.5mm o.d. the junction Pt-tinned copper wire was pulled into the inner PTFE tube so that no contamination could take place. The protruding Pt wire was then fused to approximately 2 cm length of Ag wire 2 mm o.d. for the reference electrode and Pt flag for the secondary electrode. To establish electrical contact between the electrodes and the bulk electrolyte, many attempts were made: sintered PTFE plug, PTFE rod with a small groove at its side, PTFE tape wrapped alongside a solid PTFE plug, carbon rod plug with a groove at its side, PTFE plug divided into two halves and a carbon cloth sandwiched between the two halves, all these gave unsatisfactory results. In addition to that, a reference electrode based on the Ag/Ag^+ couple was found to be unsuitable for use in hydroxide melts due to the following reaction:

$$2Ag\,NO_3 + 2NaOH \rightleftarrows \underset{\substack{\downarrow \\ Ag.AgO\,\downarrow\ \text{black precipitate}}}{Ag_2O} + H_2O + 2Na\,NO_3 \qquad (5\text{-}1)$$

where the Ag^+ concentration could not be defined because it was not in solution. Other metal/metal ion reference half-cells were tested e.g. Ni/Ni^{2+} as $Ni/Ni(NO_3)_2.6H_2O$ or Ni/unhydrated $NiCl_2$ and Cu/Cu^{2+} as Cu/CuO. The Ni salts dissolved in nitrate melt but reacted with hydroxide melt forming a black precipitate. The CuO did not dissolve in nitrate melt while it dissolved in hydroxide melt forming a deep blue solution. A reference electrode design used in hydroxide melts by G. Bombi et al.(47) was tested next. It consisted of a reference half-cell based on the Cu/Cu^+ couple, several problems were met in testing this reference electrode in hydroxide melts. In order to obtain Cu^+ ions Cu_2O was dissolved in the melt, but these ions were oxidized straight away to Cu^{2+} ions even under N_2 gas atmosphere. The threaded PTFE plug used in the original design to establish electrical contact between the melt solution inside the reference electrode compartment and the bulk melt failed to do so probably due to the problem of finding the right pitch size of the threads as it was not mentioned in the original paper even though ten different pitch sizes were tested. If it was large obviously the melt would leak through from the reference electrode compartment into the bulk melt and if it was small, gases or solids produced by chemical or electrochemical reactions inside or outside the electrode could easily block it. To overcome these problems many techniques were tried e.g. sucking the melt from the bulk melt into the reference electrode compartment; N_2 gas was blown into the reference electrode compartment to get rid of any trapped gases in the threads; maintaining a N_2 gas atmosphere inside the reference electrode and in the reactor, etc.

Eventually alumina tube was used (see section 4.10 for details) and it gave satisfactory results as far as the necessary electrical contact was concerned.

The first few experiments carried out were based on the industrial methods of $KMnO_4$, K_2MnO_4 and K_3MnO_4 production (89). The aim of these experiments was to investigate the possibility of oxidizing MnO_2 added to a nitrate melt containing high concentrations of K/NaOH by bubbling oxygen into the melt, and the expected reactions are:

$$2MnO_2 + 2KOH + O_2 \rightarrow 2KMnO_4 + H_2 \qquad (5-2)$$

or $$2MnO_2 + 4KOH + O_2 \rightarrow 2K_2MnO_4 + 2H_2O \qquad (5-3)$$

the ratio of $KOH:MnO_2$ was varied in the range 10:1 to 50:1. The main observations were that at low ratio and bubbling oxygen for several hours $KMnO_4$ was produced, which was detected by the purple colour of the melt, while at high ratio the formation of K_2MnO_4 and/or K_3MnO_4 was detected by the bluish-green colour of the melt.

The preliminary experiments provided useful practical experience of working with molten (Na-K)OH and in constructing the electrodes. With this knowledge the apparatus and an experimental procedure were developed and then used in the electroanalysis of manganates in molten (Na-K)OH.

5.2 Experimental Procedure

Electroanalysis of manganates in molten (Na-K)OH eutectic was performed using vibrating and stationary Pt wire electrodes with some confirmatory experiments using Ni electrodes. The electroanalysis cell consisted of a Pyrex tubular reactor with a detachable reactor head containing four B10 sockets and two SQ24 screw-thread sockets. Into the reactor via the sockets was placed the three electrodes system and an adjustable gas inlet tube which allowed gas to be bubbled into or above the melt. The remaining socket was left open when bubbling gas through the melt so that the gas could then escape. The reactor was positioned in the centre of a tubular furnace and maintained at 523K by an Ether "Digi" temperature controller. The system has been described in more detail in chapter 4.

The (Na-K)OH eutectic consisted of 49.04g of A.R. grade NaOH and 43.429g of A.R. grade KOH. These solids were placed in the reactor with the electrodes and gas tube, then heated in the furnace to 523K to give the required melt. The water concentration in the melt was monitored by passing dry, O_2-free N_2 through a Dreschel bottle containing NaOH solution, the concentration of NaOH solution was varied according to the required partial pressure of H_2O in the nitrogen at room temperature (approximately 20°C). The amount of H_2O dissolved in the melt was then calculated using Henry's law (23). A second Dreschel bottle was employed between the molten salt and the NaOH solution as a safeguard against suckback.

Using this method it was possible to vary the water concentration in the melt by bubbling saturated N_2 through it. Oxygen could be added to the melt in a similar way to nitrogen when required.

A water concentration of 1.0 Molar ($pH_2O=0$) was normally used although higher or lower pH_2O values were sometimes needed. The melt can thus be regarded as a "wet" melt; the melt was deliberately left wet as many of the organic reactions would produce water and the necessity of a dry melt for each chemical reaction in industry would be costly. With water present, the formation of O_2^{2-} and O_2^- would be prevented and this eliminates the possible formation of hazardous organic peroxides.

When the gas inlet tube was not being used to bubble gas through the melt, the tube was raised and connected to a system whereby a positive pressure of

N_2 could be maintained in the reactor. The system consisted of N_2 from the nitrogen purification system being passed into a glass test tube containing some water. Just above the entry of the N_2 line into the water a T-piece was inserted into the line and a connection from this then made to the reactor. The reactor was sealed by stoppering the remaining sockets. The reactor was normally reasonably gas tight and N_2 was forced to flow out through the water. The formation of bubbles of N_2 indicated that a positive pressure of N_2 was being maintained above the melt. This system was used rather than the simpler purge system as it was thought that N_2 flowing through the system might upset equilibria by diluting any gaseous components. The chemicals used in the form of solid A.R. grade were added through a SQ24 socket using a funnel fitted in a PTFE tube with a length that could reach the top of the PTFE beaker inside the reactor. In each addition N_2 was bubbled through the melt to increase mixing and aid solid dissolution. Voltammetry with a vibrating platinum electrode was performed using "forward linear sweeps"(f.s.) from positive to negative potentials and then "reverse linear sweeps" (r.s.) from negative to positive potentials. The sweep rate used was 9.6 $Vmin^{-1}$ and the scan range varied between 0.0 to +1.5V, the approximate electrochemical decomposition potential of the melt. The amplitude of the vibrating electrode in each experiment was kept constant and usually approximately 0.1 cm. The positive N_2 atmosphere also purged out the vibrating electrode's PTFE sleeve and so stopped any air unintentionally entering the system. Also a PTFE foam gasket was placed between the ground glass flanges of the reactor and reactor head as this gave a better seal.

Electroanalysis of the system after each chemical addition was performed using the vibrating Pt indicator electrode. Analysis of the voltammetric waves produced using the vibrating Pt indicator electrode was performed by applying the Herovsky-Ilkovic equation (H.I.E.) to ascertain whether the electrode réactions were reversible (and hence the number of electrons involved in the reaction) or irreversible. All potentials were measured relative to the cathodic limit of the solvent. The individual waves were identified by further confirmatory experiments. These included the use of cyclic voltammetry. In cyclic voltammetry a stationary electrode is employed in a quiescent solution. A potential scan is performed so as to reduce or oxidize the electrochemical species under study. The scan is then reversed and the products formed in the original scan, which have remained at the electrode surface since the solution is calm, are then respectively oxidized or reduced. Cyclic potential scans were carried out and peak potentials for the oxidized and reduced forms of the electrochemical species found. From these values it could be found whether the reactions were reversible and if so the number of electrons involved in the reaction or irreversible. With the results from the voltammograms obtained with the vibrating Pt indicator electrode and cyclic voltammogramsusing the stationary Pt wire indicator electrode the electrochemical reactions causing the voltammetric waves were postulated.

5.3 Pure (Na-K)OH Eutectic

Goret and Tremillon (20) investigated the chemical and electrochemical reactions in molten alkali hydroxides. Their work has been discussed in Chapter 3. The Pourbaix diagram of the melt and the various couples with their $E_{\frac{1}{2}}$ values were also presented in the same chapter.

In most of the experiments carried out in this work, a voltammogram of the pure melt was obtained before adding any chemicals, in order to compare these voltammograms with each other for the reproducibility of the various waves and to identify the adsorption waves if any. Also the difference between acidic and slightly acidic melts was studied. In Fig. 5-2 is presented a typical voltammogram of pure (Na-K)OH melt at 523K and $pH_2O = 0$, obtained using the vibrating Pt electrode, it is interesting that no significant difference between the voltammograms obtained using vibrating or stationary working electrodes was noticed.

The half-wave potentials were measured versus the cathodic limit of the solvent, which is the water reduction. The water reduction potential at $pH_2O = 0$ is 0.78±0.05V against the normal sodium electrode, thus voltammetric curves can be compared, ±50mV, by superimposing the limiting cathodic potential.

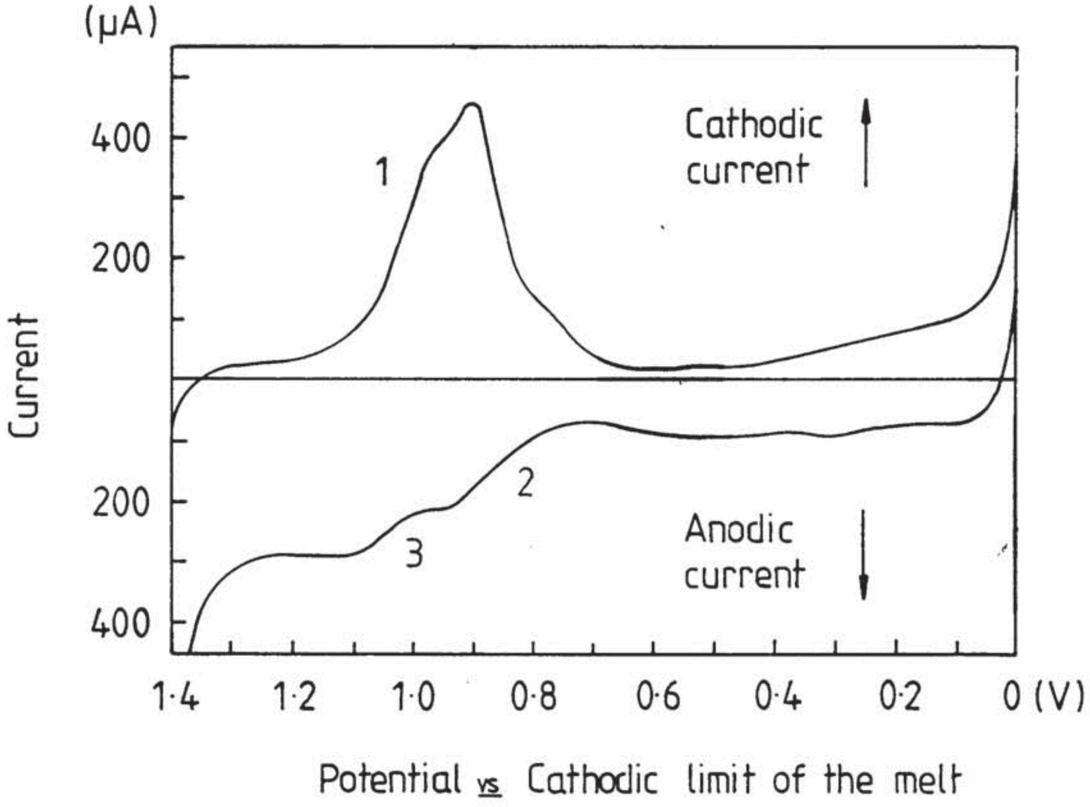

Figure 5-2 Voltammogram of acidic (Na-K)OH eutectic at 523K under N_2 using a vibrating Pt indicator electrode.

On the (f.s.) one cathodic peak was found which has been assigned wave number 1, its E_p value was in the range (0.9-1.0V). The i_p value of wave 1 was not constant and it was dependant on the Pt electrode condition. Mamantov Strong and Clayton (90) found that a plot of E vs. log $(i_p - i)$ is linear in the region $(0.5-0.9) i_p$ for the reduction of Ag^+ in molten nitrates and gave a slope of 2.2RT/nF. Nicholson and Shain (92) developed an equivalent expression for aqueous solutions and a plot of nE vs log $[(i_p - i)/i]$ was found to be linear in the range $(0.35-0.7) i_p$. The linearity in only part of the current range was suggested to be due to the activity of the deposit not being constant. Analysis of wave 1 was performed using the two plots mentioned above; the plot of E vs log $(i_p - i)$ was linear in the range $(0.4-0.8) i_p$ with a slope of 0.083V and the plot of E vs log $[(i_p - i)/i]$ was linear in the range $(0-0.5) i_p$ with a slope of 0.122V. These results suggest that wave 1 is due to an irreversible process. However its E_p value compares favourably with the value given by Goret and Tremillon for Pt oxidation, so this peak is due to the dissolution of the Pt oxide film formed on the Pt electrode surface. Split of the peak into two overlapping peaks or a wave and a peak was observed in some voltammograms of acidic melts, these effects are attributed to adsorption of gases on the electrode surface. On the (r.s.) two anodic waves were found, which have been assigned wave numbers 2 and 3, the $E_{\frac{1}{2}}$ value of wave 2 lies within the range (0.8-0.9V) and that of wave 3 lies within the range (1.0-1.1V). Their i_L values were approximately the same. Analysis of wave

2 in voltammograms of acidic melts by plotting E vs log $[(i_L-i)/i]$ gave a straight line with a slope indicating that the wave was due to an irreversible reaction, but a plot of E vs $\log[(i_L-i)^2/i]$ gave a straight line with a slope of 0.048V, Fig. 5-3, indicating a reversible two electron transfer reaction, together with the $E_{\frac{1}{2}}$ value that compares favourably with the value given by Goret and Tremillon for Pt oxidation potential according to the reaction:

$$Pt + 2OH^- - 2e^- \rightleftarrows PtO + H_2O \qquad (5\text{-}4)$$

suggests that wave 2 is due to the first step of Pt oxidation. Analysis of wave 3 also suggested a reversible two electron transfer reaction, Fig. 5-4, which could well be due to the following reaction:

$$PtO + 2OH^- - 2e^- \rightleftarrows PtO_2 + H_2O \qquad (5\text{-}5)$$

as the second step of Pt oxidation.

A voltammogram of slightly acidic melt presented in Fig. 5-5 showed that the two waves 2 and 3 had shifted towards more positive potentials and the analysis of wave 2 by H.I.E. plot suggested a reversible one electron transfer reaction, therefore wave 2 in this voltammogram was attributed to the following reaction:

$$O_2^- - e^- \rightleftarrows O_2 \qquad (5\text{-}6)$$

rather than to the Pt electrode oxidation because the new $E_{\frac{1}{2}}$ value and the wave analysis were in favour of the superoxide oxidation. Also in the same voltammogram a wave was found on both the (f.s) and the (r.s) at about 0.3V. This value suggests that it is due to the couple PtO_2^{2-}/Pt according to the following reaction:

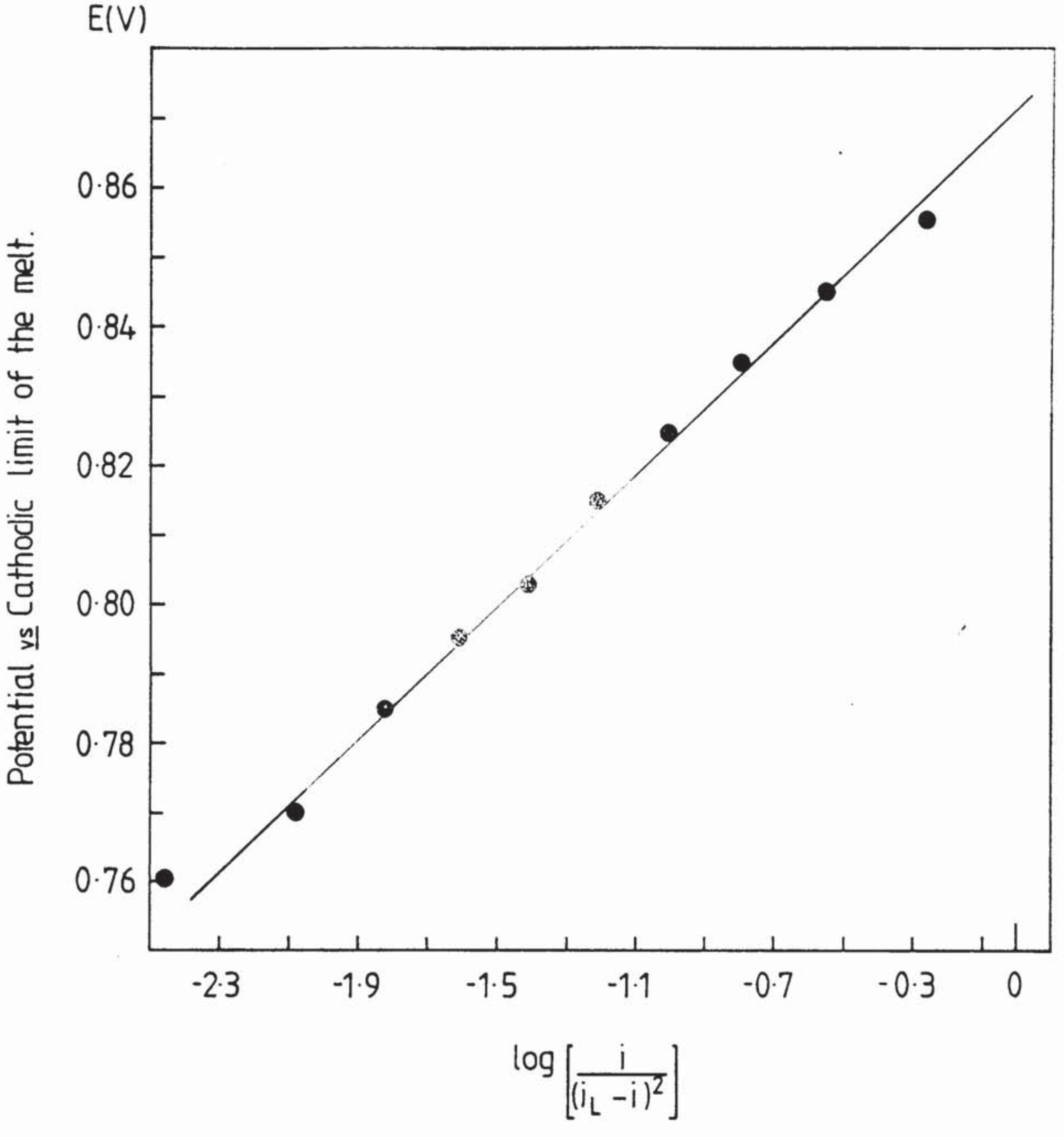

Figure 5-3 H.I.E. Analysis of voltammetric oxidation wave 2.

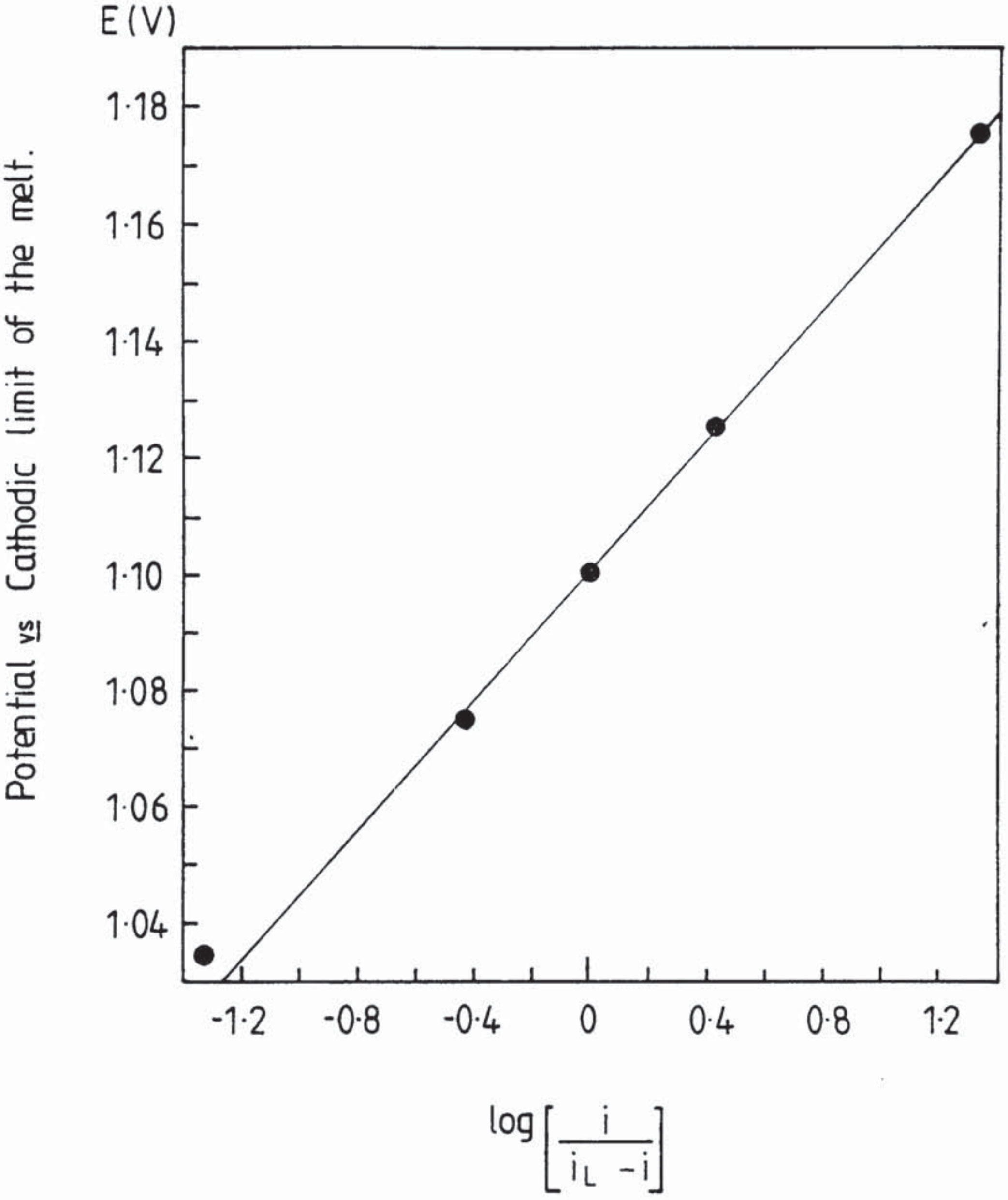

Figure 5-4 H.I.E. Analysis of voltammetric oxidation wave 3.

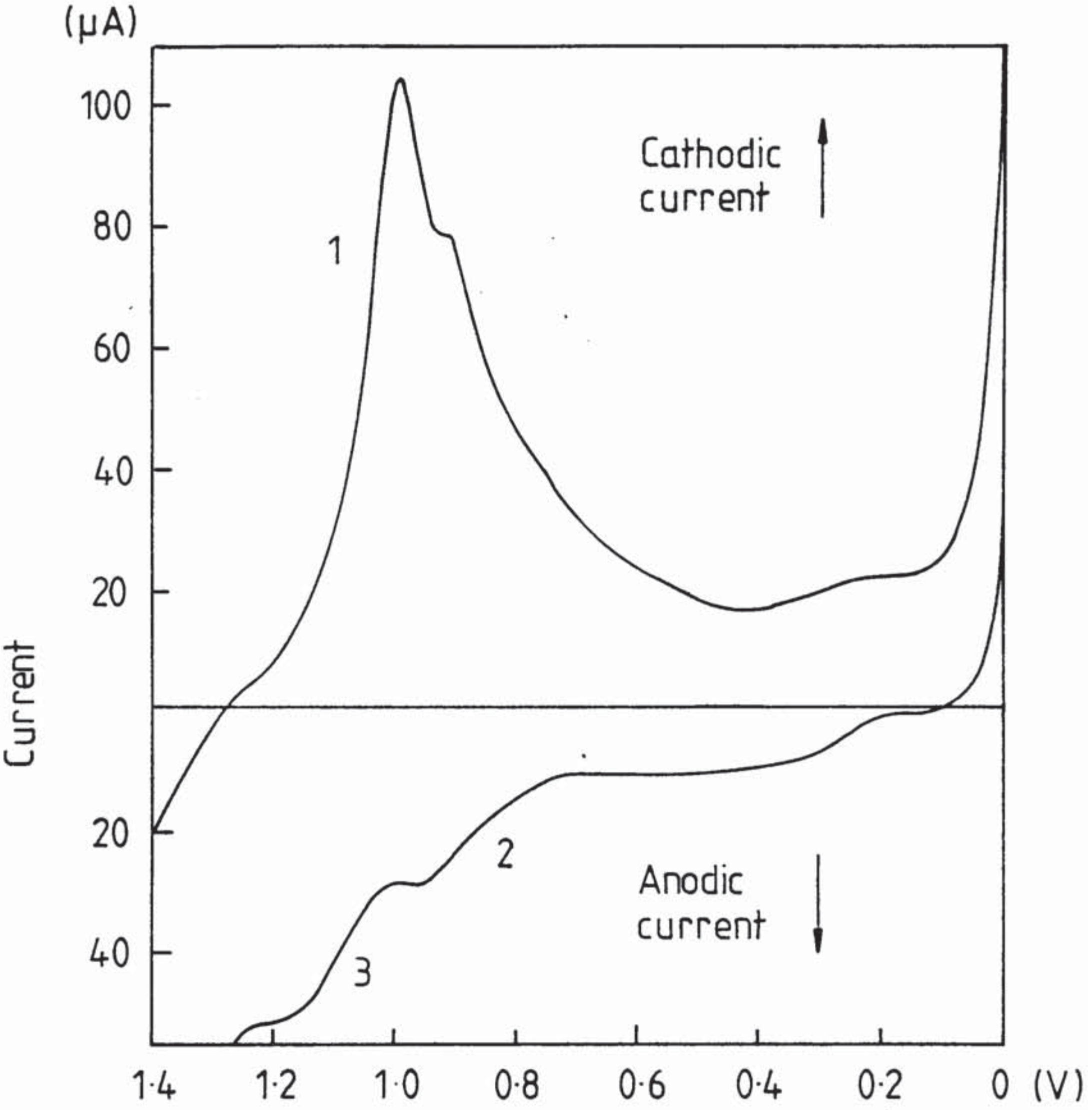

Potential vs Cathodic limit of the melt.

Figure 5-5 Voltammogram of slightly acidic (Na - K)OH eutectic at 523K under N_2 using a vibrating Pt indicator electrode.

$$Pt + 2O^{2-} - 2e^- \rightleftarrows PtO_2^{2-} \qquad (5\text{-}7)$$

Goret and Tremillon found a wave due to the reaction above in voltammograms of basic melts.

In some voltammograms of the acidic melt a wave was found on both the (f.s) and the (r.s) at approximately 1.3V, this wave only appeared using a stationary working electrode. The analysis of the wave gave a straight line with a slope indicating a reversible three electron transfer reaction and this wave was attributed to the following reaction:

$$O_2^- + 2H_2O + 3e^- \rightleftarrows 4OH^- \qquad (5\text{-}8)$$

Most voltammograms of the pure melt showed several small waves and peaks apart from the main waves mentioned above and these waves were found to be dependent on the Pt electrode state e.g. the method used for cleaning, and the age of the electrode. Some of these waves were adsorption waves.

5.3.1 Discussion

The observation that the voltammogram of the pure hydroxide melt obtained using the vibrating Pt working electrode was almost identical to the voltammogram obtained using the stationary Pt working electrode is not restricted to the hydroxide melts, W.D. Read (49) in his work with nitrate melts also reported that voltammograms of the pure nitrate melt whether obtained using vibrating or stationary Pt electrodes were very similar.

From the work of Goret and Tremillon (20) it is difficult to draw a firm conclusion about the O_2^- ions existence in acidic hydroxide melts. They reported that O_2^- ions are stable in basic melts and in acidic melts are reduced to the hydroxide ion according to:

$$O_2^- + 2H_2O + 3e^- \rightleftarrows 4OH^- \qquad (5\text{-}8)$$

without mentioning the reversibility of that reaction. It was also reported in their paper that the O_2^- ions reacts with water according to:

$$4O_2^- + 2H_2O \rightleftarrows 3O_2(g) + 4OH^- \qquad (5\text{-}9)$$

but the equilibrium constant is unfavourable except at high local concentrations of O_2^- and water, and that in acidic melts the observed evolution of O_2 on oxidation at Pt electrodes can be explained on this basis.

Eluard and Tremillon (4) found that the standard potential of the couple $O_2(g)/O_2^-$ is highly oxidizing and more positive than the standard potential of the couple O_2^-/OH^- in this melt, which indicates that O_2 evolution should not be possible on oxidation in the melt, although the unfavourable potential is so small that it is in fact easily overcome. In the present work the wave found at 1.3V in some voltammograms of the acidic melt, using a stationary Pt working electrode and attributed to the couple O_2^-/OH^- supports the existence of O_2^- ions in acidic melts in low concentrations and the proposition that it is probably unstable.

In the acidic melt, the theoretical analysis of the oxidation wave 2 by a plot of E vs. $\log[(i_L-i)/i]$ suggested an irreversible electrode reaction, while a plot of E vs. $\log[(i_L-i)^2/i]$ indicated a reversible two electron transfer reaction. This means that the Pt oxidation does not proceed according to equation (5-4) but via a reaction involving O_2^- ions such as:

$$2Pt + 2O_2^- - 2e^- \rightleftarrows 2PtO + O_2(g) \qquad (5\text{-}10)$$

In slightly acidic melts wave 2 shifted to more positive potential and the analysis of the wave in the voltammogram of this melt suggested a reversible one electron transfer reaction attributed to the O_2^- ions oxidation to O_2 gas. Goret and Tremillon (20) suggested that further oxidation of PtO to PtO_2 is very close to the oxidation of OH^- ions, the limiting anodic process, while in the present work wave 3 in the acidic melt voltammogram, attributed to the oxidation of PtO was not in fact very close to the anodic limit of the melt, but it moved closer to the anodic limit in slightly acidic melts.

The results of this section generally agree with the results obtained by Goret and Tremillon for the Pt electrode in pure hydroxide melts. The observations of Delimarskii and co-workers (91) are generally consistent with the data obtained in this work and those given by Goret and Tremillon, although the pH_2O of their melt is unknown.

5.4 (Na-K)OH Eutectic Containing Mn Metal

To molten (Na-K)OH, $pH_2O = 0$, at 523K was added 0.448 g of Mn metal (0.163M) with N_2 stirring. When all the metal had reacted the N_2 stirring was stopped and as usual a nitrogen blanket was maintained above the melt. The melt was colourless. A voltammogram of the melt solution using the vibrating Pt indicator electrode is shown in Fig. 5-6. Eluard and Tremillon (7) performed a similar experiment at 500K using a rotating nickel electrode. On the (f.s) four waves were found which

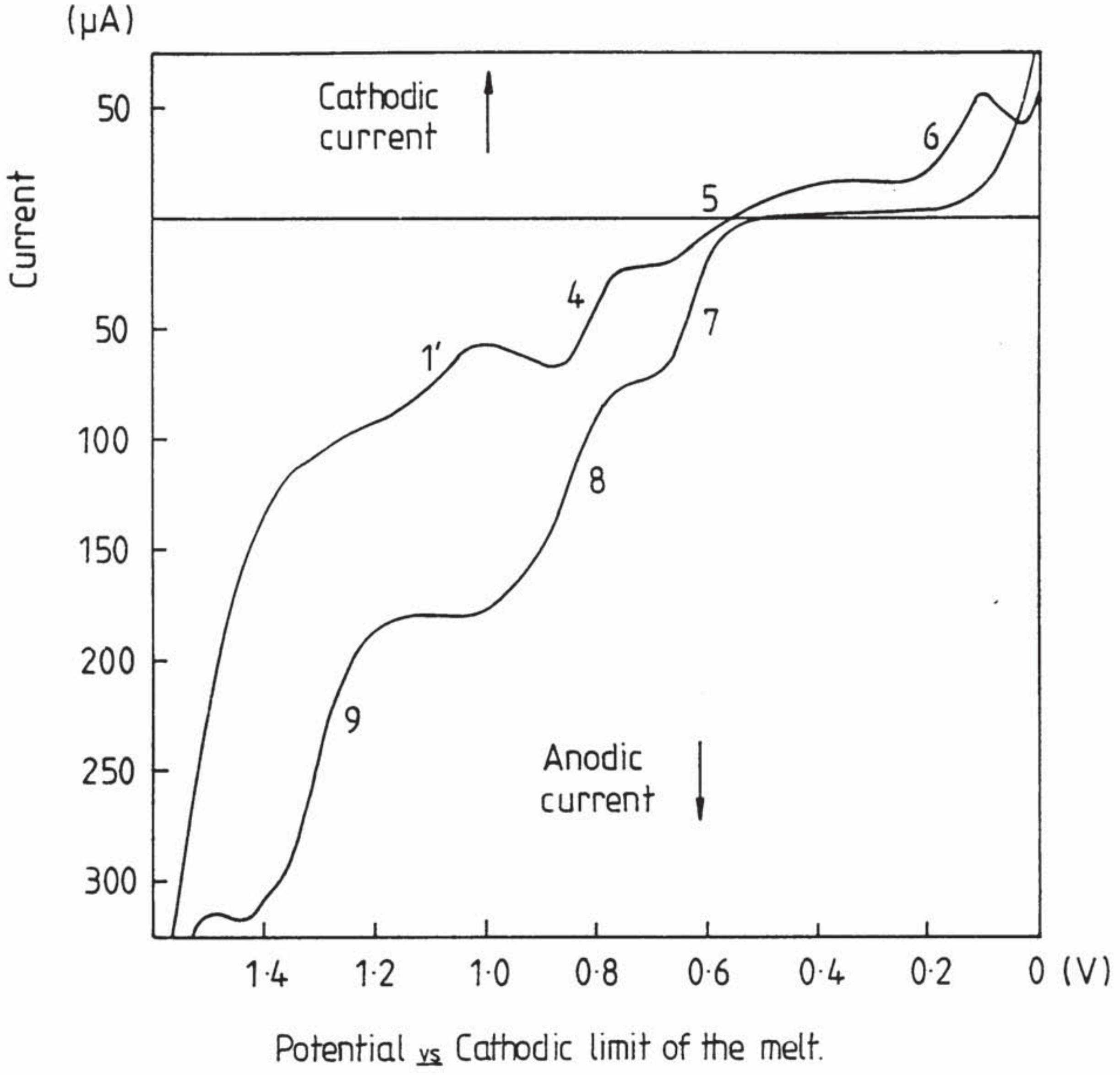

Figure 5-6 Voltammogram of (Na - K)OH eutectic containing Mn metal (0·163M) at 523K, using a vibrating Pt indicator electrode under N_2

have been assigned wave numbers 1', 4, 5 and 6. On the (r.s) three waves were found and these have been assigned wave numbers 7, 8 and 9.

The oxidation wave 1' was peak shaped and has been found to be due to the Pt electrode oxidation as the E_p value of 1.06V suggested. Analysis of the wave by H.I.E. plot gave a straight line with a slope of 0.045V. A theoretical value of 0.052V is expected for a reversible two electron transfer reaction at 523K.

There was no indication of the existance of any O_2^- ions in this melt, so wave 1' could be due to the following reaction:

$$Pt + 2OH^- - 2e^- \rightleftarrows PtO + H_2O \qquad (5\text{-}4)$$

The remaining waves are attributed to electrochemical reactions involving manganese ions, manganese oxyanions, manganese oxides and manganates.

The $E_{\frac{1}{2}}$ values for waves 4 and 8 are 0.82V and 0.87V respectively. These values compare favourably with the value given in reference (7) for the couple $MnO_4^{3-}/MnO(s)$, where the electrochemical reaction was thought to be:

$$MnO(s) + 6OH^- - 3e^- \rightleftarrows MnO_4^{3-} + 3H_2O \qquad (5\text{-}11)$$

But that reaction was thought to occur in basic melts, so there is a possibility that waves 4 and 8 are due to the couple $MnO_4^{3-}/Mn_2O_3(s)$ according to the reaction:

$$Mn_2O_3 + 10\,OH^- - 4e^- \rightleftarrows 2MnO_4^{3-} + 5H_2O \qquad (5\text{-}12)$$

which occurs in acidic melts. Analysis of the oxidation wave 4 by H.I.E. plot gave a straight line with a slope of 0.047V indicating a reversible two electron transfer reaction, Fig. 5-7. Analysis of the oxidation wave 8

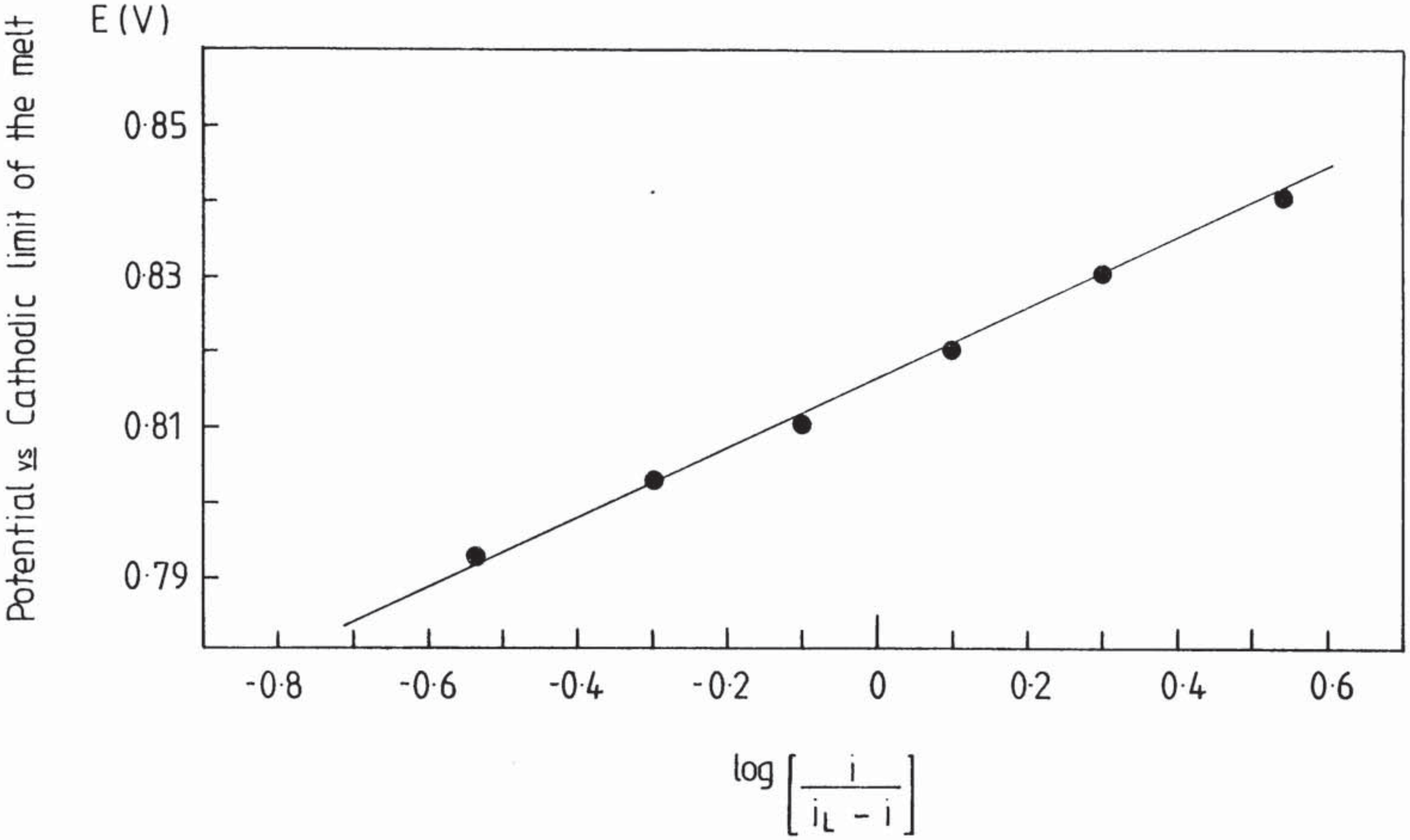

Figure 5-7 H. I. E. Analysis of voltammetric oxidation wave 4.

by H.I.E. plot of E vs. $\log[(i_L-i)/i]$ gave a straight line for $0.8i_L$ with a slope of 0.093V but for the first $0.2i_L$ the points were off the line. The slope deviates from the theoretical value of 0.104V expected for a reversible one electron transfer by 11 mV. A plot of E vs. $\log[(i_L-i)^2/i]$ gave a straight line with a slope of 0.054V indicating a reversible two electron transfer reaction, Fig. 5-8. The $E_{\frac{1}{2}}$ values for waves 5 and 7 are 0.58V and 0.62V respectively. These values compare favourably with the value given in reference (7) for the couple $Mn^{2+}/Mn_2O_3(s)$ and the electrochemical reaction is:

$$2Mn^{2+} + 6OH^- - 2e^- \rightleftarrows Mn_2O_3 + 3H_2O \qquad (5\text{-}13)$$

Analysis of the composite wave 5 by H.I.E. plot gave a straight line with a slope of 0.102V indicating a reversible one electron transfer reaction, Fig. 5-9, while the analysis of the oxidation wave 7 gave a straight line with a slope of 0.048V indicating a reversible two electron transfer reaction, Fig. 5-10.

Wave 6 just before the cathodic limit is in fact a small cathodic peak, the H.I.E. plot gave a slope of 0.047V indicating a reversible two electron transfer reaction, Fig. 5-11.

Eluard and Tremillon (7) found a similar wave when they added MnO to a slightly acidic melt and it was in a position very close to that of the reduction of water. With the E_p value of 0.115V, it is reasonable to assume that wave 6 is due to the following reaction:

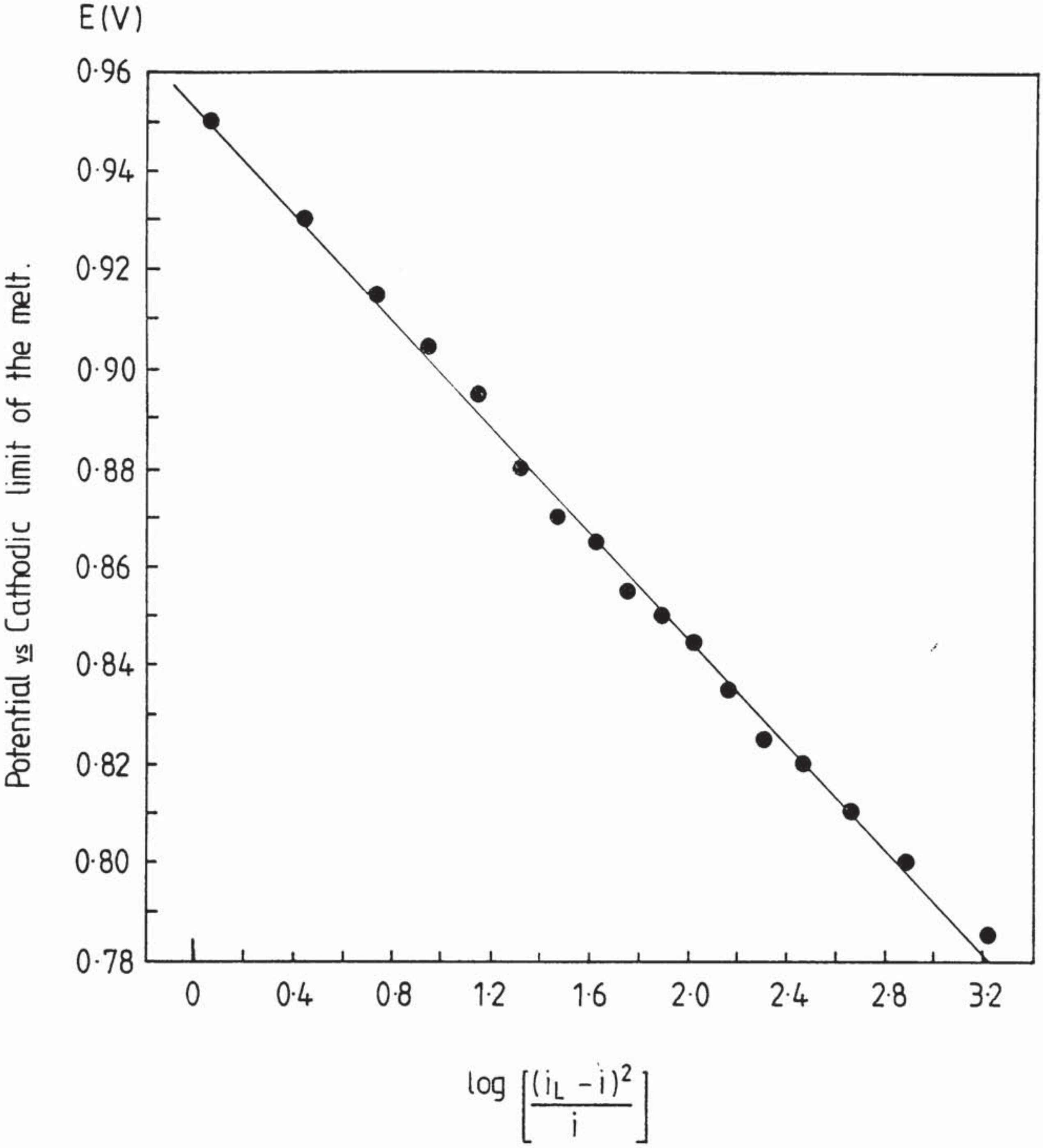

Figure 5-8 H. I. E. Analysis of voltammetric oxidation wave 8.

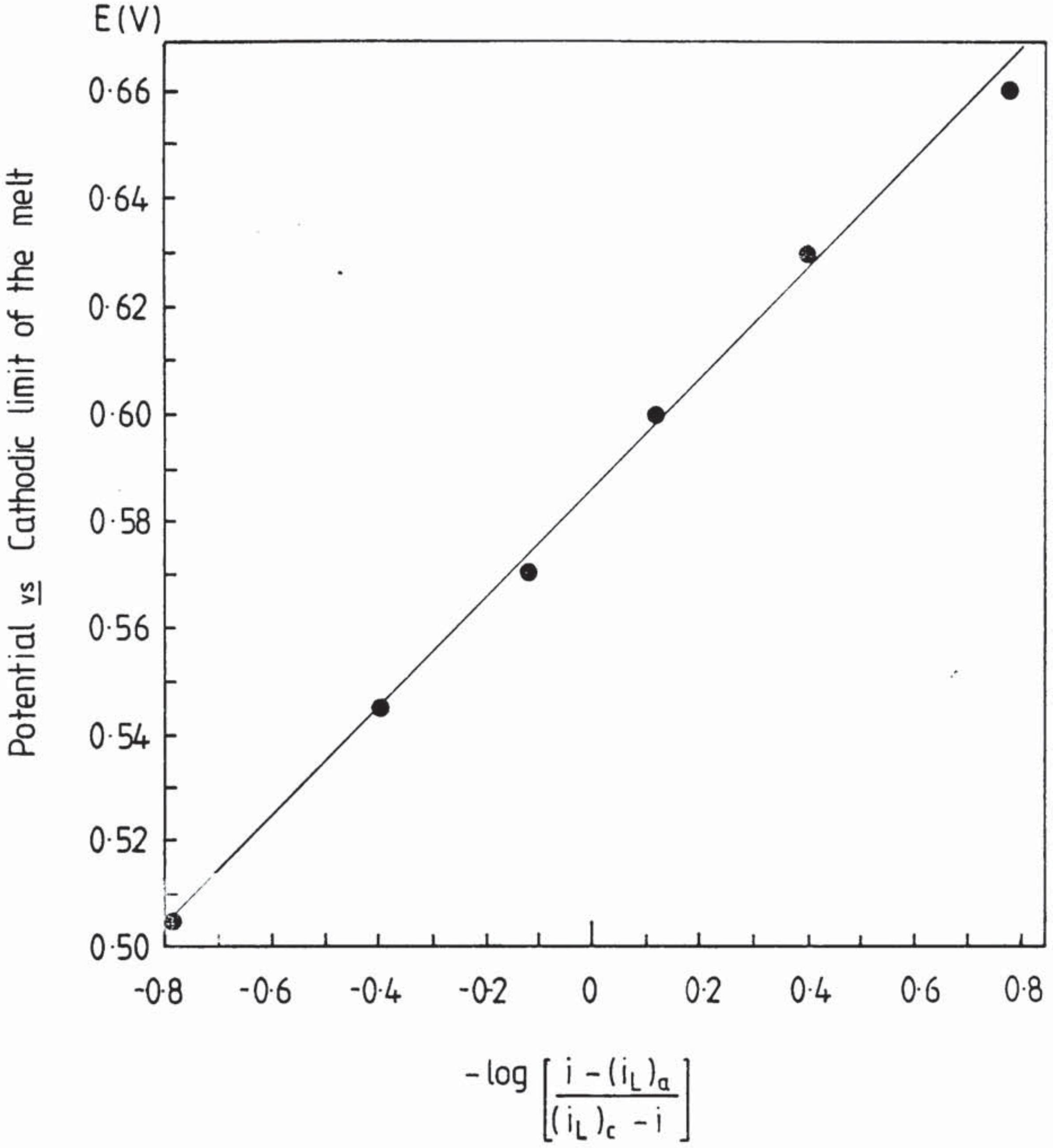

Figure 5-9 H. I. E. Analysis of voltammetric composite wave 5.

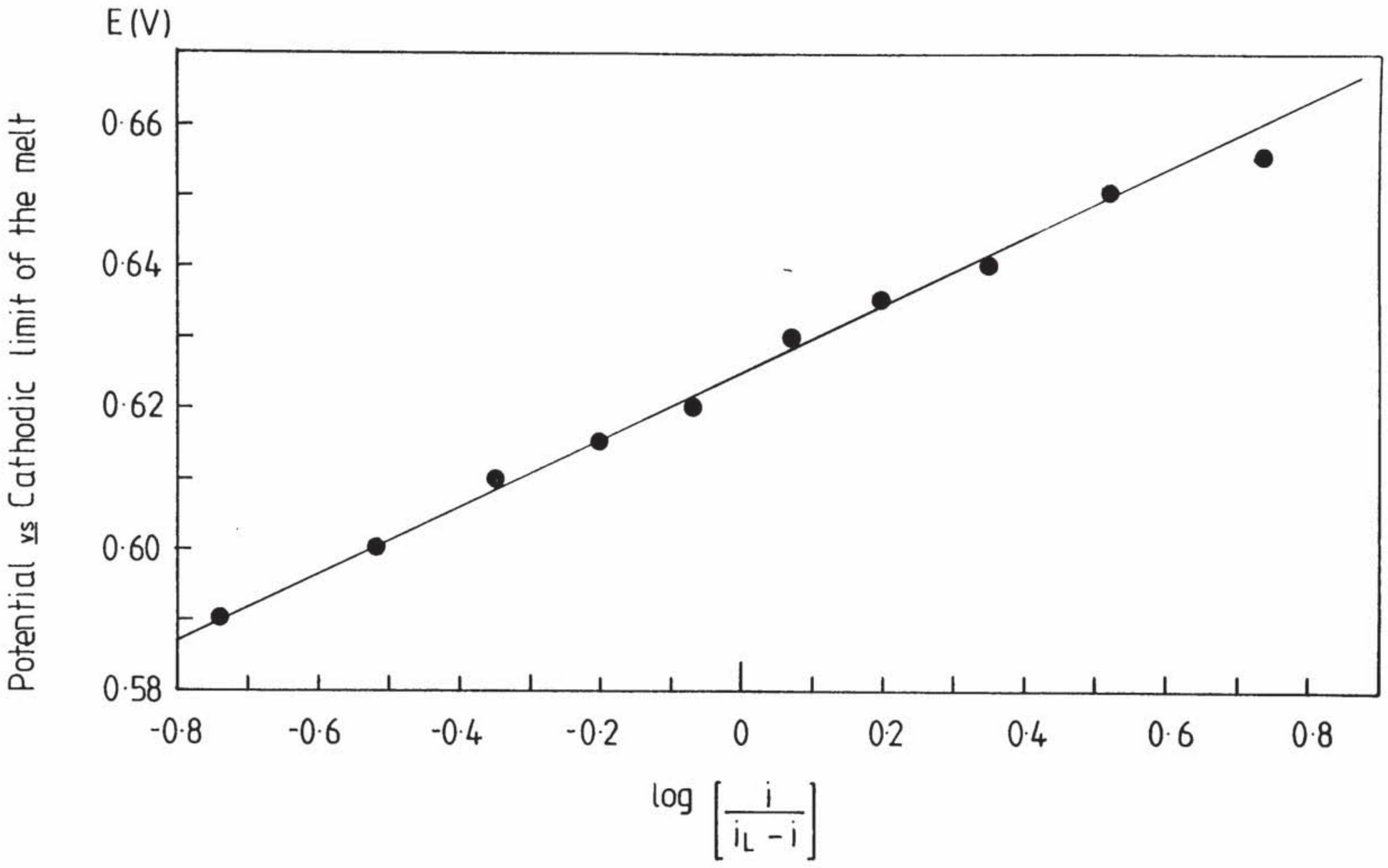

Figure 5-10 H.I.E. Analysis of voltammetric oxidation wave 7.

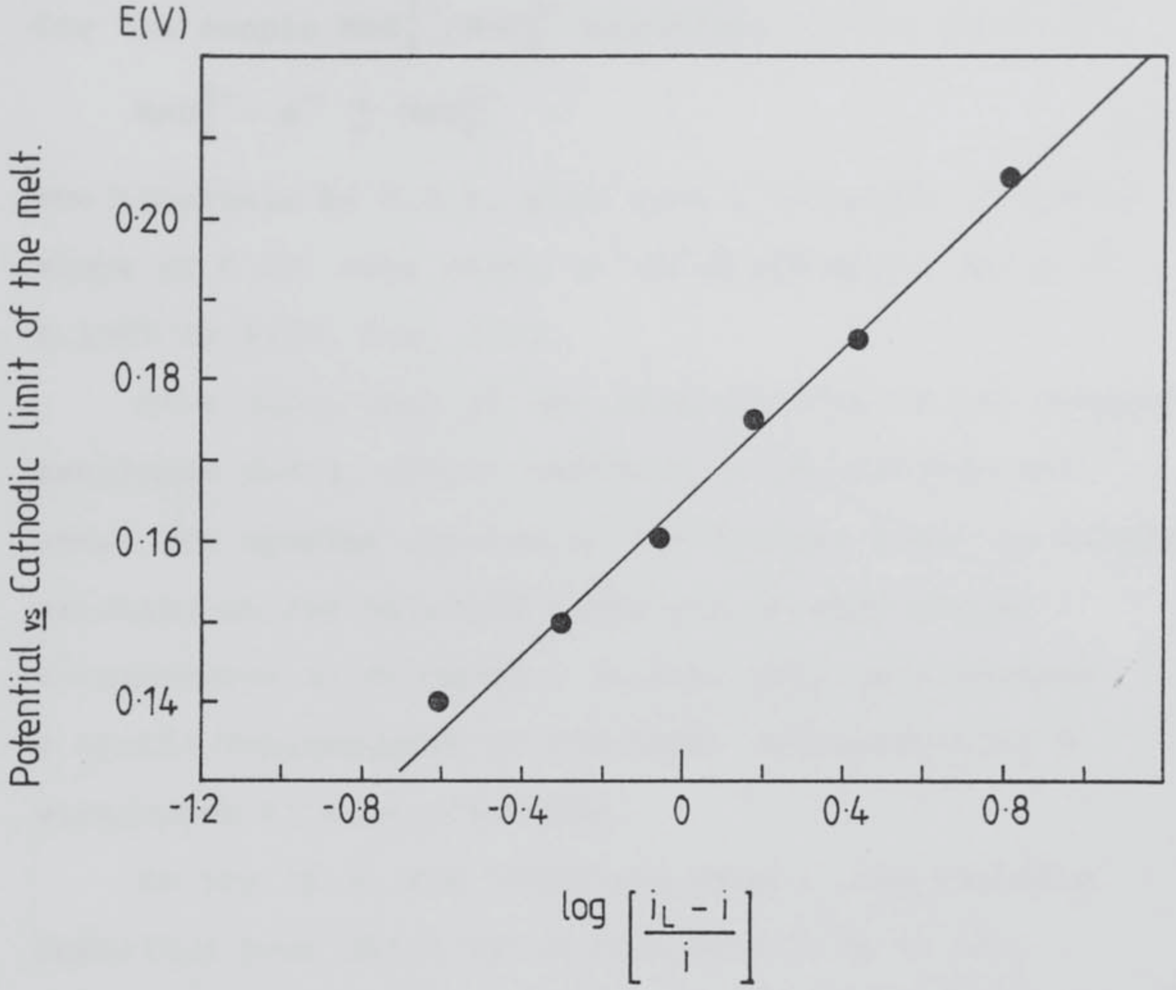

Figure 5-11 H.I.E. Analysis of voltammetric reduction wave 6.

$$2Mn^{2+} + 2OH^- + 2e^- \rightleftarrows 2MnO(s) + H_2(g) \qquad (5\text{-}14)$$

The $E_{\frac{1}{2}}$ value of the oxidation wave 9 is 1.30V which compares favourably with the value given in reference (7) for the couple MnO_4^{3-}/MnO_4^{2-} according to the reaction:

$$MnO_4^{3-} - e^- \rightleftarrows MnO_4^{2-} \qquad (5\text{-}15)$$

wave 9 analysis by H.I.E. plot gave a straight line with a slope of 0.1V, very close to the theoretical value of 0.104V at 523K, Fig. 5-12.

As a quick test of the reversibility of the couples mentioned above, cyclic voltammetry was carried out, where the species reduced on the forward sweep is usually oxidized on the backward sweep and another peaked voltammogram is produced. In Fig. 5-13 is presented a cyclic voltammogram of the melt, obtained using a stationary Pt wire electrode.

On the (f.s) the oxidation wave 1' has become a reduction peak which is in fact wave 1 as in the voltammogram of the pure melt, due to the dissolution of the oxide film formed on the Pt electrode surface. Wave 4 has also become a reduction peak which has been assigned wave number 10, but waves 5 and 6 have disappeared. On the (r.s) all three oxidation waves 7, 8 and 9 were found. The H.I.E. plot analysis of waves 7, 8 and 9 gave straight lines with slopes indicating irreversible electrode reactions. It was noticed that wave 8 became much smaller than the corresponding wave using a vibrating working electrode, indicating a charge-transfer controlled electrode process.

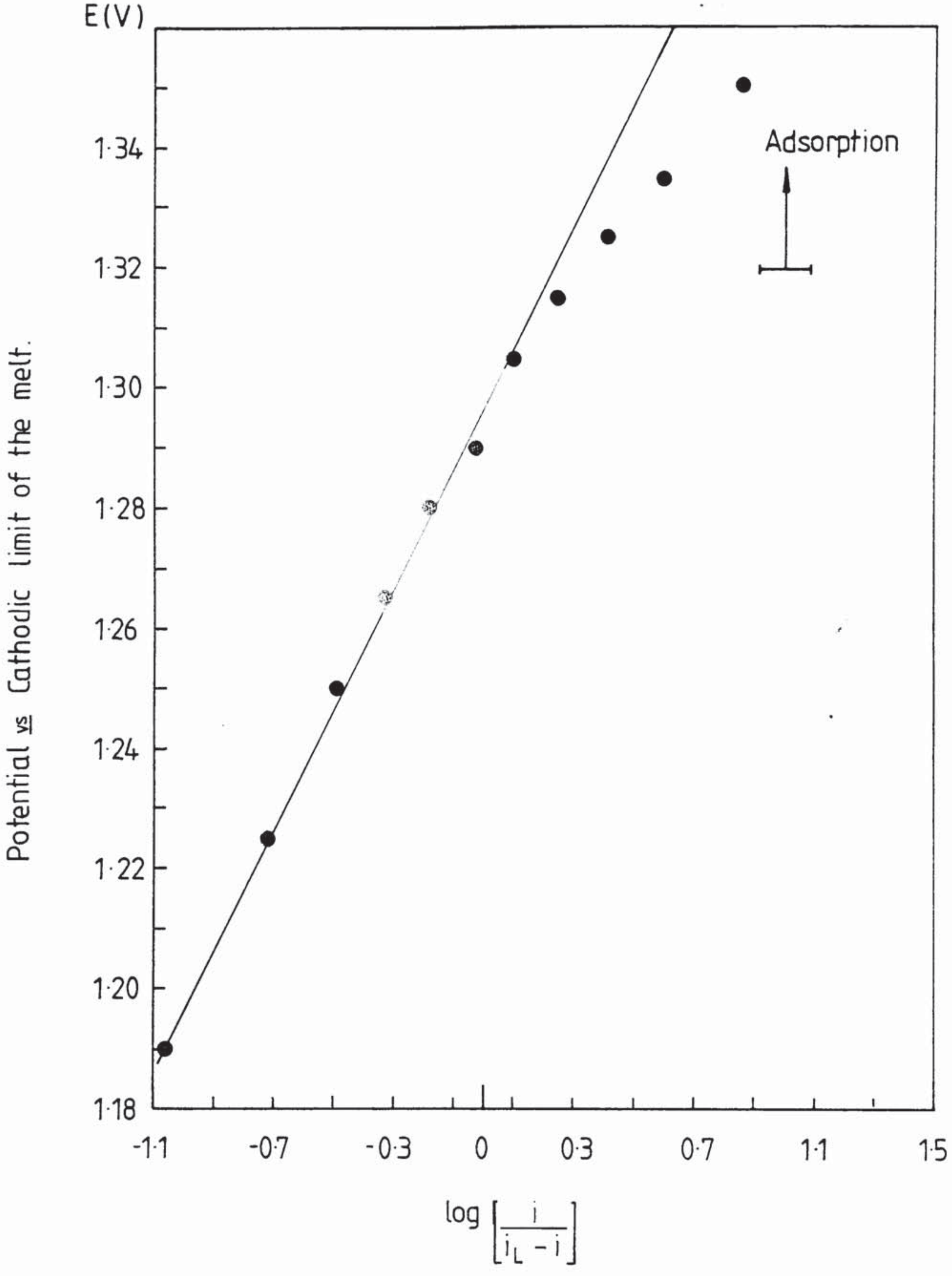

Figure 5-12 H.I.E. Analysis of voltammetric oxidation wave 9.

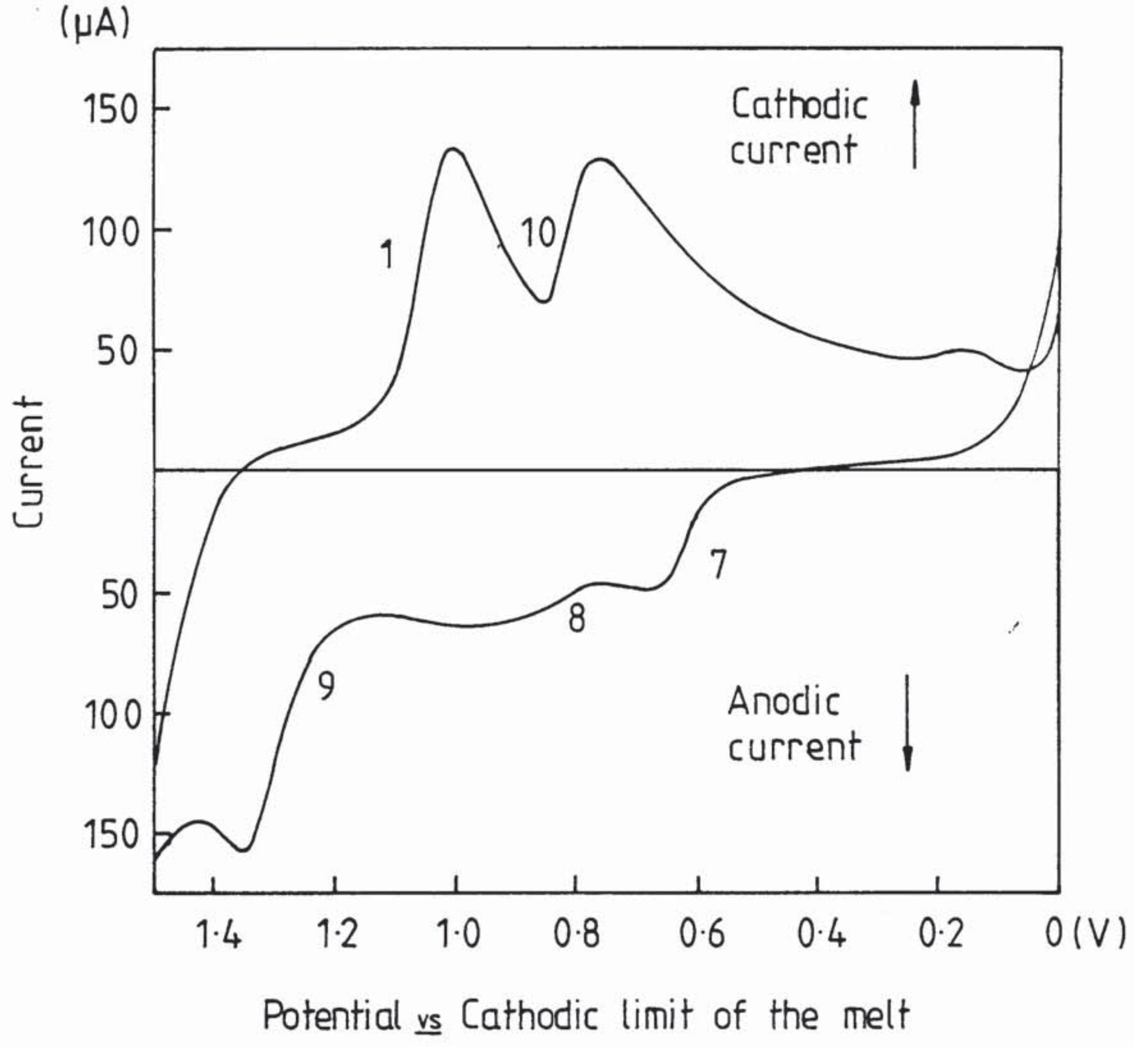

Figure 5-13 Cyclic voltammogram of (Na – K)OH eutectic containing Mn metal (0·163M) at 523K, using a stationary Pt wire indicator electrode.

5.4.1 Discussion

The results obtained from these experiments are generally in agreement with the results obtained by Eluard and Tremillon (7) but the fact that they did not produce sufficient analysis of the various waves in their paper made it necessary to reinvestigate the electrochemical reactions and their reversibility. When pure Mn metal is added to an acidic (Na-K)OH eutectic it reacts according to:

$$Mn + 2H_2O \rightleftarrows Mn^{2+} + 2OH^- + H_2 \qquad (5\text{-}16)$$

First it seems interesting to compare this work with that of Eluard and Tremillon. Using the vibrating Pt electrode wave 4 on the (f.s) and wave 8 on the (r.s) are both oxidation waves, while they obtained a reduction wave on the (f.s) and an oxidation peak on the (r.s), they attributed the wave and the peak to reaction (5-12). Wave 5 in this work is a composite wave and wave 7 is an oxidation wave. They obtained two reduction waves corresponding to waves 5 and 7 and attributed the two waves to reaction (5-13). Apart from that, the voltammogram presented in their paper did not show any other electrochemical reactions. It was thought that waves 4 and 7 should be oxidation waves, as Mn^{2+} in the melt can only be oxidized to other species.

As for wave 6, Eluard and Tremillon had to add MnO to the melt in order to obtain that wave, so it seems that the voltammogram presented in Fig. 5-6 gives a detailed and full picture of the electrochemical reactions which enable a complete study of these reactions. The test for the reversibility of the various electrochemical reactions occuring in the melt is rather difficult because some of the reactants or products of the oxidation and reduction are insoluble in the melt, therefore the Nernst equation cannot be used because the reactants or products are not in solution. Various relationships of E vs log (i) which are modified versions of the usual H.I.E. plot of E vs log $[(i_L - i)/i]$ used by other workers in similar situations were used by the present author to interpret the results given in the previous section. When a metallic ion is reduced to the metal on a solid electrode, the wave due to this electrode reaction is reversible if a plot of E vs log $[2\ (i_L - i)/i_L]$ give a straight line with a slope of 2.3 RT/nF. But when this was applied to the waves obtained it did not give a straight line. Also other plots were applied, like E vs. log $(i_L - i)$, E vs log $(i_L - i)^2$ without getting a straight line. No appropriate relationships were given in the literature that could be applied to this work except the following (93):

$$E_{W.E} = \text{constant} + \frac{2.3RT}{\beta\ nF}\ \log K \frac{D}{K_s} \qquad (5\text{-}17)$$

where:

K_s = the rate constant of the electrode process at the standard potential cm/sec.

D = Diffusion coefficient

β = Coefficient of the electrode transfer process

This relationship was used for electro-oxidation or reduction of variable valency ions accompanied by the formation of a sparingly soluble compound on the surface of an inert electrode with subsequent electro-dissolution of these compounds, e.g. $M^{m+} \rightleftharpoons M^{(m\pm n)+} \pm ne$ (5-18)

$$M^{(m\pm n)+} + (m\pm n)A^- \rightleftarrows MAm\pm n\downarrow \qquad (5\text{-}19)$$

for (m+n)e the process is anodic

for (m-n)e the process is cathodic

But the values of D, K_s, β are unknown and cannot be calculated from the results obtained.

Eventually it was decided to use the normal H.I.E. plot of E vs. log $[(i_L - i)/i]$ to test the reversibility of the waves regardless as to whether the reaction involves an insoluble compound or not, because even if the compound is insoluble ordinarily in the melt, it might be soluble in the vicinity of the electrode. Alternatively if the half-reaction yields an insoluble substance that is adsorbed on the electrode surface then the adsorbed substance may be reduced or oxidized reversibly.

If wave 4 on the (f.s) and wave 8 on the (r.s) are regarded as two waves representing the same reaction, their i_L values should be about the same, but as can be seen in Fig. 5-6, the i_L value of wave 4 is approximately half that of wave 8.

Consequently if wave 4 is due to a reversible two electron transfer reaction as the H.I.E. plot analysis showed, then wave 8 should be due to a four electron transfer reaction. Assuming that waves 4 and 8 are due to the same electrode reaction and that wave 4 could have been affected by the Pt electrode oxidation wave that preceded it, then wave 8 is due to:

$$Mn_2O_3 + 10\,OH^- - 4e^- \rightleftarrows 2MnO_4^{3-} + 5H_2O \qquad (5\text{-}12)$$

and wave 4 is due to:

$$\tfrac{1}{2}Mn_2O_3 + 5OH^- - 2e^- \rightleftarrows MnO_4^{3-} + 2.5\ H_2O \qquad (5\text{-}20)$$

But this is unlikely to happen, especially as the analysis of wave 8 (using the same H.I.E. plot used for the analysis of wave 4) suggested an irreversible electrode reaction. Moreover a wave separation of 50 mV was found between the $E_{\frac{1}{2}}$ values of the two waves which is not expected for a reversible electrode process of the same reaction, therefore waves 4 and 8 are not due to the same electrode reaction.

According to the analysis of wave 4, it could be due to the following reaction:

$$MnO + 2OH^- - 2e^- \rightleftarrows MnO_2 + H_2O \qquad (5\text{-}21)$$

Eluard and Tremillon (7) did not consider the possibility of MnO_2 formation in the melt but they reported that MnO_2 disproportionates in acidic melts. The analysis of wave 8 by plotting E vs $\log[(i_L-i)^2/i]$ is interesting as it suggests a reversible two electron transfer reaction. However, it is more likely that wave 8 is due to an irreversible electrode reaction or a mixed electrode process that involves reaction (5-21) above and reaction (5-11) which is:

$$MnO + 6OH^- - 3e^- \rightleftarrows MnO_4^{3-} + 3H_2O$$

Again the i_L value of wave 5 was found to be about half that of wave 7, suggesting that these two waves are not due to the same electrode reaction. The H.I.E. plot analysis supported this suggestion, since it indicated a reversible two electron transfer reaction for wave 7 and a reversible one electron transfer reaction for wave 5. Wave 7 was thought to be due to reaction (5-13):

$$2Mn^{2+} + 6OH^- - 2e^- \rightleftarrows Mn_2O_3 + 3H_2O$$

and wave 5 was also thought to be due to reaction (5-13) but the fact that wave 5 is a composite wave may have affected the number of electrons involved in the electrode reaction.

The cyclic voltammogram shown in Fig. 5-13 failed to show the expected results for a reversible system, where the products of oxidation are subsequently reduced, except for wave 8, where a reduction peak (wave 10) appeared. Although the analysis of the waves of the cyclic voltammogram by H.I.E. plots gave results which suggested that the electrode processes were irreversible, the deviation from reversibility could be due to a significant contribution of activation polarization involving surface oxides on the Pt electrode.

5.5 (Na-K)OH Eutectic Containing $KMnO_4$ Only

Pure hydroxide melts containing $KMnO_4$ were intended to be used for the oxidation of organic compounds and more specifically MnO_4^{3-} was intended to be the oxidizing agent, therefore it was necessary to investigate the electrochemistry of these melts. Eluard and Tremillon (7) suggested the following equation:

$$E_{\frac{1}{2}} = 2.25 + 0.1 \log \frac{[MnO_4^{2-}]}{[MnO_4^{3-}]} \qquad (5\text{-}22)$$

to calculate the change in the $E_{\frac{1}{2}}$ value of the couple MnO_4^{2-}/MnO_4^{3-} as a function of the concentration change of MnO_4^{2-} and MnO_4^{3-} at $pH_2O < 0$. Equation (5-22) was one of the equations used to establish the Pourbaix diagram shown in Fig. 3-3. When the $E_{\frac{1}{2}}$ value of the couple MnO_4^{2-}/MnO_4^{3-}, measured in a previous experiment at $pH_2O = 0$ was substituted into equation (5-22), the concentrations of MnO_4^{2-} and MnO_4^{3-} were found to be approximately equal. In order to increase the concentration of MnO_4^{3-} and decrease that of MnO_4^{2-} in the melt, the pH_2O value had to be increased, in which case equation (5-22) does not apply. Hence a pH_2O value of 0.5 was used so that the predominant species of manganates in the melt was MnO_4^{3-} and not a mixture of MnO_4^{3-} and MnO_4^{2-}. Normally the melt was prepared twenty four hours before scanning took place, with a nitrogen blanket always maintained above the melt. In this experiment scanning was carried out on the same day as well as after twenty four hours to see if that affected the results. To molten (Na-K)OH at 523K was added 0.73g $KMnO_4$(0.09M) with N_2 stirring, when all the $KMnO_4$ had dissolved, the N_2 stirring was stopped, the melt colour was blue. First scanning was carried out on the same day and a voltammogram of the melt solution using the vibrating working electrode is shown in Fig. 5-14, while that of the same melt scanned after twenty four hours is shown in Fig. 5-15. As far as the (f.s) was concerned there was no difference between these two voltammograms, only one cathodic wave was found. This wave was in fact wave 10 as its $E_{\frac{1}{2}}$ value indicated and its analysis suggested a reversible four electron transfer reaction, Fig. 5-16, due to reaction (5-12). On the (r.s) Fig. 5-14 shows one

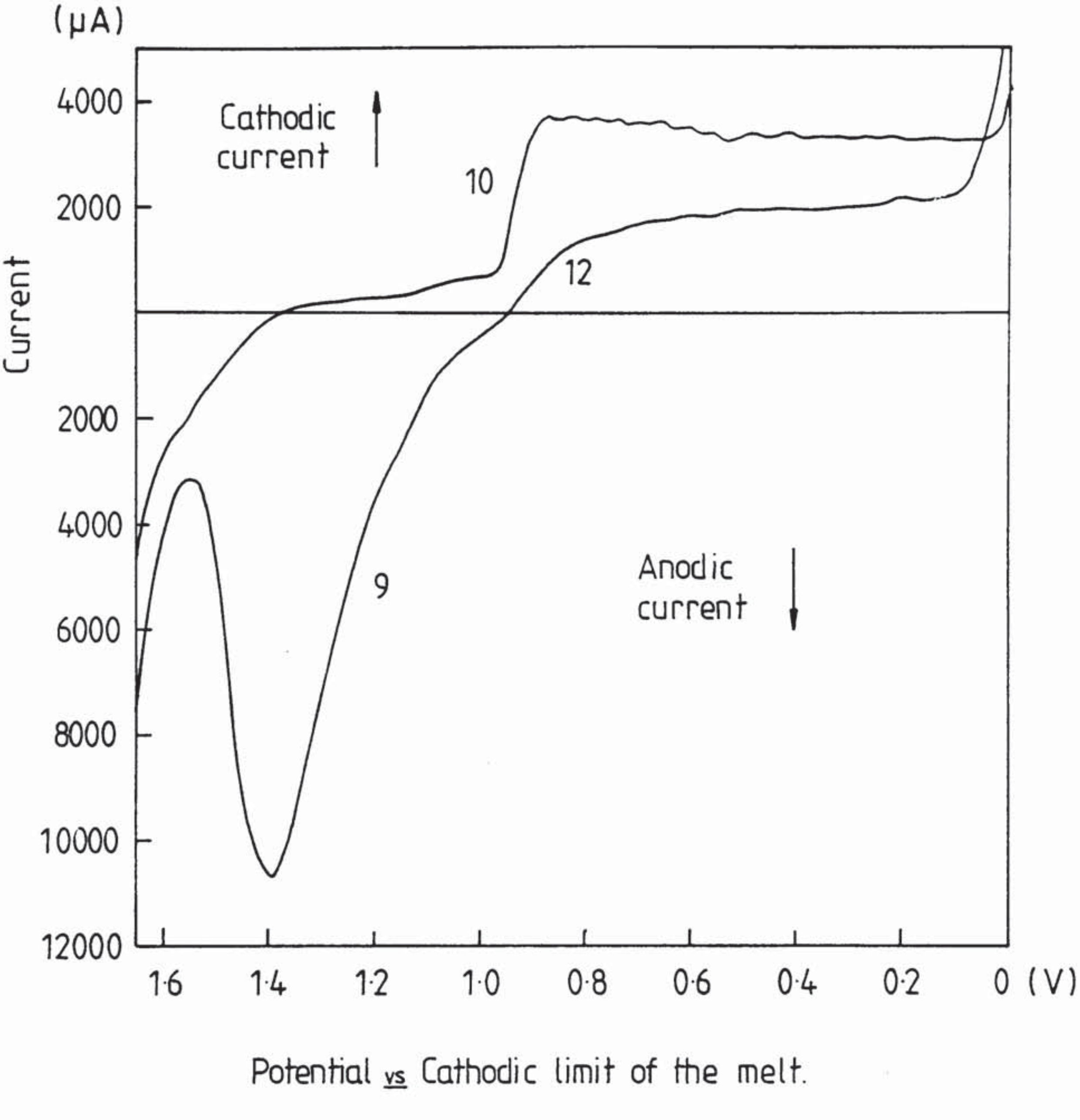

Figure 5-14 Voltammogram of (Na - K) OH eutectic containing $KMnO_4$ (0·09M) at 523K, using a vibrating Pt indicator electrode under N_2 (The scanning performed on the same day of preparing the melt)

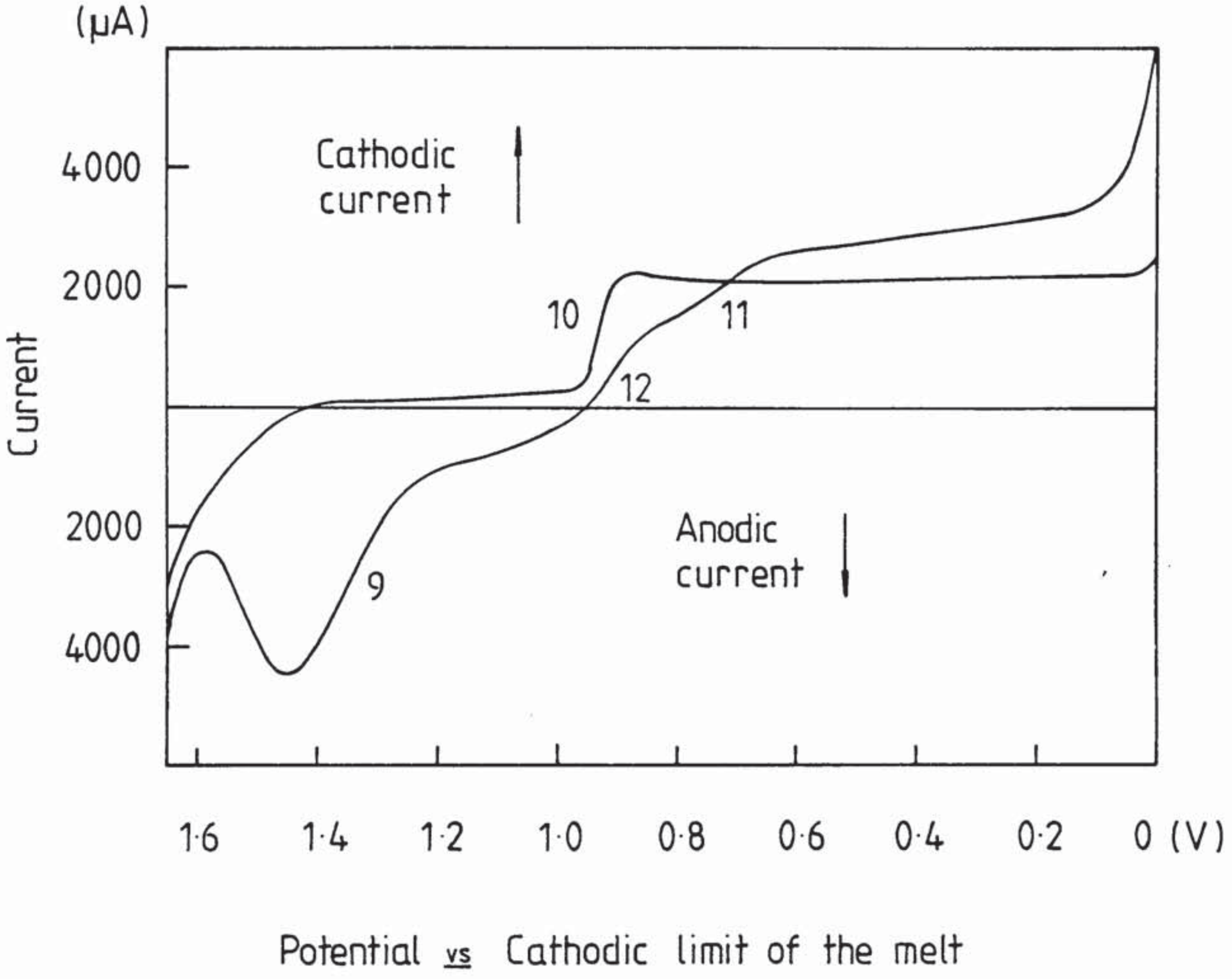

Figure 5 - 15 Voltammogram of (Na-K)OH eutectic containing K MnO_4 (0·09M) at 523K, using a vibrating Pt indicator electrode, under N_2.
(The scanning performed 24 hours after preparing the melt)

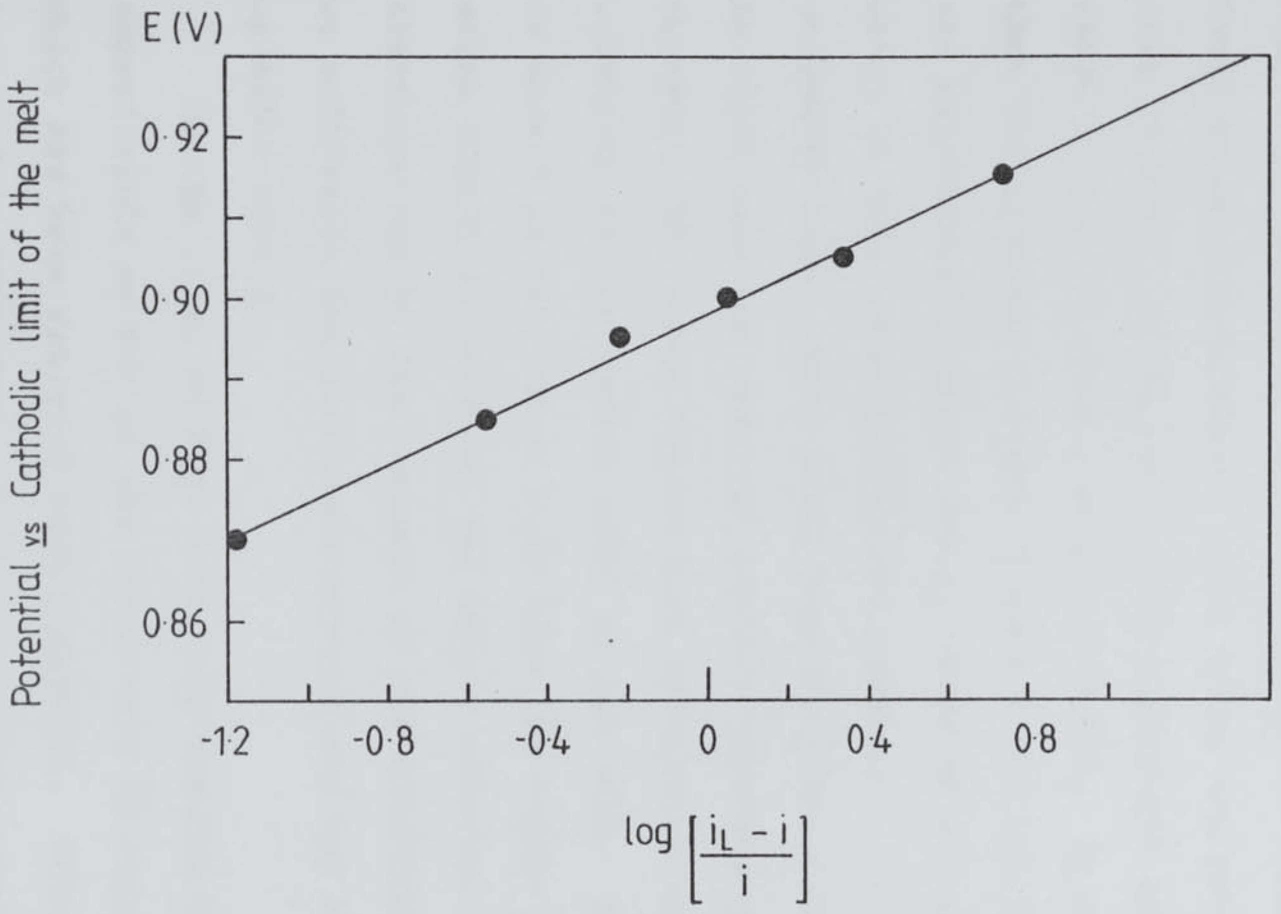

Figure 5-16 H. I. E. Analysis of voltammetric reduction wave 10.

composite wave which has been assigned wave number 12, and an anodic peak due to the MnO_4^{3-} oxidation (wave 9). The H.I.E. plot analysis of wave 12 gave a straight line for the cathodic component of the wave with a slope of 0.097V, Fig. 5-17, indicating that the cathodic component of wave 12 is due to a reversible one electron transfer reaction. The small anodic component of wave 12 was found to be irreversible. Wave 9 was analysed and a plot of E vs. $\log[(i_L-i)/i]$ gave a straight line over the range (0-0.64)i_p with a slope of 0.09V. It was noticed that the limiting current of wave 9 was not constant and reproducible, while the i_L value of all the other waves in this voltammogram are constant. It is also unusually high, which means that MnO_4^{3-} is weakly adsorbed, in which case the wave may exhibit enhancement of peak current. The other factor that influences wave 9 is its proximity to the anodic limit of the melt. The $E_{\frac{1}{2}}$ value of wave 9 is only about 0.1V from the anodic limit, where oxygen is produced and easily adsorbed on the Pt electrode and by its presence at the electrode surface it influences the electrode process and may shift, deform or split wave 9.

On the (r.s) of Fig. 5-15, the results were not reproducible as far as the first wave is concerned which has been assigned wave number 11. This wave appeared in some scans with an $E_{\frac{1}{2}}$ value suggesting that it is due to the same reaction of wave 7, reaction (5-13) and in other scans it disappeared. When wave 11

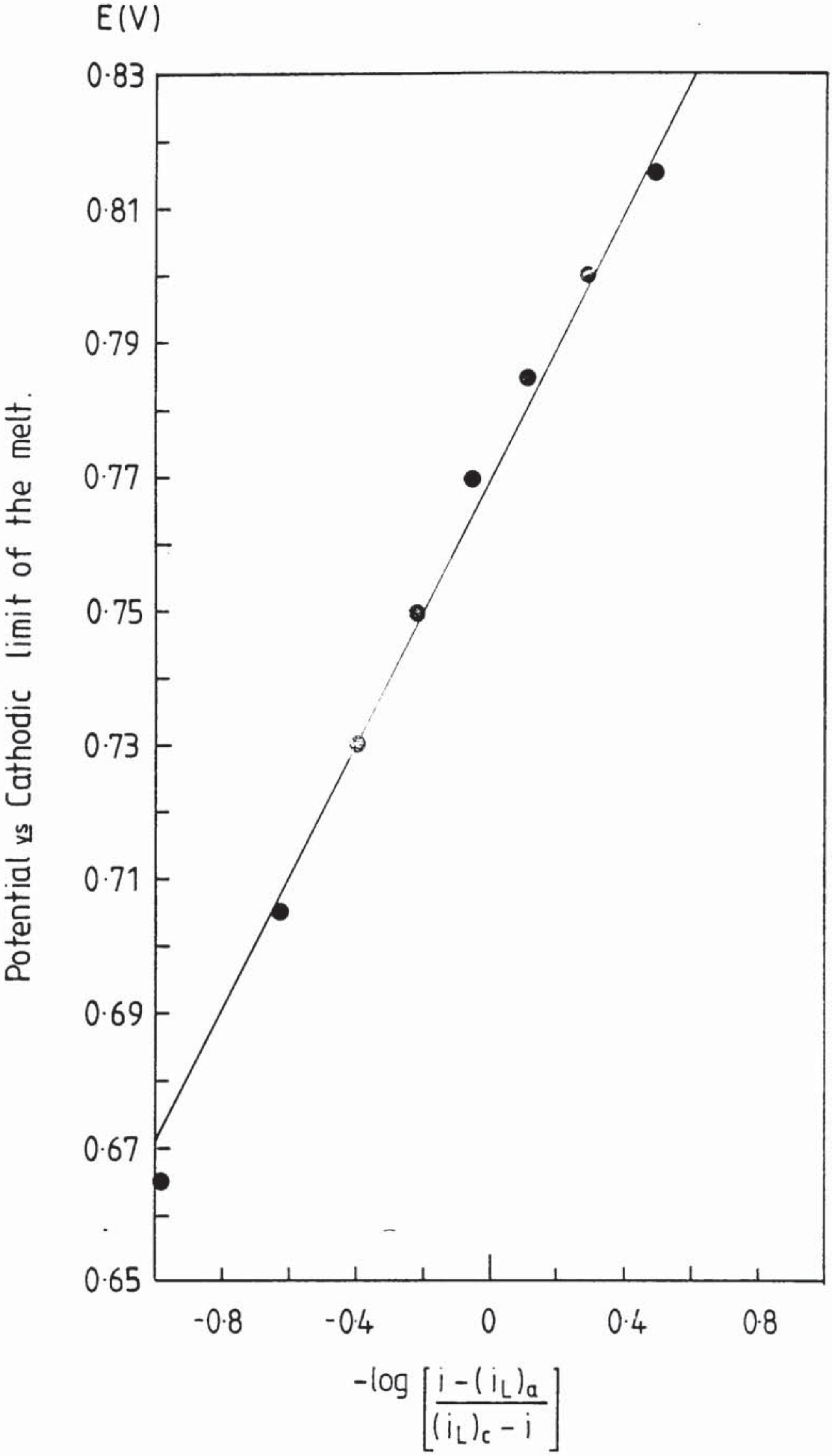

Figure 5-17 H.I.E. Analysis of voltammetric composite wave 12.

appeared it was always followed by the composite wave 12 which was found in all voltammograms whether it was preceded by wave 11 or not. In Fig. 5-15, waves 11 and 12 were found to be due to an irreversible electrode reaction, but the $E_{\frac{1}{2}}$ value of wave 12 suggests that it is due to reaction (5-12). No change was observed as far as wave 9 was concerned. However as the pH_2O value of the melt increased (i.e. drying of the melt) to approximately $pH_2O=1$, wave 9 (which is now a wave and not a peak as was at lower pH_2O values) has become due to a reversible one electron transfer reaction.

A cyclic voltammogram of the melt solution using the stationary working electrode is presented in Fig. 5-18. On the (f.s) two cathodic waves were found, they were in fact peaks, the first peak is wave 1 as its $E_{\frac{1}{2}}$ value indicated, due to the Pt oxide dissolution from the electrode; wave 1 as mentioned earlier depends on the working electrode condition, so its appearance was associated with the electrode condition. However, it was generally found when a stationary working electrode was used but not when a vibrating working electrode was used. The analysis of wave 1 suggested that it is due to a reversible four electron transfer reaction, Fig. 5-19, so wave 1 in Fig. 5-18 is attributed to the following reaction:

$$PtO_2 + 2H_2O + 4e^- \rightleftarrows Pt + 4OH^- \qquad (5\text{-}23)$$

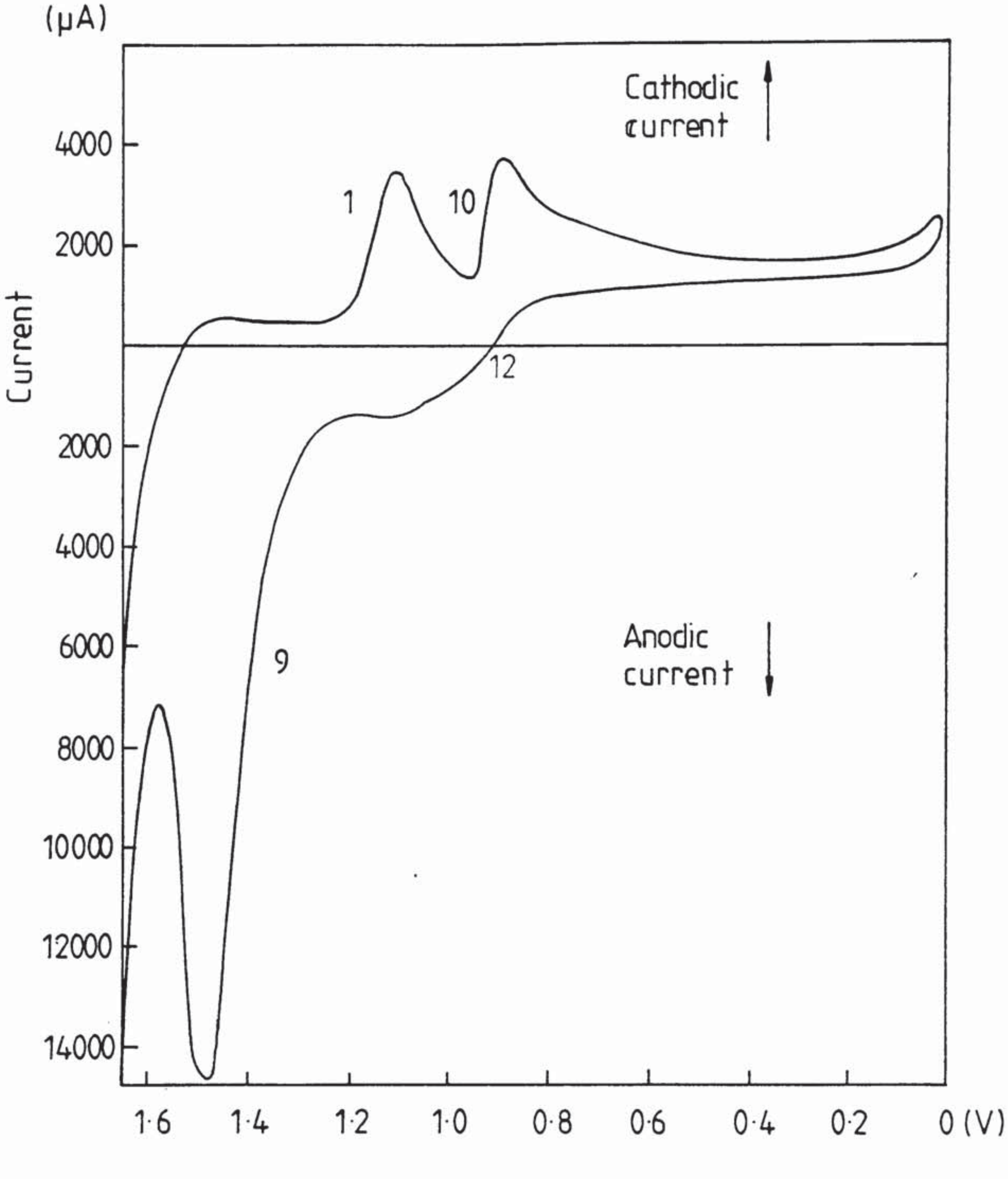

Potential vs Cathodic limit of the melt.

Figure 5–18 Cyclic voltammogram of (Na-K)OH eutectic containing $KMnO_4$ (0·09M) at 523K, using a stationary Pt wire indicator electrode under N_2.

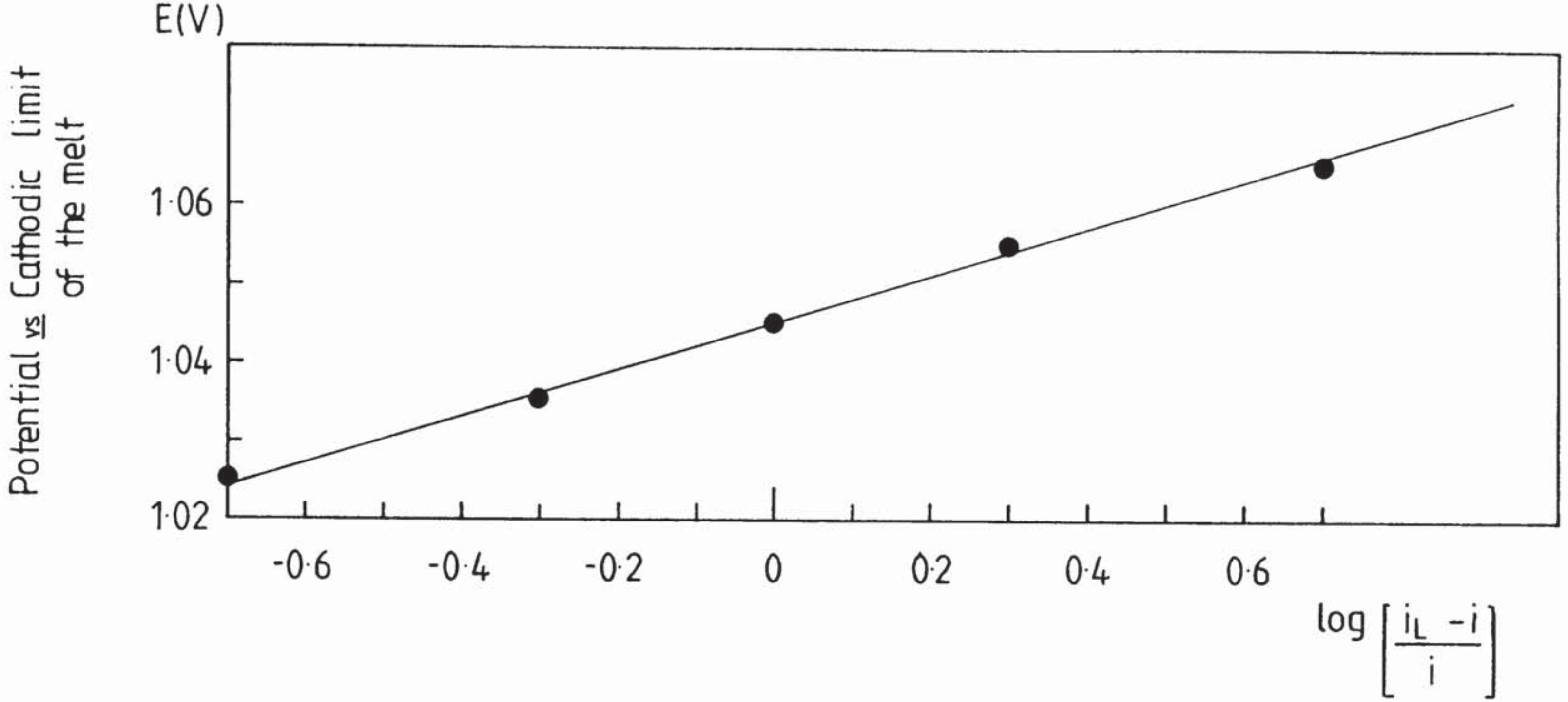

Figure 5-19 H. I. E. Analysis of voltammetric reduction wave 1.

In the voltammogram shown in Fig. 5-20 of the same melt solution used to obtain the voltammograms of Fig. 5-15 and Fig. 5-18, an anodic wave was found on the (r.s) with an $E_{\frac{1}{2}}$ value indicating that it is wave 3, due to the Pt electrode oxidation. The analysis of the wave indicated a reversible two electron transfer reaction, Fig. 5-21, which suggests that Pt oxidation occurs in two stages first to PtO and then to PtO_2.

The second wave on the (f.s) of the cyclic voltammogram of Fig. 5-18 is wave 10 as its $E_{\frac{1}{2}}$ value indicated. On the (r.s) two waves were found, the composite wave 12 and the anodic wave 9. Analysis of wave 12 by H.I.E. plot, again as when the vibrating working electrode was used, showed that melts prepared and scanned on the same day gave a reversible one electron transfer reaction, Fig. 5-22, while melts scanned after twenty four hours from preparing, the analysis gave an irreversible reaction for that wave.

5.5.1 The Voltammograms of (Na-K)OH Eutectic Containing $KMnO_4$ Using a Ni Working Electrode

Goret and Tremillon (31) in their investigations of the pure hydroxide melt used three different working electrodes, rotating Ni and Pt as well as a carbon electrode, apparently to study the electrochemical reactions involving the electrode material in the melt Eluard and Tremillon (7) used rotating Ni and Pt working electrodes in hydroxide melts containing $KMnO_4$. It was thought that using a Ni working electrode in the present work would confirm the results obtained in Section 5.5.

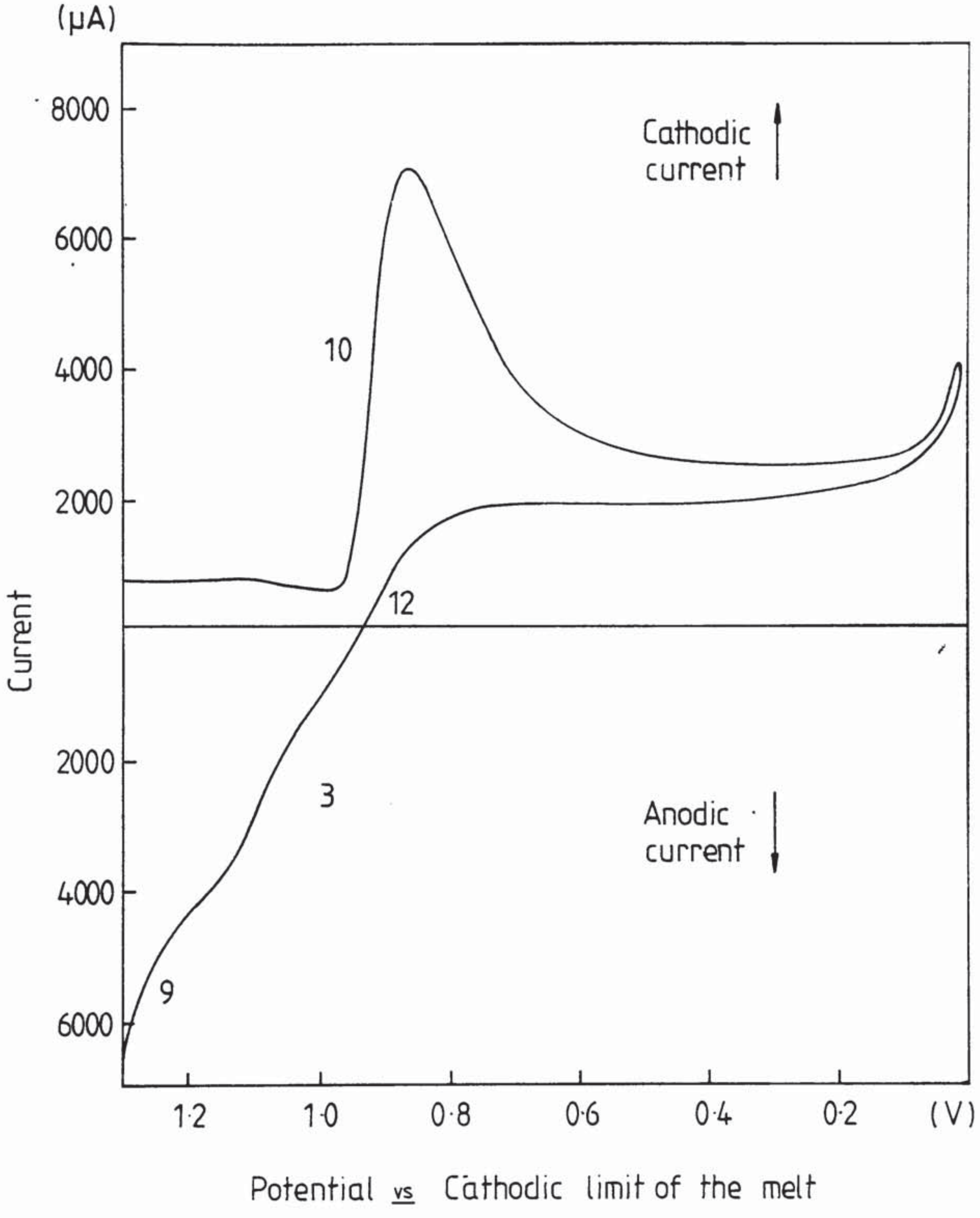

Figure 5-20 Cyclic voltammogram of (Na - K)OH eutectic containing $KMnO_4$ (0·09M) at 523K, using a stationary Pt wire indicator electrode. (showing wave 3)

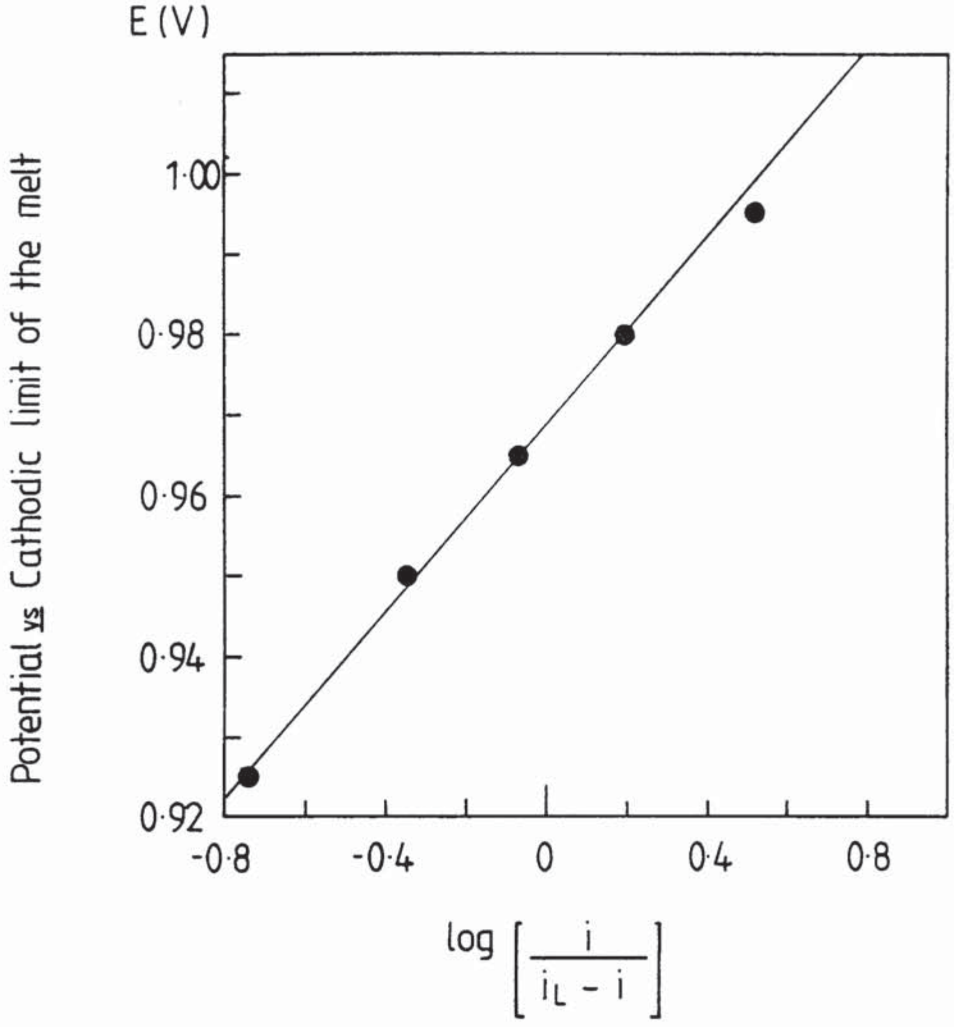

Figure 5-21 H.I.E. Analysis of voltammetric oxidation wave 3.

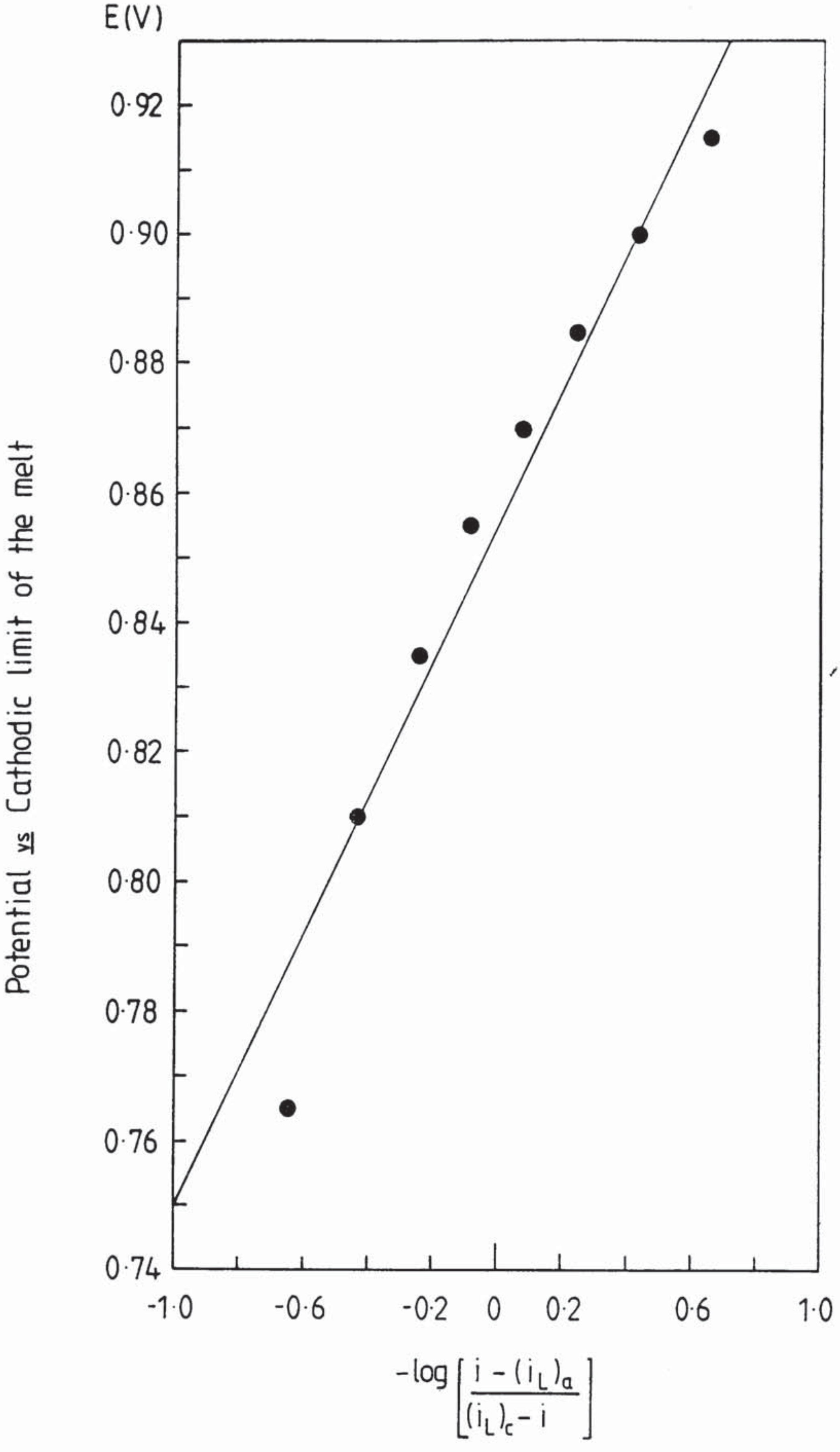

Figure 5-22 H.I.E. Analysis of voltammetric composite wave 12.

It was expected to find the same waves and peaks attributed to manganese oxides and manganates but obviously not those attributed to Pt electrode reactions with the melt. A voltammogram of the pure hydroxide melt ($pH_2O=0.5$) obtained using the vibrating Ni working electrode is presented in Fig. 5-23. On the (f.s) two cathodic waves close to the cathodic limit were found, which have been assigned wave numbers 14 and 15, their $E_{\frac{1}{2}}$ values are 0.24V and 0.08V respectively. Analysis of wave 14 by H.I.E. plot gave a straight line with a slope of 0.055V indicating a reversible two electron transfer reaction. The $E_{\frac{1}{2}}$ value of wave 14 compares favourably with the value given by Goret and Tremillon (31) for the reaction:

$$NiO + H_2O + 2e^- \rightleftarrows Ni + 2OH^- \qquad (5\text{-}24)$$

wave 15 was found to be irreversible and appears only in basic or slightly acidic melts and not in acidic melts, its $E_{\frac{1}{2}}$ value suggest that it is due to the couple NiO_2^{2-}/Ni. Goret and Tremillon found a wave due to that couple only in basic melts.

On the (r.s) two waves were found which were assigned wave numbers 16 and 17. Wave 16 is a small peak with an E_p value close to the $E_{\frac{1}{2}}$ value of wave 14. Wave 17 is a large anodic peak its E_p value of 0.55V compares closely with the value obtained by Goret and Tremillon for the reaction:

$$NiO + 2OH^- - 2e^- \rightleftarrows NiO_2 + H_2O \qquad (5\text{-}25)$$

To the same melt 0.73g of $KMnO_4$ (0.09M) was added with N_2 stirring. A voltammogram of the melt solution using

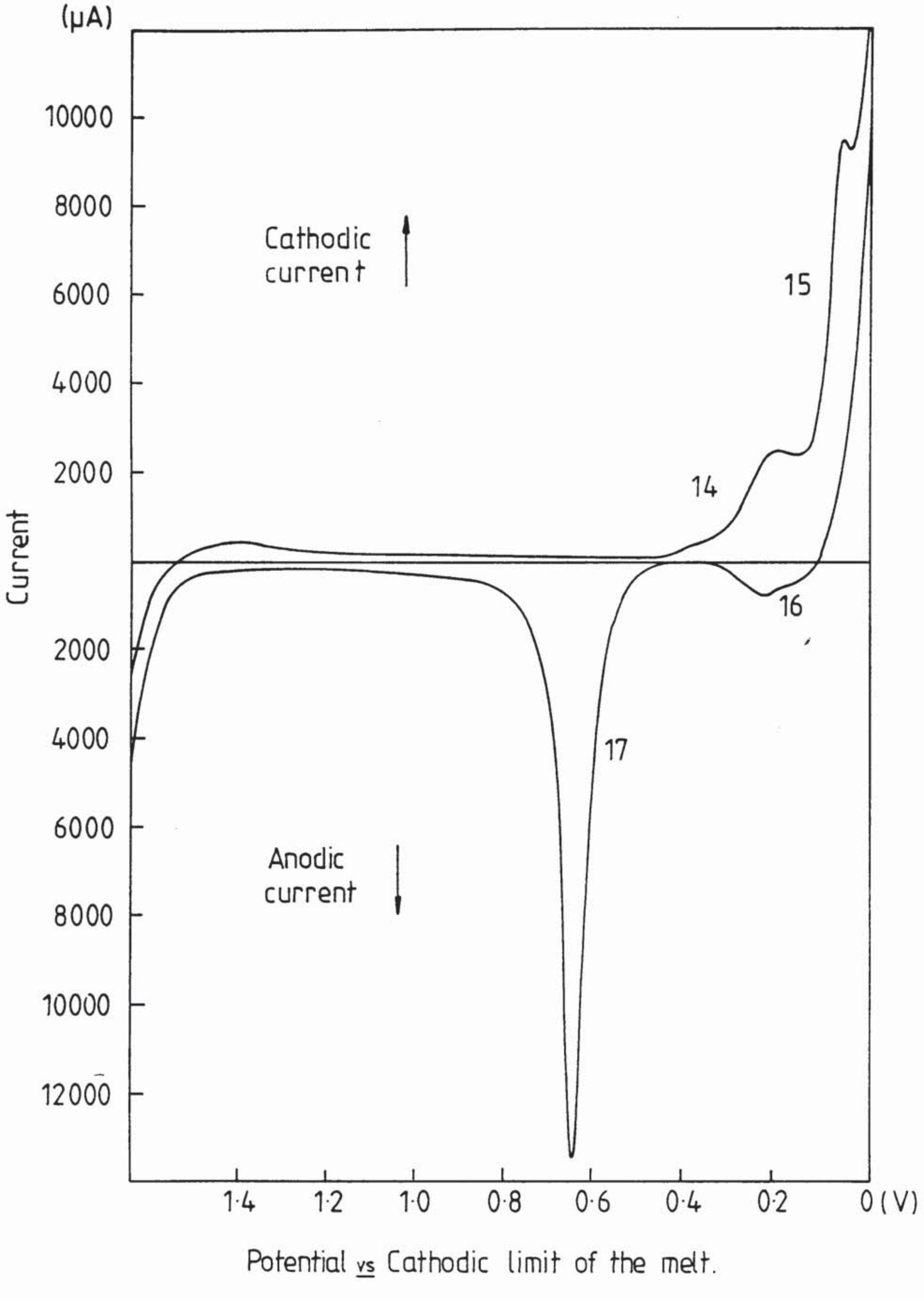

Figure 5-23 Voltammogram of (Na-K)OH eutectic at 523K, under N_2 using a vibrating Ni indicator electrode.

the vibrating Ni working electrode is shown in Fig. 5-24. In addition to the waves found in the voltammogram of the pure melt two more waves were found, one cathodic on the (f.s) and one anodic on the (r.s). The cathodic wave has been assigned wave number 18 and the anodic wave number 19, the $E_{\frac{1}{2}}$ values of waves 18 and 19 were very close and it was thought that these two waves due to the couple MnO_4^{3-}/Mn_2O_3. Waves 18 and 19 were found to be irreversible. It was surprising that the wave due to the oxidation of MnO_4^{3-} to MnO_4^{2-} did not appear.

5.5.2 Discussion

Eluard and Tremillon (7) added $KMnO_4$ to molten (Na-K)OH and suggested that the following reaction occured:

$$3MnO_4^- + 8OH^- \rightleftarrows 3MnO_4^{3-} + 2O_2^- + 4H_2O \qquad (5\text{-}26)$$

They then carried out voltammetric analysis of the solution using a rotating disc electrode. By scanning from positive to negative potentials at 1.2 V/min they obtained a voltammogram which exhibited two cathodic waves, the first wave being approximately twice as large as the second. They suggested the waves were due respectively to the following reactions:

$$Mn(V) + 2e^- \rightleftarrows Mn(III) \qquad (5\text{-}27)$$

$$Mn(III) + e^- \rightleftarrows Mn(II) \qquad (5\text{-}28)$$

At a slower scan speed of 0.24 V/min only one wave was found and this formed a maximum, the wave corresponded to the first wave found at 1.2 V/min. The electrode surface was found to be covered by a black precipitate probably Mn_2O_3. They suggested at the higher scan speed

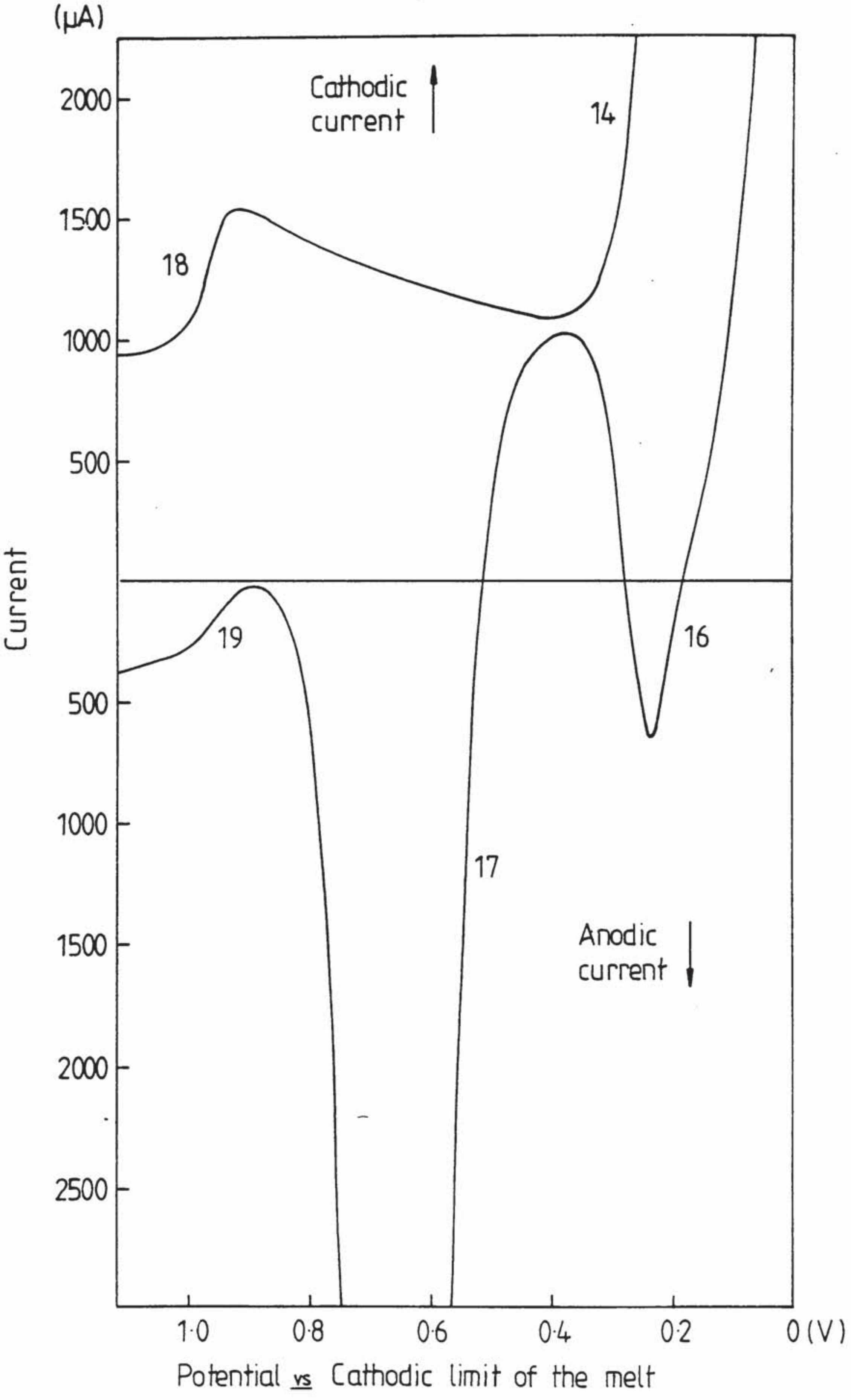

Figure 5-24 Voltammogram of (Na-K)OH eutectic containing $KMnO_4$ (0·09M) at 523K, using a vibrating Ni indicator electrode.

the precipitate is not given sufficient time to form on on the electrode and therefore prevent the second wave being seen. The results obtained in the present work suggest a rather different interpretation for the corresponding waves found by Eluard and Tremillon. The following reaction is proposed based on these results as a follow-up reaction to reaction (5-26):

$$MnO_4^{3-} + 4OH^- + 5O_2 \rightleftarrows MnO_2 + 7O_2^- + 2\,H_2O \qquad (5\text{-}29)$$

The O_2 in this reaction is thought to have originated from the reaction of O_2^- [produced from reaction (5-26)] with water according to reaction (5-9):

$$4O_2^- + 2H_2O \rightleftarrows 3O_2 + 4OH^-$$

Reaction (5-29) suggests that MnO_2 rather than Mn_2O_3 exist in the melt for some time after adding $KMnO_4$ to the pure melt. Also O_2^- produced from reaction (5-26) will exist in the melt for a similar length of time to that of MnO_2 (approximately 2-3 hrs) and continue to produce O_2 via reaction (5-9). Hence the indication of a reversible one electron transfer reaction resulted from analysing the composite wave 12 on the (r.s) of the voltammogram in Fig. 5-14 can be attributed to the following reaction:

$$MnO_4^{3-} + 3O_2 + e^- \rightleftarrows MnO_2 + 4O_2^- \qquad (5\text{-}30)$$

On the (r.s) of the voltammogram of Fig. 5-15, the appearance of wave 11 did not depend on the scan rate, as Eluard and Tremillon reported on the corresponding wave, but it was dependent on the chemical reactions that was taking place in the melt.

Wave 11, as mentioned in Section 5.5 is due to reaction (5-13):

$$Mn_2O_3 + 3H_2O + 2e^- \rightleftarrows 2Mn^{2+} + 6OH^-$$

as can be seen in the Pourbaix diagram of the melt, Fig. 3-3, the Mn^{2+}ions should not exist in a melt with a pH_2O value of 0.5 therefore it must have been produced electrochemically according to reaction (5-13).

Mn_2O_3 on the other hand was also produced electrochemically via the cathodic reaction represented by wave 10.

$$2MnO_4^{3-} + 5H_2O + 4e^- \rightleftarrows Mn_2O_3 + 10\ OH^- \qquad (5-12)$$

Hence wave 11 did not appear in Fig. 5-14 while it did in Fig. 5-15 when MnO_2 would have disporportionated according to:

$$4MnO_2 + 6OH^- \rightleftarrows Mn_2O_3 + 2MnO_4^{3-} + 3H_2O \qquad (5-31)$$

Therefore Mn_2O_3 is available for reduction, giving rise to wave 11.

Analysis of wave 9 showed that a plot of E vs.log $[(i_L-i)/i]$of the rising portion of the curve before the peak produced a straight line until a potential was reached such that the anode surface becomes inhibited with adsorbed material. The deviation from linearity is observed to correspond to a point approximately one third of the way up the rising portion of the curve, the expected slope value of 0.104V for a reversible one electron transfer reaction was not obtained but the value obtained deviates by only 14 mV from the theoretical value. That might have been caused by the presence of some MnO_4^{2-}ions in the melt which are strongly adsorbed. The regaining of the reversibility by drying the melt (eliminating MnO_4^{2-} ions totally) proves that MnO_4^{2-} ions were the reason for the deviation from reversibility. That wave 1 was generally found using a stationary working electrode but not when a vibrating working electrode was used is because using a vibrating electrode forced diffusion of the platinum oxide into the bulk solution is induced away from the electrode surface, therefore preventing wave 1 from being seen.

The voltammogram of this melt is in contrast with that of the pure melt where wave 1 was due to an irreversible reaction, while here because of the oxidizing nature of this melt (presence of manganates), the Pt was oxidized reversibly into PtO_2 as indicated from the analysis of wave 1. The use of the nickel working electrode has failed to give a clearer picture about the various electro chemical reactions occuring in the melt compared with the Pt working electrode. Clearly the Ni electrode proved to be inconvenient to use in the electrochemical analysis of the (Na-K)OH eutectic.

5.6 <u>(Na-K)OH Eutectic Containing Mn Metal and $KMnO_4$</u>

To molten (Na-K)OH containing Mn metal (0.163M) at 523K was added 0.73g of $KMnO_4$ (0.09M) with N_2 stirring, the pH_2O of the melt was about 0. The melt colour was bluish-green. A voltammogram using the vibrating Pt indicator electrode of the melt solution is shown in Fig. 5-25. Two waves were found on the (f.s), a reduction peak which has been assigned wave number 20 attributed to the electrochemical reduction:

$$MnO_4^{2-} + e^- \rightleftarrows MnO_4^{3-} \qquad (5-15)$$

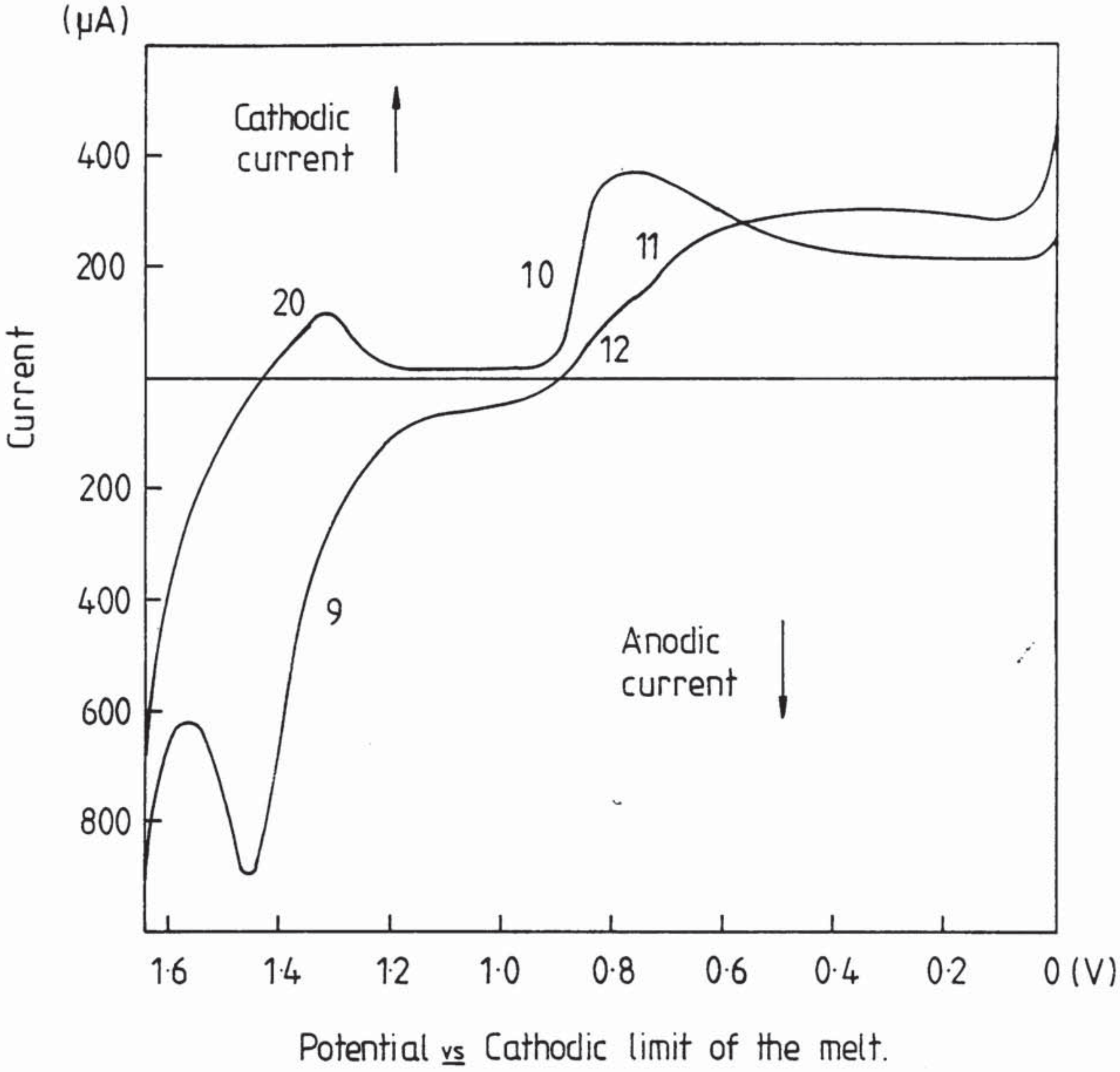

Figure 5–25 Voltammogram of (Na–K)OH eutectic containing Mn metal (0·163M) and $KMnO_4$ (0·09M) at 523K, under N_2, using a vibrating Pt indicator electrode.

The second wave is wave 10 which is peak shaped. On the (r.s) three waves were found, the first one is a cathodic wave, the second is mainly cathodic, slightly composite, i_L between these two waves is poorly defined. These two waves are in fact waves 11 and 12. The third wave is an anodic peak which is wave 9. Analysis of wave 10 by H.I.E. plot gave a straight line with a slope of 0.031V, Fig. 5-26. The theoretical value of 0.034V is expected for a reversible three electron transfer reaction at 523K therefore wave 10 in this voltammogram is due to reaction (5-11):

$$MnO_4^{3-} + 3H_2O + 3e^- \rightleftarrows MnO(s) + 6OH^-$$

Analysis of wave 11 by H.I.E. plot gave a straight line with a slope of 0.091V while that of wave 12 gave a slope of 0.088V indicating that these two waves are due to irreversible electrode reactions, however from their $E_{\frac{1}{2}}$ values, wave 11 is attributed to reaction (5-13) and wave 12 is attributed to reaction (5-11). It was noticed that if the water concentration of the melt increased, the $E_{\frac{1}{2}}$ value of wave 11 increased to the value of the couple Mn_2O_3/MnO according to the following reaction:

$$Mn_2O_3(s) + H_2O + 2e^- \rightleftarrows 2MnO(s) + 2OH^- \qquad (5\text{-}32)$$

The fact that waves 9 and 20 are peaks in spite of using a vibrating indicator electrode is due to adsorption which can cause undesirable phenomena in voltammetric analysis.

Again the limiting current of wave 9 in Fig. 5-25 as in the voltammograms of section 5.5 was not constant

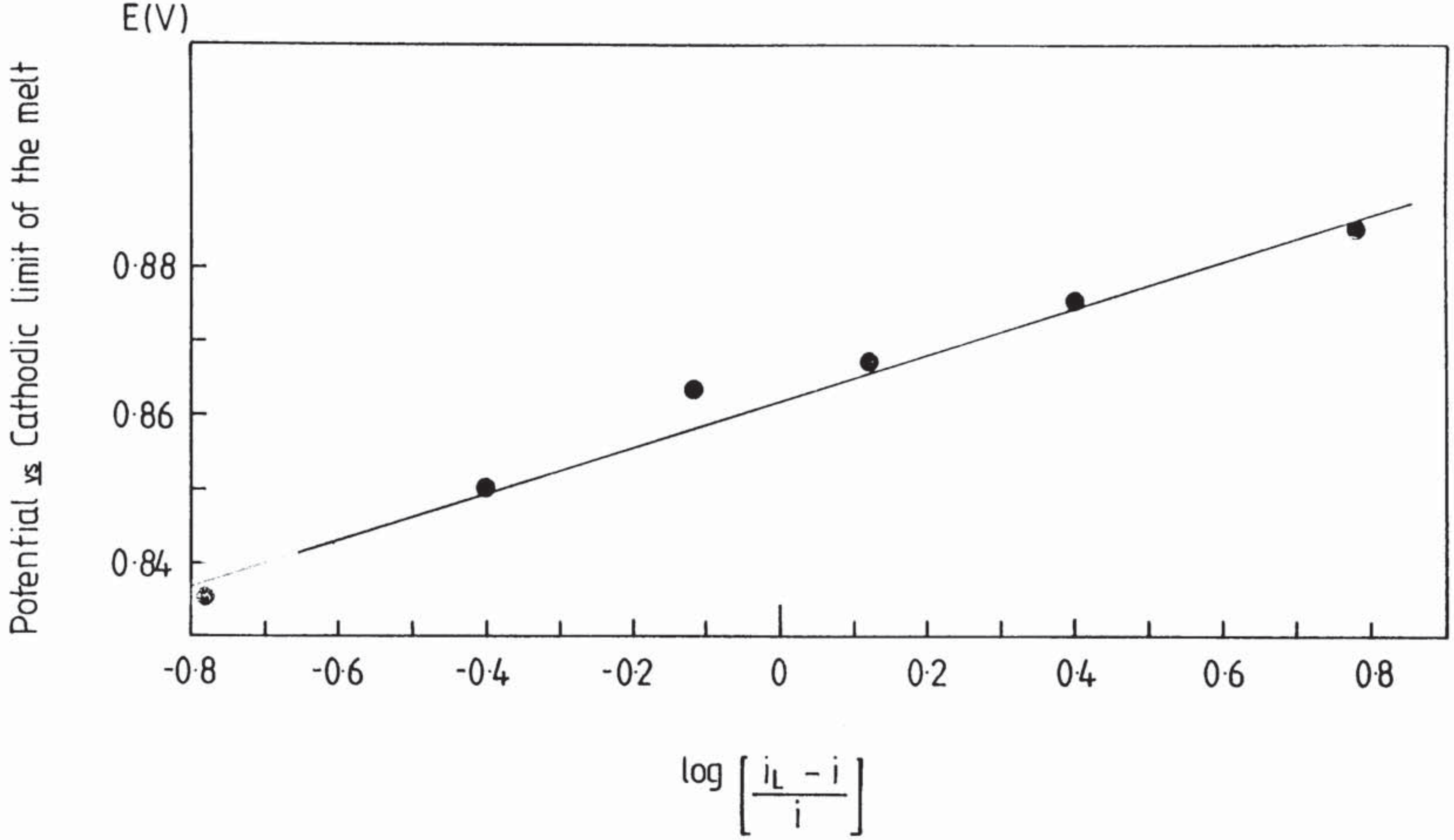

Figure 5-26 H.I.E. Analysis of voltammetric reduction wave 10.

while the i_L values of all the other waves, including i_p for wave 20, were constant. All the other observations and the factors that influenced wave 9, were mentioned in section 5.5, these are applicable for wave 9 in this voltammogram too. Clearly, there is no point in measuring i_p for wave 9, because it is not the true i_p, which is essential in testing for the reversibility of waves 20 and 9 due to the couple MnO_4^{3-}/MnO_4^{2-}.

However, the peak potential separation was 0.14V compared with the theoretically expected 0.104V for a reversible one electron transfer reaction at 523K. Analysis of wave 9 by H.I.E. plot, E vs. log $[(i_L-i)/i]$ gave a straight line over the range $(0.0-0.58)i_p$ with a slope of 0.125V, but E vs. log $[(i_L-i)^{0.5}/i]$, a plot suggested by Reinmuth (94) gave a straight line over the whole range of current with a slope of 0.123V which is still indicative of an irreversible electrode process. Single-sweeps were also carried out using the vibrating indicator electrode from the anodic to the cathodic limit and vice versa, no significant change of the voltammogram was observed.

The effects of other scan rates than the normal one of 9,6V/min, were studied. The scan rates used were 3.2, 4.8 and 19.2V/min. Using the vibrating indicator electrode with the high scan rate of 19.2 V/min, Fig.5-27, on the (f.s) wave 20 has disappeared but on the (r.s) wave 9 has become a wave and not a peak as it was at the normal scan rate. H.I.E. plot analysis gave a straight line with a slope of 0.1V, Fig. 5-28, suggesting

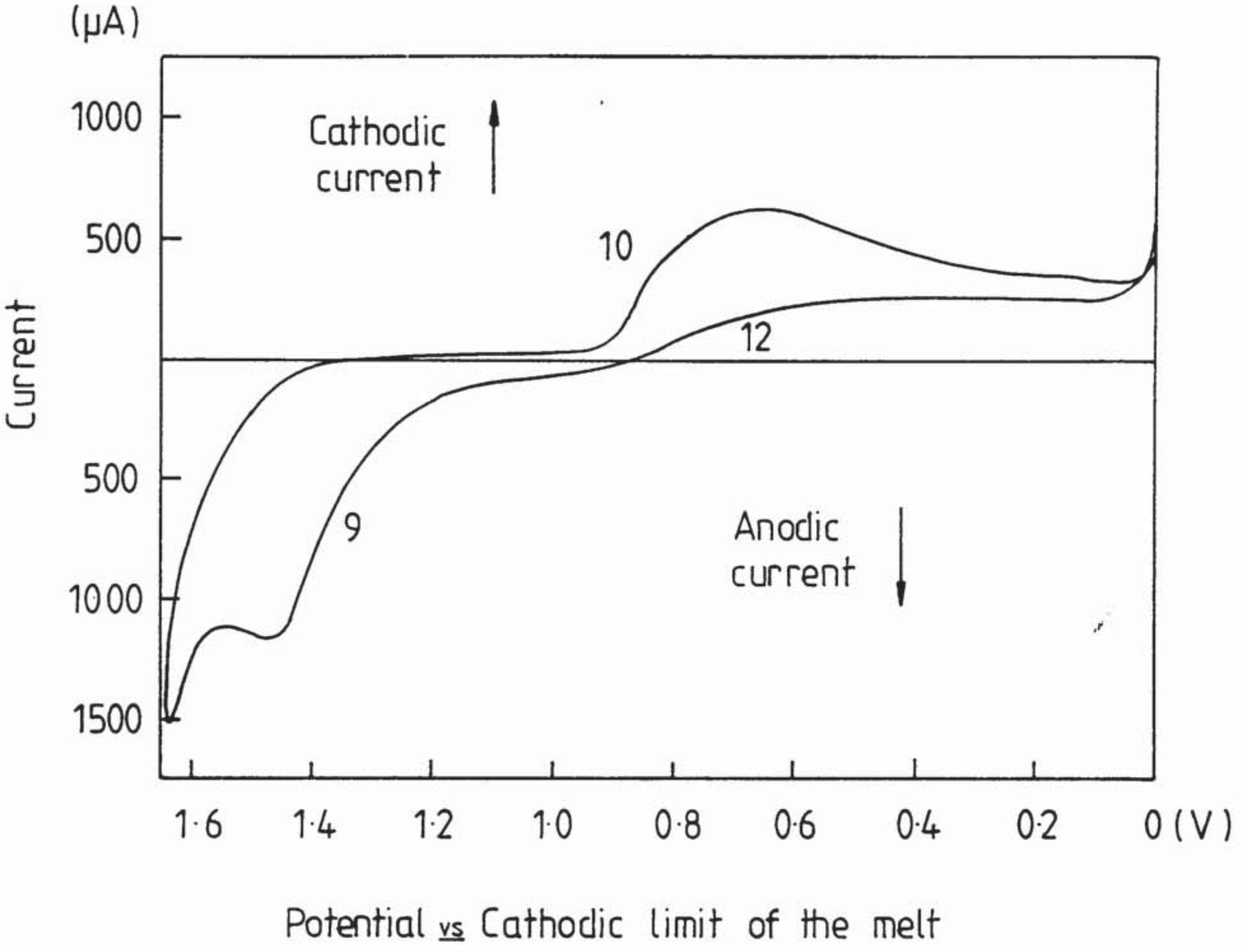

Figure 5-27 Voltammogram of (Na-K)OH eutectic containing Mn metal (0·163M) and $KMnO_4$ (0·09M) at 523K, under N_2, using a vibrating Pt indicator electrode. (Scan rate = 19·2 V min^{-1})

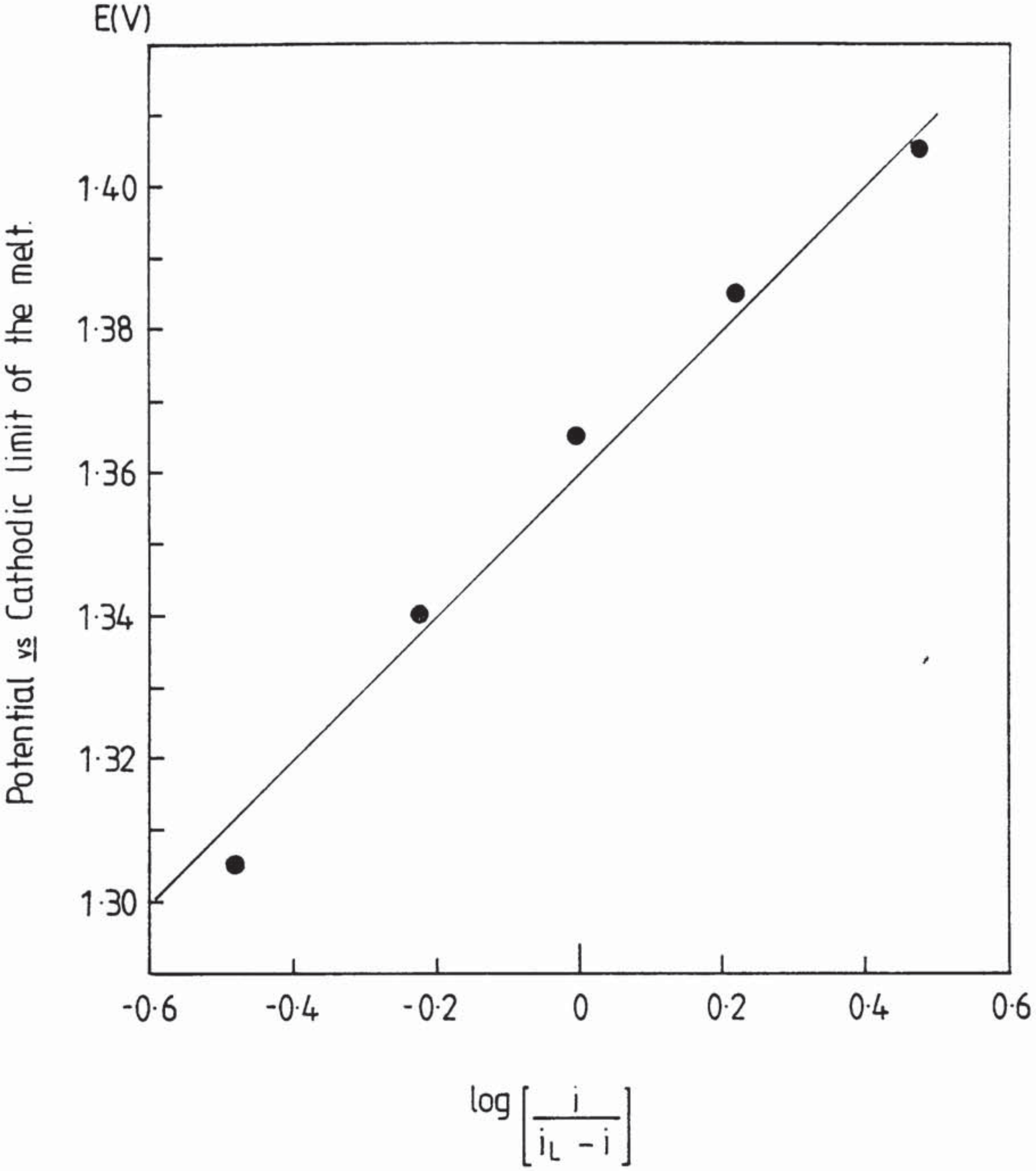

Figure 5-28 H. I. E. Analysis of voltammetric oxidation wave 9.

that wave 9 has become due to a reversible one electron transfer reaction. It is clear therefore that at fast scan rates the time is insufficient for adsorption to take place on the electrode and influence the electrode reaction, the $E_{\frac{1}{2}}$ value of wave 9 has not changed. The H.I.E. plot analysis of the peak shaped cathodic wave 10 gave a straight line with a slope of 0.104V, Fig. 5-29, indicating that at the high scan rate of 19.2V/min the electrode reaction becomes a reversible one electron transfer, which could be attributed to the following reaction:

$$MnO_4^{3-} + 2H_2O + e^- \rightleftarrows MnO_2 + 4OH^- \qquad (5\text{-}33)$$

Waves 11 and 12 have become one large composite wave ($E_{\frac{1}{2}}$ = 0.76V) which is due to an irreversible electrode reaction attributed to the couple Mn_2O_3/MnO, [reaction (5-32)]. At the lower scan rates of 3.2 and 4.8V/min the voltammograms obtained were more or less similar to the normal voltammogram obtained at 9.6V/min. At 3.2V/min the peak potential separation between waves 20 and 9 is 0.11V compared with 0.14V at the normal scan rate of 9.6V/min, which is expected, knowing that the faster the scan rate, the larger the separation in peak potential becomes. Again cyclic voltammetry was carried out as a further check on the reversibility of the various couples in this melt. In Fig. 5-30 is shown a cyclic voltammogram of the melt using a stationary working electrode. On the (f.s) there are three reduction waves, wave 20 is the peak due to MnO_4^{2-} reduction, wave 1 is a small cathodic peak due to Pt electrode dissolution of the oxide film formed on the (r.s), wave 10 is also a peak

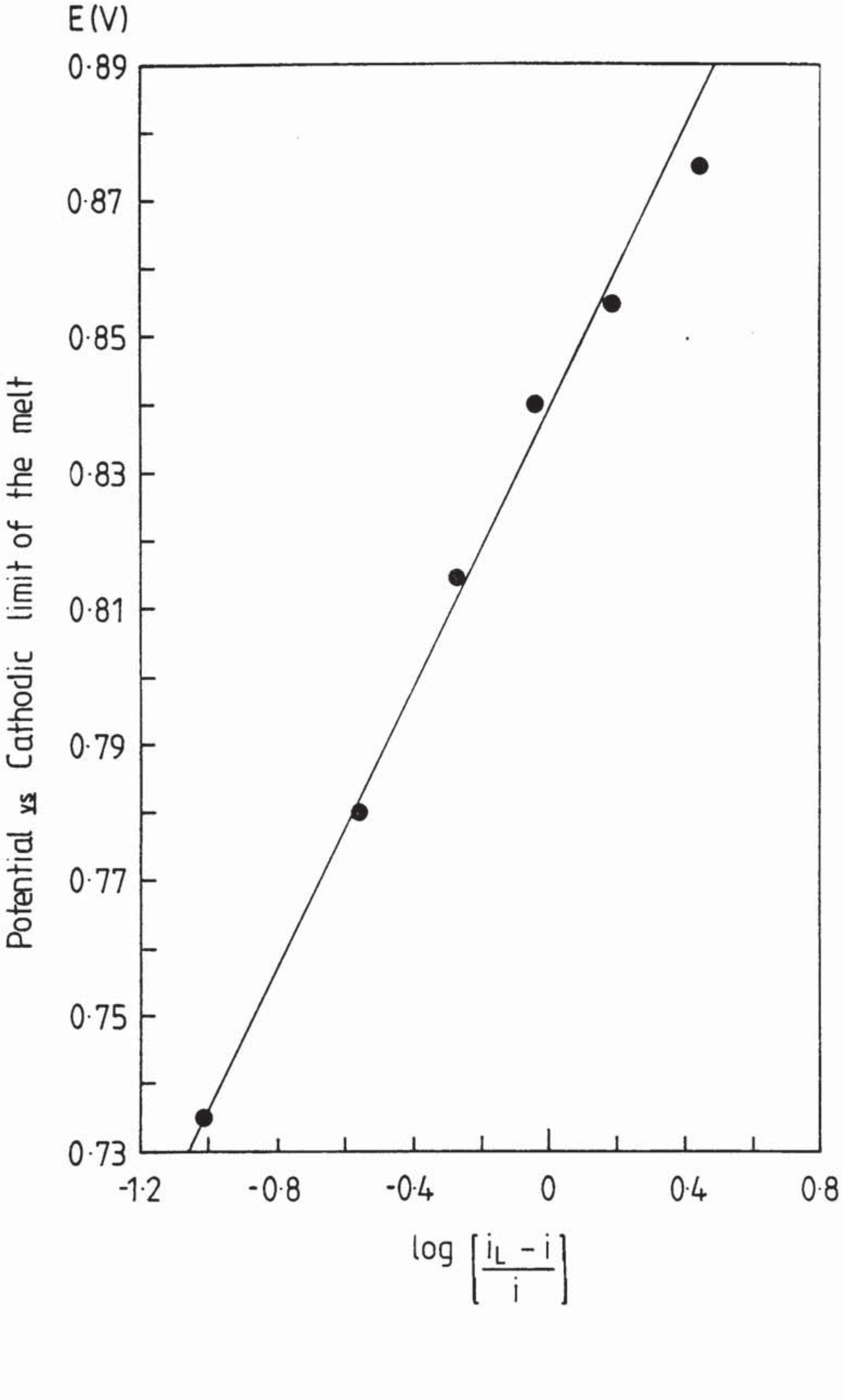

Figure 5-29 H.I.E. Analysis of voltammetric reduction wave 10.

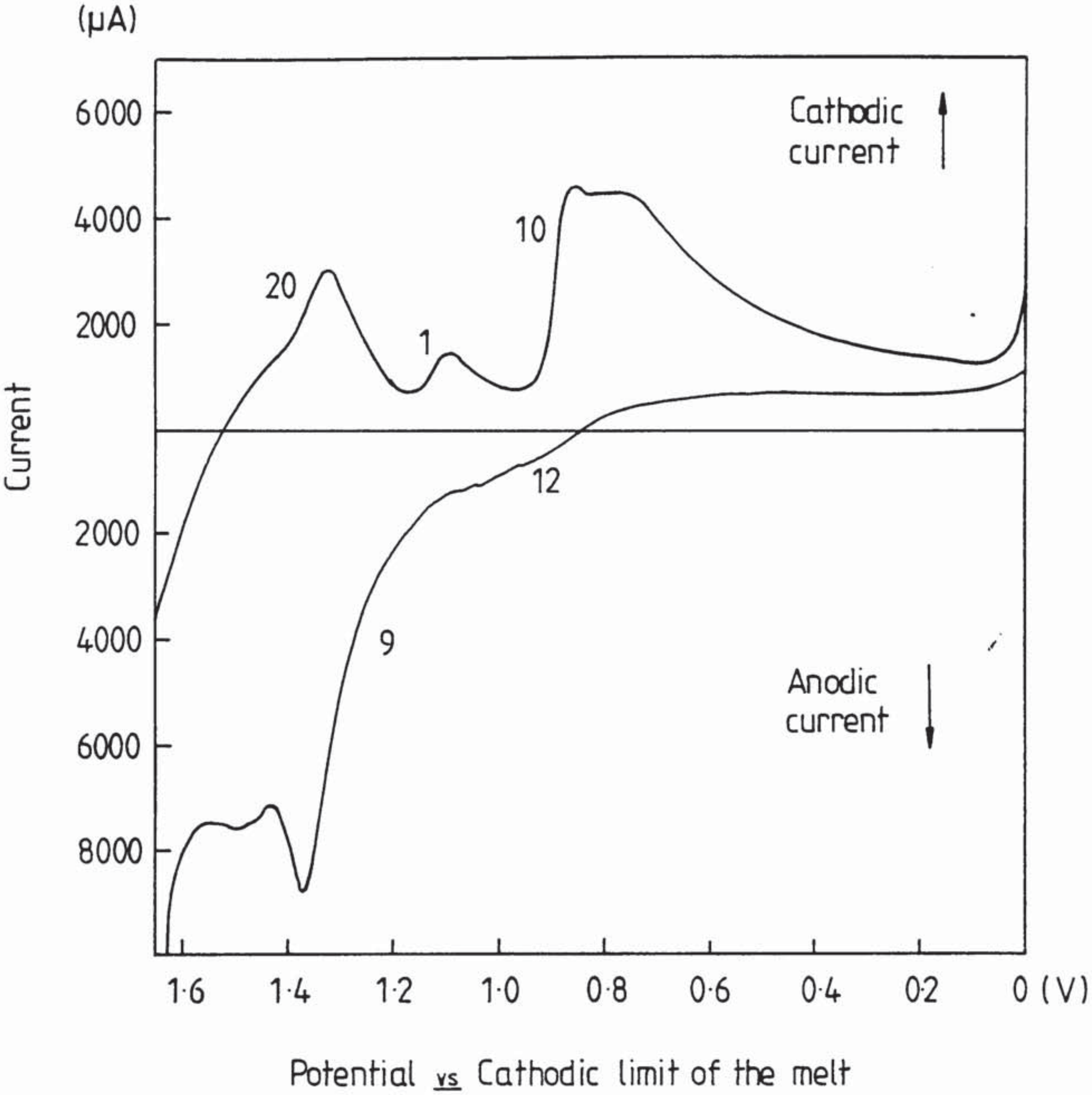

Figure 5-30 Cyclic voltammogram of (Na - K)OH eutectic containing Mn metal (0·163M) and K MnO_4 (0·09M) at 523K, under N_2 using a stationary Pt wire indicator electrode.

but here, the current rises steeply followed by a plateau then the current drops, wave 10 is obviously due to the same elctrode reaction using the vibrating working electrode, reaction (5-11). On the (r.s) an irreversible composite wave was found, its $E_{\frac{1}{2}}$ value suggested that it is due to the couple MnO_4^{3-}/MnO reaction (5-11). This wave was not easily reproducible; in some voltammograms it did not look like a wave and when it appeared its i_L was poorly defined. Wave 9 was distrubed by adsorption to a greater degree than when the vibrating working electrode was used, its $E_{\frac{1}{2}}$ value stayed unchanged but the wave was followed by a small adsorption wave or peak. Wave 9 appeared in some voltammograms as a wave and in others as a peak or semipeak. Its analysis by H.I.E. plot showed that it is irreversible. Clearly, by using a vibrating electrode, the adsorbed molecules e.g. O_2 or H_2, are forced to diffuse away from the electrode surface before they can react chemically or electrochemically.

Using lower scan rates of 3.2 and 4.8V/min, the voltammograms were not very different from the voltammogram obtained using the scan rate of 9.6 V/min, except that the $E_{\frac{1}{2}}$ value of the waves on the (f.s) becomes closer to the corresponding ones on the (r.s). Unlike the voltammogram obtained using the vibrating electrode and a high scan rate, Fig. 5-27, where waves 9 and 10 became clearly due to reversible one electron transfer reactions, using the stationary electrode and the same high scan rate, waves 9 and 10 stayed irreversible.

also wave 20 did not disappear as was the case in Fig. 5-27.

5.6.1 (Na-K)OH Eutectic Containing Mn Metal and $KMnO_4$ With O_2 Passage

Using the same melt containing Mn metal (0.163M) and $KMnO_4$ (0.09M) at 523K, $pH_2O = 0$, O_2 was bubbled through the melt for one hour. In Fig. 5-31 is presented the voltammogram (using the vibrating working electrode) of the melt immediately after the O_2 bubbling was stopped. On the (f.s) as found previously two waves were present wave 20 (peak) and wave 10. On the (r.s) one reduction wave, slightly composite, and the oxidation wave due to MnO_4^{3-} oxidation (wave 9) were found. Analysis of wave 10 by H.I.E. plot gave a straight line with a slope of 0.024V, Fig. 5-32, indicating a four electron transfer electrode process. The theoretical value expected for a reversible four electron transfer reaction at 523K is 0.026 V. The $E_{\frac{1}{2}}$ value of wave 10 has increased to 0.925V which is nearer to the $E_{\frac{1}{2}}$ value for the couple Mn_2O_3/MnO_4^{3-}, therefore wave 10 in this voltammogram is attributed to reaction (5-12).

The first wave on the (r.s) was found to be irreversible, however its $E_{\frac{1}{2}}$ value suggested that it is due to reaction (5-11). A split of wave 9 (peak) has taken place and that is expected because as previously mentioned, adsorption of O_2 produced at the anodic limit of the melt on the electrode surface causes various undesirable phenomena to wave 9, so bubbling O_2 will obviously enhance these effects. That split might also be caused because the product of the elctrode

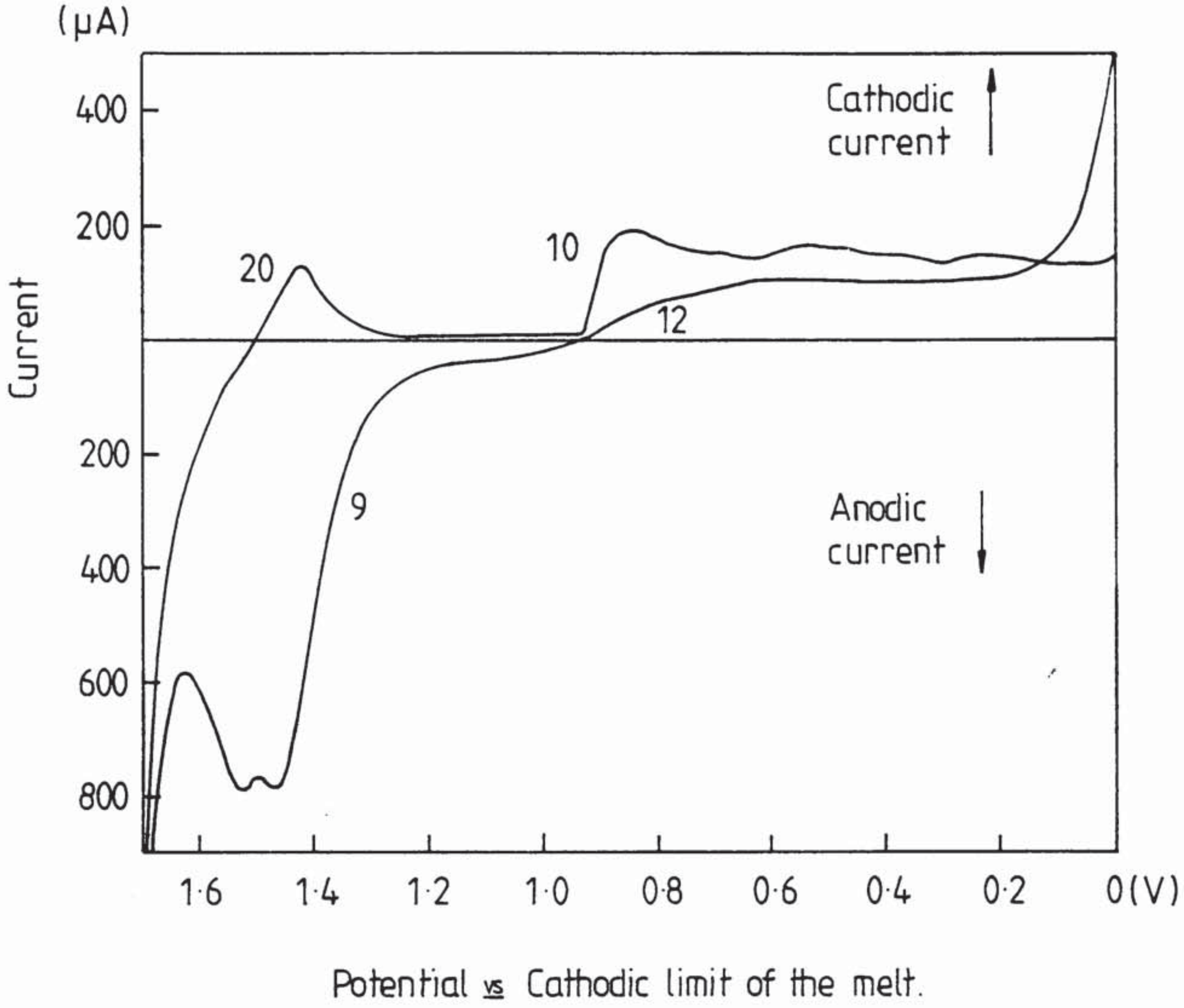

Figure 5-31 Voltammogram of (Na-K)OH eutectic containing Mn metal (0·163M) and $KMnO_4$ (0·09M) at 523K, under O_2 using a vibrating Pt indicator electrode.

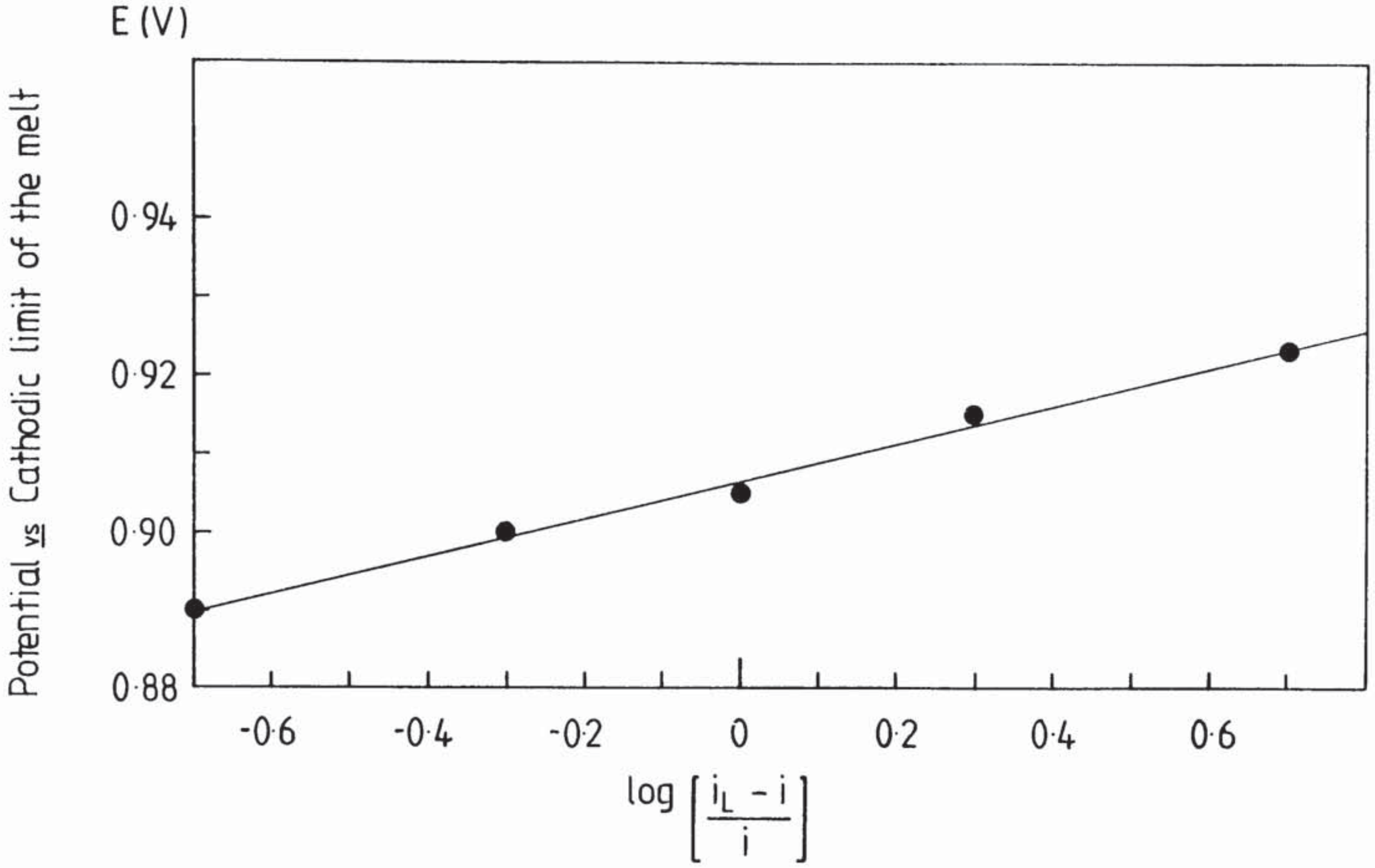

Figure 5-32 H. I. E: Analysis of voltammetric reduction wave 10.

reaction i.e. MnO_4^{2-} is strongly adsorbed (95).

Cyclic voltammetry (using a stationary electrode) gave a voltammogram similar to that obtained using the vibrating electrode except that when wave 12 on the (r.s) was analysed by H.I.E. plot, it gave a straight line with a slope of 0.103V, Fig. 5-33, which is the expected theoretical value for a reversible one electron transfer reaction at 523K.

5.6.2 Discussion

Eluard and Tremillon (7) reported that MnO_4^{2-} ions only existed in hydroxide melts when an atmosphere of O_2 was maintained above the melt and that the melt had to be very acidic. They found a wave due to the reduction of MnO_4^{2-} in a voltammogram of the melt containing $KMnO_4$ under these conditions. Lux and Niedermaier (36) also made a similar observation.

The results in the present work are in direct conflict with the results reported by these other workers, since a wave due to MnO_4^{2-} reduction to MnO_4^{3-} according to reaction (5-15)

$$MnO_4^{2-} + e^- \rightleftarrows MnO_4^{3-}$$

was found (wave 20) in a voltammogram of the melt containing Mn metal and $KMnO_4$ (pH_2O = 0) whether the melt was under N_2 or O_2. Also the melt did not need to be very acidic. Consequently the melt contained both Mn(V) and Mn(VI) at the water concentration mentioned above and it must have come from the added $KMnO_4$ because Mn metal is not expected to produce Mn(VI) as discussed

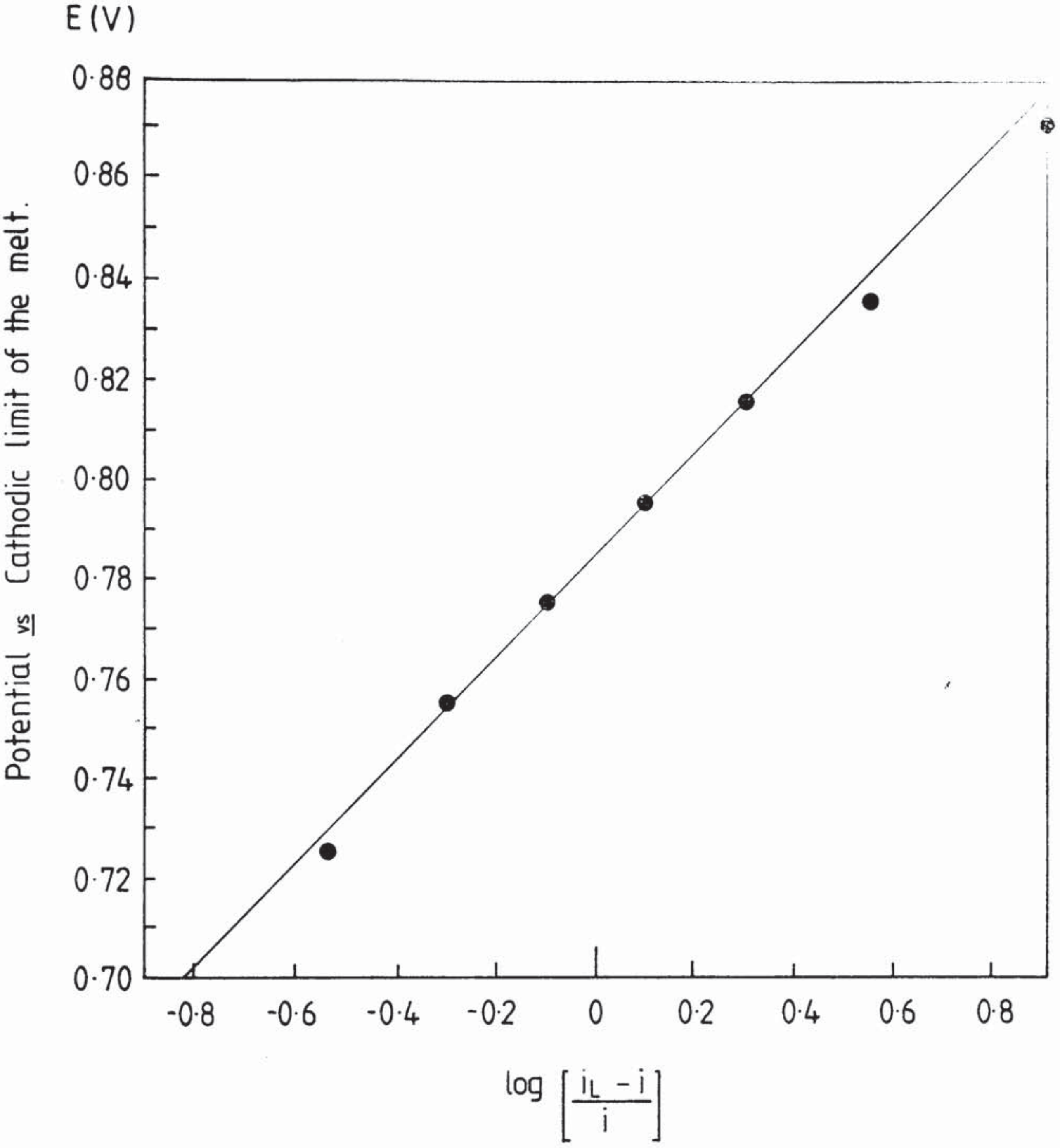

Figure 5-33 H. I. E. Analysis of voltammetric reduction wave 12.

in section 5.4. The reason for the disappearance of wave 20 from the voltammogram of Fig. 5-27 using a vibrating working electrode and high scan rate can be explained on the same basis that made wave 9 deviate from reversibility in the voltammograms in sections 5.5 and 5·6. Knowing that MnO_4^{2-} ions are strongly adsorbed on the Pt electrode, they are reduced as long as they are adsorbed on the electrode surface. Using a vibrating Pt electrode and high scan rate, these ions were desorbed by the action of vibration and were not given sufficient time to be adsorbed because of the high scan rate, which has prevented the reduction wave being seen. The reappearance of the wave using a stationary working electrode and the same high scan rate supports this argument. Wave 9 on the other hand was not affected by the presence of Mn metal or the bubbling of O_2, its interpretation remains the same as that of section 5.5. Wave 10 in sections 5.5 and 5.6 has been attributed to two different electrode reactions, the first was due to the couple MnO_4^{3-}/Mn_2O_3 and the second was due to the couple MnO_4^{3-}/MnO. Furthermore in the voltammogram of the melt solution containing Mn metal and $KMnO_4$, using a high scan rate wave 10 was attributed to the couple MnO_4^{3-}/MnO_2. No new wave numbers were assigned to the wave representing these reactions because the $E_{\frac{1}{2}}$ value of wave 10 was changing within a small potential range (about 0.1V). The $E_{\frac{1}{2}}$ values of each of the couples mentioned above was close to each other. The proposed reactions were based on wave analysis as well as the slight changes in the half-wave potential. However it was concluded that wave 10 was dependant on the melt solution and its contents. It seems that if the melt contains Mn^{2+} ions, the electrode reaction would involve MnO or MnO_2 rather than Mn_2O_3.

Mn_2O_3 was produced by the electrochemical reduction of MnO_4^{3-} and as mentioned in section 5.5, it exists in a melt containing $KMnO_4$ after a certain period of time needed for MnO_2 to disproportionate to Mn_2O_3 and MnO_4^{3-}.

A wave with a half-wave potential value that lies between those of wave 11 and wave 12 was found in the voltammograms of Fig. 5-25 and Fig. 5-27. The wave has been attributed to the couple Mn_2O_3/MnO and no new wave number has been assigned to this wave because it appeared as if that wave 11 has shifted towards more positive potential values or that wave 12 has shifted towards more negative potential values. This wave was found when two parameters were changed. The first was the water concentration of the melt; as it was increased to values more than $pH_2O = 0$, the $E_{\frac{1}{2}}$ value of wave 11 shifted slightly to a more positive value, which was in fact the $E_{\frac{1}{2}}$ value of the couple Mn_2O_3/MnO. The second parameter changed was the scan rate; at the higher scan rate of 19.2V/min, the $E_{\frac{1}{2}}$ value of the composite wave 12 shifted slightly to a more negative value which again was the $E_{\frac{1}{2}}$ value of the couple Mn_2O_3/MnO. This suggests that at higher water concentrations and scan rates, the wave due to the couple Mn_2O_3/MnO appears in preference to that of the couples Mn_2O_3/Mn^{2+} or MnO_4^{3-}/MnO.

In the cyclic voltammogram of the melt containing Mn metal and $KMnO_4$ with O_2 passage, wave 12 which was due to an irreversible electrode reaction using the vibrating electrode became due to a reversible one electron transfer reaction, using the stationary electrode. That could be explained in three steps, the first is that O_2 reacts with the melt to produce O_2^{2-} according to:

$$O_2 + 4OH^- \rightleftarrows 2O_2^{2-} + 2H_2O \qquad (5\text{-}34)$$

The second step also involves O_2, where it oxidizes the Mn_2O_3 which exists in this melt to MnO_2:

$$2Mn_2O_3 + O_2 \rightleftarrows 4MnO_2 \qquad (5\text{-}35)$$

and the third step is the electrochemical reduction to which the wave is due:

$$MnO_2 + O_2^{2-} + e^- \rightleftarrows MnO_4^{3-} \qquad (5\text{-}36)$$

It is assumed that MnO_2 had to be adsorbed onto the Pt electrode surface in order to react electrochemically therefore using a vibrating electrode would subject the adsorbed MnO_2 to forced diffusion into the bulk solution and away from the electrode surface and another electrode reaction then takes place.

As mentioned before the Pt oxide stripping peak was always found in voltammograms of the melt under a N_2 atmosphere using a stationary working electrode. In the cyclic voltammogram of the melt with O_2 passage, that peak was not found, which suggests that the Pt electrode was acting as a Pt oxide electrode and not as a Pt metal electrode as long as the melt was under an O_2 atmosphere, and that a chemical oxidation of the platinum rather than the usual electrochemical oxidation had taken place.

5.7 The Effect of Adding Carbonate and Peroxide To (Na-K)OH Eutectic Containing $KMnO_4$

5.7.1 (Na-K)OH Eutectic Containing $KMnO_4$ and Na_2CO_3

Goret and Tremillon (31) reported that carbonate ions are electrochemically inactive, but carbon was oxidized electrochemically in acidic melts according to the reaction:

$$C + 6OH^- - 4e^- \rightleftarrows CO_3^{2-} + 3H_2O \qquad (5\text{-}37)$$

and in basic melts according to:

$$C + 3O^{2-} - 4e^- \rightleftarrows CO_3^{2-} \qquad (5\text{-}38)$$

P.G. Zambonin (96) in his work with molten nitrates found that carbonates can be oxidized at a Pt electrode according to the reaction:

$$CO_3^{2-} \rightleftarrows CO_2 + \tfrac{1}{2}O_2 + 2e^- \qquad (5\text{-}39)$$

at about 0.5V before the anodic limit of the nitrate melt which makes it very close to the oxidation potential of the hydroxide ion in that melt. Consequently if the hydroxide melt had already contained carbonate ions via the reaction of carbon dioxide (from the atmosphere) with the melt, wave 9 in sections 5.4, 5.5 and 5.6 would probably be due to a mixed process involving the oxidation of MnO_4^{3-} and CO_3^{2-}. Therefore it was decided to investiage such a melt electrochemically. To molten (Na-K)OH, pH_2O = 0.5 at 523K, containing 0.09M $KMnO_4$, 0.053g (0.01M) of Na_2CO_3 was added with N_2 stirring. A voltammogram using the vibrating working electrode is shown in Fig. 5-34
Only the potential range of interest was scanned. On the (r.s) an anodic wave was found with an $E_{\frac{1}{2}}$ value close

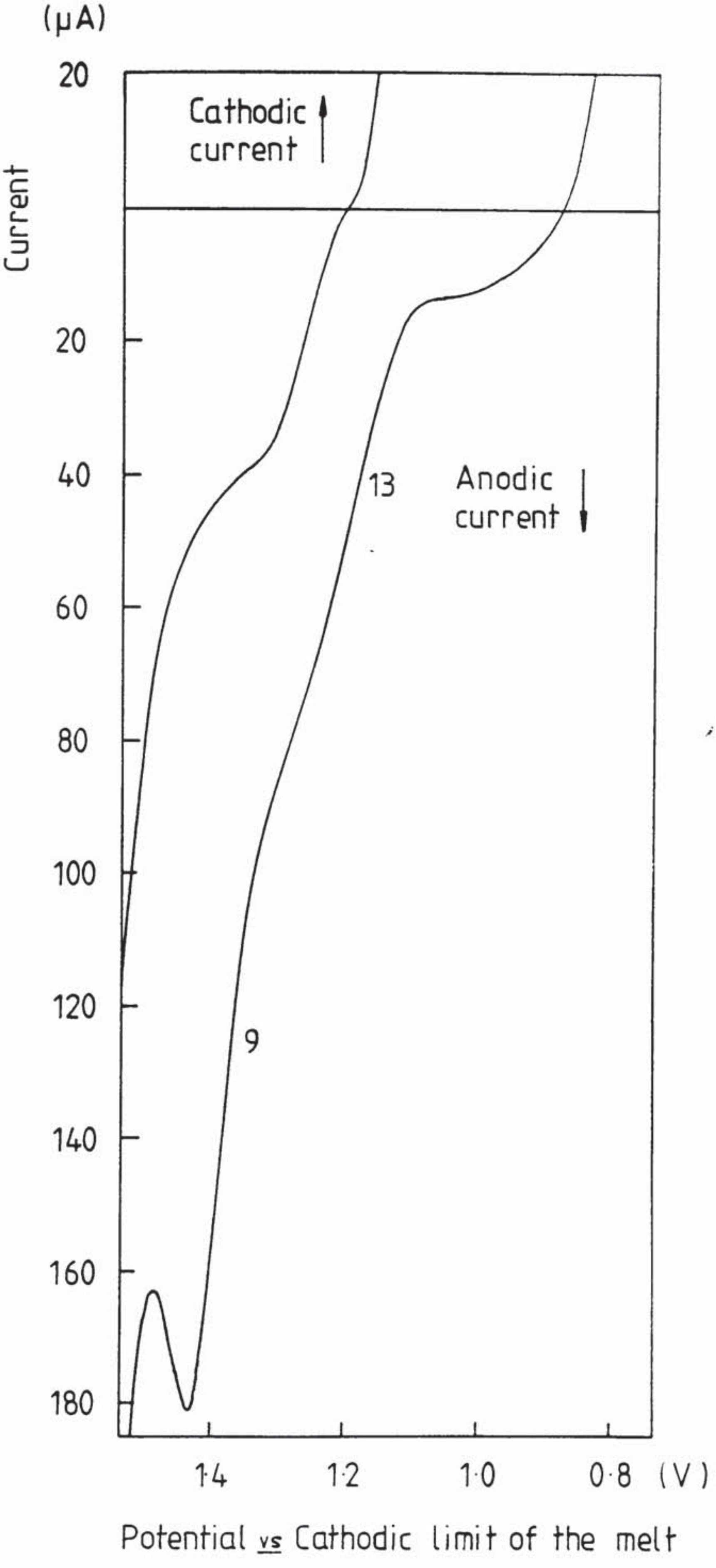

Figure 5-34 Voltammogram of (Na-K)OH eutectic containing $KMnO_4$ (0·09M) and Na_2CO_3 (0·01M) at 523K, under N_2, using a vibrating Pt indicator electrode.

to that of the MnO_4^{3-} oxidation wave and it has been assigned wave number 13. Analysis of that wave by H.I.E. plot gave a straight line with a slope of 0.050V, Fig. 5-35, indicating a reversible two electron transfer process. As the only difference between this experiment and that of section 5.5 was the addition of carbonate, it is reasonable to attribute wave 13 to the oxidation of carbonate according to reaction (5-39).

5.7.2 (Na-K)OH Eutectic Contining Na_2O_2 and $KMnO_4$

From the work of Kerridge et al (97) it is known that Na_2O_2 in molten (Na-K)NO_3 was capable of stabilizing Mn(V) or Mn(VI) or both depending on the molal ratio of O_2^{2-}: Mn. At high molal ratios of O_2^{2-}: Mn, Mn(V) was found as the only stable species; as the ratio decreases both Mn(V) and Mn(VI) were found and eventually at low molal ratios only Mn(VI) was found. In acidic hydroxide melts containing $KMnO_4$ Eluard and Tremillon (7) using a rotating Pt electrode found a wave due to O_2^- reduction at a potential slightly less positive than the reduction potential of MnO_4^{2-}, they attributed the wave to reaction (5-8):

$$O_2^- + 2H_2O + 3e^- \rightleftarrows 4OH^-$$

the superoxide was presumably produced from the reaction of the added permanganate and the melt according to reaction (5-26):

$$3MnO_4^- + 8OH^- \rightleftarrows 3MnO_4^{3-} + 2O_2^- + 4H_2O$$

because O_2^- is unstable in acidic melts.

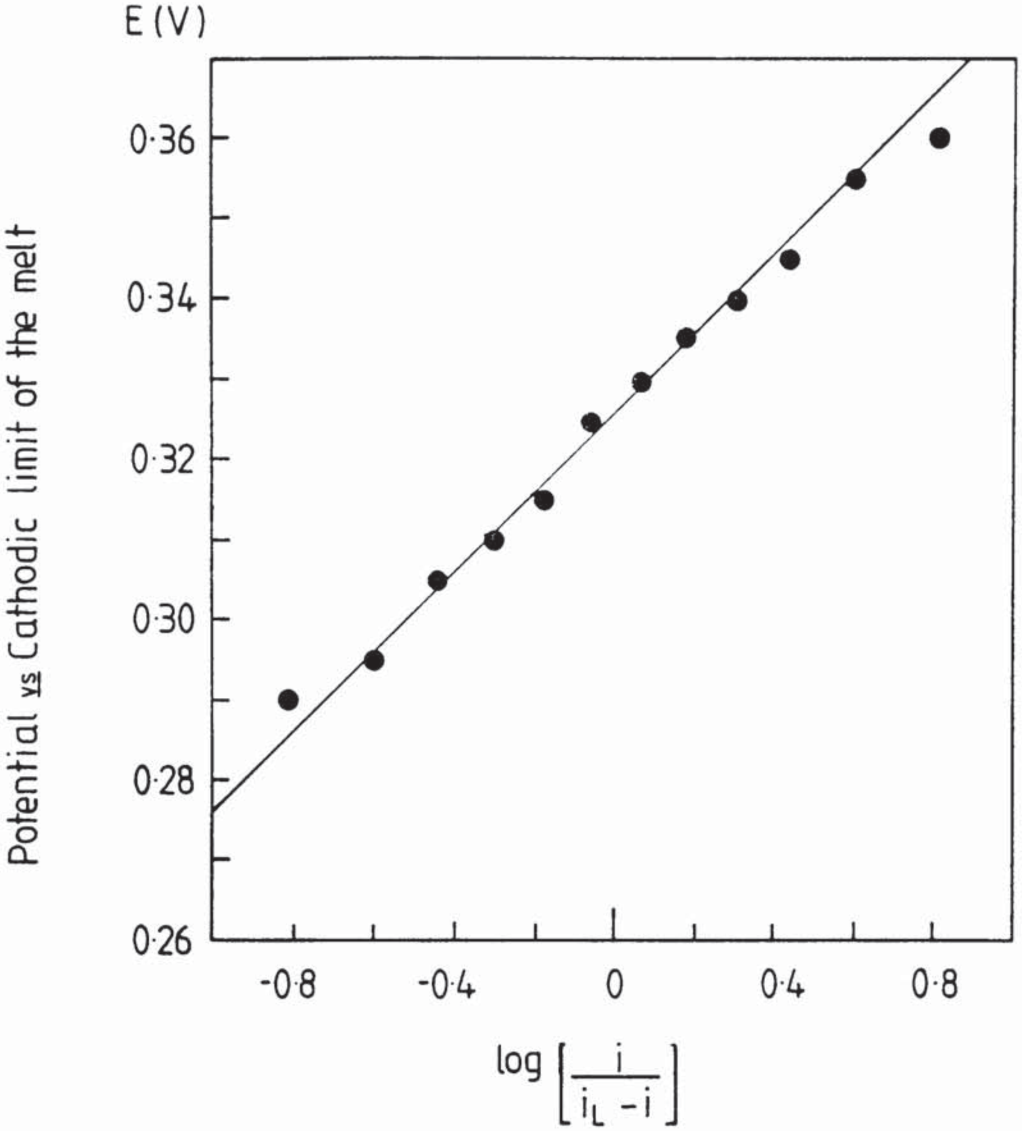

Figure 5-35 H.I.E. Analysis of voltammetric oxidation wave 13.

In this experiment the effect of O_2^{2-} added as Na_2O_2 on the various manganese species in an acidic hydroxide melt was investigated. To a melt containing Na_2O_2 (0.1M), $KMnO_4$ was added (0.09M), when all the $KMnO_4$ had dissolved the voltammogram of the melt solution was obtained using the vibrating working electrode is presented in Fig. (5-36)

On the (f.s) three cathodic waves were found. The first one with an $E_{\frac{1}{2}}$ value of 1.2V, has been assigned wave number 21. This was analysed by H.I.E. plot and gave a straight line with a slope of 0.0375V, Fig. (5-37), indicating a reversible three electron transfer reaction.

If O_2^{2-} ions are added to an acidic melt it will react with water to produce O_2^- according to:

$$3O_2^{2-} + 2H_2O \rightleftarrows 4OH^- + 2O_2^- \qquad (5\text{-}40)$$

wave 21 was therefore attributed to reaction (5-8):

$$O_2^- + 2H_2O + 3e^- \rightleftarrows 4OH^-$$

No wave due to MnO_4^{2-} reduction was found and that is because the E° value for the couple O_2^-/OH^- is less positive than the E° value for the couple Mn(VI)/Mn(V). Mn(VI) therefore reacts with O_2^- leaving Mn(V) as the main species in the melt. The second cathodic wave (peak shaped) with an E_p value of 1.00V is in fact wave 1, due to Pt oxide stripping and it was found to be an irreversible wave. The third cathodic wave which has been assigned wave number 22 was also irreversible with an $E_{\frac{1}{2}}$ value of 0.74V. This value suggests that the wave is due to the couple Mn_2O_3/MnO according to reaction (5-32). On the (r.s) three waves were also found. The first which has been assigned wave number 23, was cathodic at $E_{\frac{1}{2}} = 0.77V$; when analysed it gave a

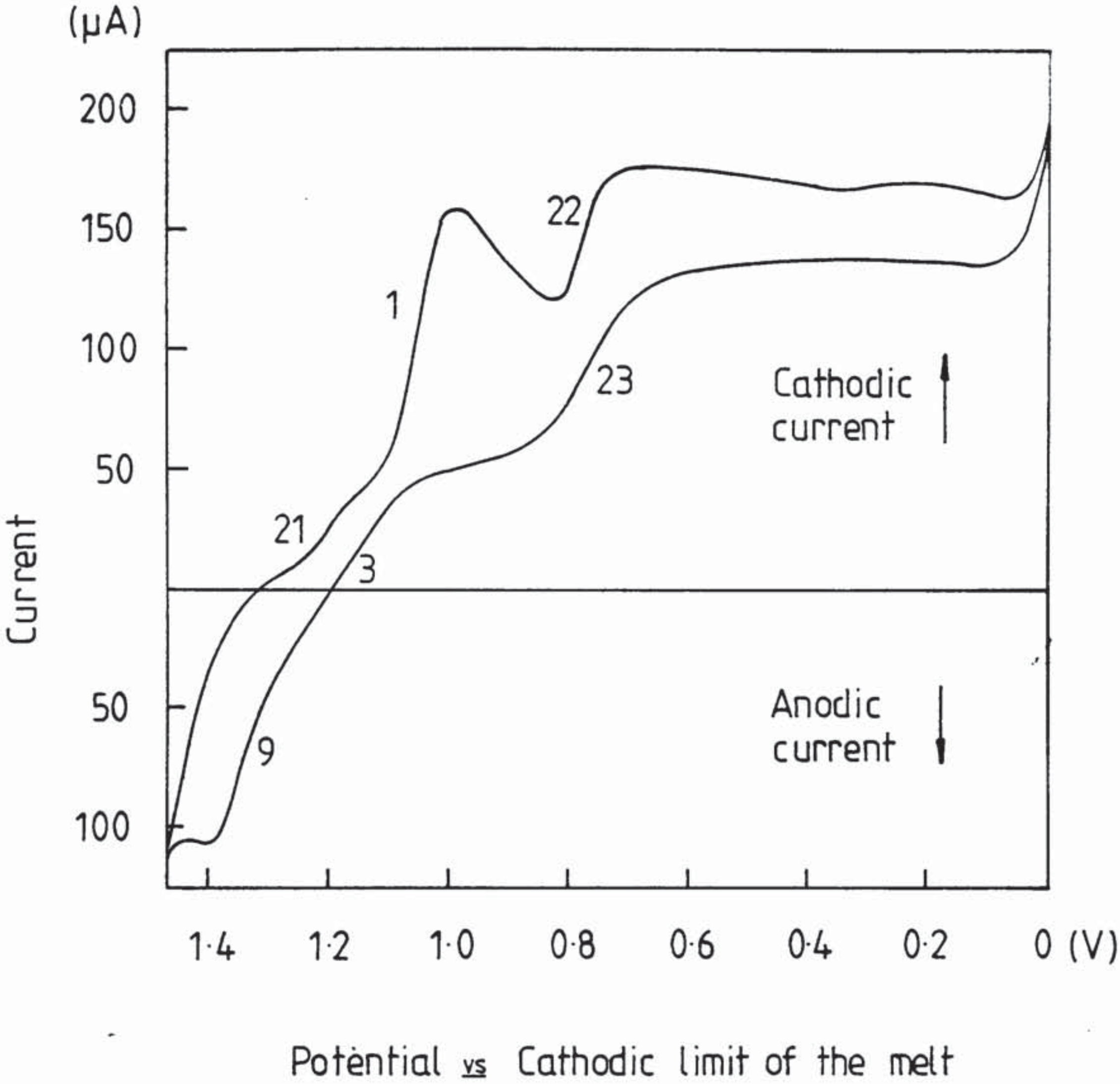

Figure 5-36 Voltammogram of (Na-K)OH eutectic containing Na_2O_2 (0·1M) and $KMnO_4$ (0·09M) at 523K, under N_2, using a vibrating Pt indicator electrode.

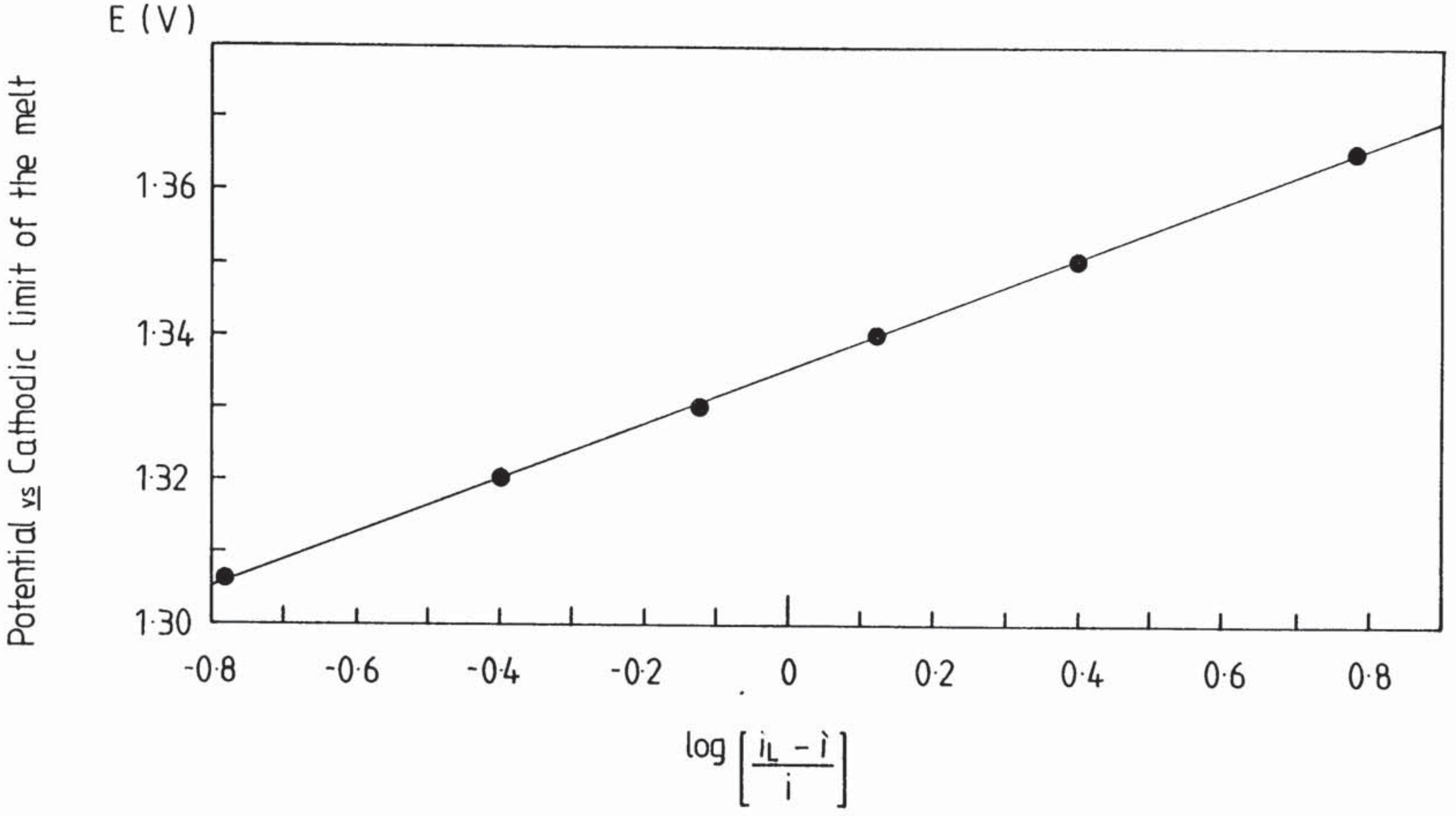

Figure 5-37 H.I.E. Analysis of voltammetric reduction wave 21.

straight line with a slope of 0.097V, Fig. 5-38, indicating a reversible one electron transfer reaction. This electrode reaction is believed to be due to the same reaction represented by a wave found in a voltammogram of the melt solution using the stationary working electrode (section 5.6.1). The only difference here is that O_2^{2-} was added to the melt instead of bubbling O_2 into the melt to produce O_2^{2-}, section 5.6.1. The proposed reactions here are:

$$Mn_2O_3 + O_2^{2-} + H_2O \rightleftarrows 2MnO_2 + 2OH^- \qquad (5\text{-}41)$$

hence:

$$MnO_2 + O_2^{2-} + e^- \rightleftarrows MnO_4^{3-} \qquad (5\text{-}36)$$

The second wave has a $E_{\frac{1}{2}}$ value approximately equal to 1.1V. The wave analysis indicated a reversible two electron transfer reaction when the wave is a composite wave, but in a duplicate voltammogram it was an irreversible cathodic wave, which suggests that the wave was not reproducible. However, the $E_{\frac{1}{2}}$ value of this wave suggests that it is due to the Pt electrode reaction with the melt. The third wave is anodic and it is in fact wave 9 due to the oxidation of MnO_4^{3-}. In table 5-1 is presented a list of reactions that have been proposed for the waves which have been discussed in this chapter.

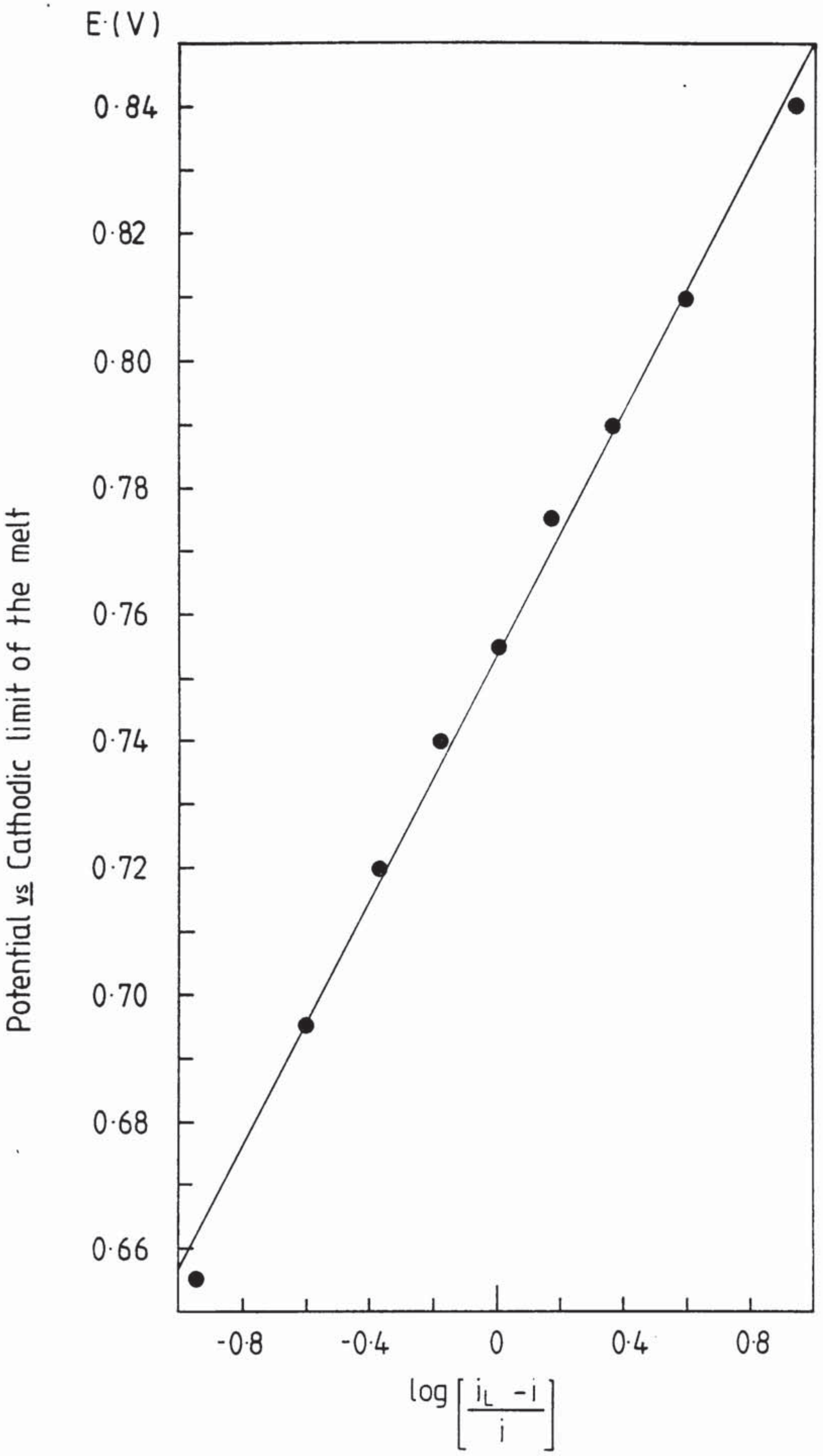

Figure 5-38 H.I.E. Analysis of voltammetric reduction wave 23.

Wave	$E_{\frac{1}{2}}$ or E_p (V)	i_L or i_p (μA)	Couple	Reaction	Comments
1 (f.s)	0.9 - 1.0	variable		Pt Oxide Stripping	Irrev. Red. Peak
	1.00	variable	PtO_2/Pt	(5-23)	Rev. Red. Peak
1'(f.s)	1.06	25	Pt/PtO	(5-4)	Rev. Oxid. Wave
2 (r.s)	0.8 - 0.9	125	Pt/PtO	(5-10)	Rev. Oxid. Wave
	0.92	20	O_2^-/O_2	(5-6)	Rev. Oxid. Wave
3 (r.s)	1.0 - 1.1	85	PtO/PtO_2	(5-5)	Rev. Oxid. Wave
4 (f.s)	0.82	40	MnO/MnO_2	(5-21)	Rev. Oxid. Wave
5 (f.s)	0.58	35	Mn^{2+}/Mn_2O_3	(5-13)	Irrev.Comp.Wave
6 (f.s)	0.115	38	Mn^{2+}/MnO	(5-14)	Rev. Red. Peak
7 (r.s)	0.62	65	Mn^{2+}/Mn_2O_3	(5-13)	Rev. Oxid. Wave
8 (r.s)	0.87	95	MnO/MnO_4^{3-}, MnO_2	(5-21), (5-11)	Irrev. Oxid Wave
9 (r.s)	1.30	125	MnO_4^{3-}/MnO_4^{2-}	(5-15)	Rev. Oxid. Wave
	1.45	variable	MnO_4^{3-}/MnO_4^{2-}	(5-15)	Irrev.Oxid. Peak
10(f.s)	0.865	350	MnO_4^{3-}/MnO	(5-11)	Rev. Red. Wave
	0.925	1875	MnO_4^{3-}/Mn_2O_3	(5-12)	Rev. Red. Wave
	0.840	530	MnO_4^{3-}/MnO_2	(5-33)	Rev. Red. Wave
11(r.s)	0.65	150	Mn_2O_3/Mn^{2+}	(5-13)	Irrev. Red. Wave
	0.74	165	Mn_2O_3/MnO	(5-32)	Irrev. Red. Wave
12(r.s)	0.88	200	MnO_4^{3-}/MnO	(5-11)	Irrev. Red. Wave
	0.93	960	MnO_4^{3-}/Mn_2O_3	(5-12)	Irrev.Comp. Wave
	0.835	740	MnO_4^{3-}/MnO_2	(5-30) & (5-36)	Rev. Comp. Wave
	0.76	250	Mn_2O_3/MnO	(5-32)	Irrev. Red. Wave
13(r.s)	1.25	65	CO_3^{2-}/CO_2	(5-39)	Rev. Oxid. Wave

14(f.s)	0.24	2120	NiO/Ni	(5-24)	Rev. Red. Wave
15(f.s)	0.08	6544	NiO_2^{2-}/Ni		Irrev. Red. Wave
16(r.s)	0.21	variable	Ni/NiO	(5-24)	Irrev. Oxid. Peak
17(r.s)	0.60	variable	Ni/NiO_2	(5-25)	Irrev. Oxid. Peak
18(f.s)	0.915	600	MnO_4^{3-}/Mn_2O_3	(5-12)	Irrev. Red. Wave
19(r.s)	0.91	320	Mn_2O_3/MnO_4^{3-}	(5-12)	Irrev.Oxid. Wave
20(f.s)	1.32		MnO_4^{2-}/MnO_4^{3-}	(5-15)	Irrev. Red. Peak
21(f.s)	1.20	28	O_2^-/OH^-	(5-8)	Rev. Red. Wave
22(f.s)	0.74	48	Mn_2O_3/MnO	(5-32)	Irrev. Red. Wave
23(r.s)	0.77	76	MnO_4^{3-}/MnO_2	(5-36)	Rev. Red. Wave

Table 5-1 Proposed Reactions of Voltammetric Waves Found in Electroanalysis Experiments.

CHAPTER 6

The Reactions of Molten Hydroxides with Organic Compounds

Molten sodium and potassium hydroxides or (Na-K)OH eutectic have been widely used for the degradation of organic compounds, by the process known as "alkali fusion". In addition to this, alkali fusion has a number of synthetic uses, it provides a general method for the preparation of phenols and is used to effect a number of important syntheses in the dyestuffs field, e.g. the first synthesis of a natural dye (alizarin), (62).

The reactions which occur under such drastic conditions are sometimes complex. The amount of water present in the hydroxides greatly affects the temperature at which they melt and plays an important role in many of the reactions which take place.

A wide variety of compounds has been submitted to alkali fusion, especially compounds that have a carboxyl, phenolic hydroxyl, or other group conferring solubility in alkali. Although a homogeneous system is an advantage it is not a prerequisite for investigation. Some examples of this class of compounds are: carboxylic acids, ketones, alcohols, arylsulfonic acids, arylhalides, phenols, pyrones, anthraquinones and benzanthrones.

In the present work, special interest is focused on the reactions of alcohols with molten hydroxides and a literature survey of these reactions, as well as the reactions of related organic compounds such as aldehydes and ketones with molten hydroxides, are dealt with in this chapter. In a series of papers published early this century under the title "The Liberation of Hydrogen from Carbon Compounds" Fry, Schulze, Otto and Weitkamp, (63, 64, 65), investigated the interaction of methyl alcohol, ethyl alcohol, n-propyl alcohol, isopropyl alcohol, isobutyl alcohol, tertiary butyl alcohol, formaldehyde, acetaldehyde, acetone, methyl formate and methyl acetate, with fused caustic alkalies. They proposed a general reaction of the type:

$$RH_n + nMOH \rightarrow R(OM)_n + nH_2 \quad (M{=}Na \text{ or } K) \qquad (6\text{-}1)$$

and

$$R(CH_3)_n + nMOH \rightarrow R(OM)_n + nCH_4 \qquad (6\text{-}2)$$

in which R is a more or less complex radical containing carbon. In the investigations of the behaviour of the compounds mentioned above, equations for the reactions occurred, were developed by applying equations (6-1) and (6-2), to the molecule of the compounds investigated. Fry, Schulze, Otto and Weitkamp found that the data obtained substantiated the occurence of the reactions predicted in conformity with the developed equations, so in every instance, oxidation of the carbon compound by the fused caustic alkalies yielded carbonates, hydrogen and methane. The following equations were suggested as possible mechanisms of reactions involved in oxidizing methyl alcohol successively to the formaldehyde, formic acid and carbonic acid stages:

$$CH_3OH + NaOH \rightarrow CH_3ONa + H_2O \qquad (6\text{-}3)$$

$$CH_3ONa + NaOH \rightarrow CH_2(ONa)_2 + H_2 \qquad (6\text{-}4)$$

$$CH_2(ONa)_2 + H_2O \rightarrow CH_2O + 2NaOH \qquad (6\text{-}5)$$

and the sum of equations (6-3), (6-4) and (6-5) is:

$$CH_3OH \rightarrow CH_2O + H_2 \qquad (6\text{-}6)$$

then,

$$CH_2(ONa)_2 + NaOH \rightarrow CH(ONa)_3 + H_2 \qquad (6\text{-}7)$$

$$CH(ONa)_3 + H_2O \rightarrow HCO_2Na + 2NaOH \qquad (6\text{-}8)$$

and the sum of equations (6-3), (6-4), (6-7) and (6-8) is:

$$CH_3OH + NaOH \rightarrow HCO_2Na + 2H_2 \qquad (6\text{-}9)$$

then,

$$CH(ONa)_3 + NaOH \rightarrow C(ONa)_4 + H_2 \qquad (6\text{-}10)$$

$$C(ONa)_4 + H_2O \rightarrow Na_2CO_3 + 2NaOH \qquad (6\text{-}11)$$

and the sum of equations (6-3), (6-4), (6-7), (6-10) and (6-11) is:

$$CH_3OH + 2NaOH \rightarrow Na_2CO_3 + 3H_2 \qquad (6\text{-}12)$$

In the investigation of the behaviour of methyl alcohol, duplicate series of runs were made, extending over a wide range of temperatures ($250^\circ C$ - $450^\circ C$). It was confirmed that certain intermediate reactions occurred according to the proposed equation, (6-1).

It was found that increasing the temperature above $250^\circ C$, made the extent of the oxidation of methyl alcohol also increase and the reaction followed equation, (6-12) which was 100% complete at $450^\circ C$. At temperatures below $300^\circ C$, the presence of formates in the reaction residues indicated the occurrence of the intermediate reactions represented by equations, (6-4), (6-7) and (6-8). Separate runs with formic acid showed its complete decomposition at 300°C but accompanied by some carbonization. The presence of methylates in the reaction residues at temperatures up to 370°C proved the occurrence of reaction (6-3).

The conversion of formaldehyde to carbonate with the liberation of hydrogen in conformity with the equation:

$$CH_2O + 2NaOH \rightarrow Na_2CO_3 + 2H_2 \qquad (6\text{-}13)$$

was quantitatively verified at 300°C. At that temperature formaldehyde underwent complete oxidation to carbonate with only minute traces of intermediately formed alkali formates.

In applying equation (6-1), to ethyl alcohol at 250°C, Fry and Schulze proposed that the hydrogen atoms of the CH_2OH radical would be the most susceptible to replacement, so the reactions were summarised as follows:

$$CH_3CH_2OH + NaOH \rightarrow CH_3CH_2ONa + H_2O \qquad (6\text{-}14)$$

$$CH_3CH_2ONa + NaOH \rightarrow CH_3CH(ONa)_2 + H_2 \qquad (6\text{-}15)$$

$$CH_3CH(ONa)_2 + H_2O \rightarrow CH_3CHO + 2NaOH \qquad (6\text{-}16)$$

and the sum of equations (6-14), (6-15) and (6-16) is:

$$CH_3CH_2OH \rightarrow CH_3CHO + H_2 \qquad (6\text{-}17)$$

This reaction, summation of the consecutive reactions (6-14), (6-15) and (6-16), was thought to be the mechanism of the reaction for the formation of acetaldehyde.

The second stage is the formation of sodium acetate, which was thought to be as follows:

$$CH_3CHO + NaOH \rightarrow CH_3CO(ONa) + H_2 \qquad (6\text{-}18)$$

and the summation of reactions (6-14), (6-15), (6-16) and (6-18) gives:

$$CH_3CH_2OH + NaOH \rightarrow CH_3COONa + 2H_2 \qquad (6\text{-}19)$$

The third stage is the conversion of sodium acetate to carbonate, with the liberation of methane:

$$CH_3COONa + NaOH \rightarrow Na_2CO_3 + CH_4 \qquad (6\text{-}20)$$

Carroll (66), in earlier work assumed that the second stage is the dissociation of aldehyde to ketene and hydrogen in the presence of caustic soda as catalytic agent, according to the equation:

$$CH_3CHO = CH_2CO + H_2 \qquad (6\text{-}21)$$

and that the third stage is the union of ketene with sodium hydroxide to form acetate:

$$CH_2CO + NaOH = CH_3CO_2Na \qquad (6\text{-}22)$$

Fry and Schulze suggested that if the reaction also involved the hydrogen atoms of the methyl radical of ethyl alcohol then complete oxidation to carbonate and orthocarbonate is quite conceivable according to the following reaction:

$$CH_3CH_2OH + 6NaOH \rightarrow Na_2CO_3 + Na_4CO_4 + 6H_2 \qquad (6\text{-}23)$$

Ethylene was also detected in the reaction product; it was thought that a catalytic decomposition of ethyl alcohol at high temperatures took place according to:

$$CH_3CH_2OH \rightarrow C_2H_4 + H_2O \qquad (6\text{-}24)$$

As the temperature was raised from approximately 250°C to approximately 530°C, the reaction tended to conform to the reaction:

$$CH_3CH_2OH + 2NaOH \rightarrow Na_2CO_3 + 2H_2 + CH_4 \qquad (6\text{-}25)$$

which is the summation of equations (6-19) and (6-20), and at that temperature neither acetates nor ethylene were obtained. Acetaldehyde reactions with hydroxide melts at 250°C, was found to conform with the reaction:

$$CH_3CHO + NaOH \rightarrow CH_3CO(ONa) + H_2 \qquad (6\text{-}26)$$

while at higher temperatures it conforms with the reaction:

$$CH_3CHO + 2NaOH \rightarrow Na_2CO_3 + H_2 + CH_4 \qquad (6\text{-}27)$$

Acetone being structurally similar to acetaldehyde, its interaction with molten hydroxides was found to follow:

$$CH_3COCH_3 + NaOH \rightarrow CH_3CO_2Na + CH_4 \qquad (6\text{-}28)$$

$$CH_3CO_2Na + NaOH \rightarrow Na_2CO_3 + CH_4 \qquad (6\text{-}29)$$

$$CH_3COCH_3 + 2NaOH \rightarrow Na_2CO_3 + 2CH_4 \qquad (6\text{-}30)$$

At 250°C, acetone reacted according to equation (6-28), but at higher temperatures it reacted according to equation (6-30). It was proposed that, n-propyl alcohol was oxidized in three stages by the fused caustic alkalies:

$$CH_3CH_2CH_2OH + 2NaOH \rightarrow Na_2CO_3 + 2H_2 + C_2H_6 \qquad (6\text{-}31)$$

$$CH_3CH_2CH_2OH + 6NaOH \rightarrow Na_2CO_3 + Na_4CO_4 + CH_4 + 5H_2 \qquad (6\text{-}32)$$

$$CH_3CH_2CH_2OH + 10NaOH \rightarrow Na_2CO_3 + 2Na_4CO_4 + 9H_2 \tag{6-33}$$

but only equation (6-32) was verified experimentally at 500°C. At the same temperature, isopropyl alcohol reacted similarly according to the proposed equation:

$$(CH_3)_2CHOH + 2NaOH \rightarrow Na_2CO_3 + H_2 + 2CH_4 \tag{6-34}$$

It was also reported that with both n-propyl and isopropyl alcohols, some free carbon was found in the reaction residue.

Investigations of isobutyl alcohol showed extensive carbonization which precluded determination of any stoichiometric ratios.

The interaction of methyl formate with the fused caustic alkalies at 475°C was assumed to involve three principal reactions: the first equation is the saponification of methyl formate, yielding formate and methyl alcohol:

$$HCOOCH_3 + NaOH \rightarrow HCOONa + CH_3OH \tag{6-35}$$

The second reaction involves the oxidation of formate to carbonate with the liberation of hydrogen:

$$HCOONa + NaOH \rightarrow Na_2CO_3 + H_2 \tag{6-36}$$

The third equation is the oxidation of methyl alcohol to carbonate and hydrogen:

$$CH_3OH + 2NaOH \rightarrow Na_2CO_3 + 3H_2 \tag{6-12}$$

The summation of these equations gives:

$$HCOOCH_3 + 4NaOH \rightarrow 2Na_2CO_3 + 4H_2 \tag{6-37}$$

equation (6-37), was proved experimentally, and that meant the assumptions in equations (6-35), (6-36) and (6-12) were verified, so equations that are exactly parallel to those proposed for methyl formate were also assumed for methyl acetate interactions with the molten hydroxides at the same temperature:

$$CH_3COOCH_3 + NaOH \rightarrow CH_3COONa + CH_3OH \qquad (6\text{-}38)$$

$$CH_3COONa + NaOH \rightarrow Na_2CO_3 + CH_4 \qquad (6\text{-}20)$$

$$CH_3OH + 2NaOH \rightarrow Na_2CO_3 + 3H_2 \qquad (6\text{-}12)$$

and the summation of these equations gives:

$$CH_3COOCH_3 + 4NaOH \rightarrow 2Na_2CO_3 + CH_4 + 3H_2 \qquad (6\text{-}39)$$

Here again the reaction was proved to follow the summation reaction equation (6-39).

In the work of Fry, Schulze, Otto and Weitkamp (63, 64, 65) outlined here, the authors failed to specify fully the experimental conditions used, in particular whether the reactions were performed in air or in an inert atmosphere (e.g. Nitrogen), where with compounds like alcohols, ketones etc., the composition and yield of the product is altered markedly if the reaction is carried out in air (67). It is very likely that these investigations were made with compounds of questionable purity and without adequate identification of the products, also much of the early work was carried out before convenient methods of analysis and identification had been developed.

Dumas and Stass (68) reported that primary alcohols are dehydrogenated to the corresponding acids when heated with potassium hydroxide. Dytham and Weedon (67) regarded this reaction as involving two successive hydride ion transfers with the intermediate formation of the corresponding aldehyde, scheme 1.,

$$RCH_2OH + {}^{\ominus}OH \rightleftarrows RCH_2O^{\ominus} + H_2O$$

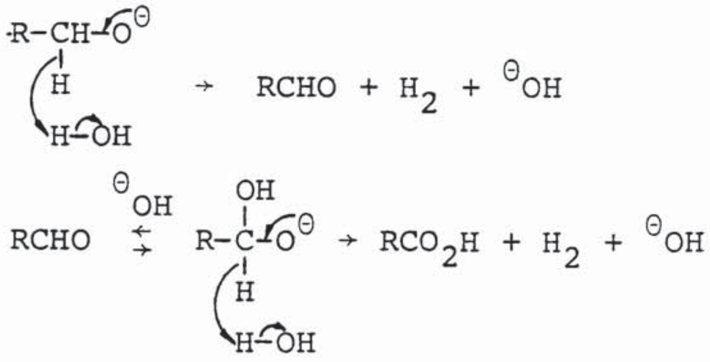

Scheme 1.

The amount of water in the hydroxides was found not to have a significant effect on these dehydrogenations where concentrated aqueous alkali metal hydroxides were also used to effect these dehydrogenations (68, 69, 70) and the addition of cadmium oxide or cadmium metal to the reaction mixture was claimed to be beneficial (71). Very good yields of the corresponding acids have been reported with many primary alcohols.

M. Guerbet (72), reported that aliphatic alcohols with fewer than six carbon atoms are partly dehydrated to olefins during the reaction, and G. Lock (73) found that the hydrogen liberated in the conversion of benzyl alcohol to benzoic acid effects partial reduction of the starting material to toluene. Both primary and secondary alcohols possessing an unsaturated methylene group at C-2, when heated with alkalies, can condense to give alcohols with two or more times as many carbon atoms as the starting material (72). The condensation is greatly favoured and the dehydrogenation reaction to the acid suppressed by essentially anhydrous conditions; these are best achieved by removing the water formed during the condensation either by azeotropic distillation or by adding a dehydrating agent to the reaction mixture. The addition of dehydrogenation catalysts is also claimed to be beneficial (74, 75, 76). A common precedure for carrying out the reaction consists in heating the alcohol with the corresponding alkali metal alkoxide rather than potassium hydroxide (70, 72). The reaction may be regarded as involving an aldol condensation, followed by hydride ion transfers from either the alcoholate, or a derived aldehyde to the ∝,β-unsaturated aldehyde and its saturated analogue, scheme 2. (67, 74, 76).

$$RCH_2CH_2OH \rightarrow RCH_2CH_2O^{\ominus} \xrightarrow{-H^{\ominus}} RCH_2CHO$$

$$2RCH_2CHO \rightarrow RCH_2\ CH(OH)CHRCHO \rightarrow RCH_2CH{=}CRCHO$$

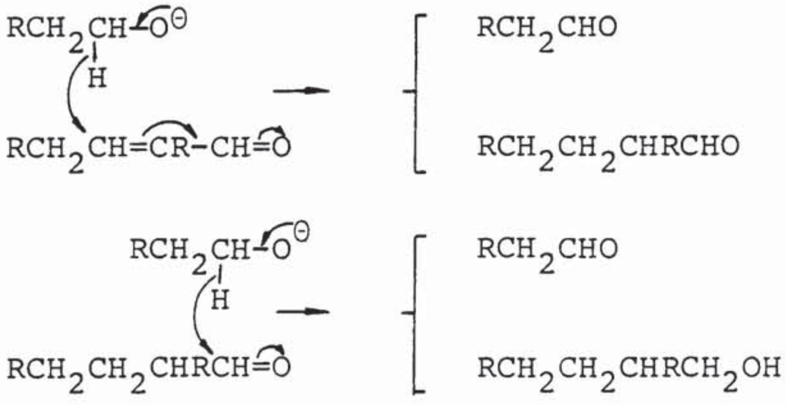

Scheme 2.

As required by this interpretation, benzyl alcohol, methyl alcohol and 2-alkyl aliphatic alcohols do not undergo this type of condensation reaction (72, 76). However, a mixture of benzyl and ethyl alcohols gives 3-phenyl propanol (77):

$$PhCH_2OH + CH_3CH_2OH \rightarrow PhCH_2CH_2CH_2OH \qquad (6\text{-}40)$$

and a mixture of isobutanol and cyclohexanol gives 2-isobutyl cyclohexanol (76):

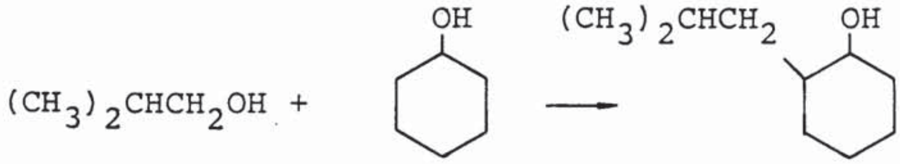

(6-41)

with primary alcohols, condensation is frequently accompanied or followed by dehydrogenation (70, 72). Some Secondary alcohols can undergo the condensation reaction, scheme 2., if heated with alkali under essentially anhydrous conditions, however in most alkali fusions the conditions are not favourable for this condensation and fissions to give products very similar in composition to those obtained from the corresponding ketones are far more frequently encountered (72). The mechanism of the fission reaction was thought to be of the type shown in scheme 3:

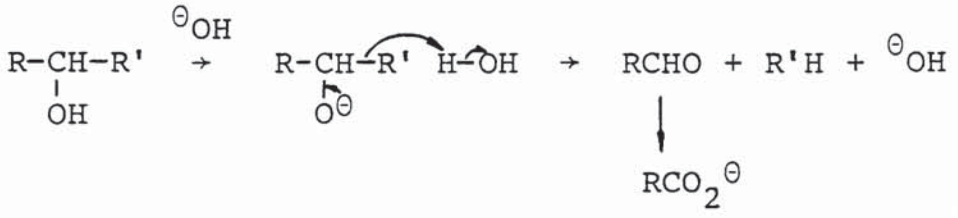

Scheme 3.

The close similarity between the products from ketones and the corresponding secondary alcohols strongly suggests that reaction of the latter compounds proceeds by an initial dehydrogenation to the ketone (scheme 4.):

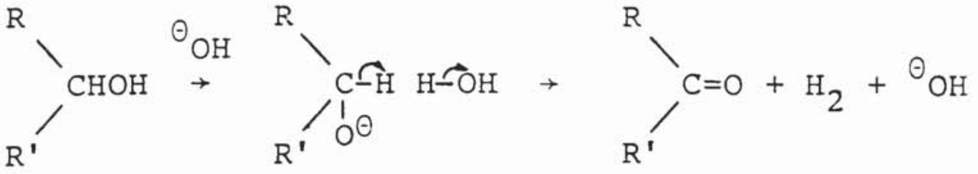

Scheme 4.

The reaction in alkali fusion of tertiary alcohol is a dehydration reaction to produce olefines (67, 78, 79). It is believed that tertiary alcohols are formed in situ during the alkali fusion of ketones, owing to attack of the carbonyl group by a carbanion. The converse of this type of reaction, (scheme 5.), may occur under suitable conditions (80, 81).

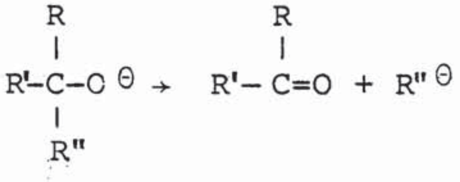

$$R'\!-\!\underset{R''}{\overset{R}{C}}\!-\!O^{\ominus} \rightarrow R'\!-\!\overset{R}{C}\!=\!O + R''^{\ominus}$$

scheme 5

Both aliphatic and aromatic aldehydes give acids in good yield on alkali fusion (64, 82, 83), although complex condensation products may be formed on treatment of aliphatic aldehydes with concentrated aqueous alkali (84).

A variety of products has been reported from alkali fusions of ketones, but recent studies with fatty acid derivatives show that the reactions involved fall mainly into three categories: (i) hydrolysis of a carbon - carbon bond adjacent to the carbonyl group, (ii) nucleophilic attack of the carbonyl group by a carbanion derived from a second molecule of the same, or another ketone, and (iii) dehydrogenation to give an α, β-unsaturated ketone followed by a fission of the retro-aldol type. Of these reactions, hydrolysis is the commonest, dehydrogenation is normally only a minor side reaction.

Aliphatic and aromatic ketones are reduced to secondary alcohols by treatment with a primary alcohol and concentrated alkali (85). Hydrogen transfers of this type show that ketones can compete efficiently with water or an alcohol as acceptors of a hydride ion from the intermediates involved in the dehydrogenation (shown in scheme 1.) of primary alcohols to acids (scheme 6.):

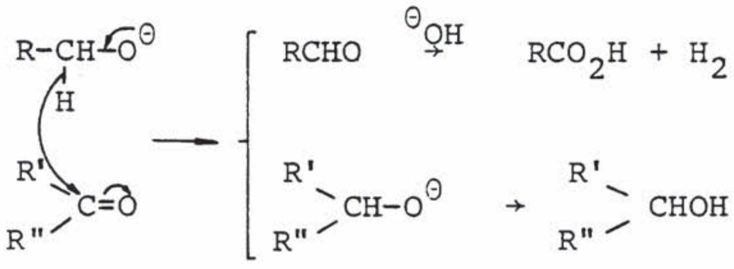

Scheme 6.

Under alkaline conditions formaldehyde and presumably other aldehydes can serve as hydride ion donors for the reduction of ketones (86).

The hydrolysis of a ketone, (A), in molten alkali may be attributed, (scheme 7.), to an initial attack of the carbonyl group by hydroxyl ion to give either (B) or (C), followed by fission of one of the adjacent carbon-carbon bonds:

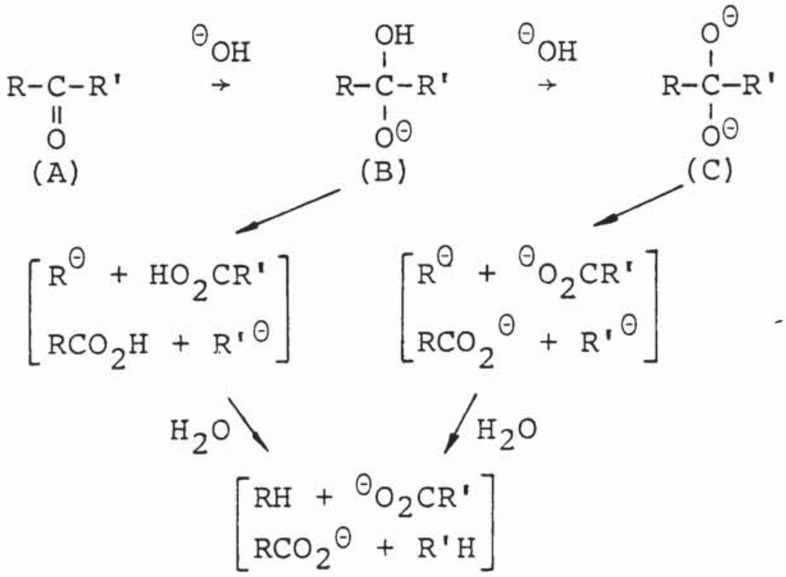

Scheme 7.

It is unlikely that the carbanions indicated in this scheme have a free existence, they are probably transferred directly to an acceptor such as water, (scheme 8), (67).

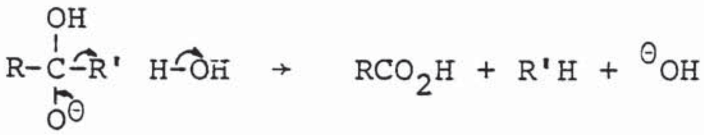

$$R\text{-}\overset{OH}{\underset{O^{\ominus}}{C}}\text{-}R'\quad H\text{-}OH \rightarrow RCO_2H + R'H + {}^{\ominus}OH$$

Scheme 8.

The simplest reaction of this type is that of acetone to give acetic acid and methane (64).

With unsymmetrical ketones the hydrolysis is accompanied by a reaction in which a carbanion is transferred from an intermediate of the type (B) or (C), to an acceptor other than water, presumably the ketone itself, scheme 9., (67).

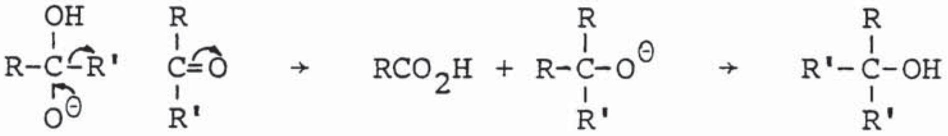

$$R\text{-}\overset{OH}{\underset{O^{\ominus}}{C}}\text{-}R'\quad \overset{R}{\underset{R'}{C}}{=}O \rightarrow RCO_2H + R\text{-}\overset{R}{\underset{R'}{C}}\text{-}O^{\ominus} \rightarrow R'\text{-}\overset{R}{\underset{R'}{C}}\text{-}OH$$

Scheme 9.

Although the resulting tertiary alcohols are unstable, evidence for reactions of this type can be inferred from the detection of dehydration and other transformation products of the alcohols. Studies on the alkali fusion of ketones (67), indicate a minor side reaction (scheme 10.), in which an initial dehydrogenation, gives rise to methyl ketones, the latter then react further, either by hydrolysis, scheme 7., or by processes similar to that shown in scheme 9.

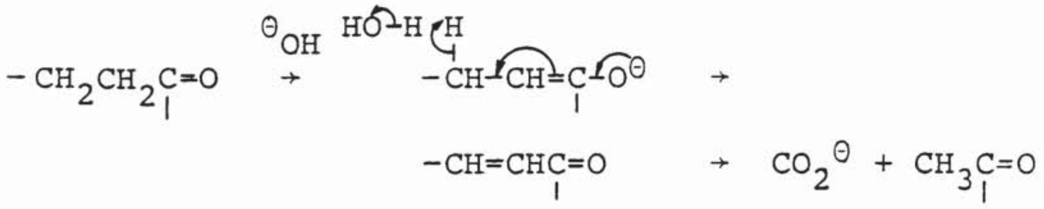

Scheme 10.

Under sufficiently drastic conditions, the long chain saturated carboxylic acids will react with molten alkali, it has been suggested that these reactions proceed, (scheme 11.), by an initial slow dehydrogenation, followed by a rapid fission of the resulting α,β - ethylenic acid (87).

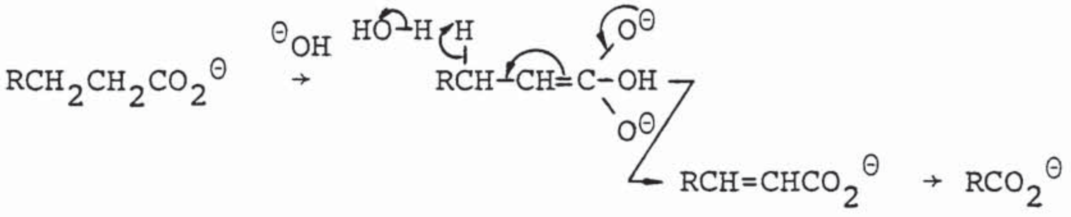

Scheme 11.

The conclusion on the reactions of organic compounds with hydroxide melts is that most organic compounds undergo one or more reactions when passed through hydroxide melts. These reactions include, dehydrogenation, fission condensation, dehydration and hydrolysis. The reaction mechanisms proposed by many workers seem to be confirmed by the analysis of reactions of organic derivatives rather than of the original compound; these derivatives were in most cases complicated with long chains and branches. However not much attention was paid to the reaction rate and yield. Even when the yield was occasionally given, it seemed to be on a qualitative basis, and the low yields were not explained. Also the reaction products need to be confirmed using more appropriate methods of analysing the melt, e.g. electro analysis.

CHAPTER 7

Oxidation of Organic Compounds by Manganates in Molten (Na-K)OH Eutectic

7.1 Introduction

Preliminary work concentrated on choosing those organic compounds that might be used as reactants for oxidation reactions in molten (Na-K)OH. The solubility and reactivity of both reactant and expected product in molten (Na-K)OH were taken into consideration. The solubility of organic compounds in concentrated alkaline solutions was taken as an indicator of the solubility of those organics in acidic hydroxide melts. It is known generally that organic compounds that are soluble in hydroxide solution usually react with it as well. Naturally the choice initially was in favour of organic compounds which are insoluble and do not react with the melt e.g. basic, neutral and inert compounds, and these include paraffins, amines, etc. However the literature survey showed that most organic compounds react to a varying degree with molten hydroxides. Consequently it was decided that a series of organic compounds would be used as reactants for oxidation reactions and these were chosen to be representative of particular functional groups.

A study of the existing methods of oxidation of the various organic functional groups by inorganic oxidants (e.g. MnO_4^-, Cr(VI), Osmium tetroxide, Lead tetracetate, etc.) was carried out as well as catalysed oxidation by O_2/air (auto-oxidation). This indicated the possible product, or products in case of multistage oxidations, and the specificity of particular oxidizing agents. Also in many of these oxidation reactions it was important that the organic compound be soluble in a suitable solvent in order to undergo oxidation and that some organics need vigorous conditions while others need mild ones. Comparisons were made between these reactions and possible reactions in molten hydroxides, especially considering regeneration of the oxidizing agent; for example the oxidation of the olefinic double bond by aqueous MnO_4^- (basic medium) containing periodate, which continuously regenerates MnO_4^- from its reduced state. The synthesis value of the oxidation reaction was also considered. In some of these reactions a mixture of products is obtained and hence there is no synthesis value. The choice of manganates as the oxidizing agent was made because of the stability of a particular oxidation state of manganese at a particular condition in the hydroxide melt and also because of the already established study of manganates in these melts most of which were confirmed in the present work. The reactions of organic compounds in molten (Na-K)OH and in the same melt containing manganates was approached with caution as explosive reactions may be possible if dangerous compounds such as organic peroxides were formed. Initial reactions were carried out with small volumes of molten hydroxide and organic reactant. These were performed in order to see if explosions resulted by passage of the organic reactant through molten hydroxides at 523K. The possible explosion volume was considered and the necessary experimental safety precautions were made (see Chapter 4). These reactions were then extended to reactions with molten hydroxides containing manganates.

The concentration of the inorganic oxidizing agent was kept to a very low value and this again made the reactions safer. No analysis was performed and observation of the melt was limited to examining it before and after reaction when the melt had been thoroughly purged with N_2. It was assumed that reaction had occurred if the original melt colour of emerald green or greenish blue had been destroyed and a new melt colour obtained, due to the change in oxidation state of the manganese.

It was therefore possible to obtain an idea of what particular organic compounds had undergone reaction. With these experiments completed more detailed experiments and analysis were performed with the Mn(V) and Mn(VI) system on a slightly larger scale. The analysis and experimental techniques were optimized and tested with specific attention being paid to the organic mass balance. Having found which organic compounds were oxidized more detailed experiments were performed on the reaction of particular organic compounds with (Na-K)OH eutectic and (Na-K)OH containing manganates.

7.2 Experimental Procedure for the Preliminary Reaction Experiments

The aim of these experiments was to test the feasibility of passing organic vapours through molten hydroxides, then through molten hydroxides containing manganate as an oxidizing agent, and to note any indications of chemical reaction. The system consisted of a melt containing A.R. grade chemicals NaOH 24.52g, KOH 21.71g and $KMnO_4$ 0.146g, contained in a 50cc PTFE beaker placed inside a tubular Pyrex glass reactor base 6cm o.d, 5cm i.d and 25cm long. The reactor head had four B10 sockets into which the organic input tube and product output tube were sealed, the other two sockets were stoppered. The reactor head and base were connected by a ground glass flange of 8.5cm o.d. The organic was admitted to the system as shown in Fig. 4-5. The reactor head was maintained at approximately 425K by heating tapes which reduced the possibility of organic reflux and the reactor was maintained at 523K by a furnace as described in Chapter 4. O_2 free N_2 was passed with the organic vapour into the reactor at approximately $100cm^3$ min^{-1} and at this rate the N_2 produced a steady stream of bubbles through the molten salt. The organic liquid was added dropwise by syringe pump to this stream, as it entered the reactor head it was entrained and vaporized and then carried down the delivery tube into the molten salt. The syringe pump was capable of delivering the organic liquid at various constant rates.

The organic vapour issuing from the reactor was not collected but fed to the laboratory extractor system where it was vented. Using the coloured nature of the manganese oxidation state - Mn(VI) was an emerald green solution, Mn(V) was greenish blue solution - reaction was assumed to have taken place when the colour of the solution changed.

7.3 Experimental Procedure for the Comprehensive Reaction Experiments

Having performed the preliminary experiments successfully without any violent reactions, a more exacting system was developed. The principal study was on the system where Mn(V) and Mn(VI) were the oxidizing agents. Electroanalysis of the molten system was performed before and after the passage of the organic reactant, using the vibrating Pt working electrode. During and after the passage of the organic through the melt the mass spectrometer was used to monitor the exit gas from the condenser. The mass spectrometer was used in the scan mode where the mass range 0 to 200 mass units was scanned and the results displayed as a continuous graph or on an oscilloscope. It was therefore possible for any new products which appeared in the exit gas stream to be observed and by fine tuning of the scan, their mass number found. The scan was made every half minute. Analysis of the organic liquid product was performed using gas liquid chromotography. The chemical reaction system consisted of a melt containing A.R. grade chemicals, NaOH 49.04g, KOH 43.429g and $KMnO_4$ 0.73g. The organic input volume was usually $5cm^3$ injected at $0.4cm^3$ min^{-1} into $100cm^3$ min^{-1} of N_2 which was then bubbled through the molten salt system. A typical experimental procedure in which a molten (Na-K)OH eutectic containing $KMnO_4$ was used to oxidize an organic compound was as follows:

Setting up

i) Charge the reactor with solid (Na-K)OH and fit reactor head.

ii) Place reactor in furnace.

iii) Wind on reactor head heating tapes.

iv) Insert thermocouple, organic delivery tube, reference electrode and secondary electrode.

v) Raise temperature in furnace to 523K, heating tapes to 425K.

vi) Bubble N_2 through melt for 2 hours to obtain the required water concentration.

vii) Insert working electrode and connect to vibro-mixer.

viii) Set up condenser system but do not attach to reactor, weigh empty condenser, switch chiller to 258K.

ix) Attach T-piece to condenser outlet and connect up mass spectrometer.

x) Put on safety visor, apron and gloves.

Measurements and Additions

i) Obtain voltammogram of molten (Na-K)OH eutectic.

ii) Add $KMnO_4$, bubble N_2 to aid dissolution.

iii) Obtain voltammogram of molten (Na-K)OH eutectic containing $KMnO_4$.

Organic run

i) Remove vibrating electrode, stopper reactor and connect condenser delivery line to reactor.

ii) Charge syringe with organic and weigh.

iii) Check all temperatures.

iv) Place major safety screen in position.

v) Start syringe pump and retire to mass spectrometer console.

vi) monitor organic/N_2 gas exit from condenser using scan mode every half minute, until organic input ceased.

vii) Continue passage of N_2 for 5 minutes to purge system then raise and maintain N_2 blanket.

viii) Disconnect the delivery line (between syringe and reactor) from the reactor and weigh together with the syringe to account for any organic liquid remaining in them.

ix) Stopper condenser dry and weigh.

x) Insert vibrating electrode and obtain voltammogram of the melt.

xi) Raise melt, note colour and if precipitate, suspension, or solution present and anything unusual.

xii) Analyse liquid product by gas liquid chromotography.

xiii) Switch off furnace and heating tapes, maintain N_2 blanket until melt has solidified.

This type of experiment was performed on all organic compounds that had been used in the preliminary experiments, firstly in a molten (Na-K)OH eutectic and then secondly in a melt containing $KMnO_4$.

7.4 Results and Discussion of the Preliminary Reaction Experiments

The first series of experiments was to pass the organics through molten (Na-K)OH eutectic at 523K to confirm that no violent reactions occurred. The organic chemicals used were, methanol, ethanol, n-propanol, butanol, iso-propanol 2 methyl propan-2-ol, benzyl alcohol, allyl alcohol, propane 1, 2 diol, n-hexane, n-heptane, 1-heptene, toluene, cyclohexane and acetone. $1cm^3$ of the organic was injected first and then if no violent reaction occurred, a further $4cm^3$. All the organics passed through the melt without any violent reaction. By looking at the melt afterwards the following organics showed signs that reaction had taken place: benzyl alcohol reacted and a white solid product was observed, also the reactor was full of white fumes; allyl alcohol and propane 1, 2 diol reacted and in both reactions a white solid was also formed; 1-heptene reacted with the melt and the melt colour was yellow after the reaction ; acetone reacted with the melt and produced a milky solution which changed later to dark brown. The remaining organics did not change the colour of the melt or produced solids, but that does not necessarily mean that they did not react with the melt, however, it does indicate that they are not as reactive as the five organics mentioned. N-hexane, n-heptane, toluene and cyclohexane were the organics that did not show signs of reaction with molten hydroxide. With these experiments completed the next stage was to pass the organics through molten (Na-K)OH eutectic containing $KMnO_4$. Two pH_2O values were used 1 and -1 to stablize Mn(V) or Mn(VI) respectively. In table 7-1 and table 7-2 are presented the results of these experiments.

Organic Input	*Final Melt Colour
Methanol	Light brown
Ethanol	Light brown
N-propanol	Emerald green
1-Butanol	Emerald green
Iso-propanol	Emerald green
2 Methyl propan-2-ol	Emerald green
Benzyl alcohol	Emerald green
Allyl alcohol	Light brown
Propane 1, 2 diol	Dark brown
N-hexane	Emerald green
N-heptane	Emerald green
1-heptene	Yellowish brown
Toluene	Emerald green
Cyclohexane	Emerald green
Acetone	Dark brown

Table 7-1 The Effect of Various Organic Compounds on the System (Na-K)OH Eutectic Containing $KMnO_4$ at 523K.

$pH_2O = -1$, Mn(VI) stabilized

(Na-K)OH(46.23g), $KMnO_4$(0.146g)

*Initial melt colour emerald green in all cases.

Organic Input	*Final Melt Colour
Methanol	Light brown
Ethanol	Greenish blue
N-propanol	Greenish blue
\-Butanol	Greenish blue
Iso-propanol	Light brown
2 Methyl propan-2-ol	Greenish blue
Benzyl alcohol	White froth
Allyl alcohol	Light brown
Propane 1, 2 diol	Dark borwn
N-hexane	Greenish blue
N-heptane	Greenish blue
1-Heptene	Yellowish brown
Toluene	Greenish blue
Cyclohexane	Greenish blue
Acetone	Dark brown

Table 7-2 The Effect of Various Organic Compounds on the System (Na-K)OH Eutectic Containing $KMnO_4$ at 523K.

pH_2O = 1, Mn(V) stabilized,

(Na-K)OH(46.23g), $KMnO_4$(0.146g)

*Initial melt colour greenish blue in all cases.

As can be seen from tables 7-1 and 7-2, methanol, allyl alcohol, propane 1, 2 diol, 1-heptene and acetone all reacted in Mn(VI) and Mn(V) melts, the melt changing colour to a brown suspension/precipitate. Ethanol reacted in the Mn(VI) melt only, Iso-propanol and benzyl alcohol reacted in the Mn(V) melt only.

These experiments showed that the passage of organic compounds through molten (Na-K)OH containing Mn(V) or Mn(VI) was possible and that reactions did occur in some cases. Furthermore the passage of the organic compounds and their subsequent reactions were not violent.

7.5 Results and Discussion of the Comprehensive Reaction Experiments

Experiments were performed on all the organic compounds in molten (Na-K)OH in the larger reactor and special attention was paid to the mass balances. In order to obtain the best possible mass balance and to check the system for leaks, if any, before carrying out the reaction experiments, the organic compounds were initially injected into the empty reactor after heating it to 523K. Dry N_2 was used to entrain the organic into and out of the reactor so that water did not affect the mass balance in any way. The results were satisfactory except for those compounds that have high vapour pressures like n-hexane and acetone where mass losses of 30 - 40% based on the input were obtained. It was noticed that increasing the injected mass of the input organic generally improved the mass balance. The maximum loss was approximately 5% based on the input mass and that occurred with n-heptane. The minimum loss was about 1% in the case of ethanol. Having optimized the mass balance, by obtaining reasonably constant losses using the available equipment, the organics were then passed through molten (Na-K)OH at 523K. The mass balances obtained when the following organics were passed through the melt resulted in mass losses of up to 50% by weight of the initial organic input: benzyl alcohol, allyl alcohol, propane 1, 2 diol and 1-heptene.

Analysis of the liquid product showed that only the unreacted organic and water were condensed. Analysis of the exit gas showed that hydrogen was produced. This suggests that the products of the reaction between these organics and the hydroxide melt stayed in the melt solution. It was therefore decided not to study the oxidation of these organics in more detail because of their dehydrogenation reactions with the hydroxide melt, which was considered beyond the scope of this research. Having spent several months on trying to improve the mass balance of n-hexane and acetone as well as analysing the reaction products of the other organics with the hydroxide melt, it was decided to concentrate the investigations on three organic compounds only, ethanol, iso-propanol and methanol as the other organics did not appear to be oxidized. Also these three represent a homologous series of compounds.

7.5.1 The Oxidation of Ethanol

In table 7-3 are shown the results of mass balances obtained when ethanol was injected into the empty reactor at 523K, purged with dry N_2 and then condensed in the glass coil condenser cooled by the chiller circulator system at 255K. In table 7-4 are presented the results of mass balances after passing ethanol through molten (Na-K)OH at 523K. Analysis of the liquid product showed that it was only water and excess ethanol. The amount of ethanol lost in reaction and shown in table 7-4 represents the net loss, i.e. the loss shown in table 7-3 and the amount of water condensed with the ethanol was taken into account. The condensed water could have come from the saturated N_2 that was bubbling through the melt or have been produced from the reaction between the melt and the alcohol or more likely from both, the saturated N_2 and the reaction. Analysis of the exit gas during the alcohol injection by the mass spectrometer showed that hydrogen was being produced indicating that the reaction was a dehydrogenation reaction. As can be seen from table 7-4 the water concentration in the melt did not affect the amount of ethanol reacted with the melt. To make sure that the rate at which the alcohol was injected ($0.4cm^3 \ min^{-1}$) was not too fast for the reaction a second passage of alcohol was made, only 1% of the amount injected was lost and this was the usual loss in the system. Hence it was concluded that approximately 10% of the alcohol injected reacts with the melt and that the reaction rate is relatively slow at the specified experimental conditions.

Mass Input (g)	Mass Output (g)	Mass Loss (g)	g% Loss Based on Input
3.204	3.155	0.049	1.53
4.36	4.302	0.058	1.33
4.826	4.78	0.046	0.95

Table 7-3 Three Runs Showing Mass Balances for Ethanol Passed Through the Empty Reactor at 523K.

pH_2O	Mass Input (g)	Mass Output (g)	Mass Loss (g)	g% Loss Based on Input
1	4.697	4.240	0.457	9.73
0	4.788	4.278	0.510	10.65
-1	4.835	4.352	0.483	9.99

Table 7-4 Results for the Passage of Ethanol Through Molten (Na-K)OH Eutectic at 523K.

The reactions of alcohol with molten hydroxides have been discussed generally in chapter 6. The reaction between ethanol and the melt will be discussed in detail after discussing the electrochemical analysis of the melt.
As stated in the preliminary reaction experiments (section 7.4) ethanol reacted with hydroxide melt containing $KMnO_4$ with a pH_2O value of -1 but it did not react with the same melt with a pH_2O value of 1, this suggests that ethanol was oxidized by Mn(VI) as MnO_4^{2-} and not by Mn(V) as MnO_4^{3-}.

As stated in Chapter 5, the predominant manganate species at pH_2O values less than 0 is MnO_4^{2-} while the predominant species at pH_2O values more than 0 is MnO_4^{3-}. At $pH_2O = 0$, the concentrations of each of these two species are about equal according to:

$$E_{\frac{1}{2}} = 2.25 + 0.1 \log \frac{\{MnO_4^{2-}\}}{\{MnO_4^{3-}\}}$$

It was therefore decided to study the reactions of ethanol with the melt containing $KMnO_4$ more closely and the three pH_2O values of 1, 0, and -1 were used. In table 7-5 are presented the results of these experiments. The concentration of $KMnO_4$ was kept constant at 0.09M. The experiments were carried out in two stages, the first in which ethanol was injected into the melt containing $KMnO_4$ at each of the pH_2O values seperately, when reaction took place in all three cases the melt colour changed. At a pH_2O value of 1 the percentage of ethanol reacted was about the same as that when ethanol was injected into the pure melt and analysis of the liquid product did not show any organic produced while analysis of the exit gas

			1st. ethanol injection into a melt containing $KMnO_4$				
pH_2O	Molar conc. of MnO_4^{3-} (approx)	Molar conc. of MnO_4^{2-} (approx.)	Melt Colour		g% ethanol lost based on input	CH_3CHO in liquid phase (product/ $KMnO_4$)mole%	Exit gaseous product
			before	after			
1	0.09	very low	blue	light brown	10.14	negligible	H_2
0	0.045	0.045	greenish blue	light brown	12.17	98.83	H_2
-1	very low	0.09	green	light brown	14.32	99.04	H_2
			2nd* ethanol injection into a melt containing $KMnO_4$				
1	0.09	very low	** light brown				
0	0.045	0.045	green	light brown	2.125	98.91	none
-1	very low	0.09	green	light brown	4.39	99.22	none

* First injection was made into pure melt and % of ethanol lost is shown in table 7-4.

** The second injection was not made because when $KMnO_4$ was added it reacted with the melt.

Table 7-5 Results of Ethanol Reactions with Molten (Na-K)OH Containing $KMnO_4$ at 523K.

from the condenser showed that hydrogen had been produced. At a pH_2O value of 0 the percentage of ethanol reacted increased. Analysis of the liquid product showed acetaldehyde had been produced and again hydrogen was detected in the exit gas.

At a pH_2O value of -1, the percentage of ethanol reacted increased again. Also acetaldehyde was found in the liquid product and hydrogen was found in the exit gas. These results suggest that at $pH_2O = 1$, ethanol reacted with the melt in the same way as it reacted with the pure melt and the product of that reaction reacted with MnO_4^{3-} and the hydrogen could have been produced from either reactions. The increase in the amount of ethanol reacted at $pH_2O = 0$ is equivalent to the amount of MnO_4^{2-} that existed in the melt at this pH_2O value assuming that one mole of ethanol reacts with one mole of MnO_4^{2-}; the hydrogen produced is due to the same reactions as occurred at $pH_2O = 1$. The reaction at $pH_2O = -1$ confirms the proposed reaction at $pH_2O = 0$, where in this case again the increase in the percentage of ethanol reacted is equivalent to the MnO_4^{2-} concentration in the melt and the hydrogen produced is due to the reaction of ethanol with the hydroxide melt. About 100 mole% of acetaldehyde was produced at pH_2O values of 0 and -1 on the basis of the number of moles of MnO_4^{2-} present in the melt. The second stage of the experiments was performed to confirm the results of the first stage. Approximately the same amount of ethanol was injected into the three pure melts with the three pH_2O values of 1, 0 and -1, then $KMnO_4$ was added to these melts (0.09M). The melt with $pH_2O = 1$ reacted with the $KMnO_4$ after it had dissolved and formed MnO_4^{3-} so there was no need to inject further ethanol.

That confirmed the reaction between MnO_4^{3-} and the product of the reaction between ethanol and the hydroxide melt. At the pH_2O value of 0 it was assumed that MnO_4^{3-} had already reacted with the product of the ethanol reaction with the hydroxide melt from the first injection and that only MnO_4^{2-} was left in the melt, so a second injection was made. The percentage of ethanol reacted was equivalent to the concentration of MnO_4^{2-} in the melt producing approximately 100% acetaldehyde. The absence of hydrogen in the exit gas proves that ethanol did not undergo further reaction with the hydroxide melt. At pH_2O =-1, assuming that all the $KMnO_4$ added was present as MnO_4^{2-}, again the percentage of ethanol reacted was equivalent to the MnO_4^{2-} concentration in the melt and approximately 100% acetaldehyde was produced.

Analysis of the gas from the condenser showed negligible traces of ethanol and acetaldehyde and no other gaseous products such as hydrogen. This shows that auto-oxidation by:

$$CH_3CH_2OH \rightarrow CH_3CHO + H_2 \qquad (7\text{-}2)$$

has not occured.

According to Dytham and Weedon (67), the final product of the reaction between primary alcohols and hydroxide melts is the corresponding acid, in the case of ethanol the product should be acetic acid or in other words acetate as the acid will react according to:

$$CH_3COOH + (Na,K)OH \rightleftarrows CH_3COO(Na,K) + H_2O \qquad (7\text{-}3)$$

It was decided then to carry out experiments to investigate the reactions between the acetate ions in the melt and manganates namely MnO_4^{2-} and MnO_4^{3-}, so acetates were added to the solid pure melt in the form of glacial acetic acid with a N_2 blanket above the melt. Assuming that the reaction between the acid and the melt was complete, the concentration of the acetates in the melt solution was calculated. $KMnO_4$ was then added to the melt and its concentration was kept constant (0.09M) while the acetate concentration was varied. As was pointed out in the previous section, MnO_4^{3-} and not MnO_4^{2-} reacted with the product of the reaction between ethanol and the hydroxide melt, therefore the pH_2O value of the melt was maintained at $pH_2O = 1$.

In table 7-6 are shown the results of these experiments.

Molar acetate concentration	Melt Colour
0.06	Greenish blue
0.08	Greenish blue
0.10	Light brown
0.12	Light brown

Table 7-6 The Reactions Between the Acetate Ions and MnO_4^{3-} in (Na-K)OH Eutectic at 523K

As a further check, $KMnO_4$ was added to a melt containing an acetate concentration of 0.10M with a pH_2O value of -1; the melt colour did not change and stayed emerald green. Clearly the change of the melt colour shown in table 7-6 when the acetate concentration exceeded that of MnO_4^{3-} in the melt indicates that the reaction is on the basis of mole:mole, $CH_3COO^-:MnO_4^{3-}$, and the reaction could proceed via one of the following reactions:

$$2MnO_4^{3-} + 2CH_3COO^- + 4H_2O \rightleftarrows 2MnO_2 + 4CO_3^{2-} + 7H_2 \tag{7-4}$$

$$2MnO_4^{3-} + 2CH_3COO^- + 3H_2O \rightleftarrows Mn_2O_3 + 4CO_3^{2-} + 6H_2 \tag{7-5}$$

H_2 gas was detected in the gas stream out of the reactor after the addition of $KMnO_4$ to the melt containing acetate by mass spectrometer.

Assuming that all the ethanol lost in the experiment of table 7-4 had reacted with the hydroxide melt and that the final reaction product was acetate according to the following reaction mechanism (67):

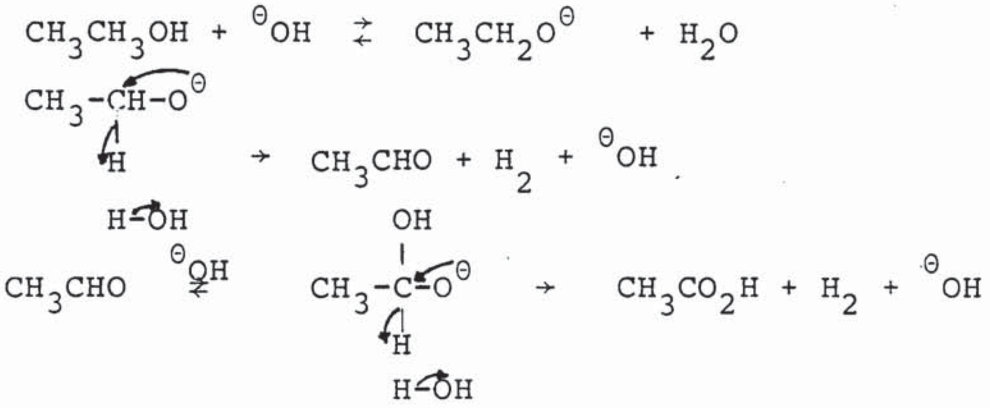

$$CH_3CH_3OH + {}^{\ominus}OH \rightleftarrows CH_3CH_2O^{\ominus} + H_2O$$

$$CH_3\text{-}CH(H)\text{-}O^{\ominus} + H\text{-}OH \rightarrow CH_3CHO + H_2 + {}^{\ominus}OH$$

$$CH_3CHO \overset{\ominus OH}{\rightleftarrows} CH_3\text{-}C(OH)(H)\text{-}O^{\ominus} + H\text{-}OH \rightarrow CH_3CO_2H + H_2 + {}^{\ominus}OH$$

therefore the acetate concentration in the melt would be 0.21M on the basis that one mole of ethanol produces one mole of acetate. This explains the results in table 7-5, where this acetate concentration is about twice the concentration of MnO_4^{3-} in the melt, so in the first injection of ethanol into a melt containing 0.09M MnO_4^{3-}, ethanol reacted with the melt first to produce the acetate ions in excess, and then these reacted with the MnO_4^{3-} ions. The same interpretation applies to the other results.

7.5.1.1 The Electroanalysis of the Experimental Melt Solutions

As a further confirmation of the results obtained in the previous section, electrochemical analysis was performed on all the melt solutions used in the reaction experiments. It was thought that using electrochemical analysis would not only help in identifying the reaction products remaining in the melt but would also be useful in monitoring the oxidation of the alcohol by MnO_4^{2-}, since the wave due to the reduction of MnO_4^{2-} should disappear after the oxidation reaction. Moreover the methods used for analysing the pure melt after its reactions with organic compounds by other workers like Weedon et al. (67,87) did not include electrochemical methods. The present work could therefore provide a new and reliable method of analysis.

A voltammogram of the melt solution after the ethanol injection using the vibrating working electrode is presented in Fig. 7-1. Four new waves were found which have been assigned wave numbers 24, 25, 26 and 27. All the waves are oxidation waves except wave 25, which is a reduction wave. Waves 24 and 25 are on the (f.s), waves 26 and 27 on the (r.s). Waves 24 and 27 are peak shaped with a small peak potential separation, their E_p values are 0.63V and 0.66V respectively.

The $E_{\frac{1}{2}}$ value of wave 25 is 0.25V, that of wave 26 is 0.23V. The $E_{\frac{1}{2}}$ values of these waves indicate that waves 24 and 27 are due to the same electrode reaction and waves 25 and 26 are due to another electrode reaction.

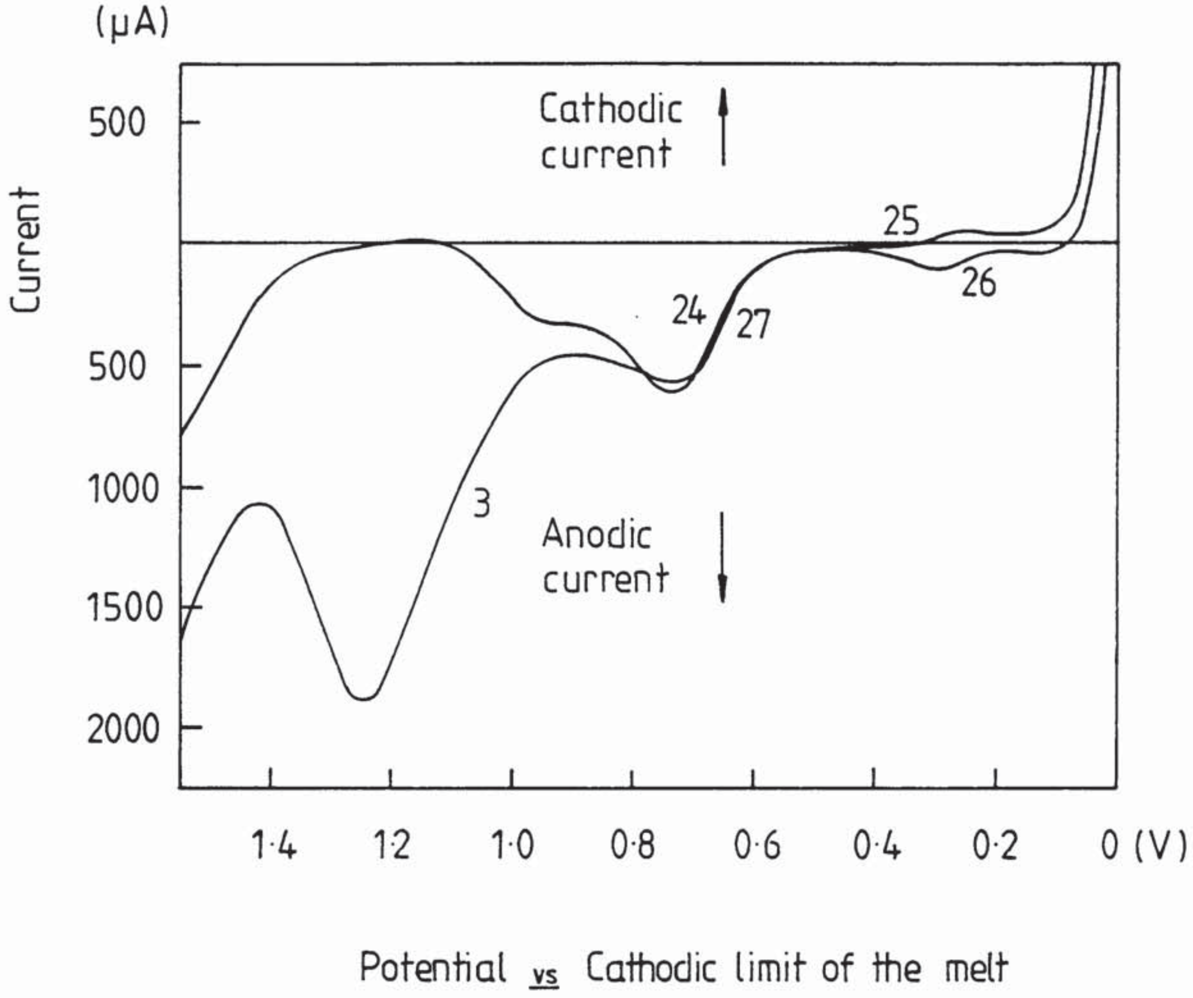

Figure 7-1 Voltammogram of (Na-K)OH eutectic after passing Ethanol at 523K, using a vibrating Pt indicator electrode, under N_2.

A large anodic peak was also found on the (r.s) with an E_p value of 1.20V. The $E_{p/2}$ value of the peak however suggests that it is wave 3 due to the Pt electrode oxidation.

The voltammogram was found to be reproducible except for wave 26 which in one voltammogram shifted towards a more positive value (by about 0.1V) without changing any of the experimental conditions. This shift will be discussed when waves 25 and 26 are discussed. Analysis of wave 24 by H.I.E. plot gave a straight line with a slope of 0.053V, Fig. 7-2, indicating a reversible two electron transfer reaction. Similarly analysis of wave 27 gave a straight line with a slope of 0.055V, Fig. 7-3. Analysis of waves 25 and 26 also gave straight lines with slopes of 0.057V, Fig. 7-4 and 0.052V, Fig. 7-5, respectively suggesting reversible two electron transfer reactions. Analysis of wave 3 gave a straight line with a slope of 0.12V indicating an irreversible electrode reaction.

Using the stationary working electrode, the voltammogram obtained was similar to that obtained using the vibrating working electrode, but the waves analysis gave straight lines with slope values indicating irreversibility as was the case when cyclic voltammograms were obtained in the investigation of the hydroxide melts containing $KMnO_4$ (Chapter 5).

One remark that can be made about the cyclic voltammogram here is that a cathodic peak (wave 1) was found with about the same peak height as that of peak 3

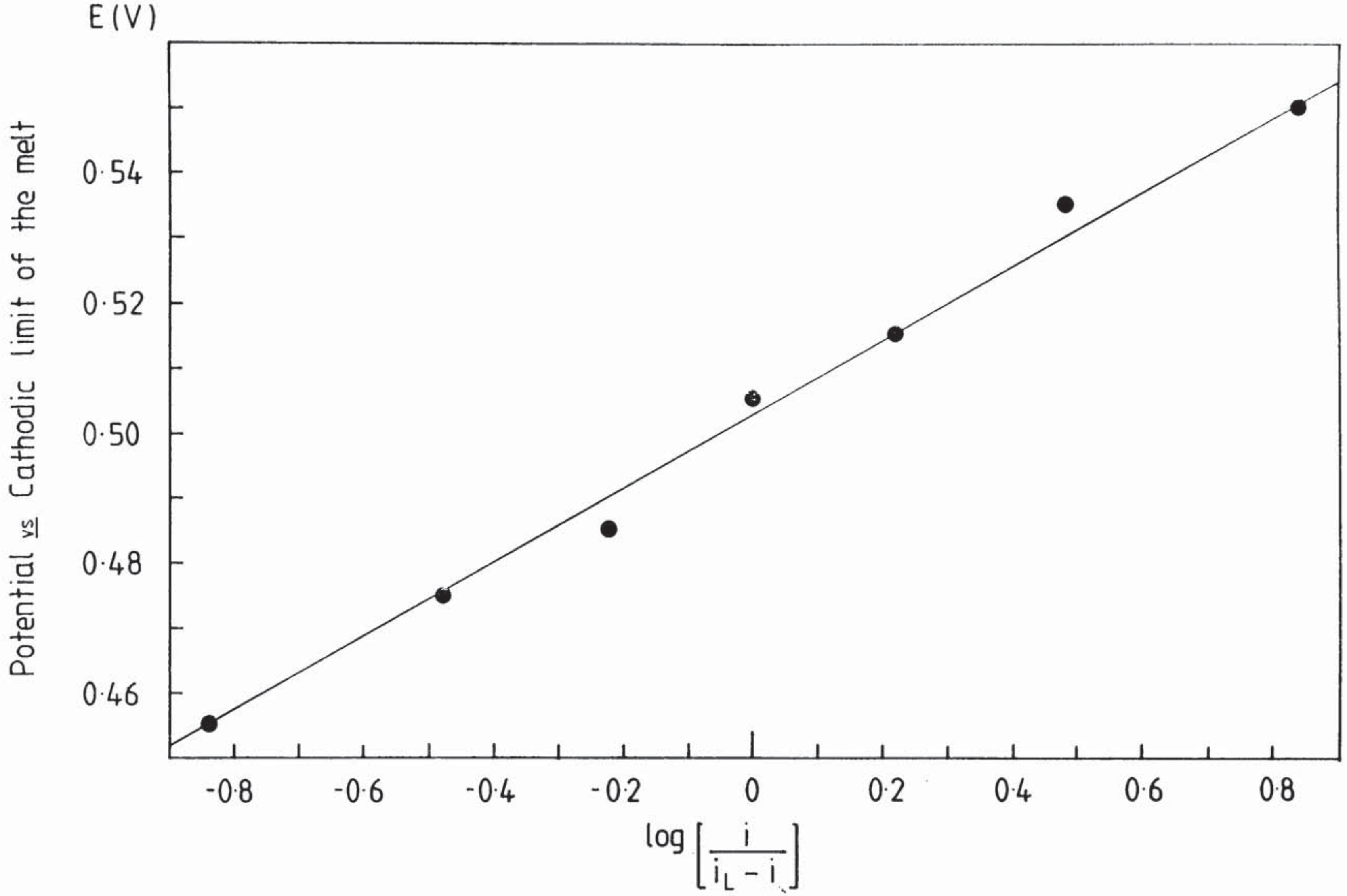

Figure 7 - 2 H.I.E. Analysis of voltammetric oxidation wave 24

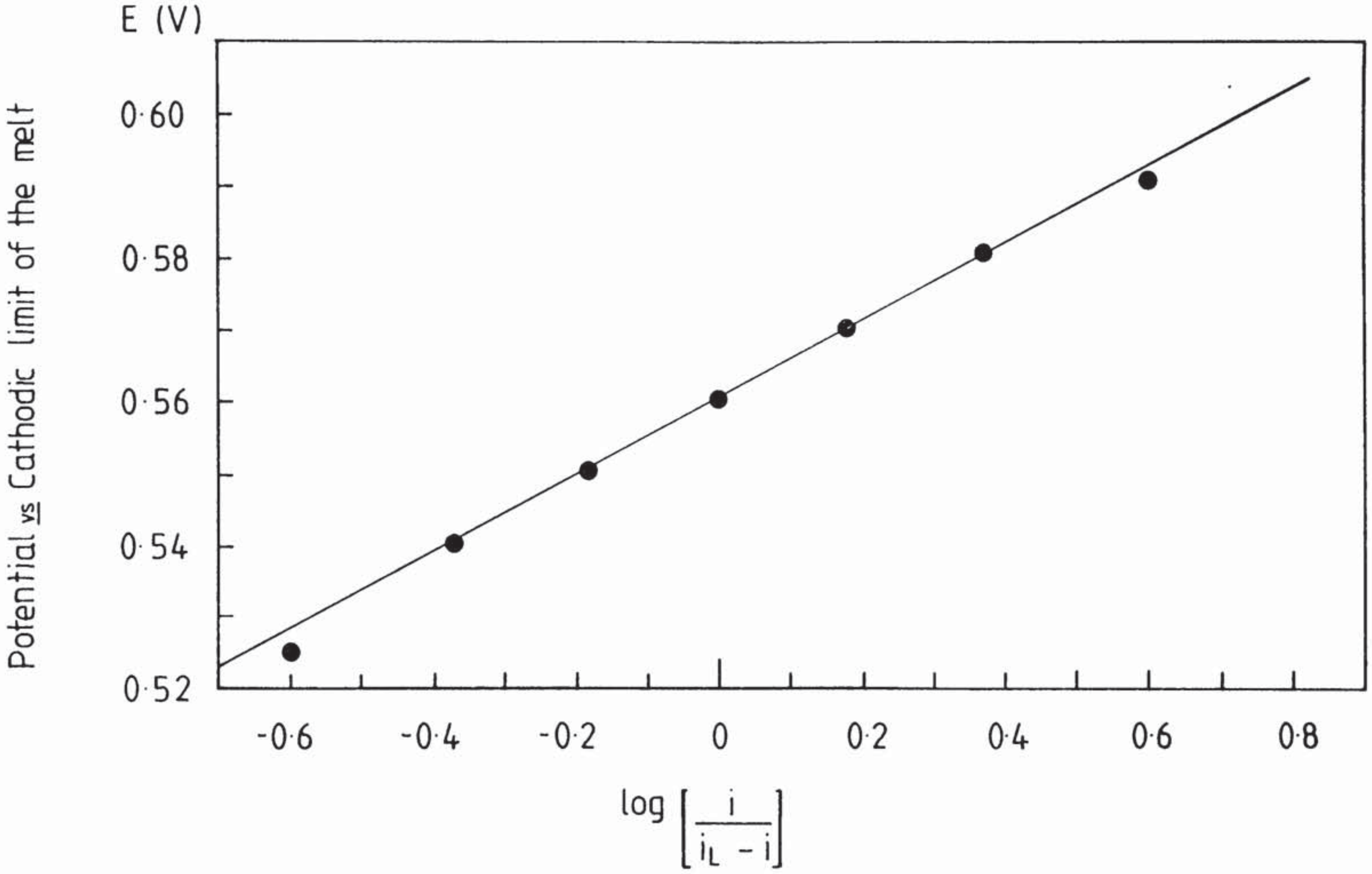

Figure 7-3 H.I.E. Analysis of voltammetric oxidation wave 27.

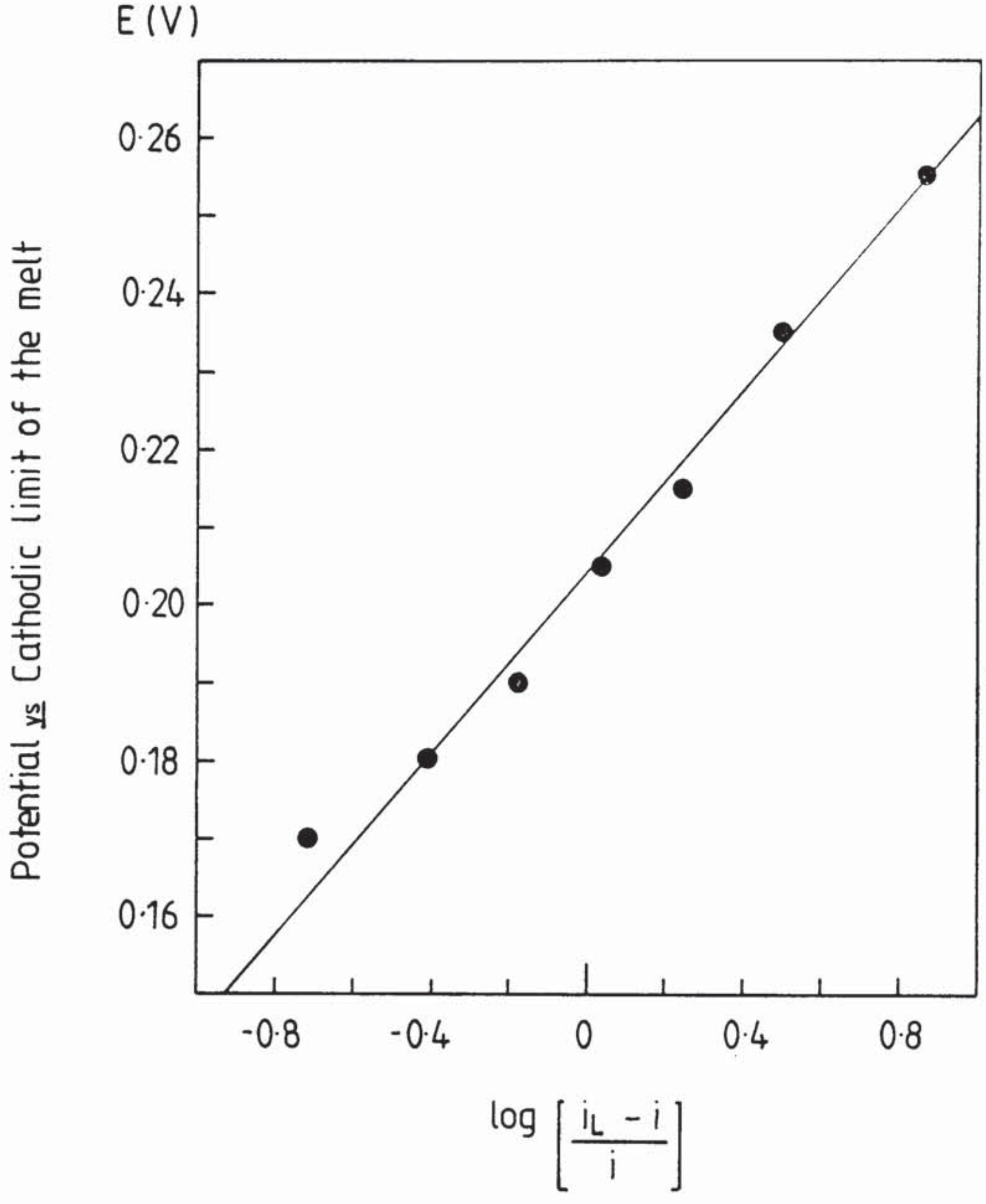

Figure 7-4 H.I.E. Analysis of voltammetric reduction wave 25.

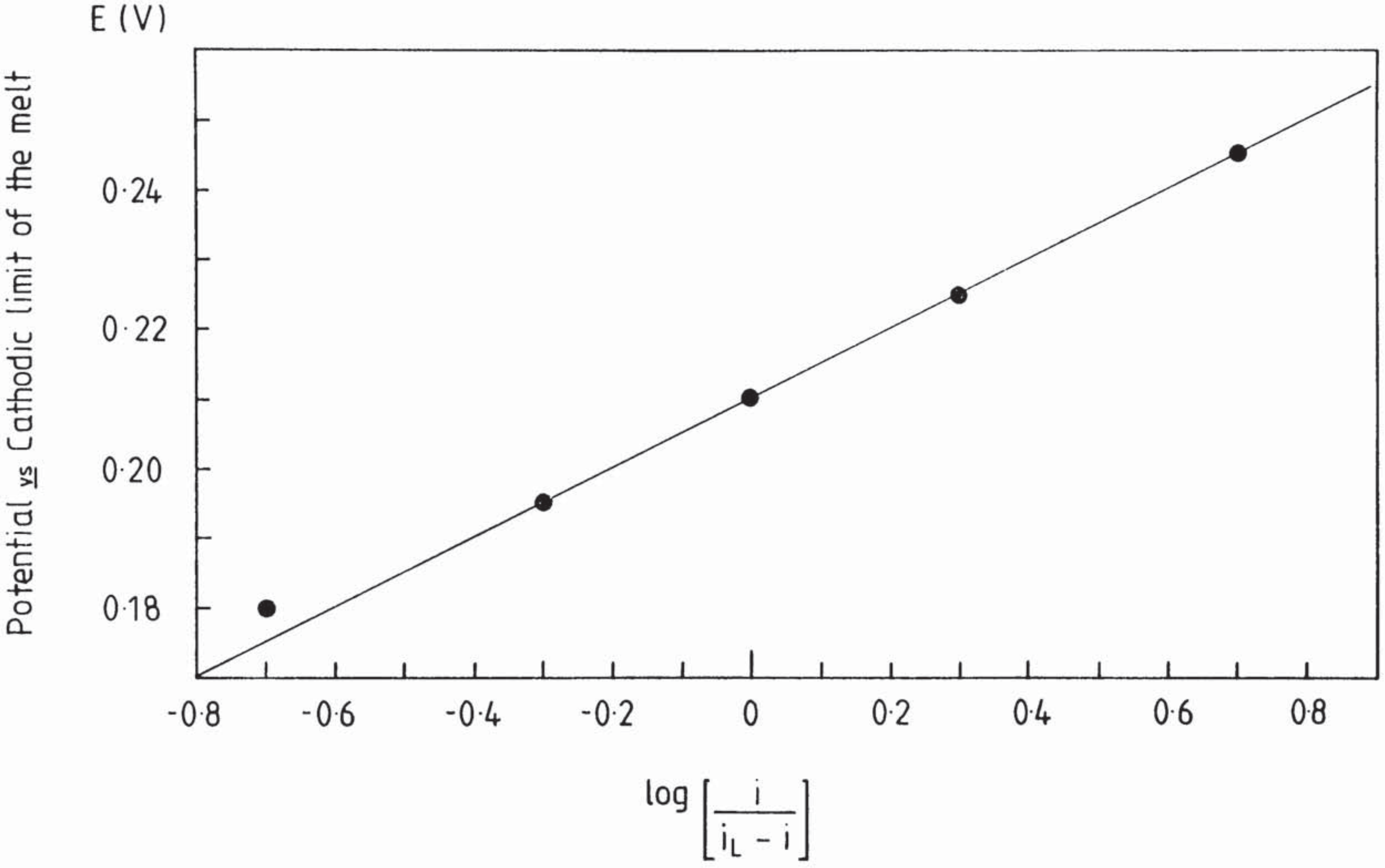

Figure 7 - 5 H.I.E. Analysis of voltammetric oxidation wave 26.

with a potential separation from peak 3 of 0.19V.

It was thought that it would be reasonable to attribute waves 24 and 27 to the following reaction:

$$CH_3COO^- + OH^- - 2e^- \rightleftarrows CO_2 + CH_3OH \quad (7-6)$$

which was proposed by Hofer and Moest (98) at the turn of the century for the oxidation of acetate in alkaline solutions at a platinum electrode. This electrode reaction will be confirmed later.

The interpretation of waves 25 and 26 was found to be more complicated as it involved adsorption of several organic and inorganic compounds on the platinum electrode surface namely H_2, CO_2, CH_3OH and C_2H_5OH, where CH_3OH and CO_2 were the products of the electrode reaction represented by waves 24 and 27, C_2H_5OH was the reactant and hydrogen was produced via more than one reaction both chemically and electrochemically. Hydrogen is one of the products of water reduction at the platinum electrode, it is also produced from the reaction between ethanol and the melt. The mechanism and nature of adsorption of organic compounds on platinum electrodes has been discussed in detail by many workers (99). A distinction has been made between a chemical mechanism and an electrochemical mechanism of adsorption. In the chemical mechanism of adsorption of methanol for example (100-102) it was suggested that it is possible that the adsorption process itself causes hydrogen atoms to split off and leads to formation of methanol dehydrogenation product on the electrode surface and therefore the anodic wave found is due to ionization of hydrogen atoms split off from the alcohol molecules. On the other hand the electrochemical mechanism of adsorption (103) suggests that the wave is due to transfer of electrons from the alcohol molecules to the platinum and that the adsorbed hydrogen atoms appear as the result of the following reaction:

$$H_2O + e^- \rightleftarrows H_{ads.} + OH^- \text{ (in alkaline solutions)} \quad (7\text{-}7)$$

Accurate determination of the composition of the chemisorbed substance presented a complicated problem for many workers as the adsorption products formed on the electrode surface during contact of the electrode with a solution of the particular adsorbate may differ greatly in nature from the original substance, as a result of dehydrogenation, hydrogenation, autohydrogenation reactions and splitting of the molecules. Therefore, adsorption of species such as CHO, C_nH_{2n+1} and RHCOH on the electrode surface is to be expected (99). It was reported (104) that the composition of the adsorbed methanol depends on the electrode potential and that CO_2 was produced via a two electron transfer oxidation reaction of the adsorbed species. In the case of chemisorbed ethanol, adsorption occurs during cathodic polarization of the electrode and ethane was found as the main hydrogenation product in the gases evolved during the polarization. It was also reported (105) that the chemisorption processes become more complicated at high temperatures and hydrogen was evolved from alkaline solutions of methanol indicating dehydrogenation of the alcohol. The potential range at which most of the work carried out by the workers referred to in the discussion above was close to the cathodic limit of the solvents used, which is in most cases the hydrogen gas evolution region and the $E_{\frac{1}{2}}$ values of waves 25 and 26 in Fig. 7-1 are also close to the cathodic limit of the melt where hydrogen is produced at the electrode. Therefore, waves 25 and 26 are comparable to the waves obtained by the other investigators. In the light of this discussion, waves 25 and 26 are probably due to one of the following three reactions:

i) $CH_3OH + OH^- \rightleftarrows CH_3O^- + H_2O$ (reaction in solution) (7-8)

then the electrode reaction is:

$2CH_3O^- + 3H_2 - 2e^- \rightleftarrows 2CH_4 + 2H_2O$ (7-9)

ii) $C_2H_5OH + OH^- \rightleftarrows C_2H_5O^- + H_2O$ (reaction in solution) (7-10)

then the electrode reaction is:

$2C_2H_5O^- + 3H_2 - 2e^- \rightleftarrows 2C_2H_6 + 2H_2O$ (7-11)

iii) $CO_2 + H_2O + 2e^- \rightleftarrows CO + 2OH^-$ (7-12)

the species in all the electrode reactions are assumed to be chemisorbed on the electrode surface. No conclusive evidence was obtained as to which of these proposed reactions waves 25 and 26 are due. The shift of the $E_{\frac{1}{2}}$ value of wave 26 towards more positive values can be interpreted as follows:

In the investigation of the interaction of ethanol with the Pt electrode surface it was reported (106-108) that when the alcohol was brought into contact with the electrode, the electrode potential shifted in the cathodic direction followed by another shift in the anodic direction, the latter process begins after some delay. In the case of alcohols containing more than one carbon atom, the shift in the anodic direction was accompanied by evolution of gaseous products. The hydrocarbons with the same number of carbon atoms in the molecule as the original alcohol predominate in the gas evolved. Similar observations (107-110) were also made concerning the shift of the electrode potential with other alcohols.

These shifts of potential were thought to be due to transition from dehydrogenation causing a shift of potential in the cathodic direction to predominant hydrogenation which shifts the $E_{\frac{1}{2}}$ value in the anodic direction. Therefore the shift of the $E_{\frac{1}{2}}$ value of wave 26 could have been caused by hydrogenation of chemisorbed ethanol on the Pt electrode.

When glacial acetic acid was added to the pure solid (Na-K)OH eutectic, electroanalysis was performed and Fig. 7-6 shows the voltammogram of the melt solution using the vibrating working electrode. The similarity beween this voltammogram and the one in Fig. 7-1 is clear.

Waves 24 and 27 were found with E_p values very close to those of the same waves in Fig. 7-1. The analysis of these waves again gave straight lines with slopes indicating a reversible two electron transfer reaction. Consequently the formation of acetate as the final reaction product for the reaction between ethanol and the hydroxide melt and the proposed electrode reaction for waves 24 and 27 have been confirmed. Moreover, the analysis of the four melt

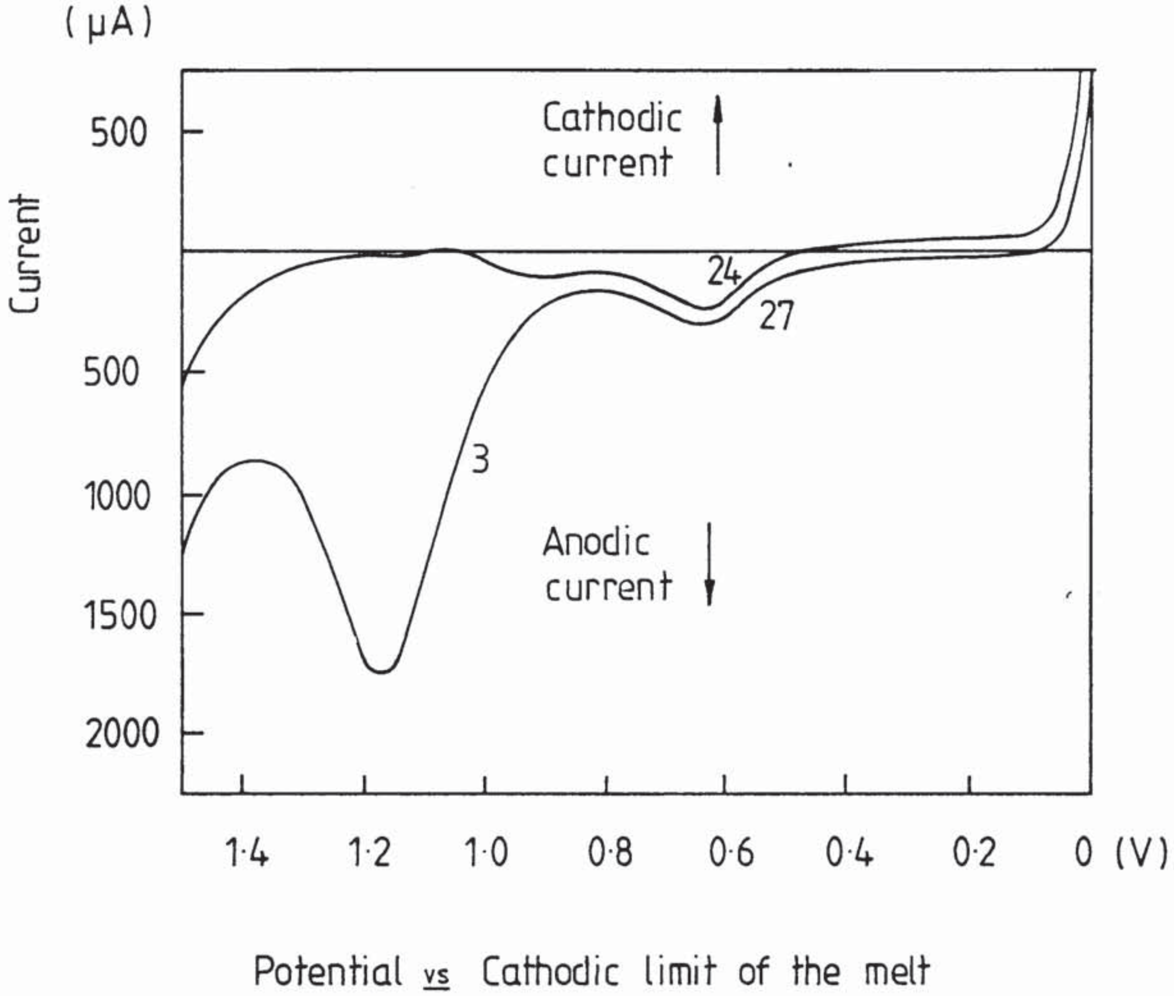

Figure 7-6 Voltammogram of (Na-K)OH eutectic at 523K containing acetate (0·1M) added as glacial acetic acid, under N_2, using a vibrating Pt indicator electrode.

solutions of table 7-6 (i.e. the melts containing four different acetate concentrations, before adding $KMnO_4$) showed that the limiting currents of waves 24 and 27 were directly proportional to the acetate concentration in the melt.

The absence of waves 25 and 26 in Fig. 7-6 suggests that in Fig. 7-1 they were due to the reduction and oxidation of chemisorbed ethanol and not to chemisorbed methanol or CO_2. After adding $KMnO_4$ (0.09M) to the melt containing acetate (0.1M), (produced from the reaction between the hydroxide melt and glacial acetic acid), the voltammogram shown in Fig. 7-7, was obtained using the vibrating working electrode. The pH_2O of the melt was approximately equal to 1. On the (f.s) two oxidation waves and one cathodic wave were found, the $E_{\frac{1}{2}}$ value of the first oxidation wave suggests that it is wave 4. (see Fig. 5-6).

The second oxidation wave has an $E_{\frac{1}{2}}$ value close to that of both waves 24 and 5. H.I.E. analysis of the wave suggested an irreversible electrode reaction. The fact that Mn^{2+} existed in the melt, which will be discussed later, suggests that the second oxidation wave is due to a mixed electrode process involving the oxidation of acetates and Mn^{2+}. The reduction wave on the (f.s) is in fact a peak with an E_p value close to that of wave 6 (in Fig. 5-6) therefore it is due to Mn^{2+} reduction.

On the (r.s) two oxidation waves were found, the first was thought to be due to the same mixed electrode

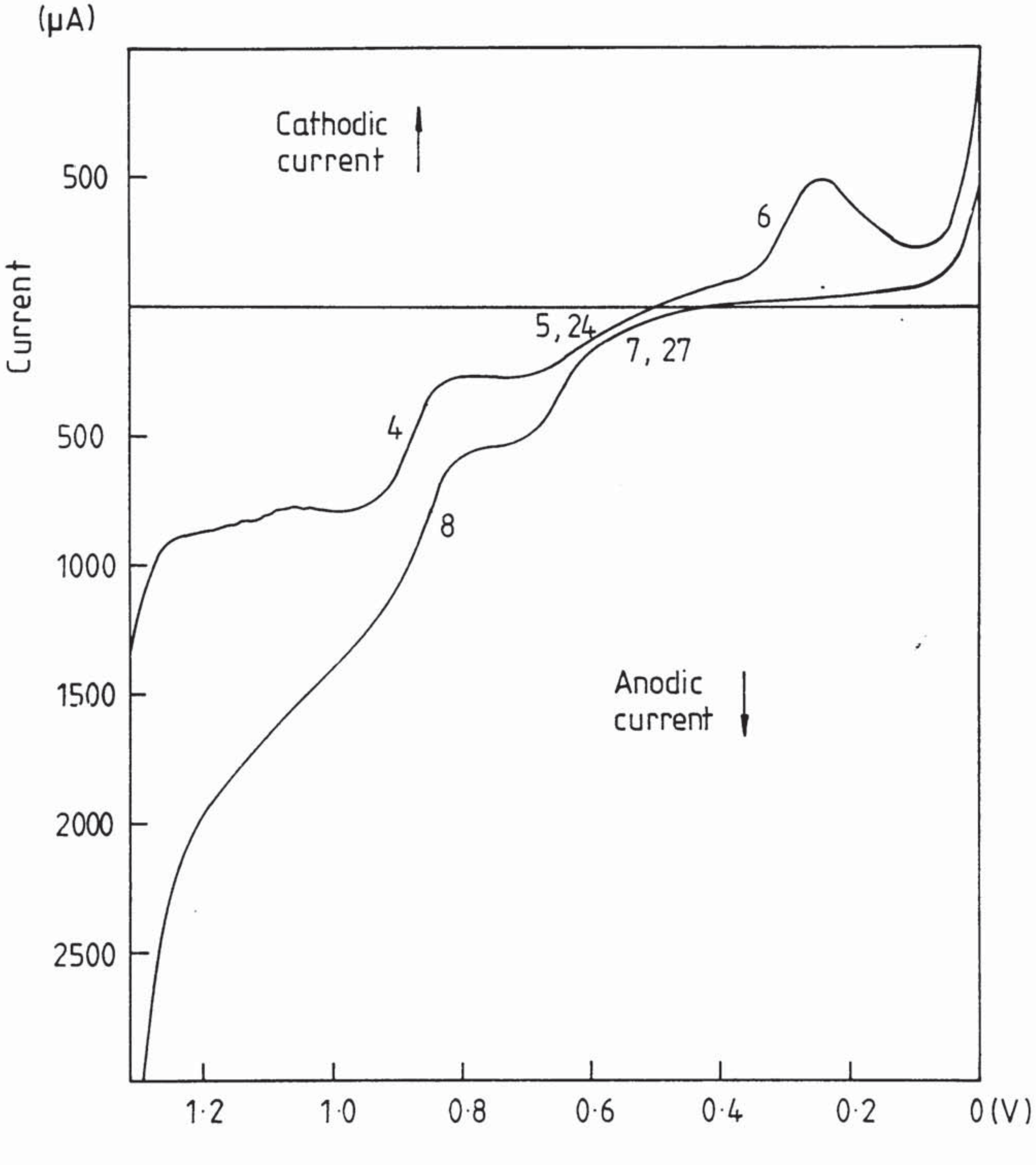

Potential vs Cathodic limit of the melt.

Figure 7-7 Voltammogram of (Na-K)OH eutectic at 523K containing acetate (0·1M) added as glacial acetic acid and $KMnO_4$ (0·09M), under N_2, using a vibrating Pt indicator electrode.

process found on the (f.s). The second wave was wave 8. The resemblance between this voltammogram and that of the melt containing Mn metal, Fig. 5-6, suggests the formation of Mn^{2+} probably from reactions such as:

$$3Mn_2O_3 + H_2O \rightleftharpoons 2MnO_4^{3-} + 4Mn^{2+} + 2OH^- \qquad (7\text{-}13)$$

and

$$MnO + H_2O \rightleftharpoons Mn^{2+} + 2OH^- \qquad (7\text{-}14)$$

These reactions are expected at $pH_2O = 1$. Consequently the reaction between MnO_4^{3-} and acetates should produce Mn_2O_3 according to equation (7-5).

Fig. 7-8 shows the same voltammogram, with the current scale reduced to show another two oxidation waves one on the (f.s) and the other on the (r.s). Their $E_{\frac{1}{2}}$ values are approximately the same. These two waves are due to the carbonate oxidation (see wave 13 in Fig. 5-34) hence the reaction between MnO_4^{3-} and acetates is confirmed once again.

The elctroanalysis of the melts used to produce the results of table 7-5 are presented in Fig. 7-9, Fig. 7-10 and Fig. 7-11. The voltammogram shown in Fig. 7-9 is of the melt solution containing $KMnO_4$ (0.09M) at $pH_2O = 0$, using the vibrating working electrode. This voltammogram has been discussed previously (see Chapter 5). Clearly both MnO_4^{2-} and MnO_4^{3-} existed in this melt as the waves 20 and 9 indicate.

The voltammogram of Fig. 7-10 is of the melt solution containing $KMnO_4$ (0.09M) at $pH_2O = 0$, after the first ethanol injection, using the vibrating working electrode.

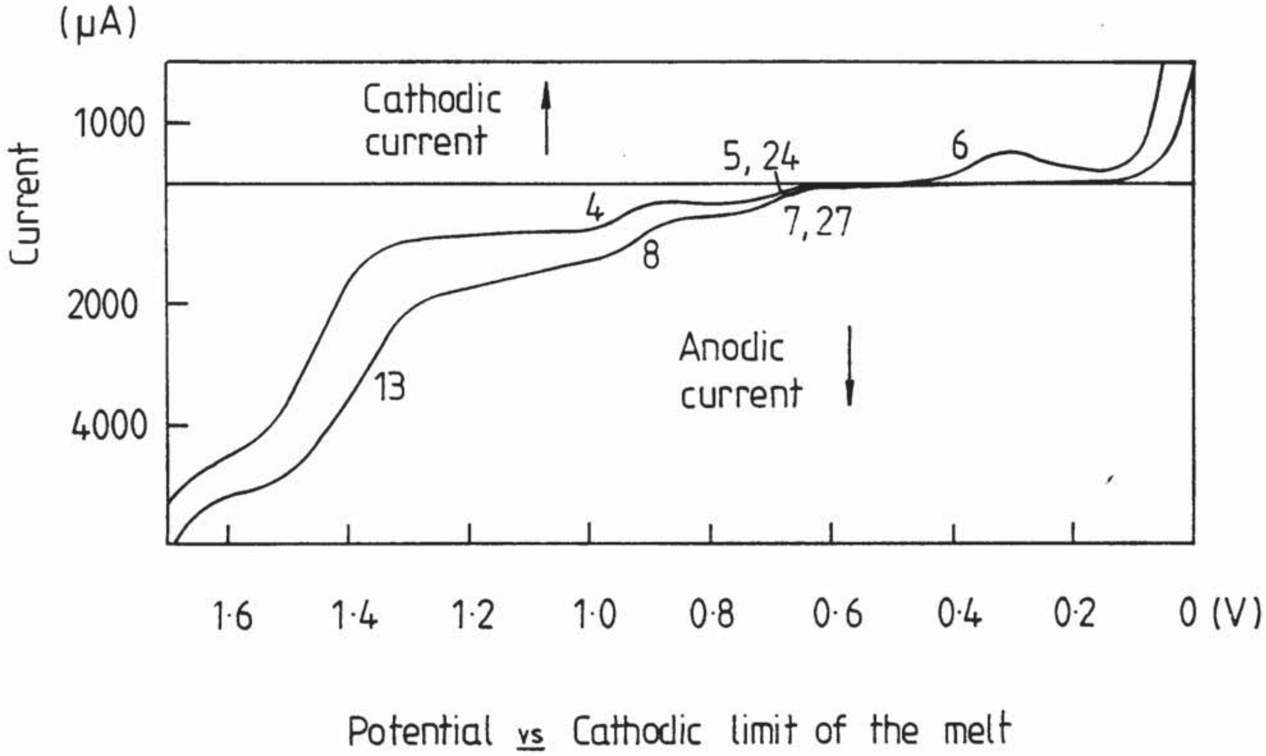

Figure 7 - 8 Voltammogram of (Na-K)OH eutectic at 523 K containing acetate (0·1 M) added as glacial acetic acid and $KMnO_4$ (0·09M), under N_2, using a vibrating Pt indicator electrode, showing wave 13.

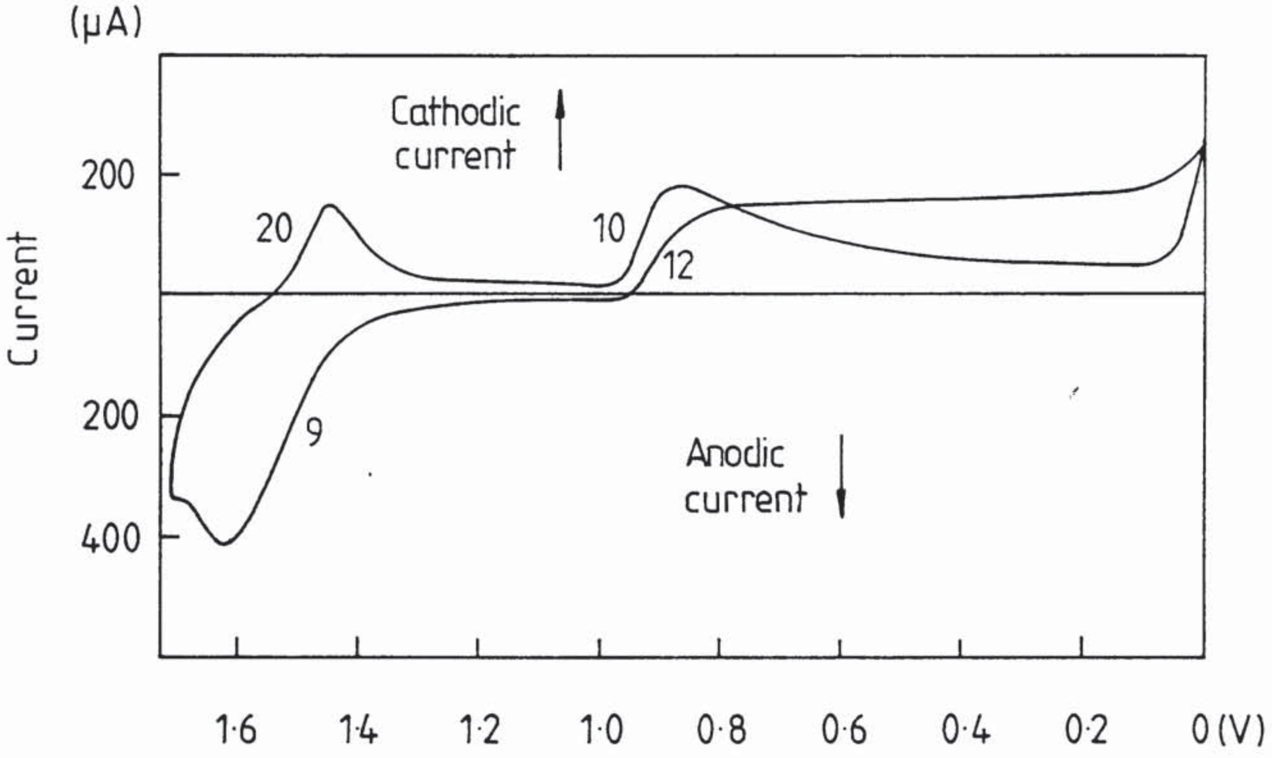

Potential vs Cathodic limit of the melt

Figure 7 - 9 Voltammogram of (Na-K)OH eutectic containing $KMnO_4$ (0·09M) at 523K and $pH_2O = 0$, under N_2, using a vibrating Pt indicator electrode.

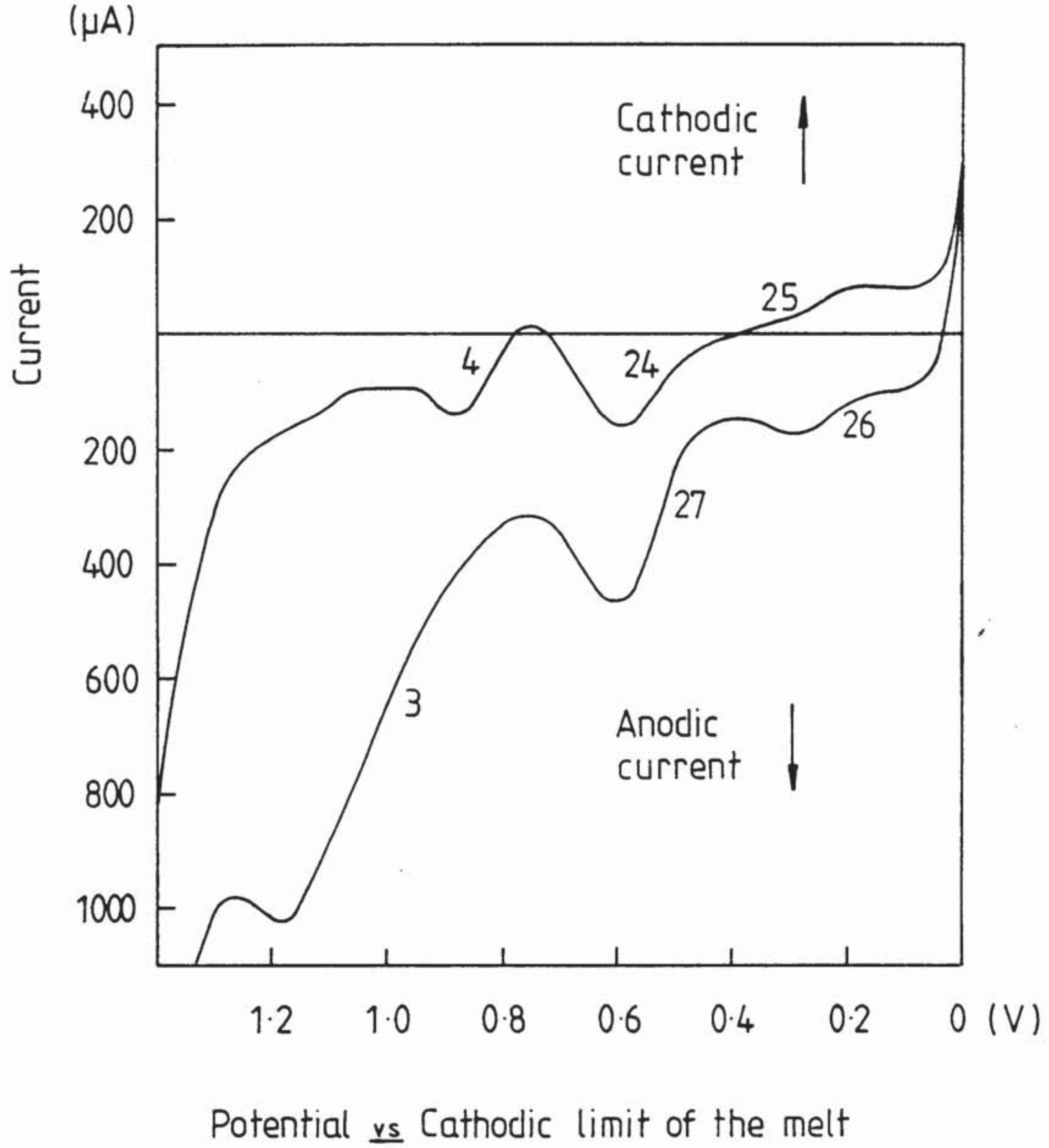

Figure 7-10 Voltammogram of (Na-K)OH eutectic containing $KMnO_4$ (0·09M) at 523K and $pH_2O = 0$ after the 1st ethanol injection, using a vibrating Pt indicator electrode.

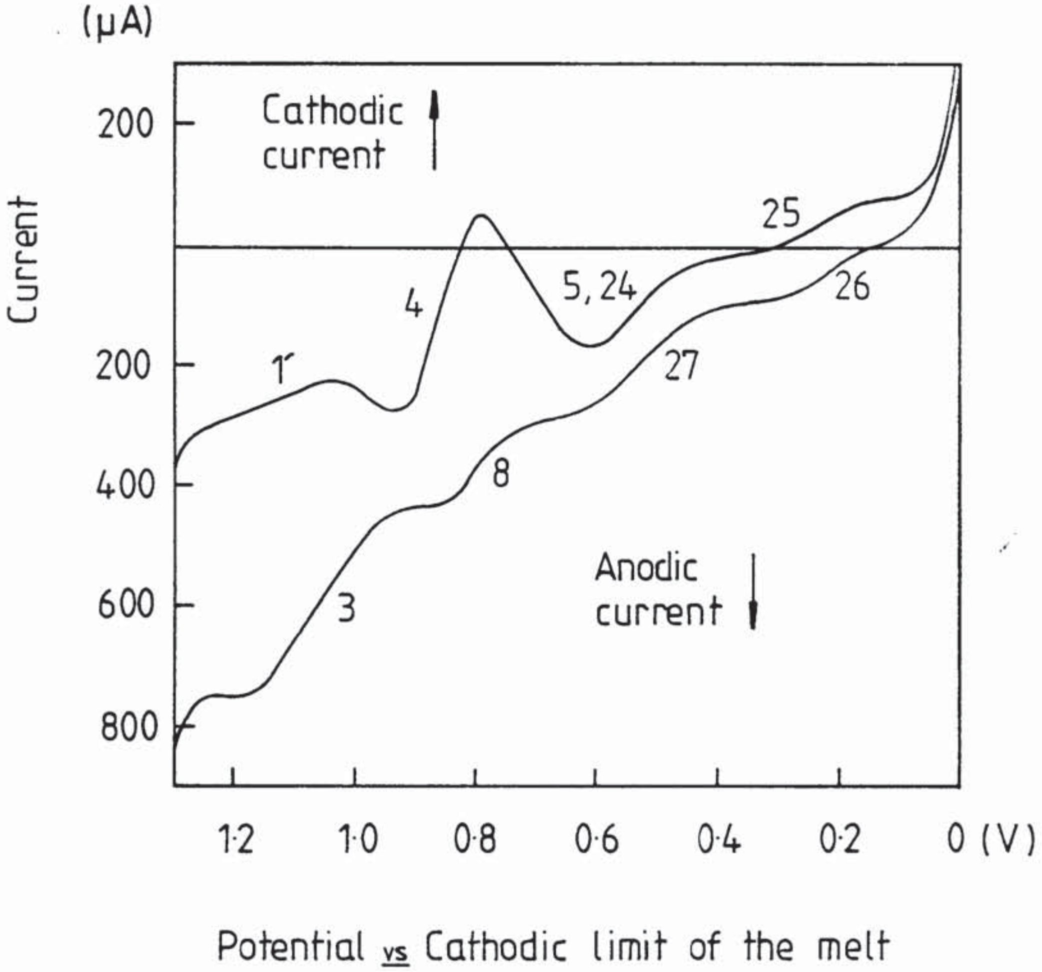

Figure 7-11 Voltammogram of (Na-K)OH eutectic containing $KMnO_4$ (0·09M) at 523K and $pH_2O = 0$ after the 2nd ethanol injection, the 1st injection was made into the pure melt before adding $KMnO_4$, using a vibrating Pt indicator electrode.

The voltammogram is similar to that of the pure melt after passing ethanol through it, Fig. 7-1, the only difference is the appearance of an oxidation peak on the (f.s) which has a $E_{p/2}$ value close to that of wave 4, therefore the peak is due to the oxidation of Mn_2O_3 produced from the reaction between MnO_4^{3-} and acetates.

In an attempt to regenerate the oxidizing agent MnO_4^{2-}, oxygen was bubbled through the melt for three hours and a voltammogram of the melt solution using the vibrating working electrode was obtained. It was exactly the same as the voltammogram of Fig. 7-1, in other words the peak due to the Mn_2O_3 oxidation has disappeared. This suggests that Mn_2O_3 has been oxidized to what probably seems an insoluble compound as it did not appear in the voltammogram as a new wave. A few green drops were observed on the inside wall of the beaker that contained the melt, suggesting that some of the Mn_2O_3 has been oxidized to MnO_4^{2-} and that bubbling oxygen through the melt for along time could regenerate the oxidizing agent which is particularly important for an industrial process. The voltammogram of Fig. 7-11 is of the melt solution containing $KMnO_4$(0.09M) at pH_2O= 0, after the second ethanol injection; the first injection having been made into the pure melt, before adding $KMnO_4$. The difference between the voltammogram in Fig. 7-11 and that in Fig. 7-10 is the appearance of wave 8 on the (r.s) which is due to the same electrode reaction of wave 4, i.e. Mn_2O_3 oxidation. The disappearance of waves 20 and 9 (found in Fig. 7-9) from

Fig. 7-10 and Fig. 7-11 confirms that MnO_4^{2-} and MnO_4^{3-} had reacted, where MnO_4^{2-} oxidized ethanol to acetaldehyde and MnO_4^{3-} reacted with the acetates in the melt.

7.5.2 The Oxidation of Iso-Propanol

The reaction of iso-propanol with molten hydroxides and its oxidation in hydroxide melts containing $KMnO_4$ has been investigated in the same way as the ethanol reactions and the same experimental procedure was used. In table 7-7 are shown the results of mass balances obtained when iso-propanol was injected into the empty reactor at 523K. In table 7-8 are shown the results of mass balances obtained after passing iso-propanol through molten (Na-K)OH at 523K. Analysis of the condensed liquid product showed that it contained water and excess iso-propanol only. The amount of iso-propanol lost in the reaction shown in table 7-8 represents the net loss where the loss shown in table 7-7 and the amount of water condensed with the iso-propanol were taken into account. Analysis of theexit gas during the alcohol injection by mass spectrometer showed that methane was being produced from the reaction between iso-propanol and the hydroxide melt. Again from table 7-8 it is clear that the water concentration in the melt did not affect the amount of iso-propanol reacted with the melt; this was also noticed in the reaction of ethanol with the melt. A second passage of the alcohol was made and the amount lost was negligible. This indicated that no further reaction took place, therefore approximately 3.0% of the alcohol injected reacts with the melt.

Mass input (g)	Mass output (g)	Mass loss (g)	g% loss based on input
4.43	4.247	0.183	4.13
4.38	4.195	0.185	4.22
4.51	4.326	0.184	4.08

Table 7-7 Three runs showing mass balances for iso-propanol passed through the empty reactor at 523K

pH_2O	Mass input (g)	Mass output (g)	Mass Loss (g)	g% loss based on input
1	3.81	3.677	0.133	3.49
0	4.08	3.952	0.128	3.14
-1	3.97	3.836	0.134	3.37

Table 7-8 Results for the passage of iso-propanol through molten (Na-K)OH eutectic at 523K

According to the results shown in table 7-8 the reaction occurred at an even slower rate than the reaction rate of ethanol with the melt. In the preliminary reaction experiments, iso-propanol had reacted with hydroxide melts containing $KMnO_4$ at pH_2O value of 1 which indicated that iso-propanol was oxidized by Mn(V) as MnO_4^{3-}. Iso-propanol was not oxidized by a melt containing Mn(VI) as MnO_4^{2-}

As before iso-propanol oxidation reactions were investigated using the same three water concentrations in the melt used in investigating ethanol oxidation reactions. In table 7-9 are presented the results of these reactions. The $KMnO_4$ concentration in the melts was kept constant at 0.09M. The experiments were carried out in two stages in the first stage iso-propanol was injected into the melt containing $KMnO_4$ at each of the pH_2O values. At $pH_2O = 1$ the melt colour changed from blue to light brown, while at the pH_2O values of 0 and -1 no colour change was observed. Therefore it was concluded that oxidation had taken place only in the melt with a pH_2O value of 1. The percentage of iso-propanol lost in reaction with this melt was the highest and the liquid phase product contained 88.6 mole% of acetone. Methane gas was also produced as the exit gas analysis showed. At $pH_2O = 0$, the percentage of iso-propanol reacted decreased and the liquid product analysis gave 86.8 mole % acetone and methane gas was again found in the exit gas.

			1st. Iso-propanol injection into a melt containing $KMnO_4$				
pH_2O	Molar Conc. of MnO_4^{3-} (approx)	Molar Conc. of MnO_4^{2-} (approx)	Melt colour		g% iso-propanol lost based on input	Acetone in liquid phase (product/ $KMnO_4$)mole %	exit gaseous product
			before	after			
1	0.09	very low	blue	light brown	9.1	88.6	CH_4
0	0.045	0.045	greenish blue	green	5.9	86.8	CH_4
-1	very low	0.09	green	green	3.2	negligible	CH_4
			2nd.*Iso-propanol injection into a melt containing $KMnO_4$				
1	0.09	very low	blue	light brown	3.45	87.3	none
0	0.045	0.045	green	green	0.32	84.7	none
-1	very low	0.09	green	green	negligible	negligible	none

* First injection was made into pure melt and % of iso-propanol lost is shown in table 7-8

Table 7-9 Results of Iso-Propanol Reactions With Molten (Na-K)OH Containing $KMnO_4$ at 523K

At pH_2O = -1 the percentage of iso-propanol reacted was about the same as that when iso-propanol was injected into the pure melt. The analysis of the liquid product gave a negligible amount of acetone produced and the analysis of the exit gas from the condenser showed that methane gas had been produced. To interpret these results, it is proposed that iso-propanol reacts with the pure hydroxide melt according to the following mechanism (72):

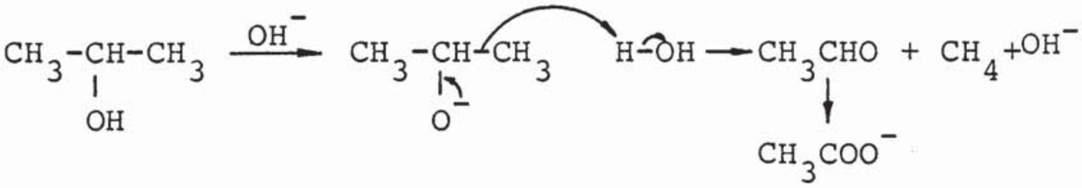

Therefore the methane gas found in the exit gas of the reactions above was produced from the reaction between the alcohol and the hydroxide melt. If it assumed that all the iso-propanol lost reacted according to the reaction mechanism above, then an acetate concentration of about 0·04M would be produced in the melt. Knowing that MnO_4^{3-} reacts with acetate (from the previous section) the results can be explained as follows:

At pH_2O = -1, assuming that the MnO_4^{2-} concentration is approximately 0·09M and that the MnO_4^{3-} concentration is very low, the iso-propanol injected was not oxidized by MnO_4^{2-} but reacted with the hydroxide melt as if the manganates were not present and consequently the green colour of the melt did not change. At pH_2O = 0, when approximately equal concentrations of MnO_4^{2-} and MnO_4^{3-} (0.045M) were present, iso-propanol was oxidized by MnO_4^{3-} to acetone. Knowing that approximately 0.00225 mole of MnO_4^{3-} existed (with the MnO_4^{3-} molar concentration of 0.045) in the melt, it was concluded that the reaction was rapid but not complete when it was found (from the results shown in table 7-9) that only about 0.002 mole of iso-propanol was oxidized to acetone on a mole:mole reaction basis.

The green colour of the melt did not change because MnO_4^{2-} did not take part in the reaction.

At $pH_2O = 1$ where the MnO_4^{2-} concentration is very low and the MnO_4^{3-} concentration was approximately 0.09M the iso-propanol was oxidized to acetone and the blue colour of the melt changed to light brown but again the reaction on a mole:mole basis was not complete as 0.004 moles of iso-propanol were oxidized by the same number of moles of MnO_4^{3-} (about 0.0045 moles of MnO_4^{3-} was present in the melt). It was concluded that the oxidation reaction of iso-propanol to acetone occurred first (the faster reaction) and this was followed by the reaction between iso-propanol and the hydroxide melt (the slower reaction). The deviation from 100% yield of acetone could be due to the formation of acetate at the same time as the iso-propanol oxidation reaction was taking place. The acetate then reacts with MnO_4^{3-} and therefore the number of moles of MnO_4^{3-} available for oxidation decreases. The second stage of the experiments was performed to confirm the results of the first stage. Approximately the same amount of iso-propanol was injected into the usual melts (at three water concentrations) before adding $KMnO_4$, then $KMnO_4$ was added to these melts (0.09M). The melt colour of all three melts was green. The second iso-propanol injection was then carried out. In the melt of $pH_2O = 1$, the amount of iso-propanol lost in the reaction and the amount of acetone produced suggests that approximately 0.0025 mole of MnO_4^{3-} was present in the melt before the second injection which oxidized iso-propanol from the second injection, to acetone. A similar number of moles of MnO_4^{3-} had reacted with the acetates produced after the first injection. No gaseous product, such as hydrogen, was detected in the exit gas which proves that auto-oxidation did not take place. At $pH_2O = 0$ the same interpretation of the results at $pH_2O = 1$ can be applied while at $pH_2O = -1$ a negligible amount of iso-propanol was lost and a similar amount of acetone was produced which confirms that iso-propanol was only oxidized by MnO_4^{3-}.

7.5.2.1 The Electroanalysis of the Experimental Melt Solutions.

Electroanalysis of the melt solutions used in the experiments was carried out as further confirmation of the results shown in table 7-9. In fig.7-12 is presented a voltammogram of the melt solution at $pH_2O = 0$, after

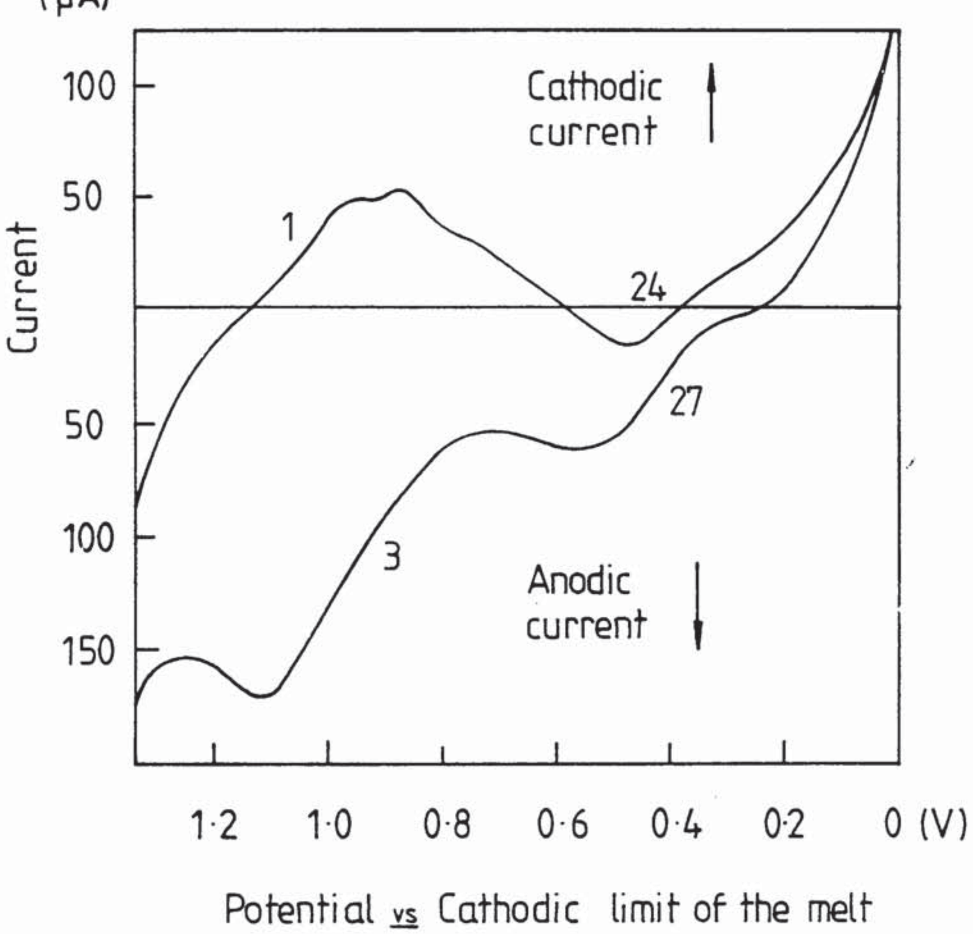

Figure 7 - 12 Voltammogram of (Na - K)OH eutectic after passing iso - propanol at 523K, using a vibrating Pt indicator electrode, under N_2.

injecting iso-propanol into the pure melt, using the vibrating working electrode. The voltammogram is similar to that of the melt solution after injecting ethanol into the pure melt (Fig.7-1). Two waves were found one on the (f.s) and the other on the (r.s) The $E_{\frac{1}{2}}$ values of these waves are similar to those of the oxidation waves 24 and 27 in Fig.7-1 indicating that they are due to the oxidation of acetate, but in Fig.7-12 the wave corresponding to wave 24 is a composite wave and that corresponding to wave 27 is an oxidation wave. It was also found that drying the melt made the first wave a cathodic wave and the second wave a composite wave. This can be explained if the following reaction is postulated:

$$CH_3COO^- + O_2^{2-} + 2H_2O \rightleftarrows CH_3OH + CO_2 + 3OH^- \qquad (7\text{-}15)$$

this reaction is based on the fact that O_2^{2-} is stable in dry melts. Therefore the cathodic electrode reaction represented by the two waves in Fig.7-12 is:

$$CH_3OH + CO_2 + 2e^- \rightleftarrows CH_3COO^- + OH^- \qquad (7\text{-}16)$$

which is the reverse of the reaction representing waves 24 and 27 in Fig.7-1. However the analysis of the two waves gave results indicating an irreversible electrode reaction which suggests that the equilibrium of reaction (7-16) lies mainly to the right if the melt was dry and the acetate concentration low. To confirm that, sodium acetate was added to the melt and a voltammogram of the melt solution was obtained. The two waves became oxidation waves, hence it was concluded that they are waves 24 and 27. Waves 25 and 26 in Fig.7-1, due to the reduction and oxidation of chemisorbed compounds on the Pt electrode surface, were only found in some voltammograms of the melt solutions used in investigating the iso-propanol reactions. Although no comprehensive experiments were carried out to investigate acetone reactions with the hydroxide melt, it was decided to investigate such reactions electrochemically because of the similarity between acetone reactions and iso-propanol reactions. Moreover acetone was earlier found to be an oxidation product of iso-propanol.

In Fig.7-13 is presented a voltammogram of the melt solution using the vibrating working electrode, after passing acetone through the pure melt. This voltammogram is virtually the same as that of Fig.7-6 of the melt solution containing acetates added to the pure melt as acetic acid. Hence Fig.7-13 shows waves 24, 25, 26 and 27. These waves have been interpreted in section 7.5.1.1. However, on the (f.s) a new anodic wave was found, its $E_{\frac{1}{2}}$ value being 0.86V. This wave has been assigned wave number 28. Studies on the alkali fusion of ketones (67) indicate minor side reactions which produce compounds other than acetic acid, therefore wave 28 is probably due to the oxidation of a side reaction product. In conclusion, the main reaction between acetone and molten hydroxides was thought to proceed according to the following mechanism:

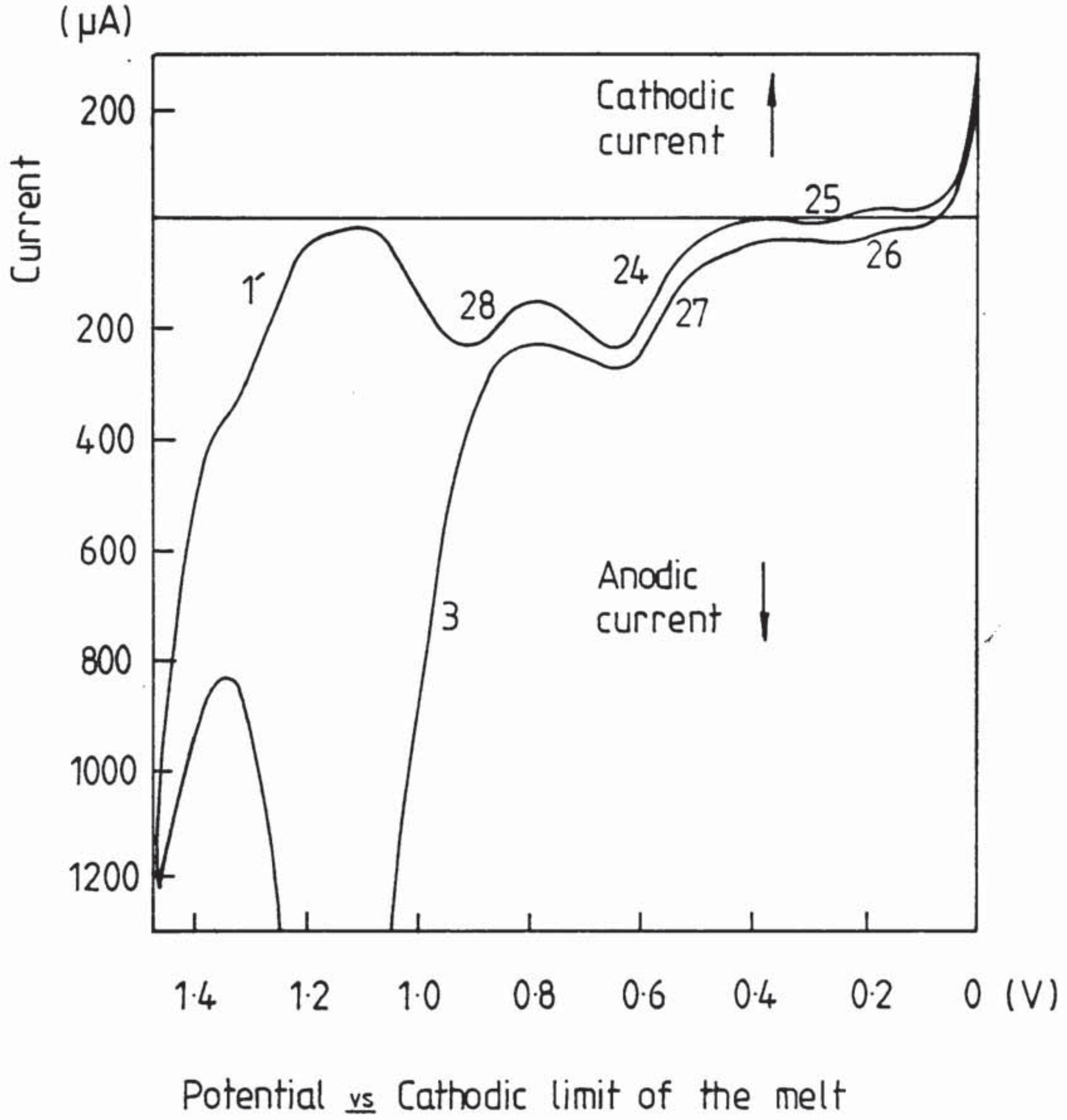

Figure 7-13 Voltammogram of (Na-K)OH eutectic after passing acetone at 523K, using a vibrating Pt indicator electrode, under N_2.

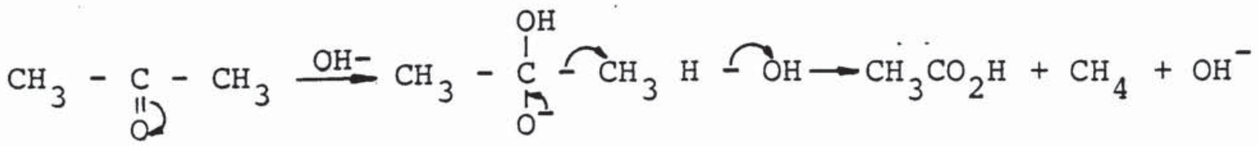

$$CH_3 - \underset{\underset{O}{\|}}{C} - CH_3 \xrightarrow{OH^-} CH_3 - \overset{\overset{OH}{|}}{\underset{O^-}{C}} - CH_3 \quad H - OH \longrightarrow CH_3CO_2H + CH_4 + OH^-$$

The second voltammogram obtained while investigating acetone reactions is shown in Fig.7-14. The melt solution used to obtain this voltammogram was the same as the one used to obtain that of Fig.7-13, except that $KMnO_4$ (0.09M) was added to it, the pH_2O value of the melt was 1. As can be seen in Fig.7-14 the appearance of the oxidation wave 9 suggests that the MnO_4^{3-} molar concentration is higher than that of the acetates in the melt because if it were lower or the same as the acetate concentration, wave 9 would not appear because of the reaction of MnO_4^{3-} with the acetates. Waves 24 and 27 in Fig.7-14 have disappeared for the reason mentioned above and instead waves 5 and 7 due to the couple Mn^{2+}/Mn_2O_3 have appeared. The rest of the voltammogram has been interpreted previously.

The voltammogram shown in Fig.7-15 is of the melt solution containing $KMnO_4$ (0.09M) initially into which acetone was then injected. In this voltammogram wave 9 has disappeared indicating that acetone was oxidized by MnO_4^{3-} probably to acetic acid. Once again that proves that the oxidation reaction is much faster than the reaction between the organics and the hydroxide melt.

A voltammogram of the melt solution ($pH_2O = 0$) containing $KMnO_4$ (0.09M) initially, after the first iso-propanol injection is shown in Fig.7-16. The

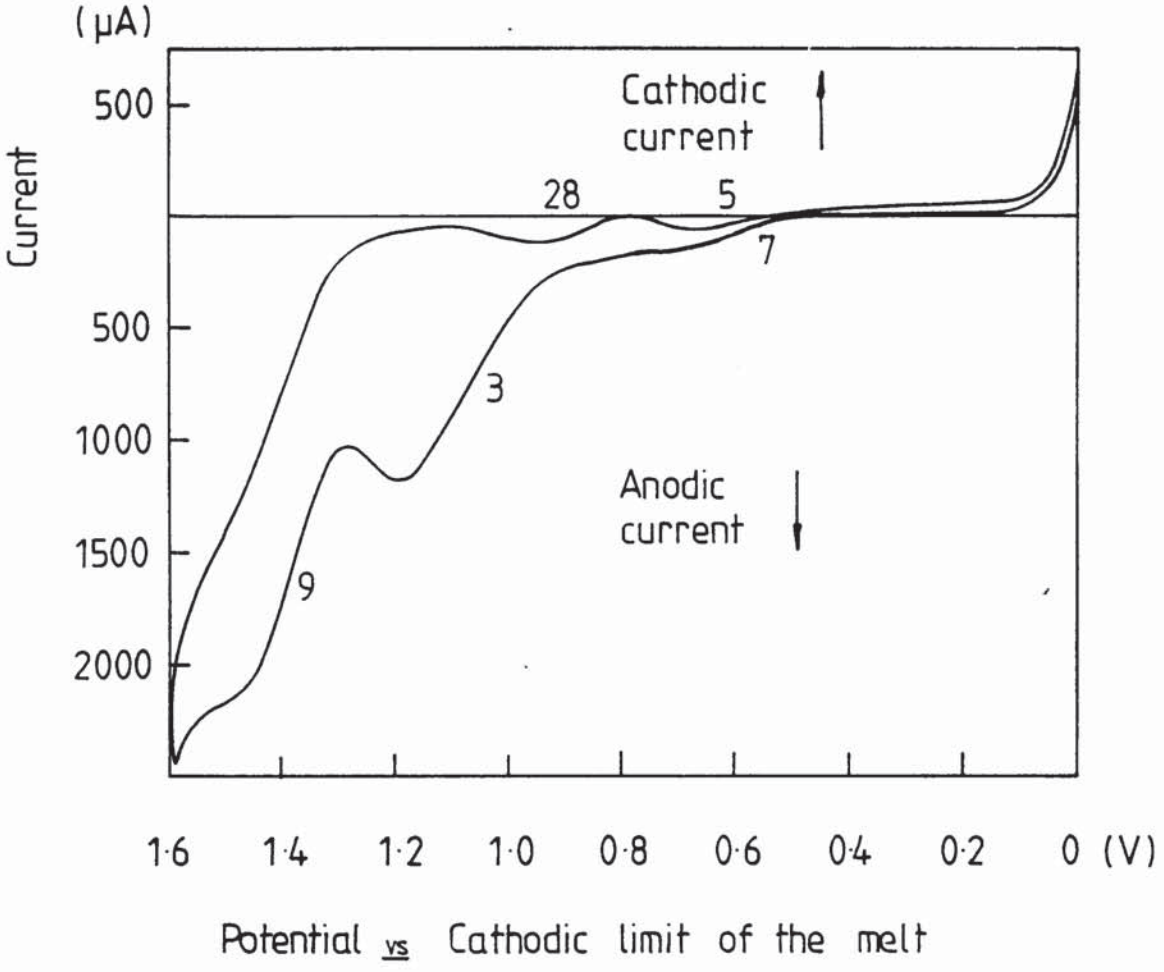

Figure 7-14 Voltammogram of (Na-K)OH eutectic after passing acetone, $KMnO_4$ (0·09M) was then added at 523K and $pH_2O=1$, using a vibrating Pt indicator electrode, under N_2.

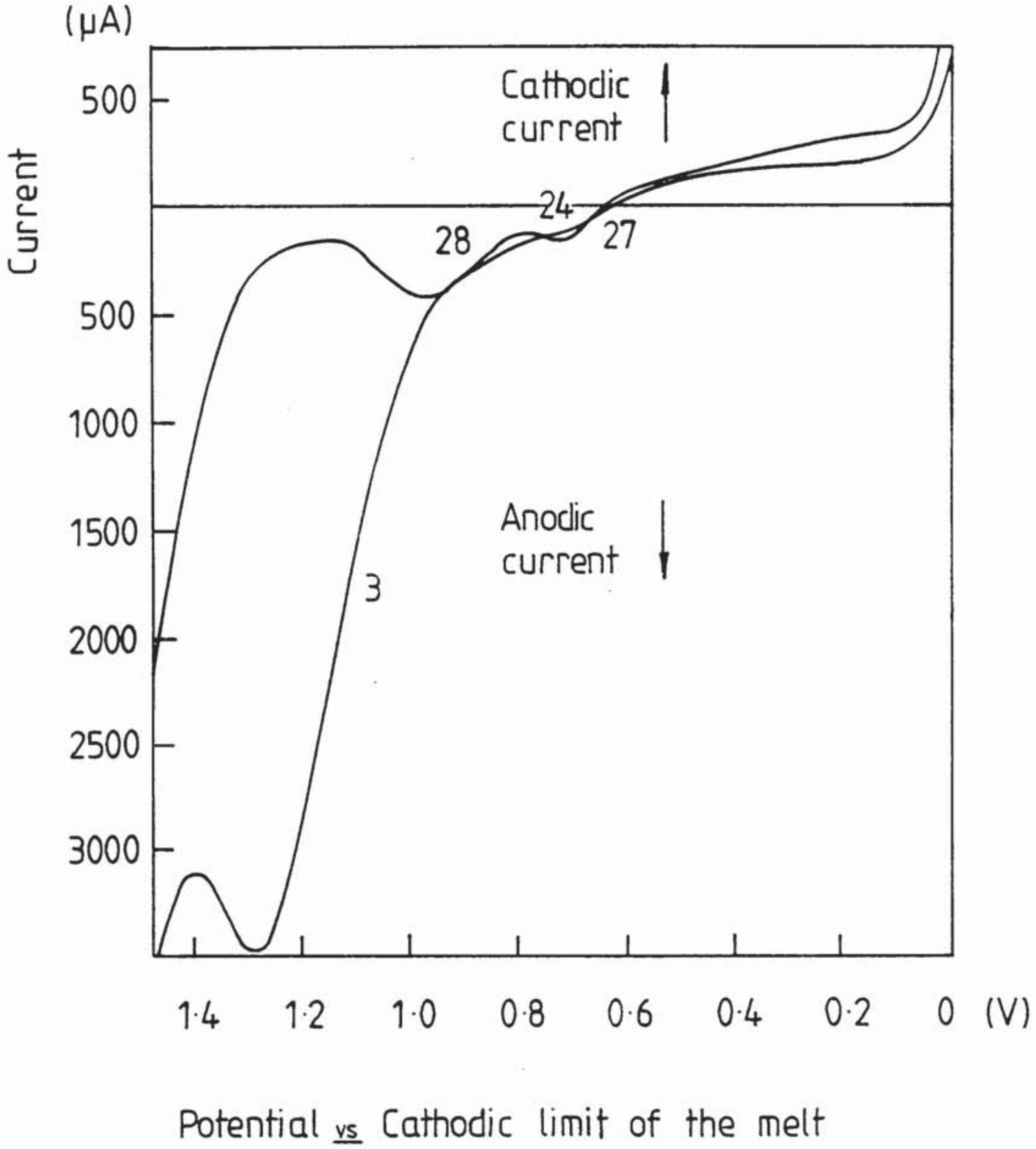

Figure 7-15 Voltammogram of (Na-K)OH eutectic containing $KMnO_4$ (0·09M) initially, into which acetone was then passed at 523K, using a vibrating Pt indicator electrode, under N_2.

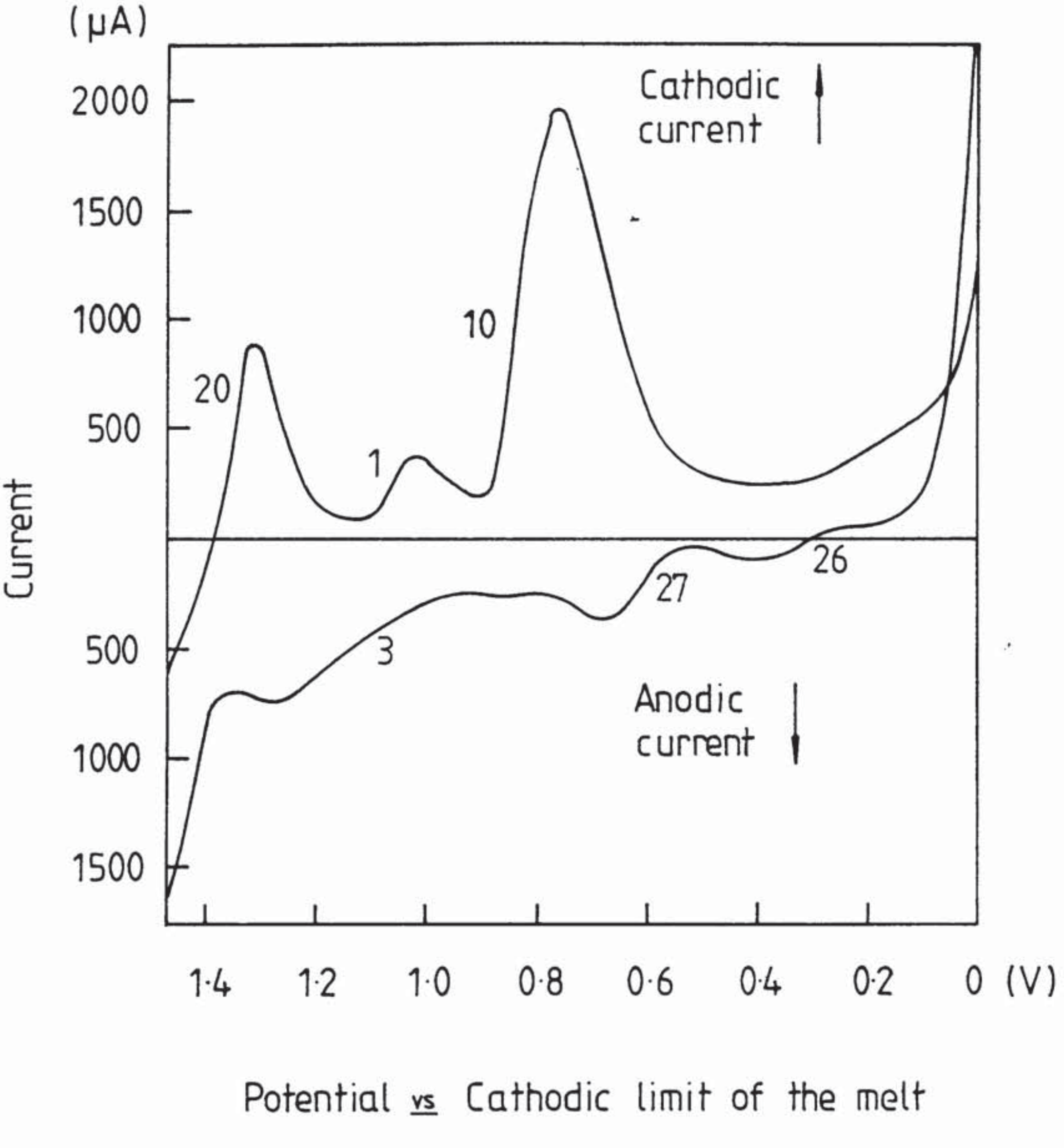

Figure 7-16 Voltammogram of (Na-K)OH eutectic containing $KMnO_4$ (0·09M) initially, after the 1st iso-propanol injection at 523K and $pH_2O=0$, using a vibrating Pt indicator electrode.

presence of wave 20 due to MnO_4^{2-} reduction and the disappearance of wave 9 due to MnO_4^{3-} oxidation clearly indicate that MnO_4^{3-} was used to oxidize iso-propanol to acetone. The remaining waves were interpreted earlier. a voltammogram of the melt solution ($pH_2O = 1$) containing acetates from the first iso-propanol injection after $KMnO_4$ (0.09M) was then added, followed by the second injection of iso-propanol, is shown in Fig.7-17. All the waves in this voltammogram have been interpreted previously. Again the disappearance of wave 9 confirms that MnO_4^{3-} has oxidized iso-propanol to acetone.

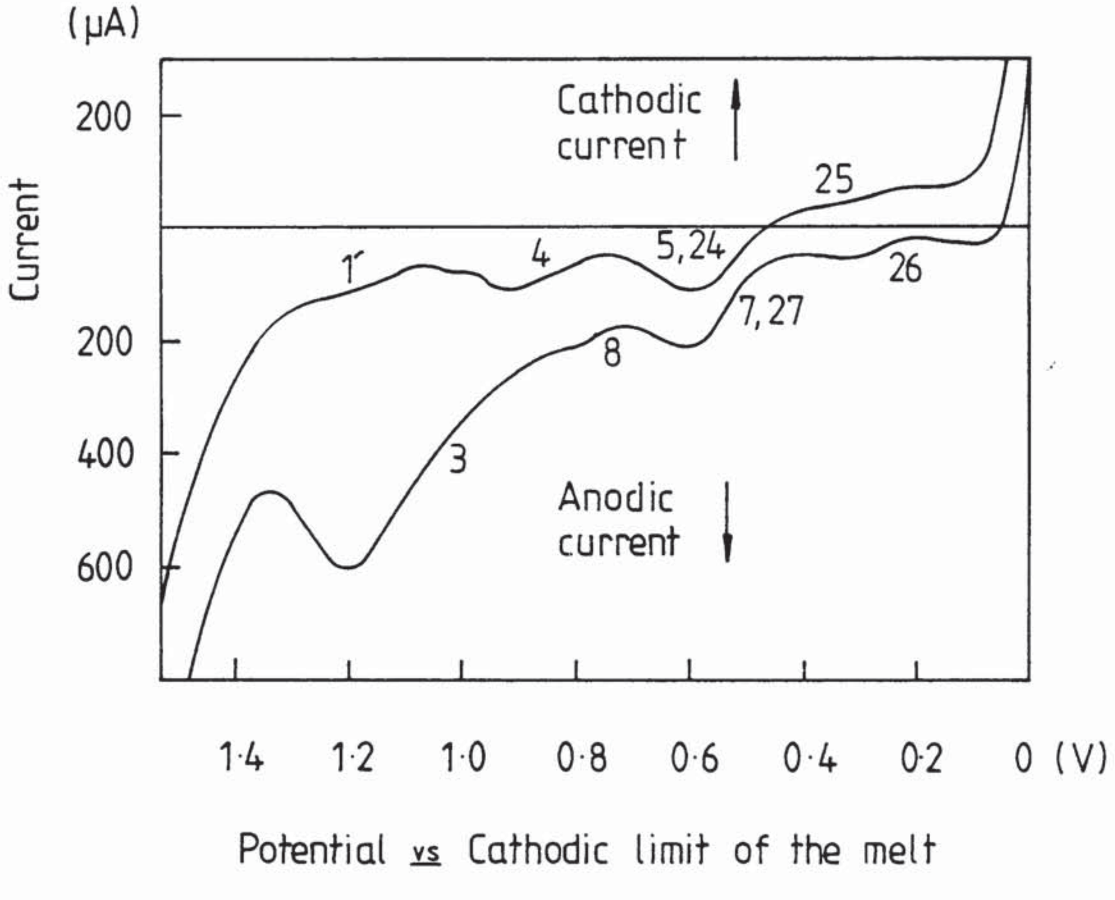

Figure 7 - 17 Voltammogram of (Na - K) OH eutectic containing $KMnO_4$ (0·09M), after the 2nd iso-propanol injection at 523K and $pH_2O = 1$, using a vibrating Pt indicator electrode. (1st injection was made into the pure melt)

7.5.3. The Oxidation of Methanol

The experimental procedure used to investigate the reactions of ethanol and iso-propanol with the pure molten hydroxides and with a melt containing $KMnO_4$, was also used for methanol. In table 7-10 are presented the results of mass balances obtained when methanol was injected into the empty reactor at 523K. In table 7-11 are shown the results of mass balances after passing methanol through molten (Na-K)OH at 523K. Analysis of the condensed liquid product showed that it contained only water and excess methanol. Here again the loss shown in table 7-11 is the net loss. Hydrogen was detected in the exit gas, indicating that a dehyrogenation reaction had occurred.

A second passage of the alcohol was made to ensure that no further reaction would take place, the amount of alcohol lost in the second passage was negligible. It was concluded therefore that approximately 15.0% of the alcohol injected reacts with the melt. From these results, it was noticed that the reaction rate of methanol with the hydroxide melt is faster than that of ethanol or iso-propanol.

The preliminary reaction experiments had shown that methanol was oxidized by hydroxide melts containing $KMnO_4$ at the pH_2O values of 1 and -1, which indicated that methanol was oxidized by both MnO_4^{2-} and MnO_4^{3-}. In table 7-12 are presented the detailed results of these reactions. The experiments were carried out as before in two stages. The first stage was performed by injecting methanol into the melts containing $KMnO_4$ (0.09M) with the pH_2O values of 1, 0, or -1.

Mass input (g)	Mass output (g)	Mass loss (g)	g% loss based on input
4.37	4.163	0.207	4.74
4.44	4.254	0.186	4.19
4.53	4.352	0.178	3.93

Table 7-10 Three Runs Showing Mass Balances for Methanol Passed Through the Empty Reactor at 523K.

pH_2O	Mass input (g)	Mass output (g)	Mass loss (g)	(g)% loss based on input
1	4.55	3.855	0.695	15.27
0	4.48	3.790	0.690	15.40
-1	4.51	3.839	0.671	14.88

Table 7-11 Results for the Passage of Methanol Through Molten (Na-K)OH Eutectic at 523K

			1st. Methanol injection into a melt containing $KMnO_4$				
pH_2O	Molar conc. of MnO_4^{3-} (approx.)	Molar conc. of MnO_4^{2-} (approx.)	melt colour		g% Methanol lost based on input	product in liquid phase	exit gaseous product
			before	after			
1	0.09	very low	blue	light brown	18.44	excess methanol and water	H_2
0	0.045	0.045	greenish blue	light brown	17.54	excess methanol and water	H_2
-1	very low	0.09	green	light brown	18.07	excess methanol and water	H_2
			2nd.* Methanol injection into a melt containing $KMnO_4$				
1	0.09	very low	blue	light brown	3.19	excess methanol and water	none
0	0.045	0.045	blue	light brown	1.64	excess methanol and water	none
-1	very low	0.09	** light brown				

* First injection was made into pure melt and % of methanol lost is shown in table 7-11.

** The second injection was not made because when $KMnO_4$ was added it reacted with the melt.

Table 7-12 Results of Methanol Reactions with Molten (Na-K)OH Containing $KMnO_4$ at 523K

From the melt colour change and the mass balances, it was found that methanol was oxidized by both MnO_4^{2-} and MnO_4^{3-} on a mole:mole basis. Analysis of the condensed liquid product showed that it contained only water and excess methanol, indicating that the oxidation product stayed in the melt. The exit gas analysis showed that hydrogen was produced indicating that a dehydrogenation reaction had taken place between methanol and the hydroxide melt according to the following mechanism (67):

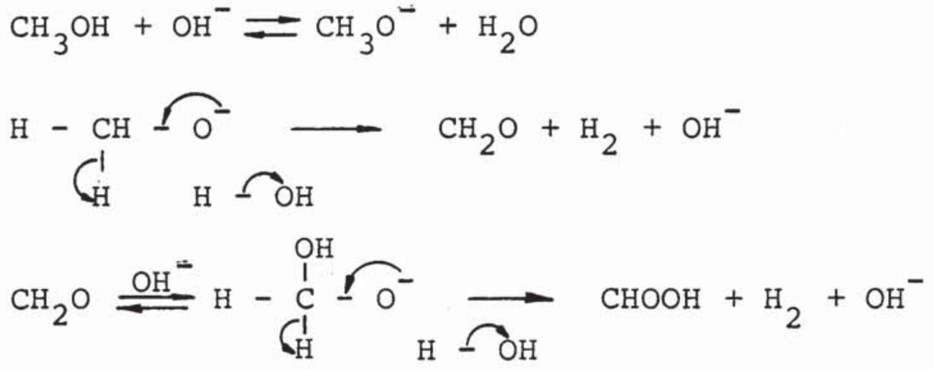

$$CH_3OH + OH^- \rightleftharpoons CH_3O^- + H_2O$$

$$H - \underset{H}{\overset{}{CH}} - O^- \quad \underset{H - OH}{} \longrightarrow CH_2O + H_2 + OH^-$$

$$CH_2O \overset{OH^-}{\rightleftharpoons} H - \underset{H}{\overset{OH}{C}} - O^- \quad \underset{H - OH}{} \longrightarrow CHOOH + H_2 + OH^-$$

but this reaction is much slower than the oxidation reaction. The product from both reactions is believed to be formate, but whether the formates are stable in the melt or not could only be confirmed by performing electroanalysis of the melt.

As shown in table 7-12 the percentage of methanol lost when it was injected into the melt with a pH_2O value of 0 is lower than that lost in melts with pH_2O values of 1 and -1. Also the percentage of methanol lost when it was injected into the melt with a pH_2O value of -1 is slightly lower than that lost in the melt with a pH_2O value of 1. Knowing that methanol was oxidized by both MnO_4^{2-} and MnO_4^{3-}, the results suggest that the oxidation by MnO_4^{3-} was complete i.e. the same number of moles of methanol were oxidized as of MnO_4^{3-} reduced (about 0.0045 moles at $pH_2O = 1$). However, the oxidation by MnO_4^{2-} was not complete or in other words, not all the MnO_4^{2-} which existed in the melt (about 0.0045 moles at $pH_2O = -1$) was used to oxidize methanol. This suggests that some of the MnO_4^{2-} reacted with possibly formates according to:

$$2MnO_4^{2-} + 4HCOO^- \rightleftarrows 2MnO_2 + 4CO_3^{2-} + 2H_2 \qquad (7\text{-}17)$$

as the formate concentration in the melt was in excess. In the second stage of the experiments, approximately the same amount of methanol was injected into the pure melts, then $KMnO_4$ was added to the melts (0.09M). The colour of the melts with pH_2O values of 1 and 0 was blue indicating the existance of MnO_4^{3-} while that with a pH_2O value of -1 was light brown indicating that MnO_4^{2-} had reacted with the formates according to equation (7-17). A second injection of methanol was then made into the melts with pH_2O values of 1 and 0. The percentage of methanol lost and the melt colour change indicated that methanol was oxidized by MnO_4^{3-}. Analysis of the condensed liquid product showed that it contained water and excess methanol. No gaseous product was detected in the exit gas.

7.5.3.1 The Elctroanalysis of the Experimental Melt Solutions.

In Fig.7-18 is presented a voltammogram of the melt solution after the passage of methanol through it, using the vibrating working electrode. The scan was performed

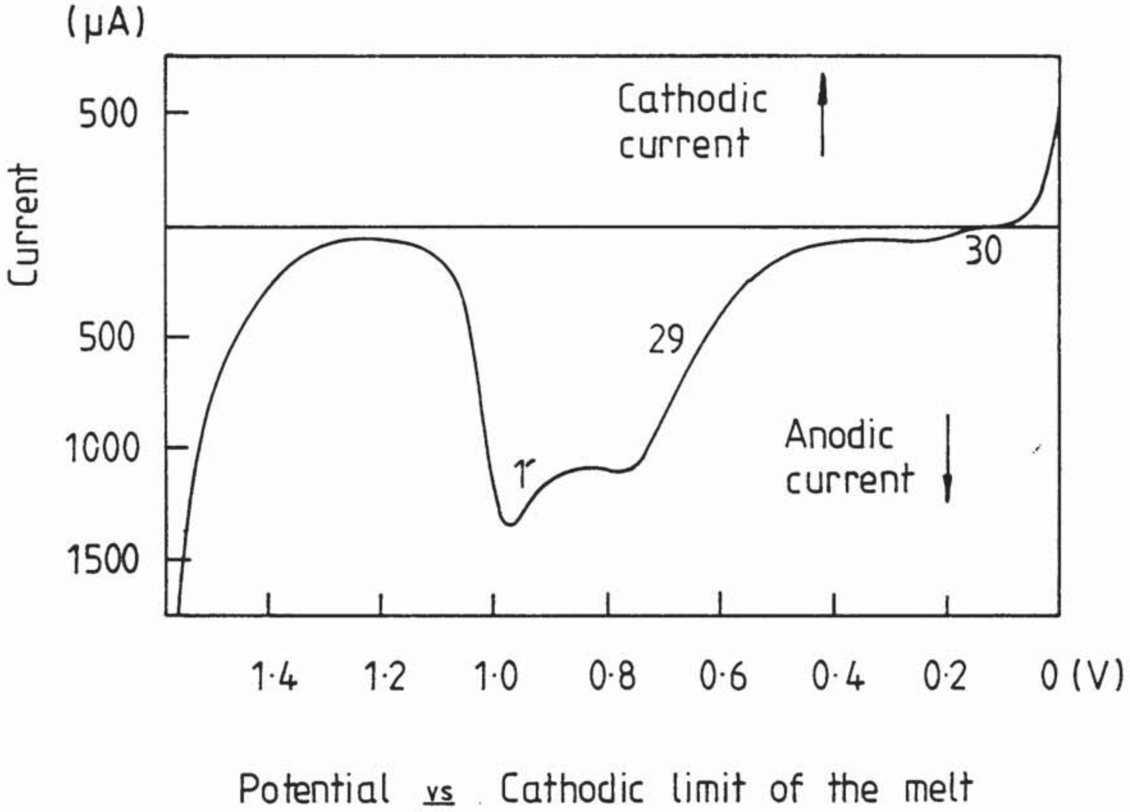

Figure 7-18 Voltammogram of (Na-K)OH eutectic after the passage of methanol at 523K, using a vibrating Pt indicator electrode. (f. s.)only.

on the (f.s) only. Instead of the normal Pt electrode surface oxidation peak (which appeared in most of the voltammograms of melt solutions after passing an organic) in the potential range (0.9 → 1·1V), the current shifts rapidly to an anodic limiting value at a potential of about 1.0V, followed by an anodic wave. This anodic wave is thought to be wave $1'$ with an $E_{\frac{1}{2}}$ value of 0.95V, due to the Pt electrode surface oxidation. Thermodynamic calculations from free energy of formation data show that CO_2, H_2, CO and H_2O can be formed from the decomposition of formic acid in water (111). However it was shown (112) that formic acid reacts with Pt electrodes in aqueous solutions to form an adsorbed species which behaves in a way similar to carbon monoxide. This adsorbed species blocks the surface of the electrode and prevents the adsorption of other species. The electrode can be cleaned by allowing the voltage of the electrode to decrease to about that for Pt oxide formation where the adsorbed species is oxidized. In basic aqueous solutions, the rate of electrolytic oxidation of formate to CO_2 at a platinized porous carbon anode was reported to be slow (113). If the hypothesis mentioned above applies to molten hydroxides, then the current shift in Fig.7-17 is because the Pt electrode oxidation was hindered by an adsorbed species like CO.

After the current shift the rest of the voltammogram is apparently normal.

An anodic wave was found at an $E_{\frac{1}{2}}$ value of 0.64V and has been assigned wave number 29. H.I.E. plot analysis of the wave indicated a reversible two electron transfer reaction, therefore wave 29 is thought to be due to the formate oxidation according to:

$$HCOO^- + OH^- - 2e^- \rightleftarrows CO_2 + H_2O \qquad (7\text{-}18)$$

A small anodic wave which has been assigned wave number 30 was also found close to the cathodic limit of the melt, this wave is thought to be due to the chemisorbed CO oxidation. In Fig.7-19 is shown the (f.s) and the (r.s) of the voltammogram of Fig.7-18. On the (r.s) another small anodic wave, assigned wave number 31, was found. Wave 31 is thought to be due to the oxidation of chemisorbed CH_3O^-, according to equation (7-9). Wave 31 is followed by a wave at approximately the same $E_{\frac{1}{2}}$ value of wave 29, which was assigned wave number 32 and is attributed to the formate oxidation as the wave analysis also indicated a reversible two electron transfer reaction. The voltammogram shown in Fig.7-20 is of the melt solution with a pH_2O value of 1 containing $KMnO_4$, added after the first injection of methanol. The voltammogram is similar to that shown in Fig.7-19 apart from the appearance of wave 9 due to MnO_4^{3-} oxidation indicating that MnO_4^{3-} was not affected by the presence of the formates. The voltammogram of the melt solution containing $KMnO_4$ initially through which methanol was then passed was not different from that shown in Fig.7-19. Also the voltammogram of the melt solution after the second methanol injection was

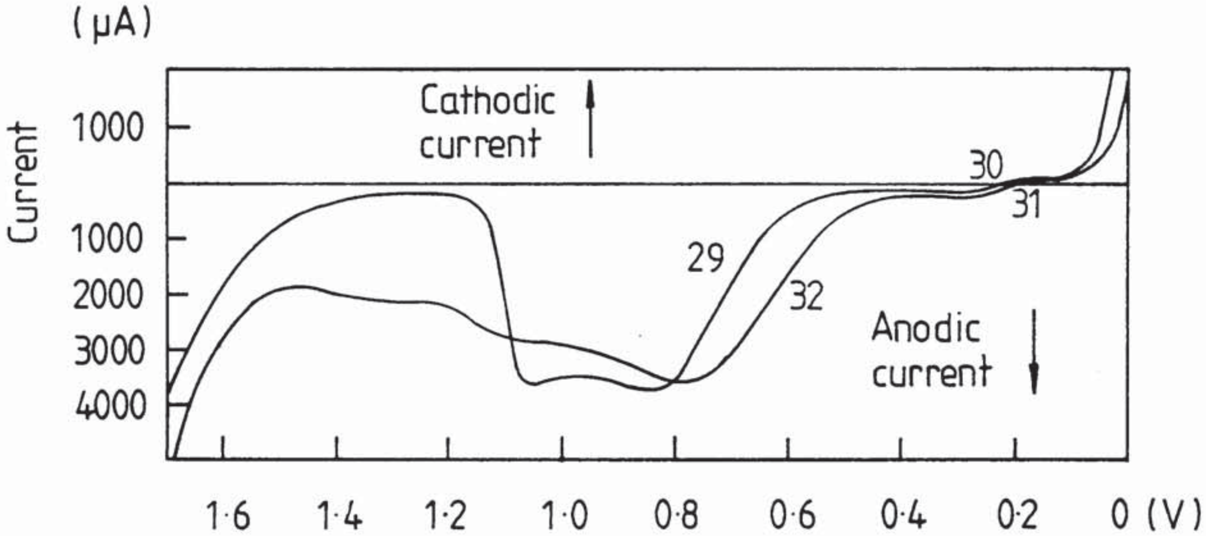

Potential vs Cathodic limit of the melt

Figure 7 - 19 Voltammogram of (Na-K)OH eutectic after the passage of methanol at 523K, using a vibrating Pt indicator electrode. (f. s) and (r.s)

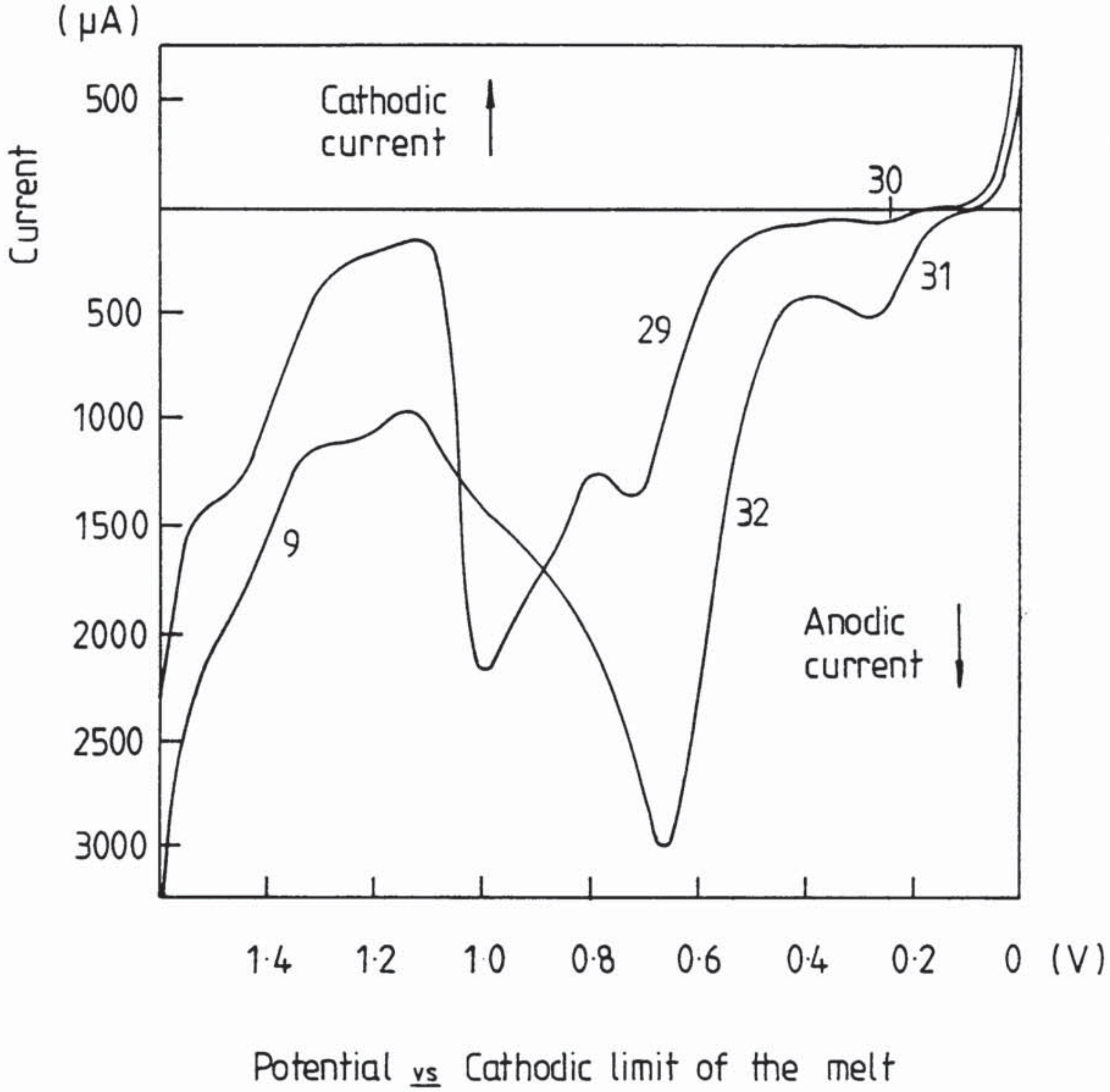

Figure 7 - 20 Voltammogram of (Na-K)OH eutectic after passing methanol initially, then $KMnO_4$ (0·09M) was added at 523K and $pH_2O = 1$, using a vibrating Pt indicator electrode.

similar. An experiment was carried out to show the effect of bubbling oxygen through the melt solution with a pH_2O value of 1 containing $KMnO_4$ initially, after the first methanol injection. Oxygen was bubbled through the melt for three hours and in Fig.7-21 is presented the voltammogram of the melt solution using the vibrating working electrode. As can be seen the two waves, wave 29 and wave 32 due to the formates oxidation have disappeared because the formates were oxidized by oxygen to CO_2. Two cathodic waves were found one on the (f.s) and the other on the (r.s). Their $E_{\frac{1}{2}}$ values were 0.75V and 0.70V respectively. These two waves were thought to be due to the following reaction:

$$Mn_2O_3 + H_2O + 2e^- \rightleftarrows 2MnO + 2OH^- \qquad (7\text{-}19)$$

as their $E_{\frac{1}{2}}$ values and their analysis suggested. Adding formate to the melt in the form of formic acid showed that it decomposes as a voltammogram of the melt after adding the acid proved. The voltammogram obtained was exactly the same as that of the pure melt.

In table 7-13 is presented a list of reactions that have been proposed for the waves which have been discussed in this chapter.

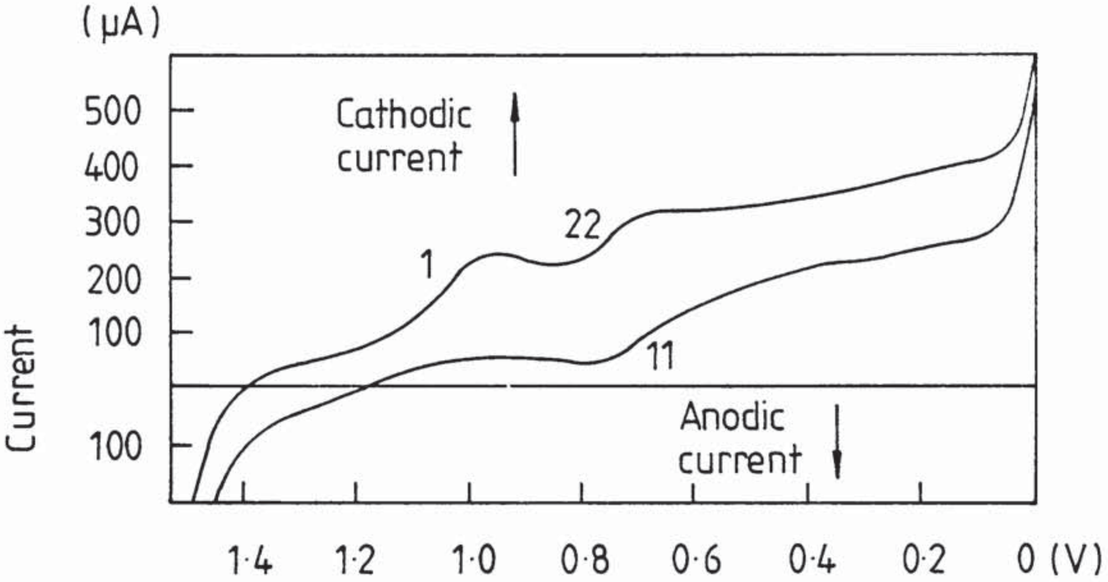

Potential vs Cathodic limit of the melt

Figure 7-21 Voltammogram of (Na-K)OH eutectic containing $KMnO_4$ (0·09M) initially, after the 1st methanol injection at 523K and $pH_2O = 1$, O_2 bubbled through for 3hrs, using a vibrating Pt indicator electrode.

Wave	$E_{\frac{1}{2}}$ or E_p (V)	i_L or i_p (μA)	Couple	Reaction	Comments
24(f.s)	0.63	615	CH_3COO^-/ CO_2,CH_3OH	(7-6)	Rev. Oxid. Peak
25(f.s)	0.25	95	$C_2H_5O^-$/ C_2H_6	(7-11)	Rev. Red. Wave
26(r.s)	0.23	115	$C_2H_5O^-$/ C_2H_6	(7-11)	Rev. Oxid. Wave
27(r.s)	0.66	595	CH_3COO^-/ CO_2,CH_3OH	(7-6)	Rev. Oxid. Peak
28(f.s)	0.86	96		Acetone+ (Na-K)OH	Irrev.Oxid. Wave
29(f.s)	0.64	variable	$HCOO^-/CO_2$	(7-18)	Rev. Oxid. Wave
30(f.s)	0.19	75	CO/CO_2	(7-12)	Rev. Oxid. Wave
31(r.s)	0.18	80	CH_3O^-/CH_4	(7-9)	Rev. Oxid. Wave
32(r.s)	0.66	variable	$HCOO^-/CO_2$	(7-18)	Rev. Oxid. Wave

Table 7-13 Proposed Reactions of Voltammetric Waves Found in Electroanalysis Experiments

CHAPTER 8

Conclusions and Recommendations for Future Work

The objective of this research was the oxidation of organic compounds in molten hydroxides containing manganates. It has been shown that controlled oxidation can be readily achieved with high specificity to give products in high yield with very short reaction times. In this chapter the achievements of this research are listed together with recommendations for future work.

(i) Using the vibrating Pt electrode the electroanalysis of chemical species which are present in acidic or neutral (Na-K)OH eutectic at 523K contained in a PTFE cell has been studied. The following systems in molten (Na-K)OH at 523K have also been studied using the vibrating Pt electrode, Mn metal, $KMnO_4$, Mn metal and $KMnO_4$, $KMnO_4$ and Na_2CO_3, $KMnO_4$ and Na_2O_2 and the effect of O_2 on some of these systems has been studied. Voltammetric waves were found and reactions have been proposed and in some cases validated, for each system.

(ii) Henry's law constants for water in molten (Na-K)OH have been measured and used to calculate the water concentration in the melt, therefore the existence and stability of Mn(II), Mn(III), Mn(IV), Mn(V) and Mn(VI) added to the melt as $KMnO_4$ or Mn metal were investigated. The existence and stability of these manganese oxidation states were found to be dependent on the water concentration in the melt.

(iii) Electroanalysis has been performed on stabilized Mn(V) and Mn(VI) and it has been concluded that Mn(V) is the predominant and stable manganese oxidation state at a pH_2O value of about 1 and that Mn(VI) is the predominant and stable manganese oxidation state at a pH_2O value of about -1. In a melt of pH_2O value of about 1, an oxidation wave has been found which is due to the oxidation of Mn(V) to Mn(VI) ($E_{\frac{1}{2}}$ = 1.45V) and no wave due to Mn(VI) reduction was found. In a melt of pH_2O value of about -1, a reduction wave has been found which is due to the reduction of Mn(VI) to Mn(V) at a similar $E_{\frac{1}{2}}$ value to that of the oxidation of Mn(V) to Mn(VI) and no wave due to Mn(V) oxidation was found. In a melt of pH_2O value of about 0, both the oxidation and the reduction waves were found. These waves were used to monitor the existence of Mn(V) or Mn(VI) before and after the passage of organic compounds through the melt.

(iv) The following organic chemicals have been passed through molten (Na-K)OH at 523K : Methanol, allyl alcohol, propane 1, 2 diol, 1-heptene, acetone, ethanol, iso-propanol, benzyl alcohol, n-propanol, butanol, 2 methyl propan-2-ol, n-hexane, n-heptane, toluene and cyclohexane. They have also been passed through Mn(V) and Mn(VI) melt solutions. In none of these experiments did violent reactions occur. Future research could extend the range of organic chemicals studied in this research project e.g. aliphatic amines, paraffins and others.

(v) Chemical oxidation by Mn(V) and Mn(VI) has been shown to occur with methanol, allylalcohol, propane 1, 2 diol, 1-heptene and acetone. Ethanol was only oxidized by Mn(VI), iso-propanol and benzyl alcohol were only oxidized by Mn(V). The reaction times were of the order of one eighth of a second and high reaction conversions were achieved e.g. for ethanol a conversion of 100%.

(vi) The reaction products of some of the organic chemicals mentioned above (from their reaction with the pure hydroxide melt) have been identified by analysing the melt solutions electrochemically. Research into the reactions of other organic chemicals with the pure hydroxide melt with controlled water concentrations could be performed using electro-analytical methods to analyse the melt solutions.

(vii) The complete oxidation of methanol by Mn(V) and Mn(VI) in molten (Na-K)OH at 523K to formates which were decomposed by bubbling oxygen through the melt could be used as a basis to develop an industrial process by which unwanted methanol could be eliminated from an output line.

The major areas where future work into organic oxidation reactions are feasible are therefore:

Oxidation using Mn(V) or Mn(VI) with other organic chemicals and the study of the present ones which have not been studied in detail. Research into the oxidation of those organic chemicals which apparently do not react with the hydroxide melts e.g. hydrocarbons, by other oxidizing agents e.g. chromates.

The regeneration of Mn(V) and Mn(VI) by air, O_2, electrolysis or other chemical additions.

The development of an industrial process which incorporates all the normal research studies such as; economic viability, safety, scale-up and comparison with existing reactor systems.

APPENDIX

Supporting Publication

Henry's Law Constant for Water in the Eutectic Molten Salt System NaOH-KOH

E. Al-muslih, P. J. Iredale and J. K. Maund

Journal of Chemical and Engineering Data,
28, 245 - 246 (1983)

NOMENCLATURE AND ABBREVIATIONS

E^o	Standard electrode potential
$E_{w.e}$	Electrode potential of working electrode
E_p	Voltammetric peak potential
$E_{p/2}$	Voltammetric half-peak potential
$E_{\frac{1}{2}}$	Voltammetric half-wave potential
F	Faraday constant
f.s	Forward sweep
F.I.D	Flame ionization detector
G.L.C	Gas-Liquid Chromatograph
H.I.E	Herovsky-Ilkovic equation
i_d	Diffusion current
i_L	Limiting current
i_p	Peak current
i.d	Internal diameter
m	Molal concentration
M	Molar concentration
n	Number of electrons
o.d	Outside diameter
R	Universal gas constant
r.s	Reverse sweep
T	Temperature (K)

REFERENCES

(1) G.Von Hevesy, Z.Phys.Chem. 73, 667(1910).

(2) H.W.Otto and R.P.Seward, J.Chem.Eng.Data 9, 507 (1964).

(3) N.A.Reshetnikov and N.I.Vilutis, Zh.Neorg.Khim. 4, 123 (1959).

(4) A.Eluard and B.Tremillon, J.Electroanal.Chem.18, 277 (1968).

(5) A.Eluard and B.Tremillon, Anal.Lett.2, 221 (1969).

(6) A.Eluard and B.Tremillon, J.Electroanal.Chem.27, 117 (1970).

(7) A.Eluard and B.Tremillon, J.Electroanal.Chem.26, 259 (1970).

(8) A.Eluard and B.Tremillon, J.Electroanal.Chem.30, 323 (1971).

(9) K.Arndt and G.Ploetz, Z.Phys.Chem.121, 439 (1926).

(10) S.Zecchin, G.Schiavon and G.G.Bombi, J.Electroanal. Chem. 50, 261 (1974).

(11) M.A.Klochko and M.M.Godneva, Zh.Neorg.Khim.4, 2136 (1959).

(12) C.Dauby, J.Glibert and P.Claes, Electrochimica Acta.24, 35 (1979).

(13) C.Dauby, J.Glibert and P.Claes, Electrochimica Acta.25, 1077 (1980).

(14) B.Newmann and E.Bergve, Z.Elektrochem.21, 143 (1915).

(15) D.Inman and D.G.Lovering "Ionic Liquids" Plenum Press, New York and London (1981).

(16) J.Greenberg and L.J.Hallgreen, J.Chem.Phys.35, 180 (1961).

(17) R.Oyamada, J.Phys.Soc.Jpn.26, 1068 (1969).

(18) V.P.Shvedov and I.A.Yvanov, Russ. J.Phys.Chem. 39, 396 (1965).

(19) J.Goret, Bull.Soc.Chim.Fr., 1074 (1964).

(20) J.Goret and B.Tremillon, Bull.Soc.Chim.Fr., 67 (1966)

(21) D.D. Williams, J.A.Grand and R.R.Miller, J.Amer. Chem.Soc. 78, 5150 (1956).

(22) G.G.Bombi, S.Zecchin and G.Schiavon, J.Electroanal. Chem. 50, 261 (1974).

(23) E.Almuslih, P.J.Iredale and J.K.Maund, J.Chem.Eng. Data 28, 245 (1983).

(24) A.Rahmel and H.Krueger, Z.Phys.Chem.55, 25 (1967).

(25) E.Hoyt, J.Chem.Eng. Data 12, 461 (1967).

(26) A.Eluard, Ph.D.thesis, Faculte des Sciences de l'Universite de Paris (1970).

(27) W.M.Vogel and S.W.Smith, J.Electroanal.Chem.18, 215 (1968).

(28) W.M.Vogel, K.J.Routsis, V.J.Kehrer, D.A.Landsman and J.G.Tschinkel, J.Chem.Eng.Data 12, 465 (1967).

(29) J.N.Agar and F.P.Bowden, Proc.Roy.Soc.Ser. A169, 206 (1938).

(30) K.H.Stern and J.K.Carlton, J.Phys.Chem.58, 965 (1954).

(31) J.Goret and B.Tremillon, Electrochim.Acta 12, 1065 (1967).

(32) J.Goret, Ph.D. thesis, Faculte des Sciences de l'Universite de Paris (1966).

(33) H.Lux, Z.Elektrochem.45, 303 (1939); 52, 220 (1948); 53, 41 (1942); Naturwissenschaften 28, 92 (1940).

(34) H.Flood and T.Forland, Acta Chem.Scand. 1, 592 (1947).

(35) J.N.Agar and F.P.Bowden, Proc.R .Soc. London 169, 206 (1939).

(36) H.Lux and T.Niedermaier, Z.Anorg.Allg.Chem.282, 196 (1955); 285, 246 (1956); 298, 285 (1959).

(37) H.Lux and E.Renauer, Z.Anorg.Allg.Chem.310, 305 (1962).

(38) J.Goret and B.Tremillon, Bull.Soc.Chim.Fr.67, 2872 (1966).

(39) B.Tremillon and R.Doisneau, J.Chim.Phys.10, 1379 (1974).

(40) R.Doisneau and B.Tremillon, Bull.Soc.Chim.Fr. 9-10, 1419 (1976).

(41) R.Newman, R.Smith and C.Smith, Proc.Int.Conf.Liq. Met.Technol.Energy Prod. 2, 841 (1977).

(42) R.Doisneau and B.Tremillon, J.Chim.Phys. 71, 1445 (1974).

(43) L.Antropov, D.Tkalenko and S.Kudrya, Ukr.Khim.Zh.40, 429 (1974).

(44) G.Kern and O.Bloch, C.R.Acad.Sci.Ser. C258, 531 (1964).

(45) M.Bonnemay, L.Lacourcelle and J.Royon, Electrochim. Acta 14, 1061 (1969).

(46) D.J.G.Ives and G.J.Janz "Reference Electrodes, theory and practice", Chap.4, Academic Press (1969).

(47) G.Schiavon, S.Zecchin and G.G.Bombi, J.Electroanal. Chem. 38, 473 (1972).

(48) J.P.Wiaux and P.Claes, J.Electrochem.Soc. 129/1, 123 (1982).

(49) W.D.Read, Ph.D.thesis, University of Aston in Birmingham (1978).

(50) G.Kern, P.Degobert and O.Block, C.R.Acad.Sci.Paris 256, 1500 (1963).

(51) P.Claes, Paper presented at EUCHEM Molten Salt Meeting, Lysekil, Sweden (June 1978).

(52) H.J.Kruger, A.Rahmel and W.Schwenk, Electrochim. Acta 13, 625 (1968).

(53) B.Tremillon, Int.Symposium on Non-Aqueous Electrochemistry, Paris (1970), Butterworths, London, 395 (1971).

(54) L.I.Antropov and D.A.Tkalenko, Elektrokhimiya 6, 1557 (1970).

(55) A.B.Tsentsiper, T.I.Rogozhnikova and V.M.Bakulina, Izv.Akad.Nauk SSSR Ser.Khim.1967, 2073 (1967).

(56) A.S.Afanasev and V.P.Gamazov, Zh.Fiz.Khim.38, 2823 (1964).

(57) W.J.Hamer and J.P.Schrodt, J.Amer.Chem.Soc.71, 2347 (1949).

(58) H.A.Lehmann and K.Teske, Z.Anorg.Allg.Chem. 336, 197 (1965).

(59) H.Lux and M.Seliger, Mikrochim.Acta 1968, 683 (1968).

(60) A.Carrington and M.C.R.Symons, J.Chem.Soc., 3373 (1956).

(61) K.Sekula-Brzezinska, P.K.Wrona and Z.Galus, Electrochimica Acta 24, 555 (1979).

(62) D.Richter, "Thorpe's Dictionary of Applied Chemistry" Longmans - London, 1, 203 (1949).

(63) H.S.Fry, E.L.Schulze and H.Weitkamp, J.Amer.Chem.Soc. 46, 2268 (1924).

(64) H.S.Fry and E.L.Schulze, J.Amer.Chem.Soc. 48, 958 (1926).

(65) H.S.Fry and E.Otto, J.Amer.Chem.Soc.50/1, 1122 (1928).

(66) B.H.Carrol, J.Phys.Chem. 22, 128 (1918).

(67) R.A.Dytham and B.C.L.Weedon, Tetrahedron 8, 246 (1960).

(68) J.Dumas and J.S.Stass, Justus Liebigs Ann.Chem.35, 129 (1840).

(69) E.E.Reid, H.Worthington and A.W.Larchar, J.Amer.Chem. Soc. 61, 99 (1939).

(70) C.Weizmann and S.F. Garrard, J.Chem.Soc.117, 324 (1920).

(71) H.C.Chitwood, U.S.Patent 2, 384, 817 (1945); Chem.Abstr. 40, 354 (1946); British Patent 601, 817 (1948); Chem. Abstr. 42, 7325 (1948).

(72) M.Guerbet, Bull.Soc.Chim.Fr. 5, 420 (1909); 7, 212 (1910), 11, 164, 279 (1912); Ann.Chim.Phys.27, 67 (1902); C.R.Acad.Sci., Paris, 128, 511, 1002 (1899), 132, 207, 685 (1901), 133, 300,1220 (1902).

(73) G.Lock, Chem.Ber. 63, 551 (1930).

(74) H.Machemer, Angew. Chem. 64, 213 (1952).

(75) E.F.Pratt and D.G.Kubler, J.Amer.Chem.Soc.76, 53 (1954).

(76) C.Weizmann, E.Bergmann and M.Sulzbacher, J.Org.Chem. 15, 54 (1950).

(77) M.Guerbet, C.R.Acad.Sci., Paris, 146, 298 (1908).

(78) T.L.Cairnes, R.M.Joyce and R.S.Schreiber, J.Amer.Chem. Soc. 70, 1689 (1948).

(79) E.L.Pelton, C.J.Starnes and S.A.Shrader, J.Amer.Chem. Soc. 72, 2039 (1950).

(80) H.Pines and L.Schaap, J.Amer.Chem.Soc.79, 2956 (1957).

(81) H.D.Zook, J.March and D.F.Smith, J.Amer.Chem.Soc. 81, 1617 (1959).

(82) G.H.Hargreaves and L.N.Owen, J.Chem.Soc. 1947, 753.

(83) G.Lock, Chem.Ber.61, 2234 (1928), 62, 1177 (1929).

(84) A.T.Nielsen, J.Amer.Chem.Soc. 79, 2518, 2524 (1957).

(85) C.S.Barnes and A.Palmer, Aust.J.Chem.10, 334 (1957).

(86) J.R.Roach, H.Wittcoff and S.E.Miller, J.Amer.Chem. Soc. 69, 2651 (1947).

(87) R.G.Ackman, R.P.Linstead, B.J.Wakefield and B.C.L.Weedon, Tetrahedron 8, 221 (1960).

(88) P.G.Zambonin, J.Electroanal.Chem.24, 365 (1970).

(89) U.S.Pat.2,940,821 ; 2,940,822 (14th Jun.1960).

(90) G.Mamantov, J.M.Strong and F.R.Clayton, Anal.Chem.40, 488 (1968).

(91) Yu.K.Delimarskii, O.G.Zarubitskii and V.G.Budnik, Elektrokhimiya 6, 1635 (1970).

(92) R.S.Nicholson and I.Shain, Anal.Chem.36, 706 (1964).

(93) Kh.Z.Brainina, Talanta 18, 513 (1971).

(94) W.H.Reinmuth, Anal.Chem.33, 1793 (1961); 34, 1446 (1962).

(95) A.M.Bond, "Modern Polarographic Methods in Analytical Chemistry", 192-194, Marcel Dekker (1980).

(96) P.G.Zambonin, Anal.Chem.44, 763 (1972).

(97) B.J.Brough, D.A.Habboush and D.H.Kerridge, Inorg.Chim. Acta 6, 366 (1972).

(98) H.Hofer and M.Moest, Ann.323, 284 (1902).

(99) B.B.Damaskin, O.A.Petrii and V.V.Batrakov "Adsorption of Organic Compounds on Electrodes" Chap.8, Plenum Press, New York-London (1971).

(100) B.I.Podlovchenko and E.P.Gorgonova, Dokl. Akad.Nauk SSSR 156,673 (1964).

(101) B.I.Podlovchenko, O.A.Petrii and E.P.Gorgonova, Elektrokhimiya 1, 182 (1965).

(102) O.A.Petrii, B.I.Podlovchenko, A.N.Frumkin and Hira Lal, J.Electroanal.Chem. 10, 253 (1965).

(103) A.I.Shlygin and G.A.Bogdanovskii, Proceedings of the 4th Conference on Electrochemistry, Russ.(1956); Izd.Akad.Nauk SSSR 282 (1959); Zh.Fiz.Khim.31, 2428 (1957); 33, 1769 (1959); 34, 57 (1960); G.A.Martinyuk and A.I.Shlygin, Zh.Fiz.Khim.32, 164 (1958); A.K.Korolev and A.I.Shlygin, Zh.Fiz.Khim.36,314 (1962).

(104) T.Biegler, J.Phys.Chem.72, 1571 (1968).

(105) V.F.Stenin and B.I.Podlovchenko, Elektrokhimiya 3, 481 (1967).

(106) B.I.Podlovchenko, O.A.Petrii and A.N.Frumkin, Dokl. Akad.Nauk SSSR 153, 379 (1963).

(107) B.I.Podlovchenko, Elektrokhimiya 1, 101 (1965).

(108) B.I.Podlovchenko, O.A.Petrii, A.N.Frumkin and Hitra Lal, J.Electroanal.Chem.11, 12 (1966).

(109) J.E.Oxley, G.K.Johnson and B.T.Buzalski, Electrochim. Acta 9, 897 (1964).

(110) D.M.Drazic and U.Drazic, Electrochim.Acta 11,1235 (1966).

(111) F.D.Rossini, "Selected Values of Chemical Thermodynamics Properties" Natl.Bur.Standards, Circ.500, U.S.Dept. of Commerce, Feb.(1952).

(112) D.R.Rhodes and E.F.Steigelmann, J.Electrochem.Soc. 112/1, 16 (1965).

(113) R.P.Buck, "Mechanism and Kinetics of Reactive Groups in Organic Fuels", 15th Annual Proceedings Power Sources Conference, May 9 (1961).

(114) W.Sundermeyer, Angew.Chem. 77, 241 (1965).

(115) W.Sundermeyer, Angew.Chem.Internat.Ed.4, 222 (1965).

(116) D.H.Kerridge, Pure and Appl.Chem.41, 355 (1975).

(117) M.Parodi, A.Bonomi and G.Gentaz, European Conference on "Develoment of Molten Salts Applications" Battelle, Geneva Mar. (1973).

(118) C.Gentaz and A.Bonomi, Conference on "Molten Salts: Technology and Future Trends" Ludwigshafen Feb.(1975).